TWO-STEP RAPID SULFUR CAPTURE

FINAL TECHNICAL REPORT

Contract No. DE-AC21-90MC27200

Date Prepared

APRIL 1994

prepared for

U.S. DEPARTMENT OF ENERGY
Morgantown Energy Technology Center
P.O. Box 880
Collins Ferry Road
Morgantown, West Virginia 26507-0880

by

ENERGY TECHNOLOGY OFFICE OF
TEXTRON DEFENSE SYSTEMS
2385 Revere Beach Parkway
Everett, MA 02149

DOE/MC/27200 -- 5197
(DE96004478)

Two-Step Rapid Sulfur Capture

Final Report

April 1994

Work Performed Under Contract No.: DE-AC21-90MC27200

For
U.S. Department of Energy
Office of Fossil Energy
Morgantown Energy Technology Center
Morgantown, West Virginia

By
Textron Defense Systems
Everett, Massachusetts

DISCLAIMER

DOE/MC/27200 -- 5197
(DE96004478)
Distribution Category UC-106

Two-Step Rapid Sulfur Capture

Final Report

Work Performed Under Contract No.: DE-AC21-90MC27200

For
U.S. Department of Energy
Office of Fossil Energy
Morgantown Energy Technology Center
P.O. Box 880
Morgantown, West Virginia 26507-0880

By
Textron Defense Systems
2385 Revere Beach Parkway
Everett, Massachusetts 02149

April 1994

TABLE OF CONTENTS

		Page
List of Illustrations		iv
List of Tables		vii
EXECUTIVE SUMMARY		E-1
1.0	INTRODUCTION	1-1
1.1	BACKGROUND AND PROGRAM OBJECTIVES	1-1
1.2	TWO-STEP RAPID SULFUR CAPTURE CONCEPT	1-4
1.3	PROJECT SCOPE	1-9
2.0	TEST PLAN DEVELOPMENT AND FACILITY DESIGN	2-1
2.1	TEST PLAN DEVELOPMENT	2-1
2.1.1	EXPERIMENTAL VARIABLES	2-1
2.1.2	TEST PLAN	2-4
2.2	OVERALL FACILITY DESIGN REQUIREMENTS	2-4
2.3	TEST FACILITY DESIGN	2-5
2.3.1	ACTIVATION AND MAIN BURNER FLOWS	2-5
2.3.2	ACTIVATION AND MAIN BURNER THERMAL INPUTS	2-8
2.3.3	SULFUR DIOXIDE AND LIMESTONE FLOW RATES	2-10
2.3.4	ACTIVATION BURNER AND SORBENT FEED SYSTEMS	2-10
2.3.5	ACTIVATION DUCT	2-13
2.3.6	MAIN BURNER	2-14
2.3.7	INTERFACE MODULE	2-14
2.3.8	MAIN DUCT	2-19
2.3.9	INSTRUMENTATION	2-19
2.3.10	DATA ACQUISITION AND CONTROL	2-20
3.0	FACILITY SHAKEDOWN AND MODIFICATIONS	3-1
3.1	ACTIVATION BURNER SHAKEDOWN	3-1
3.1.1	PERFORATED COPPER DISK BURNER	3-1
3.1.2	SINTERED BURNER AND SCREW FEEDER SYSTEM	3-2
3.2	SORBENT FEED SYSTEM UNSTEADINESS	3-3
3.3	ACTIVATION BURNER TEMPERATURES	3-4
3.4	FACILITY SHAKEDOWN	3-7
3.5	SULFUR MASS CLOSURE	3-7
3.6	AXIAL TEMPERATURE PROFILE	3-10
3.7	MAIN REACTOR STOICHIOMETRY CHECK	3-10
3.8	LIMESTONE WALL LOSS CHECK	3-10
3.9	SURVEY EXPERIMENTS	3-12

TABLE OF CONTENTS
(CONTINUED)

		Page
4.0	PROGRAM EVOLUTION	4-1
	4.1 PHILOSOPHICAL REFLECTIONS	4-1
	4.2 PROGRAM HISTORY	4-3
	4.2.1 ORIGINAL PROGRAM	4-3
	4.2.2 ACTUAL PROGRAM	4-6
	4.3 FOCUS OF PRESENT REPORT	4-35
5.0	EXPERIMENTS	5-1
	5.1 INTRODUCTION	5-1
	5.2 INFLUENCE OF SORBENT QUENCH PARAMETERS	5-3
	5.3 INFLUENCE OF SORBENT ACTIVATION CONDITIONS	5-12
	5.4 INFLUENCE OF Ca/S RATIO	5-16
	5.5 INFLUENCE OF SULFATION TEMPERATURE	5-17
	5.6 INFLUENCE OF SORBENT SIZE CUT	5-19
	5.7 INFLUENCE OF SORBENT TYPE	5-23
	5.8 SORBENT PROPERTIES AFTER ACTIVATION	5-25
	5.8.1 ACTIVATED SORBENT SIZE DISTRIBUTIONS	5-26
	5.8.2 SURFACE STRUCTURE VIA ELECTRON MICROSCOPY	5-28
	5.8.3 DEGREE OF CALCINATION TRENDS	5-36
	5.8.4 SPECIFIC SURFACE AREA TRENDS	5-40
	5.8.5 POROSITY TRENDS	5-40
	5.8.6 PORE SIZE TRENDS	5-42
	5.8.7 CLOSURE TO SECTION 5.8	5-45
6.0	TWO-STEP RAPID SULFUR CAPTURE MECHANISM MODELING	6-1
	6.1 INTRODUCTION	6-1
	6.2 PHYSICAL MECHANISMS AND CORRESPONDING MODELS	6-1
	6.3 COMPUTER CODE STRUCTURE	6-2
	6.4 SAMPLE PREDICTIONS	6-5
	6.5 MODEL SUMMARY	6-10
7.0	TECHNICAL FEASIBILITY/ECONOMIC EVALUATION SUMMARY	7-1
8.0	CONCLUSIONS	8-1
9.0	REFERENCES	9-1
APPENDIX A	LISTING OF PHASE I (Base) TESTS	A-1
APPENDIX B	LISTING OF PHASE IA TESTS	B-1

TABLE OF CONTENTS
(CONTINUED)

		Page
APPENDIX C	LISTING OF PHASE IB TESTS	C-1
APPENDIX D	COMPUTER CODE INPUT FILE: CASOX.DAT	D-1
APPENDIX E	COMPUTER CODE OUTPUT FILE: CASOX.OUT	E-1
APPENDIX F	COMPUTER CODE OUTPUT FILE: CASOX.PLT	F-1
APPENDIX G	COMPUTER CODE INPUT FILE: CALCINATION CASE	G-1
APPENDIX H	COMPUTER CODE INPUT FILE: SULFATION CASE	H-1
APPENDIX I	INITIAL FEASIBILITY/ECONOMIC EVALUATION	I-1
I.1	INTRODUCTION	I-1
I.2	TWO-STEP SULFUR CAPTURE	I-1
I.3	APPLICATIONS FOR THE TWO-STEP PROCESS	I-1
I.4	ACTIVATION BURNER DESIGN	I-1
I.5	ADVANCED COAL COMBUSTION SYSTEMS CONSIDERED	I-2
I.6	ECONOMIC ANALYSIS METHOD	I-2
I.7	RILEY STOKER'S LIMB REFERENCE SYSTEM	I-2
I.8	EPRI'S REFERENCE SYSTEM	I-4
I.9	RILEY STOKER'S AFBC SYSTEM	I-5

LIST OF ILLUSTRATIONS

Figure		Page
E-1	Two-Step Rapid Sulfur Capture Process	E-2
E-2	Comparison of Actual Versus Original Program Schedules	E-4
E-3	Test Facility Schematic	E-5
E-4	Potential Application Areas for the Two-Step Rapid Sulfur Capture Process	E-6
1-1	Equilibrium Sulfur Capture in Propane/Air Mixtures	1-3
1-2	Batch Reactor Results; 90% Sulfur Capture at Ca/S = 1	1-5
1-3	Single Stage Injection Process	1-7
1-4	Two-Step Rapid Sulfur Capture Process	1-8
2-1	Conditions for Survey Experiments	2-3
2-2	Test Facility Schematic	2-6
2-3	Photograph of Test Facility	2-7
2-4	Flame Temperatures of Stoichiometric Propane/'Air'/Limestone Mixtures	2-9
2-5	Sintered Bronze Burner with Central Sorbent Injection	2-11
2-6	Perforated Copper Disk Burner and Fluidized Bed Feeder	2-12
2-7	Sorbent Quench Zone: Interface Module and Silicon Nitride Sleeve	2-15
2-8	Details of 30^{o} Silicon Nitride Mixing Sleeve	2-17
2-9	Quench Jet Configuration for 30^{o} Silicon Nitride Mixing Sleeve	2-18
3-1	Radiation Corrected Gas Temperatures 10 cm (10 ms) from the Burner	3-5
3-2	Radiation Corrected Gas Temperatures 30 cm (30 ms) from the Burner	3-6
3-3	Activation Burner Axial Temperature Profile - Propane in Carrier Jet	3-8
3-4	Baseline Sulfur Data from Several Tests	3-9

LIST OF ILLUSTRATIONS
(CONTINUED)

Figure		Page
3-5	Main Duct Gas Temperatures	3-11
4-1	Comparison of Actual Versus Original Program Schedule	4-4
4-2	Effect of Probe Cooling Water Temperature on Apparent Sulfur Capture	4-22
4-3	Batch Reactor Experimental Apparatus	4-24
4-4	Batch Reactor Rapid Gas Sampler	4-25
4-5	Effect of System Moisture on Batch Reactor Sulfur Capture	4-28
5-1	Two-Step Calcium Utilization Results	5-5
5-2	Two-Step Calcium Utilization Results	5-6
5-3	Comparison of the Performance of the 15 and 30 Degree Mixing Sections	5-9
5-4	Non-Equilibrium Sulfur Capture Profiles in the 15 Degree Mixing Section for an Activation Temperature of 2600 ^{o}K	5-10
5-5	Non-Equilibrium Sulfur Capture Profiles in the 15 Degree Mixing Section for an Activation Temperature of 2400 ^{o}K	5-11
5-6	Effect of Activation Temperature and Time on Non-Equilibrium Sulfur Capture Performance	5-14
5-7	Activation Temperature Influence on Two-Step Sulfur Capture for the 15 and 30 Degree Mixing Sections	5-15
5-8	Influence of Ca/S on Two-Step Calcium Utilization	5-18
5-9	Influence of Sulfation Temperature on Two-Step Calcium Utilization	5-20
5-10	Influence of Sorbent Size Cut on Two-Step Calcium Utilization	5-21
5-11	Influence of Different Sorbent Types on Two-Step Calcium Utilization	5-24
5-12	Limestone Size Distributions Before and After Activation	5-27
5-13	SEM Photographs of Raw Marblewhite 325 Limestone	5-29

LIST OF ILLUSTRATIONS
(CONTINUED)

Figure		Page
5-14	SEM Photographs of Marblewhite 325 Limestone Activated at 2200 ^{o}K and 10 ms.	5-30
5-15	SEM Photographs of Marblewhite 325 Limestone Activated at 2600 ^{o}K and 10 ms.	5-31
5-16	SEM Photographs of Marblewhite 325 Limestone Activated at 2600 ^{o}K and 30 ms.	5-32
5-17	Two-Step Sulfur Capture Calcination Results	5-37
5-18	Non-Equilibrium Activation Calcination Results	5-39
5-19	Specific Surface Area Results for Non-Equilibrium Mode Activation	5-41
5-20	Porosity Results for Non-Equilibrium Mode Activation	5-43
5-21	Median Pore Size Results for Non-Equilibrium Mode Activation	5-44
6-1	Physical Configuration of Computational Modeling	6-3
6-2	Modeled Particle Temperature History During Calcination	6-6
6-3	Modeled Calcium Carbonate Conversion During Calcination	6-7
6-4	Modeled Particle Temperature During Quenching and Sulfation	6-8
6-5	Modeled Mass Fraction of Calcium Sulfate During Sulfation	6-9

LIST OF TABLES

Table		Page
2-1	Experimental Variables	2-2
4-1	Parameter Ranges for the Phase I (Base) Optimization Testing	4-11
4-2	Parameter Ranges for the Phase IA Activation Optimization Testing	4-16
4-3	Parameter Ranges for the Phase IB Quench Optimization Testing	4-34
5-1	Physical Properties of Activated Limestone Particles	5-33

EXECUTIVE SUMMARY

The primary goal of this program was to test the technical and economic feasibility of a novel dry sorbent injection process called the Two-Step Rapid Sulfur Capture process for several advanced coal utilization systems. The Two-Step Rapid Sulfur Capture process consists of limestone activation in a high temperature auxiliary burner for short times followed by sorbent quenching in a lower temperature sulfur containing coal combustion gas. The Two-Step Rapid Sulfur Capture process is based on the Non-Equilibrium Sulfur Capture process developed by the Energy Technology Office of Textron Defense Systems (ETO/TDS) on a previous program[1] sponsored by the Morgantown Energy Technology Center (METC) of the United States Department of Energy (US DoE).

The principal result from the previous Non-Equilibrium Sulfur Capture experiments was that sulfur captures as high as 90% were achieved at a calcium to sulfur molar ratio of Ca/S = 1 by injecting limestone powder (Marblewhite 325) into high temperature (>2200^{o}K) combustion gases prepared in a batch reactor. The capture peaked at short times (20-60 ms) and decreased at longer times due to sorbent product decomposition. For the Non-Equilibrium Sulfur Capture process, retention of the captured sulfur was recognized as the major engineering challenge. The high calcium utilization produced by the Non-Equilibrium Sulfur Capture process was explained on the basis of the formation of an active sorbent as a result of very high particle heating rates (~10^{5} ^{o}K/s).

The ability of calcium based sorbents to retain sulfur is limited above 1500^{o}K because the sulfated compounds (calcium sulfate, sulfite, and sulfide) all decompose at high temperatures. By quenching the sorbent in a coal combustion gas below 1500^{o}K, the Two-Step process avoids the major limitation of the Non-Equilibrium process. A schematic diagram of the Two-Step Rapid Sulfur Capture process is shown in Figure E-1. Based on the Non-Equilibrium Sulfur Capture studies[1] the range of conditions for optimum sorbent activation were thought to be: activation temperature > 2200^{o}K for activation times in the range of 10-30 ms. Therefore, the aim of the Two-Step process is to create a very active sorbent (under conditions similar to the bomb reactor) and complete the sulfur reaction under thermodynamically favorable conditions.

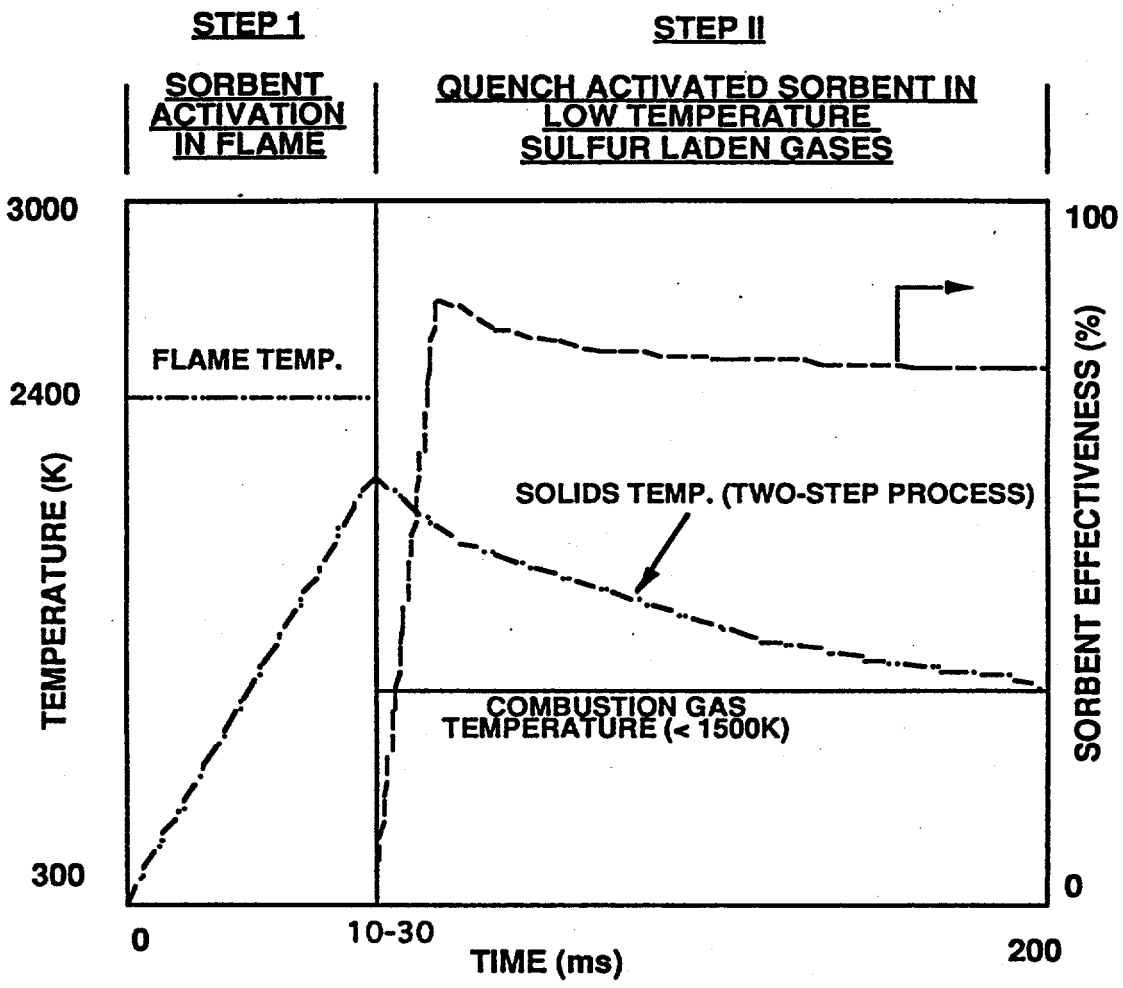

Figure E-1. Two-Step Rapid Sulfur Capture Process.

Figure E-2 gives a comparison of the actual program schedule and the original plan. The original program was a three phase 33 month program. The goals of the Phase I were to confirm the technical and economic feasibility of the two-step sulfur capture process. The subsequent phases (II and III) were structured to demonstrate optimized performance in a proof of concept advanced coal utilization facility.

Referring to Figure E-2, the actual Phase I effort consisted of five elements, namely: the base program {Phase I (Base)}; two extensions {Phases IA and IB}; and two relevant, yet not required, studies funded by TDS (which will not be discussed here but are discussed in Section 4.2.2). Most of the work planned for the original Phase I effort was carried out during Phase I (Base) in the actual program. This effort was conducted over a 15 month period. Phase I (Base) contained the following technical tasks, namely:

Task 1 Test Plan and Test Facility Design and Fabrication.
Task 2 Experimental Testing.
Task 3 Two-Step Rapid Sulfur Capture Mechanism.
Task 4 Technical/Economics Feasibility Study.

A flow facility was designed and assembled to simulate the temperature, time, stoichiometry, and sulfur gas concentration prevalent in the advanced coal utilization systems such as gasifiers, fluidized bed combustors, mixed-metal oxide desulfurization systems, diesel engines, and gas turbines. A schematic of the test facility is shown in Figure E-3. The facility consists of four functional zones for: sorbent activation, low temperature sulfur gas preparation, sorbent quenching, and sulfur capture. The activation burner and activation duct are located at the top of the central duct. The low temperature sulfur gas is prepared in the two side burners. Sorbent quenching occurs inside the cross-shaped module called the interface module. Sulfur capture is measured below the mixing zone via gas and solid sampling systems.

The objective of the original test plan was to check the feasibility of the two-step technique for sulfur capture under conditions present in advanced coal utilization systems. Figure E-4 presents a temperature/stoichiometry map for the applications considered (phi (ϕ) > 1 represents fuel-rich conditions). To meet the program objectives, the test plan was divided into

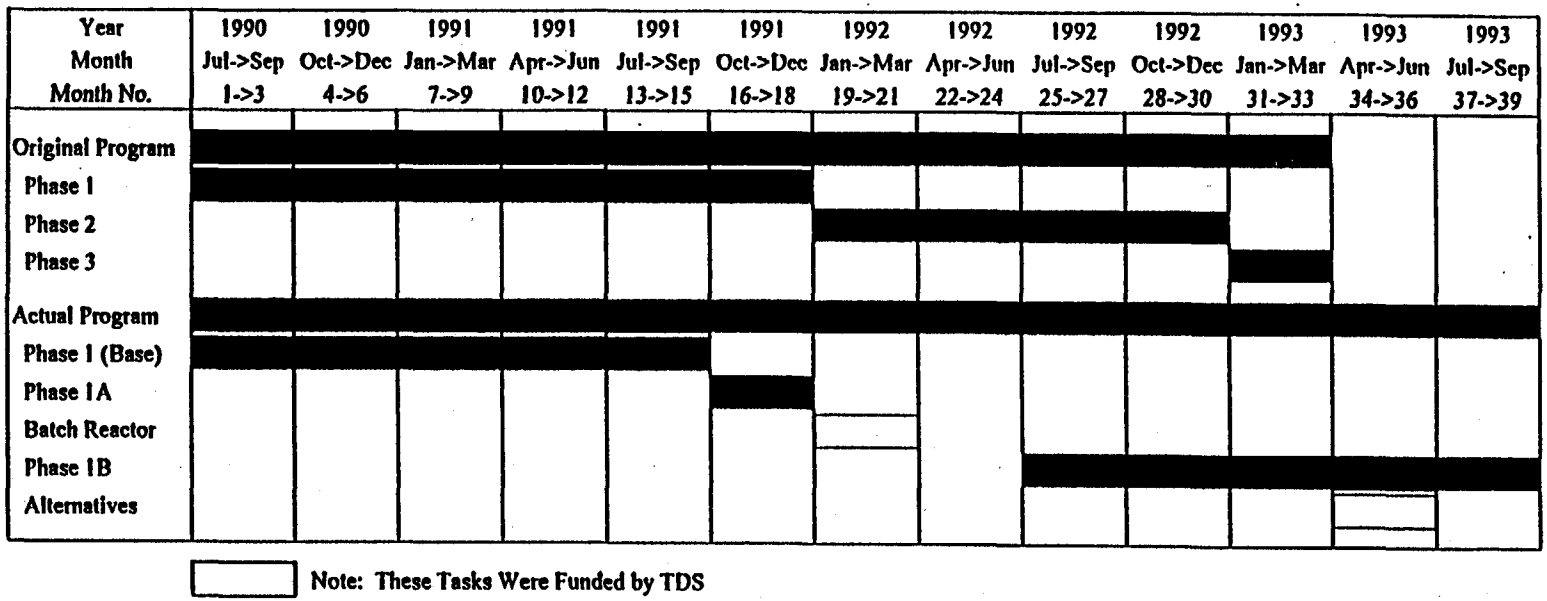

Figure E-2. Comparison of Actual Versus Original Program Schedules.

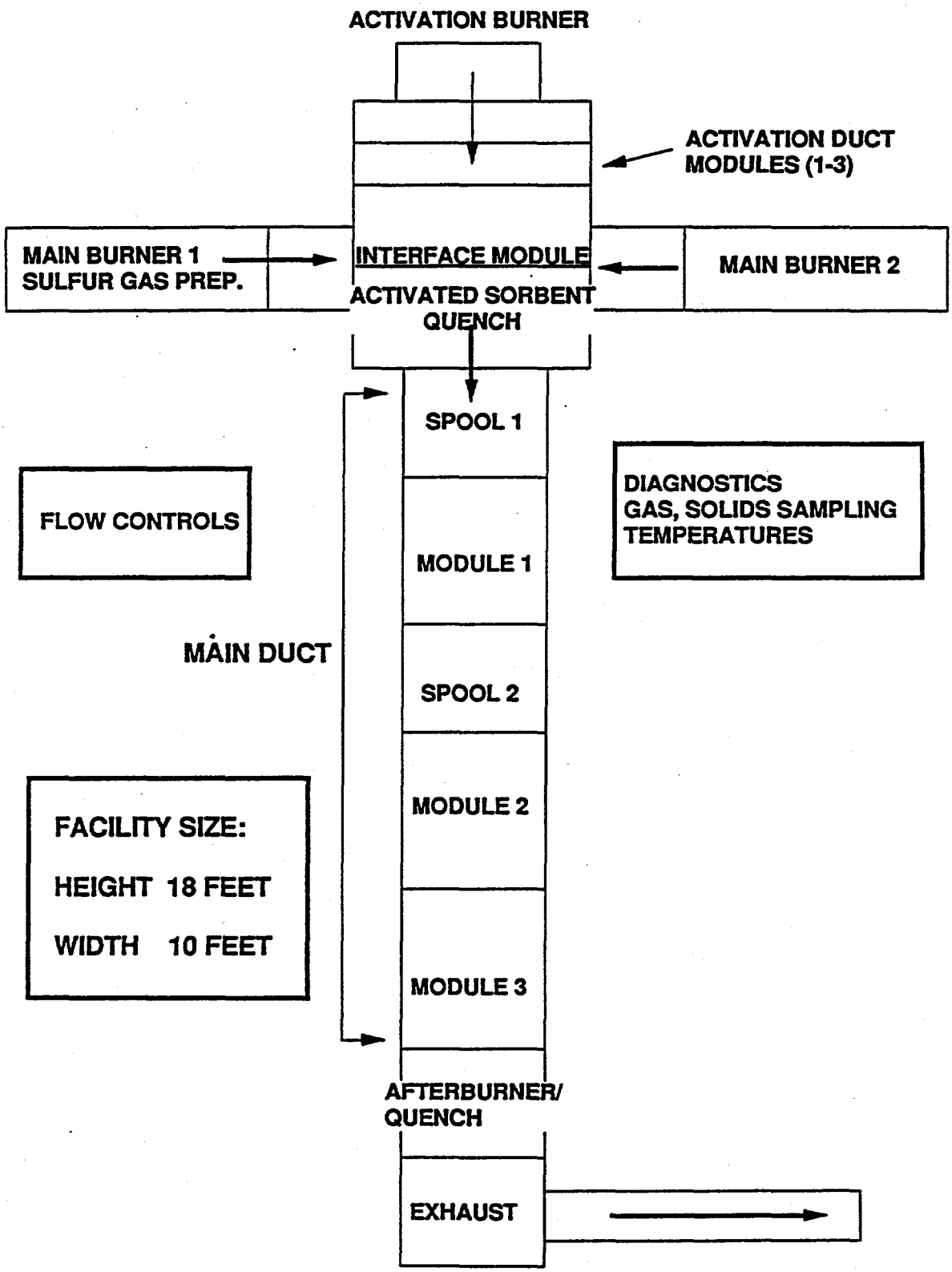

Figure E-3. Test Facility Schematic.

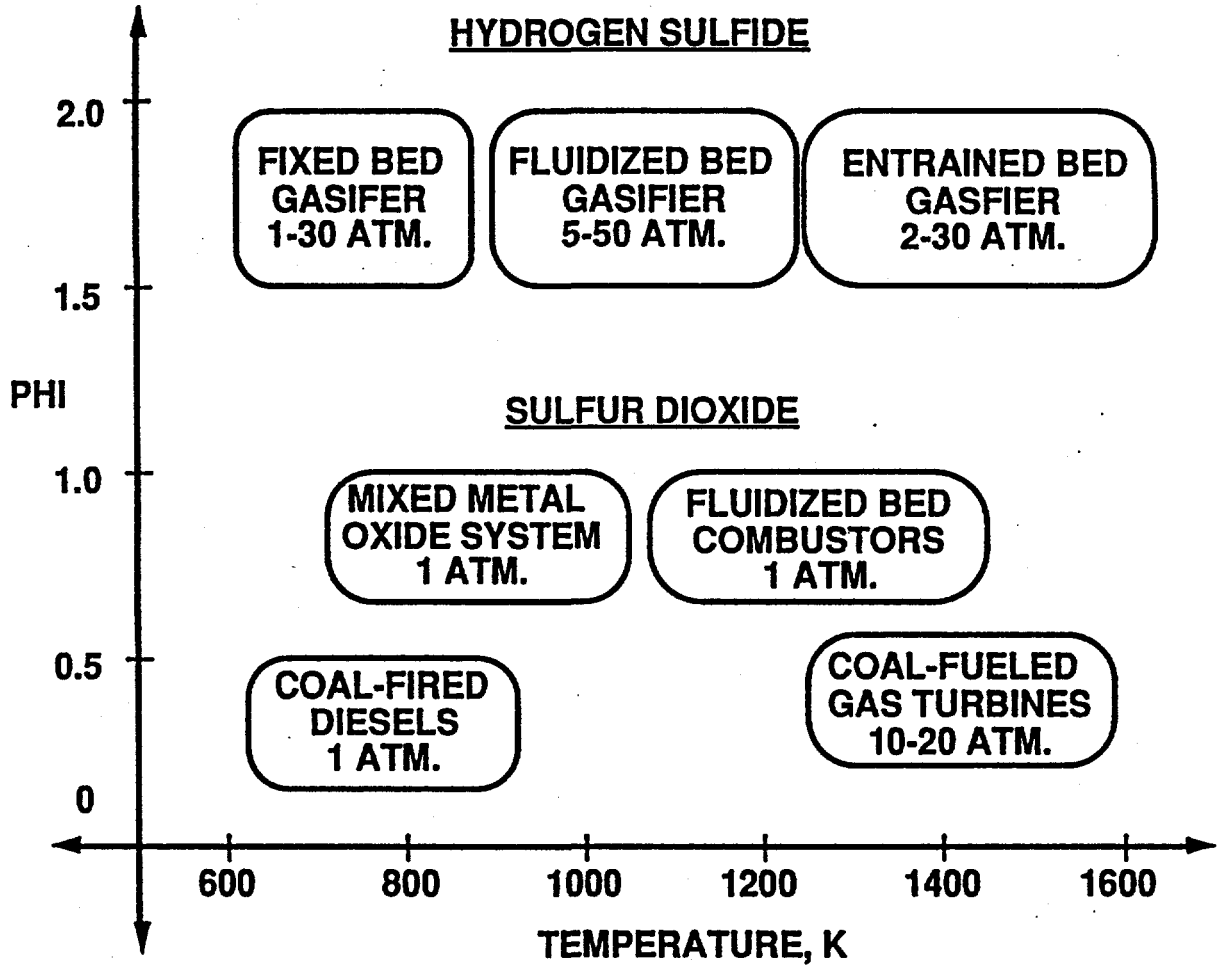

Figure E-4. Potential Application Areas for the Two-Step Rapid Sulfur Capture Process.

two phases: survey experiments and detailed scan of activation conditions for each application of interest.

The objective of the survey experiments was to identify the desulfurization temperature and stoichiometry conditions which had the greatest potential for yielding high captures. This was achieved by conducting experiments at fixed activation conditions, while scanning the desulfurization stoichiometry and temperature range shown in Figure E-4. Marblewhite 325, the limestone powder used in the earlier Non-Equilibrium experiments, was used as the sorbent. The activation conditions were: 2600°K for 20 ms. The survey experiments showed low utilization at desulfurization temperature < 1000°K under all stoichiometries, and best utilizations for temperature in the 1300-1450°K under fuel-lean conditions.

Consequently, the first detailed scan of activation conditions was conducted under fluidized bed desulfurization conditions. At fixed activation temperatures of 2400°K and 2600°K, the capture improved as the activation time was decreased from 30 ms to 20 ms to 10 ms. Reducing the time further to 5 ms did not result in any improvement over the capture at 10 ms. Under identical desulfurization conditions the sulfur capture at 2600°K was greater than at 2400°K. Thus, in later experiments the activation conditions were fixed at 2600°K and 10 ms.

Although the results of the Phase I (Base) Program were later found to be in error, they made it possible to identify an experimental anomaly, one that later led to the discovery of a systematic experimental error, namely: in-probe sulfur capture, caused by wet scrubbing, was giving erroneous gas phase sulfur capture results. This anomaly led to Phase I (Base) sulfur captures based on gas phase analysis (i.e., by on-line gas analyzer) that were a factor of three to four greater than those determined by chemical analysis of collected spent sorbent. This insidious error, once identified, invalidated most of the early work of this program.

A fair question to ask is: why was this effect not discovered earlier? The reason is that in-probe scrubbing only occurs when limestone is flowing. For example, good SO_2 baseline data (no sorbent flowing) was obtained with cold probes both before injecting sorbent and after terminating sorbent flow. In fact, with the cold probes, SO_2 levels rose quickly after terminating sorbent injection. This implies that the SO_2 capture was due to formation of a water mist (two-

phase phenomenon) in the gas sampling probes, rather than condensation on the internal surfaces of gas sampling probe. Until the in-probe scrubbing tests, these facts misled TDS into believing the cold probe utilization results. The low utilizations based on spent sorbent chemical analyses from earlier tests was a concern, but was not taken as the most reliable measure because of problems with the solids sampling system.

The main objectives of the Phase IA effort were to perform Non-Equilibrium and sorbent activation studies to obtain a better understanding of the activation process and, at the same time, to optimize the activation process and resolve the discrepancy between utilizations derived via gas phase and spent sorbent analyses. During this phase it was clearly shown that very significant in-probe wet scrubbing was occurring; which yielded higher gas analysis based sulfur capture results. After resolving this, Phase IA was concluded by performing a limited series of optimization tests to investigate the actual performance of Two-Step Rapid Sulfur Capture and Non-Equilibrium Sulfur Capture processes, with some activation tests to characterize activated sorbent properties. The results of these tests were not at all encouraging. The best Two-Step Sulfur Capture utilizations were no better than 12%. The best Non-Equilibrium Sulfur Capture utilizations were no better than 10%. The best Non-Equilibrium Sulfur Capture occurred at an activation temperature of 2600 ^{o}K with an activation time of 10 ms and a Ca/S of nominally 1.

The sorbent activation studies revealed the following: SEM photographs of collected activated limestone sorbent indicated that there are more fine particles relative to raw limestone. However, size distribution measurements, by both laser diffraction sizing and mercury porosimetry, indicate that there is little change in size distribution. The difference in these two measurements can be reconciled if it is realized that the fines constitute only a small fraction of the total mass of the sorbent.

At this point in the program (i.e., the conclusion of Phase IA), two lines of thinking dominated. First, there may be an inherent limitation in the Two-Step Rapid Sulfur Capture activation process. If the polydispersed nature of raw limestone is considered, it is conceivable that different combinations of activation temperature and time serve only to activate a specific size cut in the size distribution of the raw limestone. Sizes above this cut are not well activated (low porosity and specific surface area due to low heating rates) and sizes below this cut become

sintered because of very high heating rates. Second, if this inherent limitation does not exist, then the low utilizations, specific surface areas, and porosities are due to quench/mixing section characteristics that yield activated sorbent quenching times that are too long, which causes sintering or non-optimum activation. In an attempt to reconcile these differing lines of thinking, a Phase IB plan was developed which would investigate the influence of reduced mixing times on Two-Step Rapid Sulfur Capture performance.

Since in-probe scrubbing was found to have a drastic effect on gas phase based utilizations measured during the Two-Step Rapid Sulfur Capture program, and since even higher utilizations were measured during the Batch Reactor program[1], the natural question to ask is: was in-situ wet scrubbing occurring in the batch reactor, thereby producing high utilizations? In order to verify or refute earlier batch reactor results, a brief TDS funded batch reactor study was performed prior to starting Phase IB. Although the results of this TDS study are presented in detail in Section 4.2.2.4, let it be said here that there exists some evidence suggesting that wet scrubbing effects may have interfered with true measurements of sulfur capture in the current and previous batch reactor investigations. Based on these considerations, the previous[1] batch reactor data should be considered questionable.

The overall objective of the Phase IB extension was directed towards improving activated sorbent quenching for the purpose of increasing Two-Step Rapid Sulfur Capture calcium utilization. Tests conducted during Phase IA using the two-step sulfur capture facility yielded calcium utilizations that were less than 15%. Analysis of activated limestone samples revealed low porosities (< 10%) and relatively low specific surface areas (< 15 m^2/gm), while chemical analysis revealed up to 90% degree of calcination. Since the theoretical porosity at 90% degree of calcination is almost 45%, it appears that calcine sintering may be responsible for the low calcium utilizations observed. Particle sintering should be avoidable through more rapid quenching of the two-phase sorbent jet exiting the activation burner by lower temperature sulfur containing gases. This, in turn, would produce a sorbent of increased surface area, thus increased activity.

Calcination times for limestone particles should vary from a few milliseconds (for fine particles) to tens of milliseconds for large particles (~ 30 μm) under high temperature activation

conditions. Therefore, very fast quenching is needed, with mixing times less than 5 - 10 ms, to prevent significant sintering. The mixing of three gas streams (activation burner stream and two streams from the side duct burners) occurs in the silicon nitride quench/mixing section. This section was designed to achieve rapid quenching of the activated sorbent with minimal sorbent loss to walls. It is possible that the original 60^{o} mixing section was designed too conservatively regarding wall losses and that it may be producing mixing times that are too long. Based on SO_2 mixing studies performed during Phase IA, the quenching time for the 60^{o} mixing section has been estimated to be 50 ms. This rather long mixing time could certainly account for the low specific surface areas and porosities observed in Phase IA.

The primary objective during Phase IB was to determine optimum quench conditions for the activation/sulfation conditions that gave the highest SO_2 captures during Phase IA. Investigating optimum quench conditions involved redesigning the silicon nitride quench/mixing section. Three new silicon nitride quench/mixing sections were designed and fabricated. The number of quench jets in the quench/mixing section and their diameter, injection angle, and pattern were redefined based on a TDS computer code. The ultimate goal was to effect more rapid quenching of the two-phase sorbent jet exiting the activation burner. Mixing effectiveness, or aggressiveness, was found to be a strong function of quench jet injection angle. It was found that sorbent segregation to walls and mixing section recirculation were a function of injection angle also. The reason for fabricating three new quench/mixing sections, therefore, was to allow quench study flexibility recognizing that mixing aggressiveness and sorbent wall deposition are coupled processes.

To support exploratory efforts, cut sizes of Marblewhite 325 limestone were tested under Two-Step Sulfur Capture mode operation, as well as using 200 mesh Linwood hydrated lime as the sorbent. Sulfur capture performance using different size cuts of limestone was investigated to obtain information that might reveal inherent limitations of the Two-Step Rapid Sulfur Capture activation process. As noted earlier, the activation process may have limitations due to the polydispersed characteristics of the raw sorbent. That is, for a given set of activation conditions, it is possible that only a narrow band of sizes are being activated. Sizes below this range are probably being sintered, whereas sizes above this range are not experiencing heating rates that produce high surface area, high porosity, thus highly activated sorbent particles. Examining the

sulfur capture characteristics of specific cuts of the raw sorbent provides an indication if this limitation is present. Higher activation temperatures were investigated also during Phase IB to check if higher heating rates produce higher captures.

Phase IB revealed that the Two-Step Rapid Sulfur Capture process has inherent limitations which lead to calcium utilizations that are not sufficient to make this process economically viable. The best Two-Step Rapid Sulfur Capture calcium utilization measured during this program was nominally 10%. This level was achieved at activation temperatures in the range 2200 - 2600°K (utilization did not appear to be strongly dependent on activation temperature in this range), an activation time of 10 ms, a slightly fuel lean stoichiometry ($0.8 \leq \phi_s \leq 0.9$), a sulfation temperature of nominally 1100°C, and using the 15° mixing section. This level of calcium utilization makes the economics of the Two-Step Rapid Sulfur Capture process very unattractive.

The calcium utilizations appeared to be unaffected by quench jet injection angle or by activation temperature. The following comments can be made based on the observed influence of quench parameters on the Two-Step Rapid Sulfur Capture process. First, reduced mixing times were achieved by the 15° mixing sleeve relative to the 60° unit. The mixing time reduction was nominally 40%. It is expected that the 0° sleeve probably gives even smaller mixing times and that the 30° unit gives somewhat longer times. Regardless, it was found that the 0, 15, and 30° mixing sleeves did not produce significant improvements in Two-Step Rapid Sulfur Capture calcium utilizations. The best utilization measured was 9% using the 15° mixing sleeve with an activation temperature in the range 2200 - 2600°K, an activation time of 10 ms, a sulfation temperature of 1100°C, and Ca/S = 1.

After studying the morphology of the limestone particles before and after activation, it was seen that the following morphological characteristics are hindering the Two-Step process from achieving competitive sulfur capture performance: 1) the Two-Step process is hindered by its inability to produce a high surface area calcia sorbent; 2) the Two-Step process fails to produce a highly porous calcia sorbent; 3) the Two-Step process produces activated limestone sorbent that has a mean pore diameter that is less than the raw limestone. Thus, the Two-Step process fails to produce activated calcia that has modest pore sizes. If the Two-Step process was successful it would have produced a sorbent with high surface area, high porosity, and large pore size.

1.0 INTRODUCTION

1.1 BACKGROUND AND PROGRAM OBJECTIVES

Environmentally benign coal utilization has the potential to reduce U.S. dependence on imported oil. Coal utilization by its very nature generates significant quantities of sulfur dioxide, nitrogen oxide, and particulate emissions which must be controlled tightly. While significant nitrogen oxide and particulate emission are released during oil and natural gas consumption, the release of sulfur dioxide is primarily associated with coal consumption. For example, nearly 80% of the world wide sulfur dioxide (SO_2) emission is due to coal burning. The two-step rapid sulfur capture program aims to develop a novel dry sorbent injection technique and demonstrate its economic feasibility for a wide variety of advanced coal utilization systems.

Sulfur dioxide and to some extent nitrogen oxide emissions cause acid rain. Acid rain is known to cause widespread damage to forests, and aquatic life. Also, many historic structures are also being eroded by the acidic rainfall resulting from sulfur dioxide emission from coal fired power plants.

Sulfur emission can be controlled by some combination of the following approaches.

(1) Sulfur removal by physical and/or chemical cleaning before coal utilization (combustion, gasification, liquefaction, etc)

(2) Injection of sorbents during processing.

(3) Post processing treatment of gas (flue gas desulfurization).

The first approach includes unit operations, such as froth floatation, magnetic desulfurization, etc., that are standard in most coal preparation plants. However, standard beneficiation procedures are not sufficient to meet the Federal emission limit of 1.2 lb/MMBtu, and the use of deep cleaning methods required to meet this limit would constitute a significant increase in the capital and operating costs of the overall plant.

At present flue gas desulfurization (FGD) is the technique of choice for removing sulfur from coal flue gases. FGD while it removes greater than 95% of sulfur requires huge capital investment, has significant operating costs, and generates large volumes of slurry waste. The last option, injection of sorbents during processing, is most attractive because it requires a lower capital investment, is retrofittable, and produces less solid waste than FGD. However, a high calcium utilization is the key to the success of any dry sorbent injection process.

Although a number of alkaline and alkaline-earth based compounds have been tested as sorbents, limestone (primarily calcium carbonate) because of its wide availability, low cost, and effectiveness as a sulfur getter is the sorbent of choice. Figure 1-1 shows the predicted thermodynamic equilibrium sulfur capture as a function of temperature at various stoichiometries (phi). As can be seen, the ability of limestone to capture sulfur is limited to temperatures below $1500^{o}K$ because the reaction products (calcium sulfate, sulfite, and sulfide) decompose at higher temperatures. Since coal combustors and entrained flow gasifiers operate at temperatures higher than $1500^{o}K$, equilibrium sulfur capture in these systems is not possible.

The various curves in Figure 1-1 can be divided into two categories: fuel-lean (phi < 1) and fuel-rich (phi > 1). Under fuel-lean conditions, sulfur dioxide is the primary sulfur gas and is captured as calcium sulfate. On the other hand, under fuel-rich conditions, hydrogen sulfide is the primary sulfur gas and is captured as calcium sulfide.

The equilibrium sulfur capture curves under fuel-lean and fuel-rich conditions are very different in shape. For fuel-lean conditions up to 100% capture is predicted at low temperatures. The capture decreases at higher temperatures. Under stoichiometric (phi=1) conditions, the capture is zero above $1400^{o}K$. The presence of some free oxygen significantly shifts the equilibrium curve to higher temperatures. Therefore, excess oxygen serves to stabilize the sorbent product. In the absence of oxygen, calcium sulfite is formed which is less stable than calcium sulfate. For fuel-rich conditions, the equilibrium capture is zero at low and high temperatures because the formation of hydrogen sulfide is favored over calcium sulfide. Equilibrium sulfur capture is predicted in an intermediate temperature range ($800\text{-}1600^{o}K$).

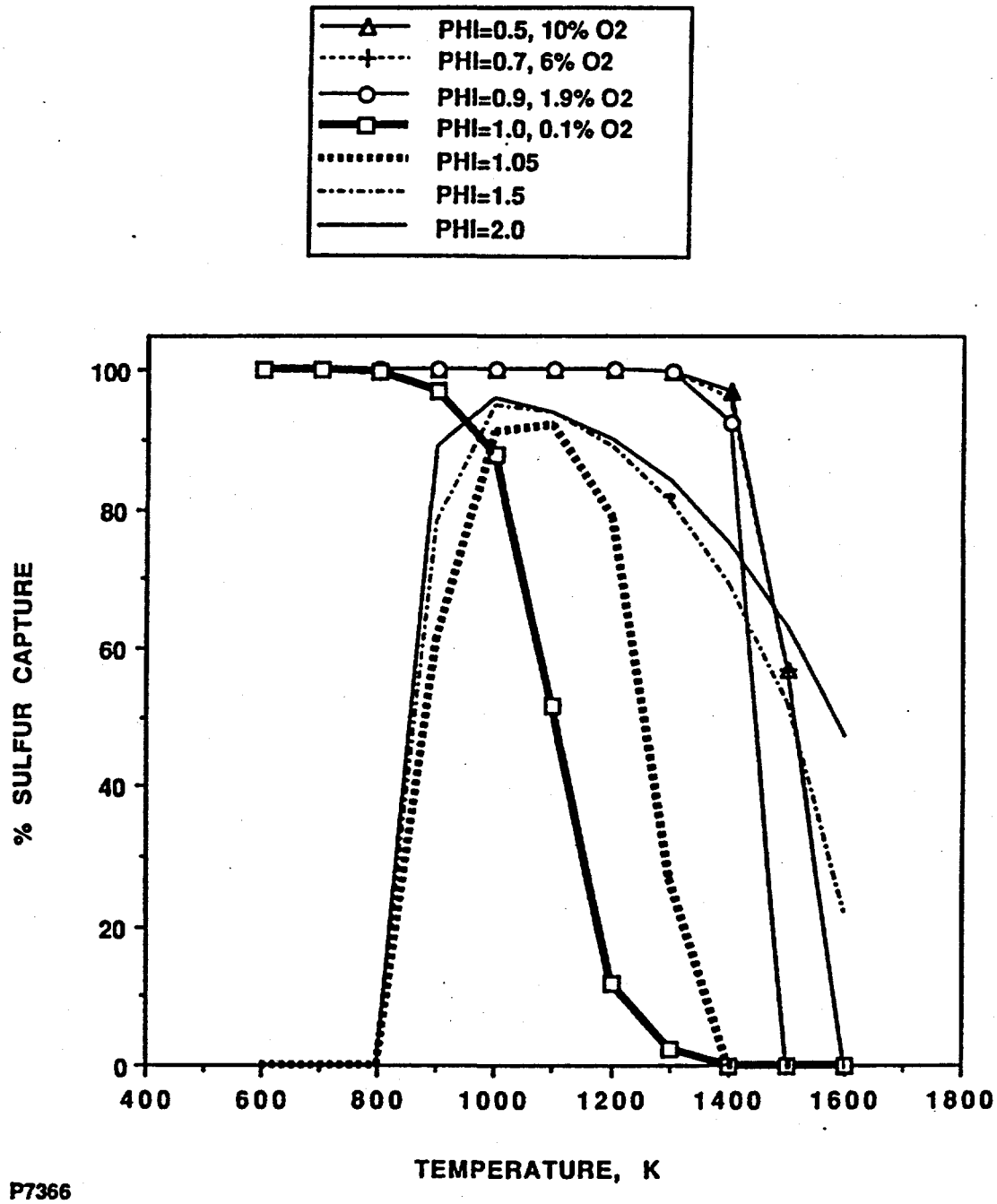

Figure 1-1. Equilibrium Sulfur Capture in Propane/Air Mixtures.

1.2 TWO-STEP RAPID SULFUR CAPTURE CONCEPT

Duct or single-stage injection is a sulfur capture process based on dry sorbent injection. In duct injection, the sorbent, typically limestone or hydrated lime, is injected into the coal combustion gas at temperatures below 1500^{o}K. To date, approximately 50-60% sulfur removal has been achieved using hydrate injection at a calcium to sulfur molar ratio of 2 (Ca/S=2) and a reaction time of several seconds. With limestone a Ca/S=4-5 is needed to achieve comparable capture. Therefore, the calcium utilization is generally below 20% for limestone, and significant solid waste is generated.

The proposed two-step sulfur capture process involves limestone activation in a high temperature auxiliary burner for short time followed by sorbent quenching in a low temperature sulfur laden coal combustion gas. The two-step sulfur capture technique is an extension of the non-equilibrium sulfur capture process investigated by TDS in high temperature combustion gases on a previous METC program[1].

The previous METC program investigated the potential of calcium based sorbents for removal of sulfur from high temperature combustion/gasification gases under non-equilibrium conditions. These experiments were conducted in a batch reactor. A typical sulfur capture versus time plot is shown in Figure 1-2. The most significant result of this program was that very high sulfur capture efficiencies, approaching 90% calcium utilization, were observed under transient conditions. However, at long times (approximately 100 ms and over), as the solids equilibrated with the hot gas, the sulfur capture reduced to low values. For practical situations retaining the high capture constitutes an engineering challenge. Higher injection temperatures were found to result in higher captures.

The high transient sulfur captures are believed to be due to the formation of an active sorbent. Limestone (of standard grind, 90% through 270 mesh) upon injection into the 2200-2600^{o}K gas is subjected to high heating rates (approximately 10^{5} ^{o}K/s). The endothermic calcination reaction constrains the particle temperature (and prevents sintering) while the carbon dioxide released results in a very porous particle. Particle shattering is also a possibility given the high dissociation pressures within the particles. Therefore, the high surface area temperature

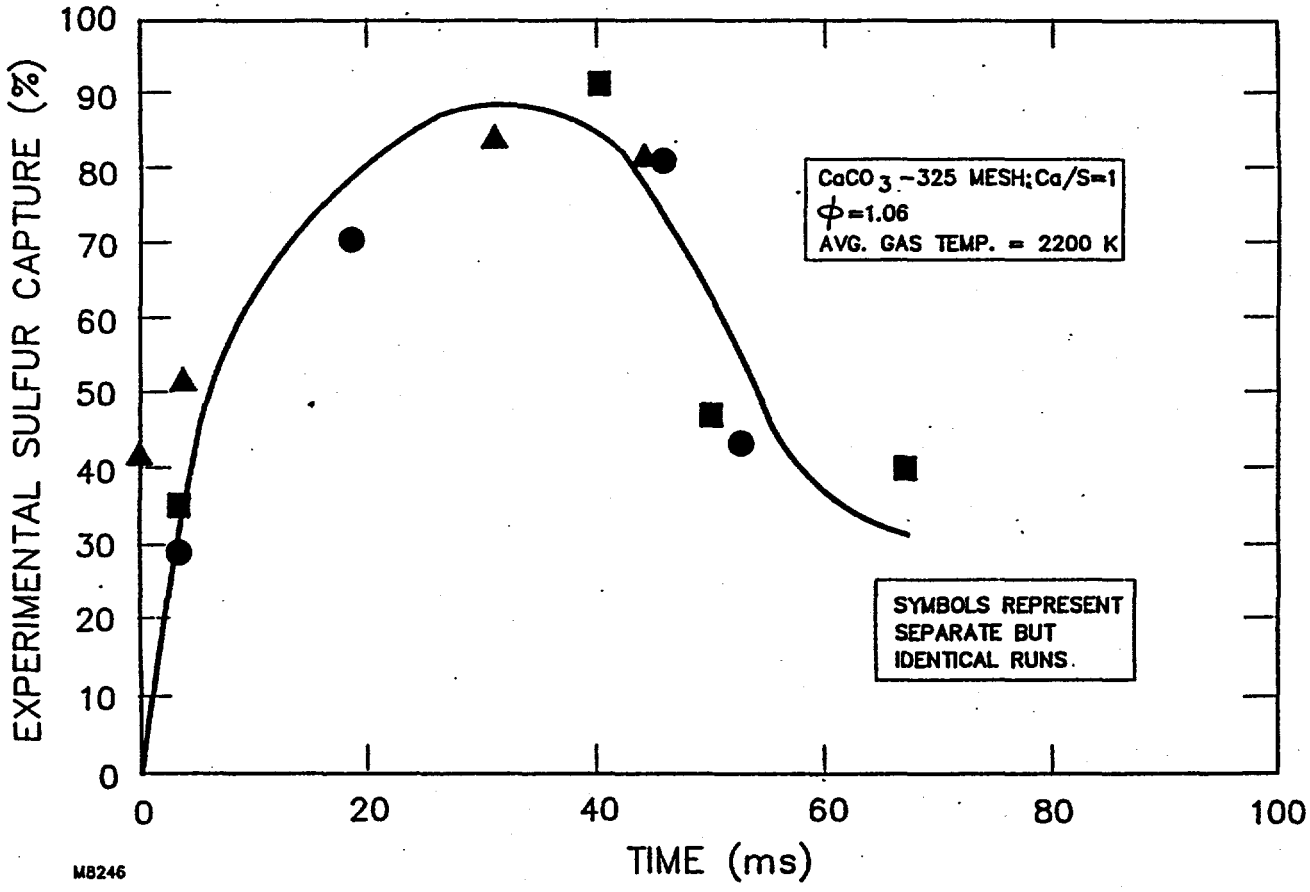

Figure 1-2. Batch Reactor Results; 90% Sulfur Capture at Ca/S = 1.

constrained sorbent is believed to be responsible for promoting very rapid sulfur capture and gaseous sulfur compound re-evolution observed in the non-equilibrium experiments.

These results suggest that a high surface area sorbent can be produced if calcium carbonate is passed through a flame front for a short time. The active sorbent should be quenched quickly otherwise sintering occurs. The quenching is best done in a low temperature sulfur containing gas; in a temperature window where thermodynamic capture is favored. In addition to providing high surface area sorbent, this technique has the advantage that the particles come in contact with the gas while they are still hot, thereby further enhancing the rate of sulfur capture.

The two-step rapid sulfur capture technique then takes advantage of the formation of the active sorbent which is expected to greatly improve the sulfur captures and sorbent utilization over standard duct injection. Calcium utilizations up to 90% at a Ca/S molar ratio of 1 were anticipated based on previous TDS results.

A comparison of the two-step process with conventional duct injection is shown in Figures 1-3 and 1-4. In a typical duct injection process (see Figure 1-3) the sorbent temperature rises slowly to the gas temperature and, therefore, the calcination and initial sulfur capture reactions occur at a temperature much lower than the gas temperature. Sorbent is injected into a gas below 1500^{o}K because of the thermodynamic constraints mentioned earlier. However, in the two-step technique, the rate controlling chemical kinetics and diffusion processes are likely to occur at a higher rate because of the formation of an active sorbent. The sulfation reactions are exothermic and tend to drive the particle temperature towards and maybe beyond the optimum value for thermodynamic sulfur capture. However, the quenching in the cold sulfur laden gases should serve to remove the heat of sulfation and stabilize the spent sorbent particles.

In duct injection, the calcination and desulfurization reactions occur simultaneously. However, in the two-step process calcination is replaced by activation in a high temperature gas (2200-2600^{o}K) for short times (15-75 ms), and sulfur capture occurs on quenching the sorbent in low temperature (< 1500^{o}K) sulfur laden coal combustion gas. Greater control, thus optimization, is possible over the two processes of sorbent preparation from desulfurization, and it should be possible to optimize the overall sulfur removal process for different applications.

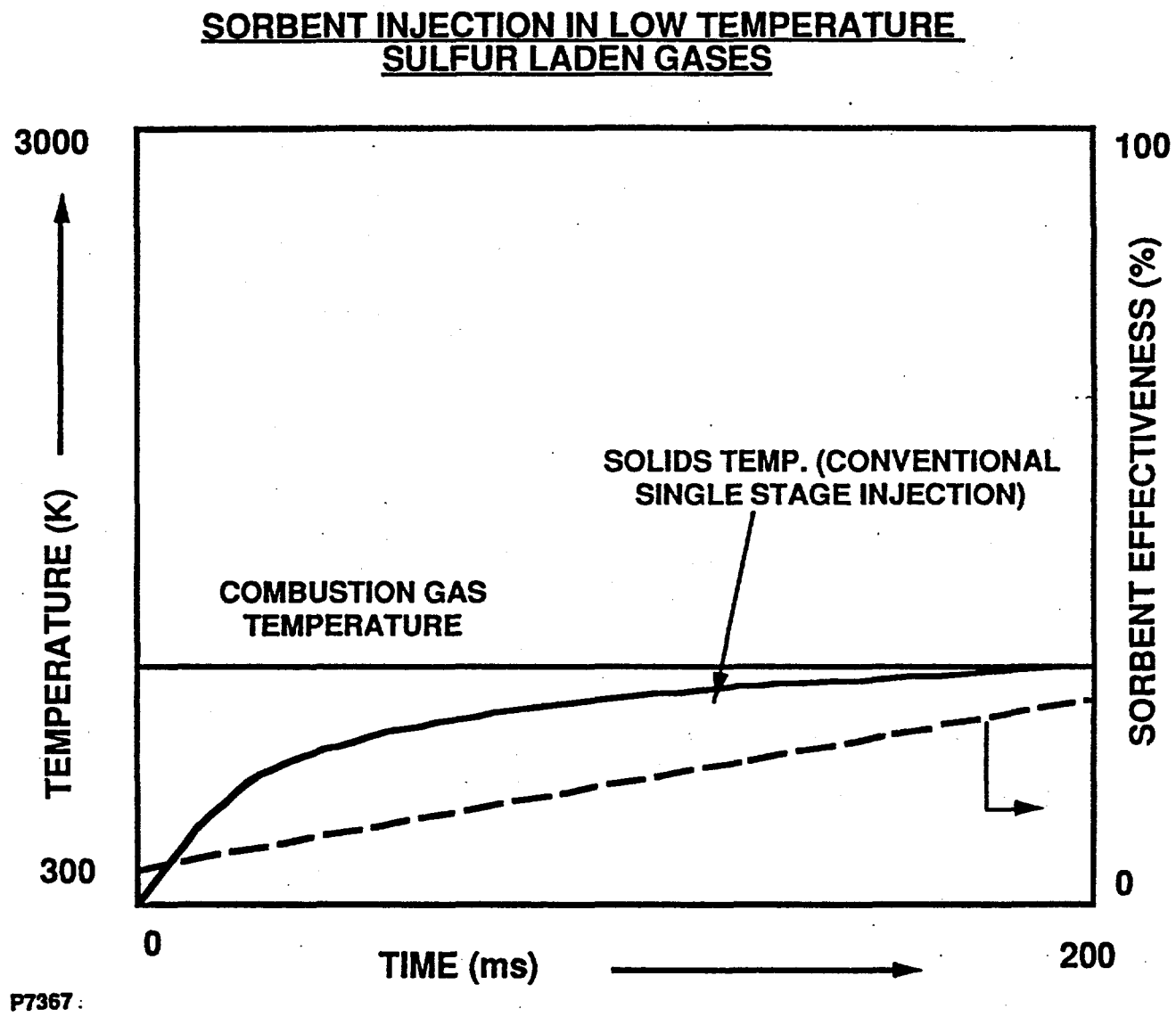

Figure 1-3. Single Stage Injection Process.

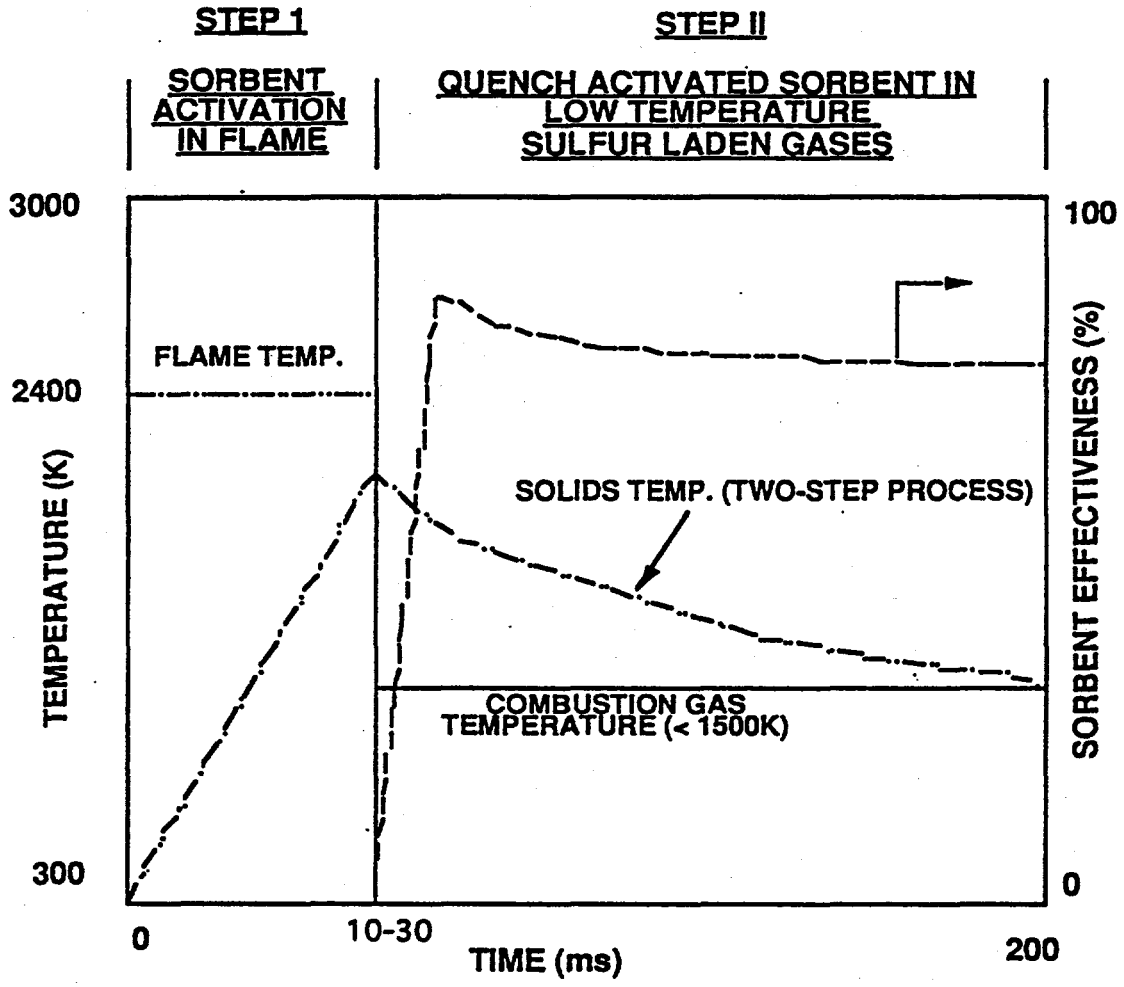

Figure 1-4. Two-Step Rapid Sulfur Capture Process.

The increased control over activation and desulfurization also implies much wider applicability for the two-step process than duct injection. The duct injection process is limited to a narrow range of injection temperatures. For example, duct injection would be very inefficient in a coal diesel exhaust (temperature < 800°K) because of inadequate calcination. In contrast, this application is well suited to the two-step process because higher sorbent quenching rates, which stabilize the product, will be attained.

1.3 PROJECT SCOPE

The objectives of this program are to evaluate the two-step rapid sulfur capture process over a wide range of process conditions (700-1500°K and for both oxidizing and reducing atmospheres), determine viable applications to advanced coal utilization systems, confirm feasibility in a proof-of-concept facility, and conduct a comparative economic evaluation with existing sulfur removal technologies. The goal is to develop this sulfur removal concept to the point where industry is willing to support its further development.

The project is divided into three phases. This document reports the progress made in Phase I. In Phase I, small-scale flow experiments were conducted over a wide range of operating conditions in order to gain a better understanding of the intricacies of limestone heat-up, calcination, and sulfur capture reactions. This information was used to determine the areas of application for the two-step sulfur removal process. Areas considered included direct coal-fueled turbines, coal-fueled diesels, fluid bed combustion/ gasification systems, fixed and entrained bed gasification systems, and the off-gases from a mixed metal oxide sulfur removal system. Phase II which is optional consists of optimizing the two-step technique at a proof-of-concept size advanced coal utilization system. Only short duration testing are to be conducted during Phase II. Phase III, which is also optional, consists of long duration testing and an economic feasibility study.

The scope of the Phase I work was broken into five tasks:

(1) Test Plan Development

(2) Test Facility Design, Fabrication, and Assembly

(3) Experimental Testing

(4) Two-Step Rapid Sulfur Capture Mechanism Determination

(5) Feasibility/Applicability Study

The progress made on each of these tasks is reported in the following chapters. The next chapter, Section 2.0, presents the work accomplished during test plan development, and test facility design, fabrication, and assembly. In Section 3.0, shakedown and baseline tests, facility modifications, and results of survey experiments are reported. Since the present program evolved in way not anticipated, Section 4.0 presents a history of this program. Section 5.0 presents the relevant experimental test results produced over the duration of this program. Section 6.0 gives a description of the progress made during this program towards producing a computer model of sulfur capture processes. Section 7.0 presents TDS' findings regarding the economic feasibility of the Two-Step Rapid Sulfur Capture process. Section 8.0 presents conclusions that can be drawn from the work performed during this program.

2.0 TEST PLAN DEVELOPMENT AND FACILITY DESIGN

This section describes test plan development, and test facility design. The primary objective of this project was to determine the applicability of the two-step sulfur capture process to advanced coal utilization systems such as fluidized bed combustor/gasifier, gas turbine, diesel, fixed and entrained bed gasifiers, and off gases from a mixed metal oxide sulfur removal system. In order to best achieve this objective, a test plan was first developed. The test plan considered all the experimental variables and their range, and contained a preliminary test matrix and a run sequence. Next, an experimental facility which could achieve the desired range of test variables was designed, fabricated, and assembled.

2.1 TEST PLAN DEVELOPMENT

The objective of the test plan was to allow a separate evaluation of limestone activation and subsequent sulfur capture by the activated sorbent. Parameters of investigation concerning the activation of limestone were: 1) both dry sorbent injection and sorbent injection as a liquid fuel/sorbent slurry, 2) temperature/heat flux of activation, 3) three different sorbents, 4) activated sorbent residence time before exposure to the sulfur containing gas stream, and 5) surface area of the sorbent as a function of time. Additional parameters to consider during the reaction of the activated sorbent and the sulfur containing gas were : 1) oxidizing and reducing gas streams, 2) temperature of the gas stream, and 3) residence time.

2.1.1 EXPERIMENTAL VARIABLES

The major experimental variables and their ranges are summarized in Table 2-1. The range of the activation conditions was obtained from previous batch reactor experiments conducted by Textron Defense Systems (TDS). The range of desulfurization conditions was obtained from a review of conditions for the potential applications of interest. The operating conditions for these application areas are shown on a stoichiometry versus desulfurization temperature map in Figure 2-1.

TABLE 2-1

EXPERIMENTAL VARIABLES

	VARIABLE RANGE	
Sorbent Treatment:		
Activation Temperature (^{o}K)	2600	2200
Activation Time (ms)	30	10
Activation Flame Stoichiometry	1 (could be varied, if necessary)	
Sulfur Capture:		
Desulfurization Temperature (^{o}K)	1500	700
Ca/S Molar Ratio	3 (few tests)	1 (most tests)
Main Flame Stoichiometry	1.5	0.5
Desulfurization Time (ms)	200 (could be extended if needed)	
Pressure (atm)	1	
Other Important Variables:		
Activation Burner Flame	Gas and Oil	
Sorbent Type	Marblewhite limestone (90% through 325 mesh and 200-270 mesh) and METC designated two other sorbents: Vicron 45-3 limestone and Linwood hydrated lime.	
Sulfur Gas Levels	300-3000 ppm	

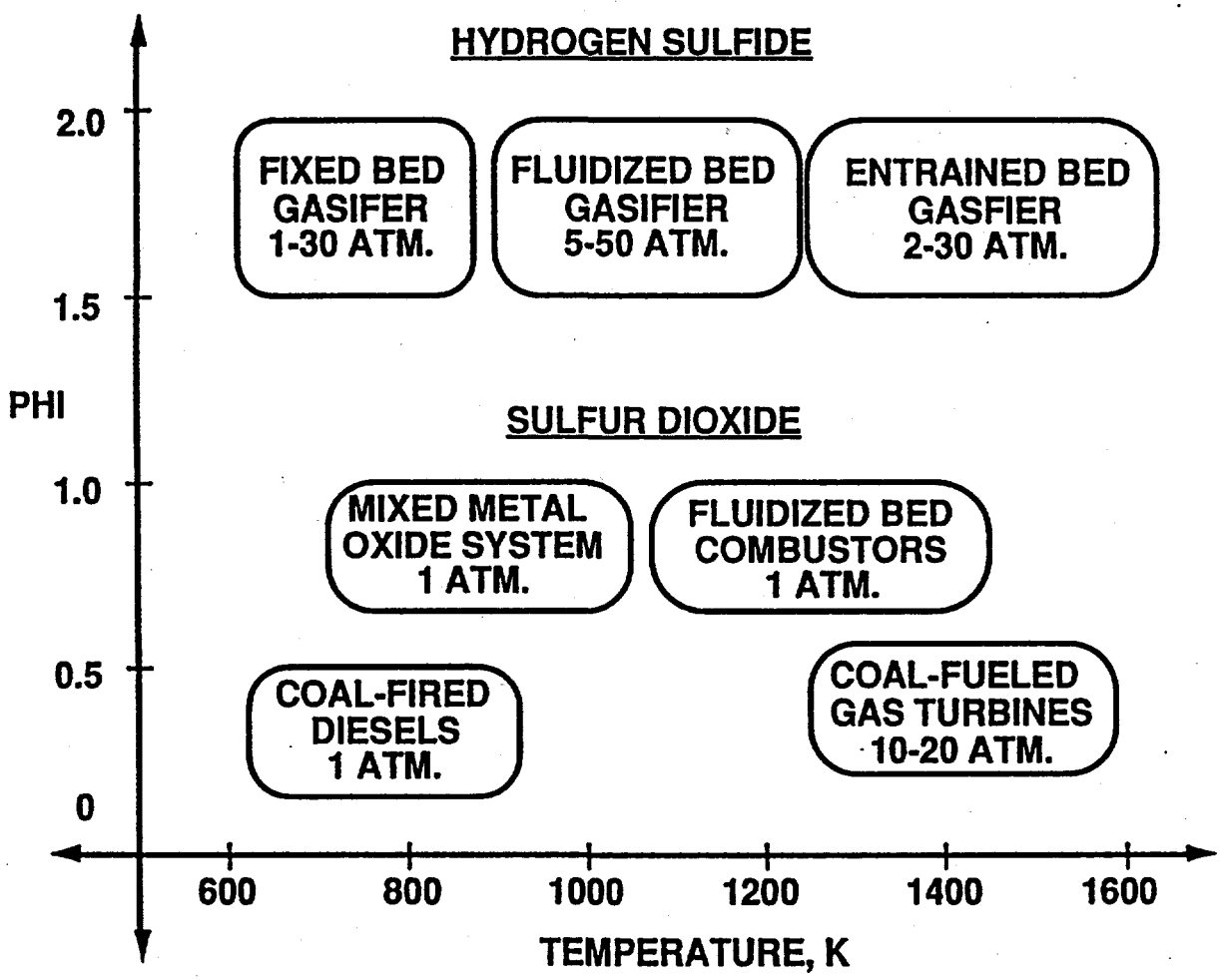

Figure 2-1. Conditions for Survey Experiments.

2.1.2 TEST PLAN

The experimental test plan consisted of a facility shakedown followed by survey experiments, a detailed scan of activation conditions for each application area of interest, confirming high sulfur captures with two other sorbents, and lastly sorbent activation in an oil flame.

Facility shakedown involved checking out all the components, establishing the desired temperature and residence time conditions in the facility, establishing sulfur mass closure in the absence of solids and in the presence of inert solids, performing a calcium mass closure experiment to determine losses on duct walls, and conducting baseline sulfur capture tests using unactivated lime.

The objective of the survey experiments was to scan the full range of stoichiometry-desulfurization temperature combinations (see bold dots in Figure 2-1) for all application areas of interest at selected activation conditions. Based on the batch reactor data, the activation temperature and time were fixed at 2600^{o}K and 20 ms respectively for the survey experiments. However, it was realized that the two processes: sorbent activation and desulfurization were not independent since the activated sorbent quench rate and possibly sulfur capture were expected to vary with the desulfurization temperature. Therefore, for maximum captures, less severe activation conditions were anticipated at higher desulfurization temperatures.

After the survey experiments, sulfur captures were to be optimized by conducting a detailed scan of the activation conditions for the major application areas of interest. In these tests, the desulfurization conditions were to be kept fixed.

2.2 OVERALL FACILITY DESIGN REQUIREMENTS

The primary design requirements of the activation unit were an ability to process sorbent in the temperature range 2200-2600^{o}K for residence times between 5-30 ms, achieve a high particle heating rate (which depends upon achieving high temperatures and rapid mixing of sorbent particles with the flame gas), create uniform temperature and velocity profiles in the duct, and

lastly avoid sorbent deposition on the walls.

The design requirements of the main duct were an ability to control the reaction temperature between 700-1500^{o}K, stoichiometry from 0.4-1.5, reaction time of at least 200 ms, achieve uniform temperature and velocity profiles, and minimize heat losses. The diagnostics required on the main duct were temperature measurements and gas and solids sampling.

2.3 TEST FACILITY DESIGN

The facility design was constrained by the existing hot flow facility which was modified for this project. The hot flow facility had been partially constructed under a previous METC program[2] (Westinghouse project) and partially using TDS funds. The afterburner, quench, and exhaust sections (see Figures 2-2 and 2-3) were fabricated and assembled under TDS funding. The design exercise consisted of estimating the activation and main burner flows and thermal inputs, and design of the activation burner, sorbent quenching zone, main duct, and diagnostics. These design details are presented next.

2.3.1 ACTIVATION AND MAIN BURNER FLOWS

The total mass flow rate through the system was estimated as follows. The existing hot flow facility constrained the main duct length to approximately 2 m. Therefore, in order to attain a residence time of 200 ms a duct velocity of 10 m/s was selected. The duct internal diameter was constrained by the size of the modules in the hot flow facility. These modules were made from 8" pipe. An internal diameter of 4" was selected as this provided adequate (2") insulation. Next, the range of total mass flow rate was calculated. It was 30 gm/s at 700^{o}K and 17 gm/s at 1500^{o}K. The Reynolds number in the main duct is in the 12,000-20,000 range.

The activation burner and main burner mass flows were calculated by doing a mass and energy balance. The energy equation was written in a form which gave the ratio of the activation burner to the total main burner mass flow as a function of activation temperature, main burner gas temperature and the final desulfurization temperature, and the gas specific heat capacity. The mass ratio was calculated at final desulfurization temperatures of 700^{o}K and 1500^{o}K using the specific

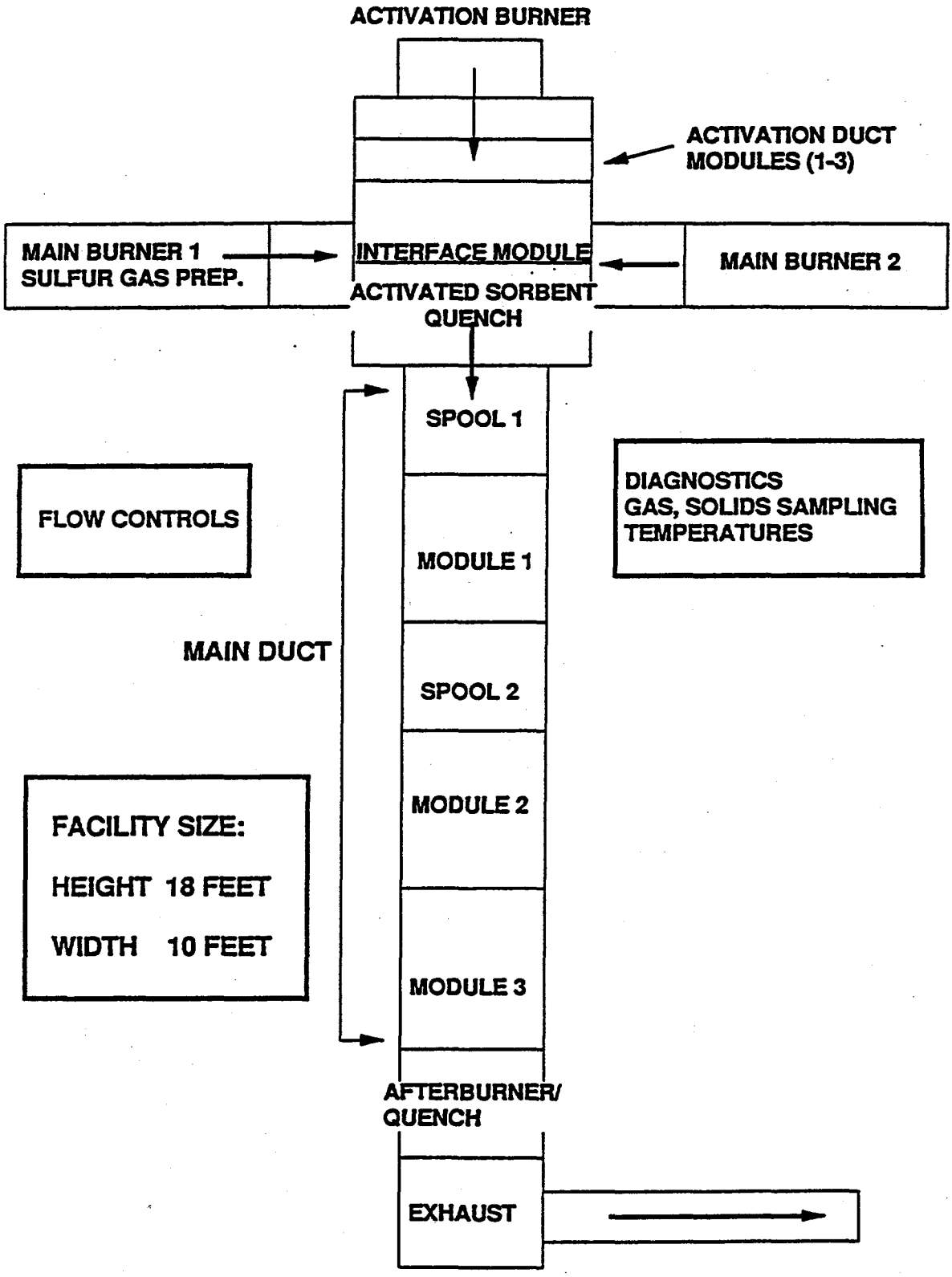

Figure 2-2. Test Facility Schematic.

heat of air. The ratio of the main burner gas temperature to final desulfurization temperature was fixed at 0.9 in order to simulate practical situations in which the activation gas flow will be less than 10% of the total flow. This means that the main burner gas temperature cannot increase by more than 10% upon mixing with the hot activation gas. Under these constraints the activation flow was calculated to range from 1.0-1.2 gm/s while the main burner flow varied from 16-29 gm/s. Thus the activation flow was 3.5% of the total flow at 700°K and 7.5% at 1500°K.

2.3.2 ACTIVATION AND MAIN BURNER THERMAL INPUTS

Given the total activation and main burner flows and the desired temperatures, the NASA thermochemical equilibrium code[3] was used to calculate the oxygen, nitrogen, and propane mass flow rates. The resulting propane flows gave the thermal inputs to the various burners. The total thermal input in the main burners was calculated to be 60,000-80,000 Btu/hr in order to achieve the range of sulfur gas temperatures, 700-1500°K. The activation burner thermal input was calculated to be about 15,000 Btu/hr. The flow ranges were next used to size flowmeters.

Oxygen enrichment was needed to achieve the high temperatures in the activation burner. Figure 2-4 shows a plot of the calculated adiabatic flame temperature in stoichiometric propane/'air' mixtures as a function of the oxygen mass fraction in the 'air' and limestone loading. As expected, all the curves show an increase in temperature with increasing oxygen mass fraction. The data also show a 150-200°K drop in flame temperature for every 10% increase in the limestone loading. Since the flame temperature is such a strong function of the solids loading, the Ca/S was varied by changing the SO_2 concentration at a fixed sorbent flow during testing. This approach was adopted to vary the Ca/S in the 1.5-2.0 range. For Ca/S=1 tests, a lower oxygen index was used because the solids loading in these tests was 50% of the loading in the Ca/S=2 tests.

Testing under fuel-rich and fuel-lean conditions at a fixed desulfurization temperature was also desired in the test plan. Fuel-rich and fuel-lean mixtures were prepared by first establishing the desired desulfurization temperature in the main duct under stoichiometric conditions and then simply increasing the fuel flow or the oxygen flow to obtain the desired stoichiometry.

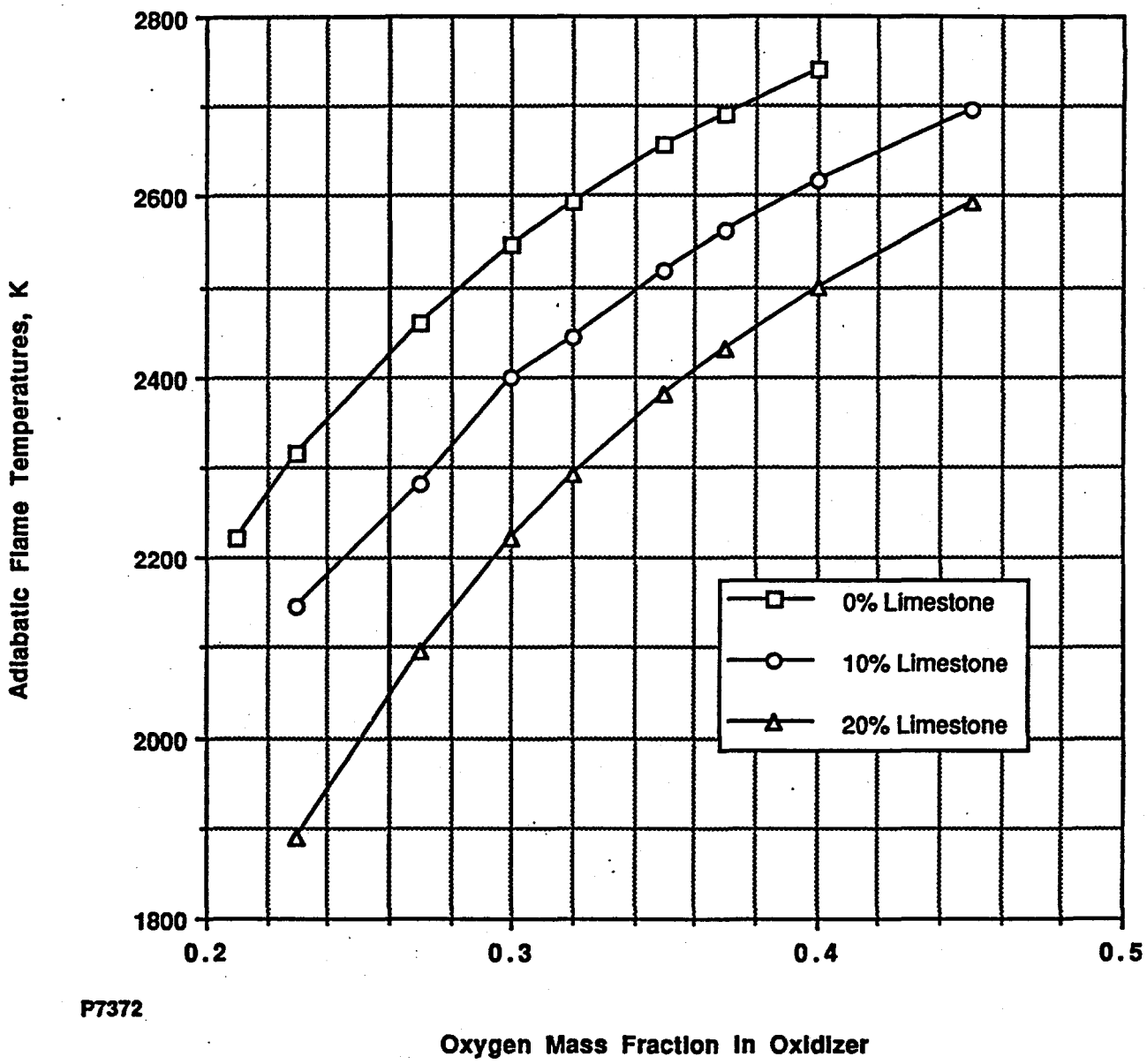

Figure 2-4. Flame Temperatures of Stoichiometric Propane/'Air'/Limestone Mixtures.

2.3.3 SULFUR DIOXIDE AND LIMESTONE FLOW RATES

Sulfur dioxide was added to the main burner flow to obtain the desired sulfur gas concentrations. At a maximum sulfur dioxide concentration of 2000 ppmv, the SO_2 flow range was 1.8 to 3.2 SLPM at 1500°K and 700°K respectively. The limestone flow varied from 0.8-1.5 lb/hr at a Ca/S molar ratio of 1 to 1.8-3.2 lb/hr at a Ca/S ratio of 3.

2.3.4 ACTIVATION BURNER AND SORBENT FEED SYSTEMS

Two activation burner designs were developed: a sintered bronze burner and a perforated copper disk burner. Both burners were fabricated and tested. The sintered burner proved more reliable and was used in all the tests.

Sintered Bronze Burner and Screw Feeder/Eductor Design: A schematic of the sintered burner is shown in Figure 2-5. The burner system consisted of a 1.5" water cooled sintered bronze plug with a 1/2" hole on axis for sorbent injection. A stoichiometric mixture of propane, oxygen, and nitrogen was supplied to the sintered burner. The flame temperature was controlled by varying the oxygen/nitrogen ratio. The sorbent flow was metered by a K-Tron T-20 screw feeder mounted on an electronic scale, and conveyed to the activation burner by a mixture of oxygen and nitrogen. To ensure high particle heating rates, propane was added in stoichiometric amounts to the carrier gas prior to injection. The particle heating rates were estimated to be approximately 10^5 °K/s. The calculated adiabatic temperatures of the carrier jet flame and the sintered burner flame were matched. Since calcination reduces the carrier flame temperature, the oxygen/nitrogen ratio in the carrier gas was greater than in the sintered burner gas. In the final design, the total activation burner flow was approximately 3 gm/s with 2/3rd of it going through the carrier jet.

The sintered burner and sorbent feed system underwent considerable evolution during shakedown testing. These changes are described in the next chapter.

Perforated Copper Disk Burner and Fluidized Bed Feeder: A schematic of the perforated copper disk burner design and sorbent feed system is shown in Figure 2-6. This design

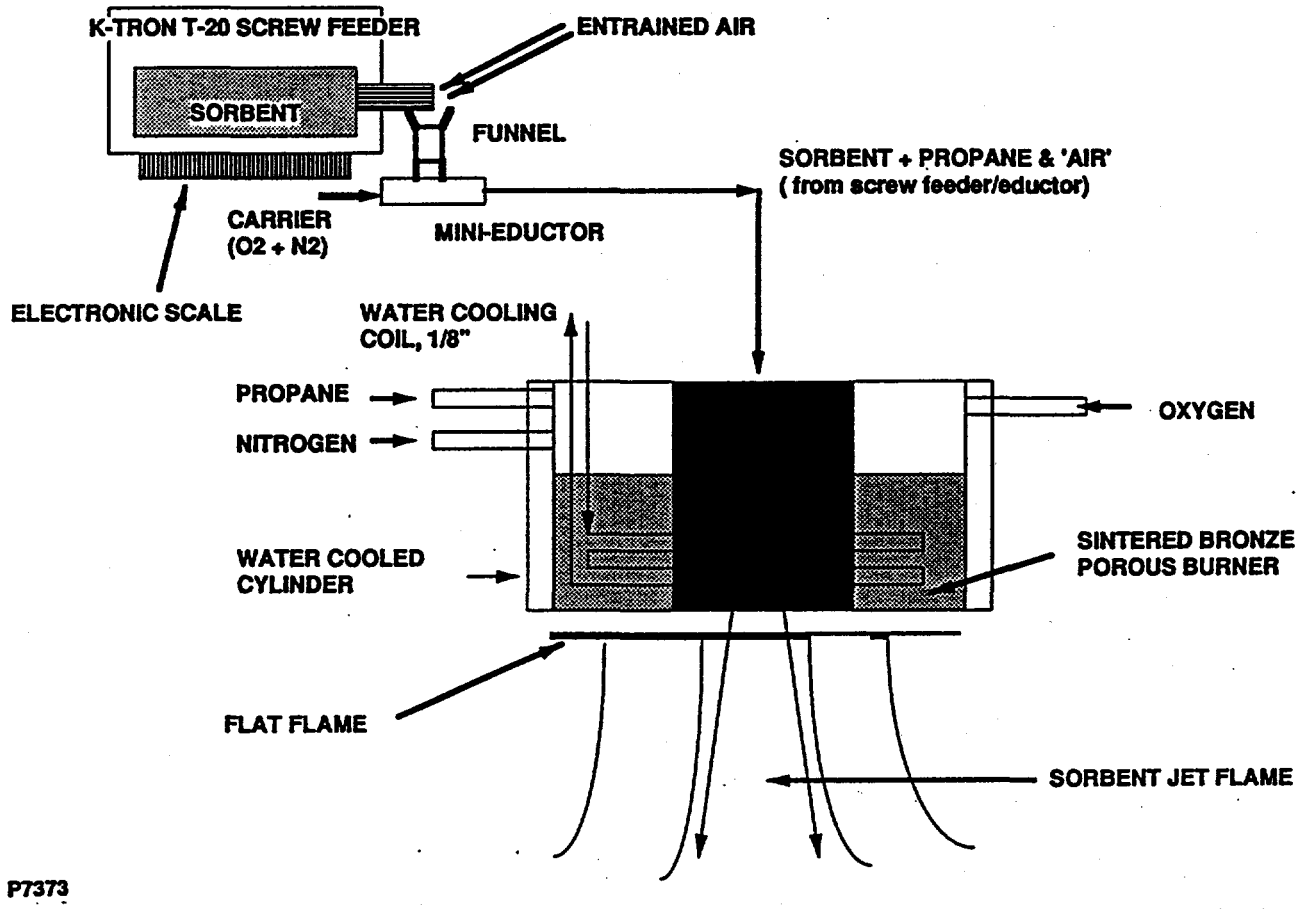

Figure 2-5. Sintered Bronze Burner with Central Sorbent Injection.

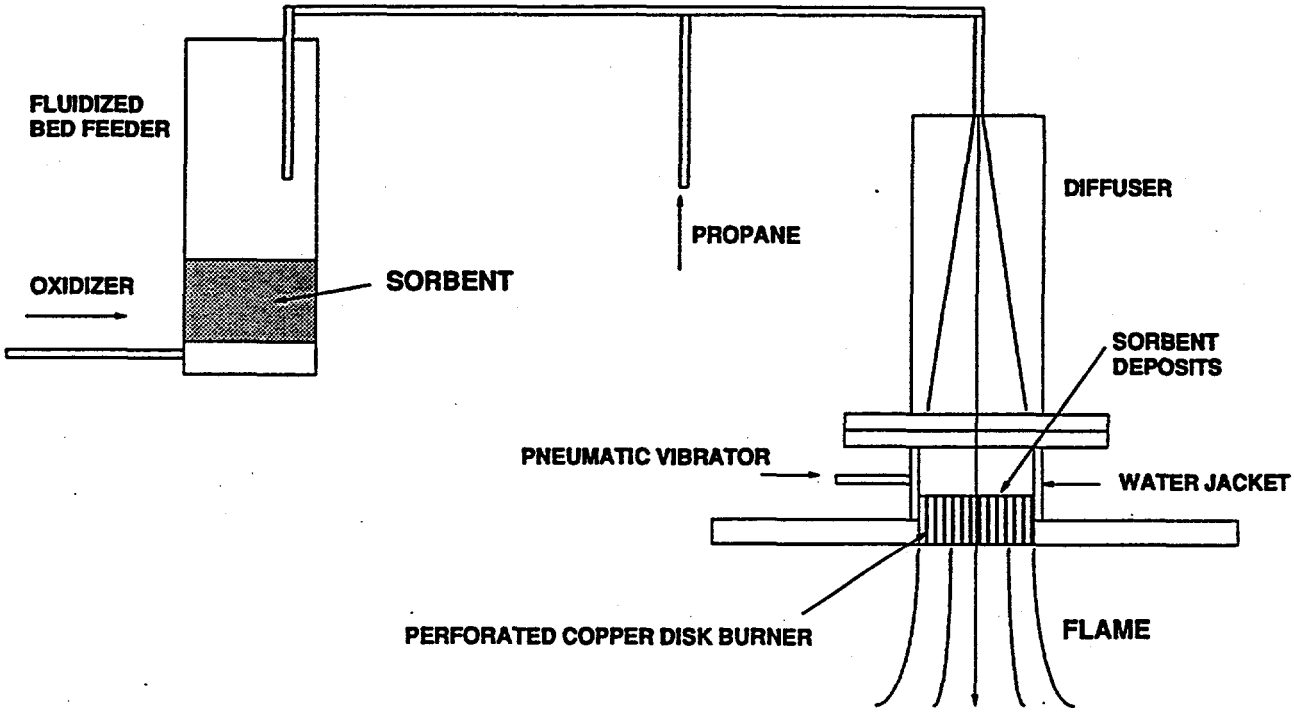

Figure 2-6. Perforated Copper Disk Burner and Fluidized Bed Feeder.

consisted of a perforated disk with 1/16" holes arranged in a hexagonal close packed pattern with a hole to hole distance of 1/8". The holes were sized to prevent flashback, and chamfered (entry angle of 45^{o}) on the back side to reduce limestone deposition. The perforated burner was 3" in diameter. It was bigger than the sintered burner because the open area in the perforated disk was only 23%. Since the activation duct was only 1.5" in diameter, the first activation duct module downstream of the perforated disk was cast in a frustrum shape in order to reduce the flow diameter from 3" to 1.5".

Due to the significant pressure drop across the perforated disk burner (1-2 psig), a screw feeder and eductor system could not be used. Instead, a fluidized bed feeder was used. An existing fluidized bed feeder was tested and found capable of supplying a dilute two phase flow at a few psig. However, the feeder required a high carrier flow and therefore, all of the oxidizer flow was supplied through the feeder. Propane was added to the carrier gas downstream of the feeder. A conical diffuser (expansion angle 7^{o}) was provided before the burner in order to achieve a uniform two phase flow pattern upstream of the copper disk. The diffuser is simply a cone 30 cm long with a total angle of 15 degrees. The diffuser is used to expand the flow from a 1/4" tube to 3" with minimum sorbent deposition on the walls. The primary advantage of this burner design over the sintered burner was that the uniform sorbent dispersion in the combustion gases, in contrast to discrete injection in the sintered porous burner. This design proved unreliable due to plugging and was not used in the tests.

2.3.5 ACTIVATION DUCT MODULES

Sorbent activation occurred in a refractory lined duct which consisted of several modules (see Figure 2.2). Each module was made from 12" pipe and was 8" long. Two ports, 1" in diameter, and located diametrically opposite to each other were provided on each module for mounting diagnostics. The modules were cast with two layers of refractory: an inner 1" thick, high temperature zirconia castable (Cotronics) and an outer layer (3.5" thick) of Resco-8G insulating refractory.

2.3.6 MAIN BURNER

The low temperature sulfur laden combustion gas was prepared in two 30" long side ducts located on opposite sides of the sorbent quench zone (see Figure 2.2). A propane/oxygen torch with a thermal input of 30,000-100,000 Btu/hr provided the high temperature gas in each side duct. The torches were mounted on water cooled flanges. Several 1" ports were provided on each duct for gas addition, and instrumentation. Nitrogen was added downstream of the torches in two locations to set the final temperature and reaction time. Sulfur dioxide was added to obtain the desired sulfur gas concentrations.

The main burner modules which were constructed from 8" pipe had an internal diameter of 3". Insulation was provided by two layers of refractory: high temperature zirconia oxide on the inside and Resco-8G on the outside. The burner modules were also water cooled by burying a copper cooling coil inside the outer refractory.

2.3.7 INTERFACE MODULE

Figure 2-7 shows a schematic of the sorbent quenching zone. The activated sorbent was quenched by the low temperature sulfur laden gases in the interface module. A silicon nitride sleeve placed inside the interface module was used to achieve rapid mixing. While the activation burner gas flows straight down the center of the sleeve, the low temperature sulfur gas is injected into the activation gas via holes in the sleeve. The number, size, and angle of the holes was designed to complete mixing in less than 25-50 ms, with minimal particle deposition and recirculation. The sleeve design was modified later in order to obtain faster quenching. In the original design there were 10 holes 5/8" in diameter at an angle of 60 degrees to the horizontal. Later, gas mixing and sorbent quenching calculations performed using a computer code developed at TDS showed that extremely slow particle quenching was occurring under the nominal flow conditions. This was because the low temperature sulfur laden quench gas jets did not penetrate into the high momentum activation gas/particle jet. The calculations showed that the original activation jet core containing the particles persisted for 25-50 ms in the quench zone.

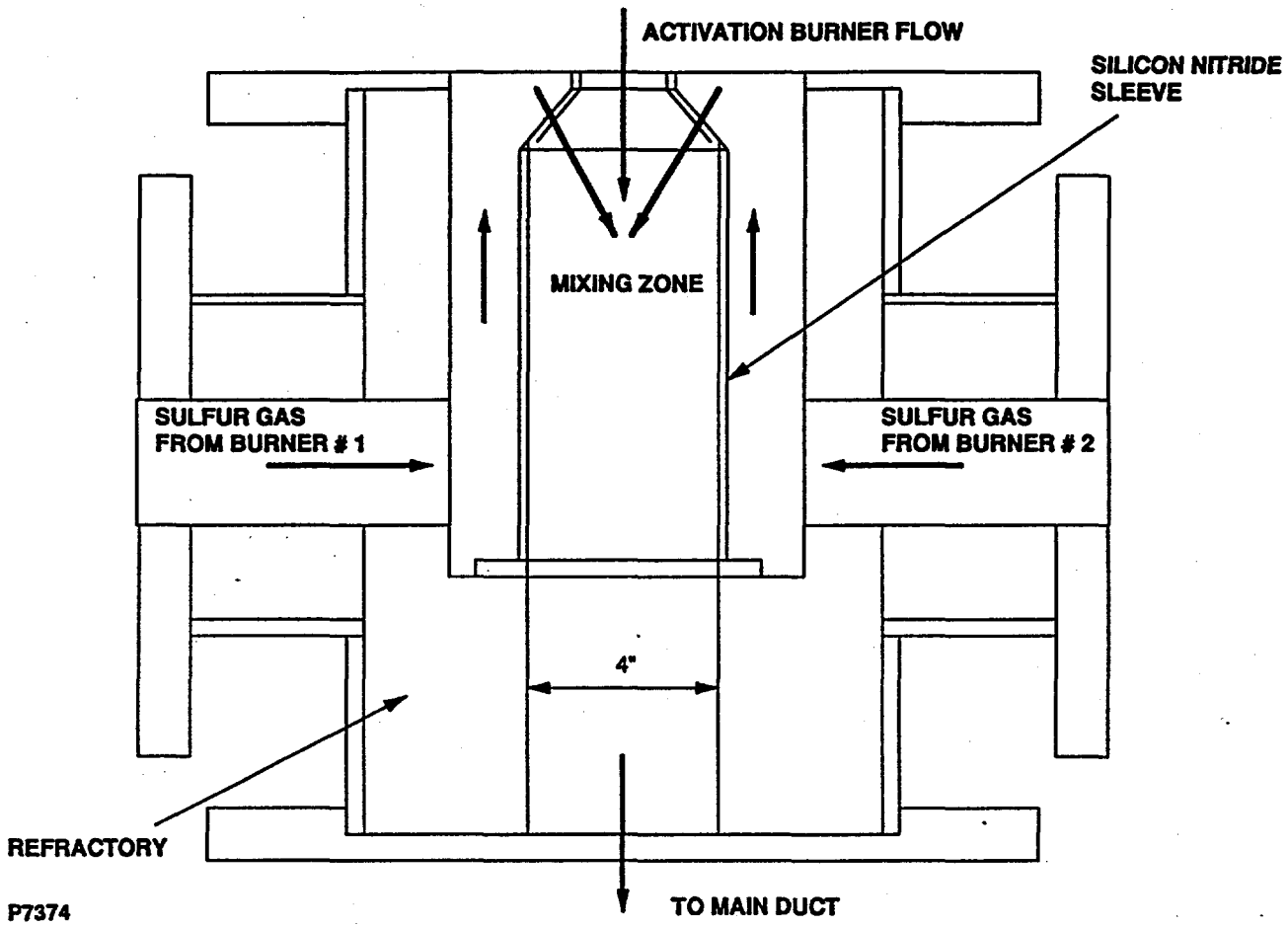

Figure 2-7. Sorbent Quench Zone: Interface Module and Silicon Nitride Sleeve.

In order to study the influence of sorbent quench conditions on Two-Step Rapid Sulfur Capture performance, three new mixing sleeves were designed and fabricated later in this program. A CFD code developed at TDS was used to arrive at final designs for the new sleeves. The CFD code enabled studies of the mixing between the two activation duct streams (i.e., the carrier burner and sintered burner streams), and the activated sorbent quenching process as a function of quench jet variables. The activation burner mixing simulation confirmed that very little mixing occurs between the outer pilot flame (sintered burner stream) and the high momentum two-phase inner flame (carrier burner stream). The calculations showed that the inner portion of the activation jet has velocities of 60 - 90 m/s upon entering the mixing sleeve. Since the sorbent particles are present in this inner core region, the quench jets must penetrate to the centerline of the mixing sleeve in order to achieve rapid quenching. Achieving this degree of jet penetration, however, leads to conditions that will induce negative axial velocities, i.e., flow reversal.

The activation burner mixing computation results were used as inputs for sorbent quenching CFD simulations. In order to reduce the number of variables and limit the overall computational effort, the number of mixing sleeve quench jets and their diameters were fixed at 10 and 0.5 inches, respectively. Next, sorbent quench CFD studies were conducted for quench jet angles of θ = 0, 15, 30, and 60^{o}. If the activation burner two-phase jet is direct vertically downward, then the angle θ is the angle between the horizon and the axis of the quench jets. Figures 2-8 and 2-9 present the details of the 30^{o} mixing sleeve. The 60^{o} mixing sleeve was used initially and the 0, 15, and 30^{o} sleeves were fabricated later in the program. CFD calculations showed that the 60^{o} sleeve was giving poor penetration of the quench jets into the center of the mixing sleeve. Similar computations showed that the 0, 15, and 30^{o} sleeves produced quench jets that penetrated very well into the center of the mixing sleeve. The 0^{0} sleeve produced the most rapid quench of the activation burner jet, yet it did produce a reversal of the mixing sleeve axial flow field just upstream of the position where the quench jets pass closest to the centerline of the sleeve. This phenomena is not desirable since it can segregate and deposit sorbent particles to the wall of the mixing sleeve, or produce an unacceptable back pressure in the activation duct. This effect, however, decreases with increasing θ, and is the reason several mixing sleeves were fabricated. It should also be noted that the two arrays of quench jets are angled so that they produce opposite swirl. The swirl produced by the quench jets labeled "A" in Figure 2-8 is canceled by the counter-swirl produced by the "B" quench jets. This configuration was adopted

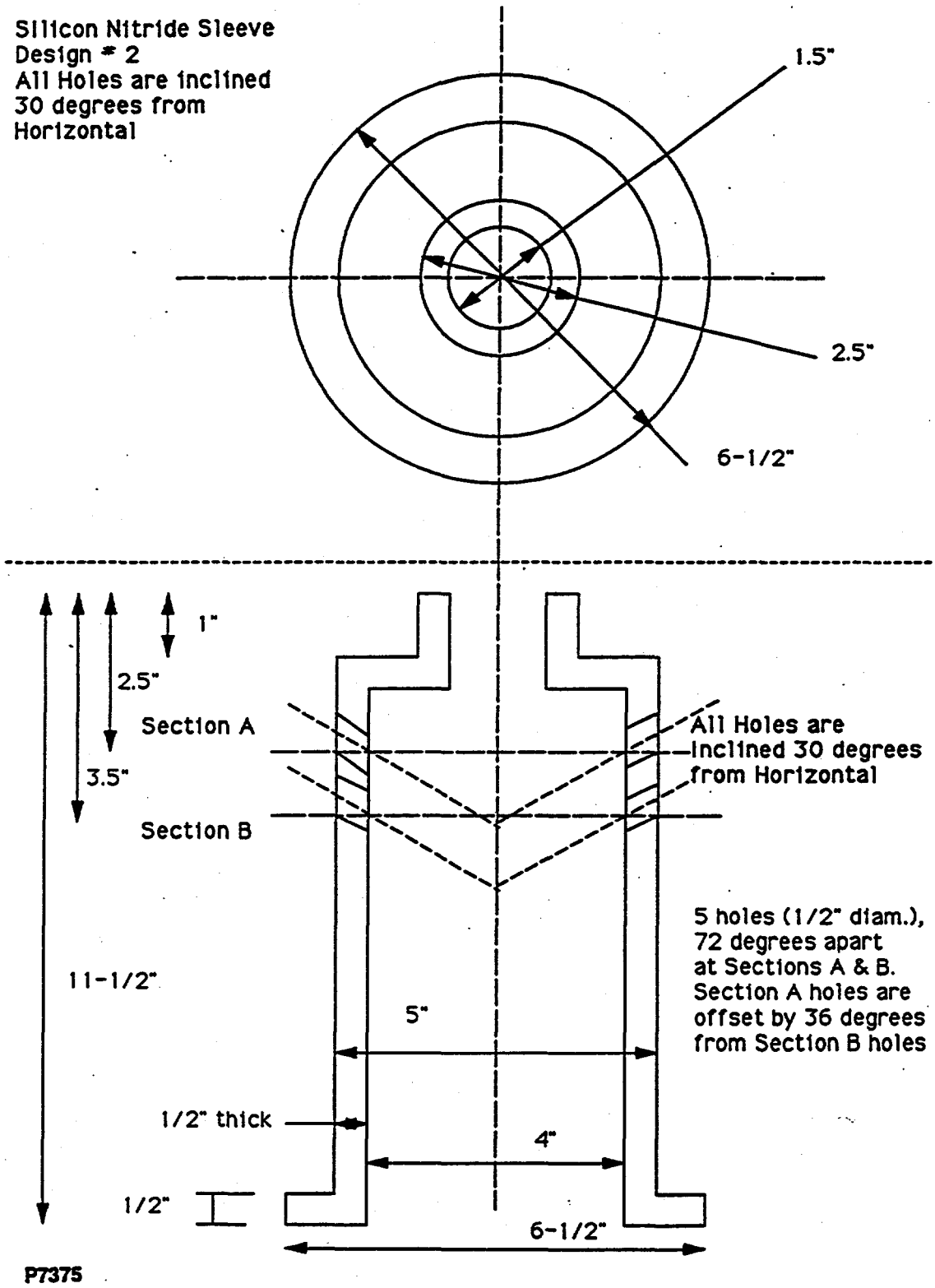

Figure 2-8. Details of 30° Silicon Nitride Mixing Sleeve.

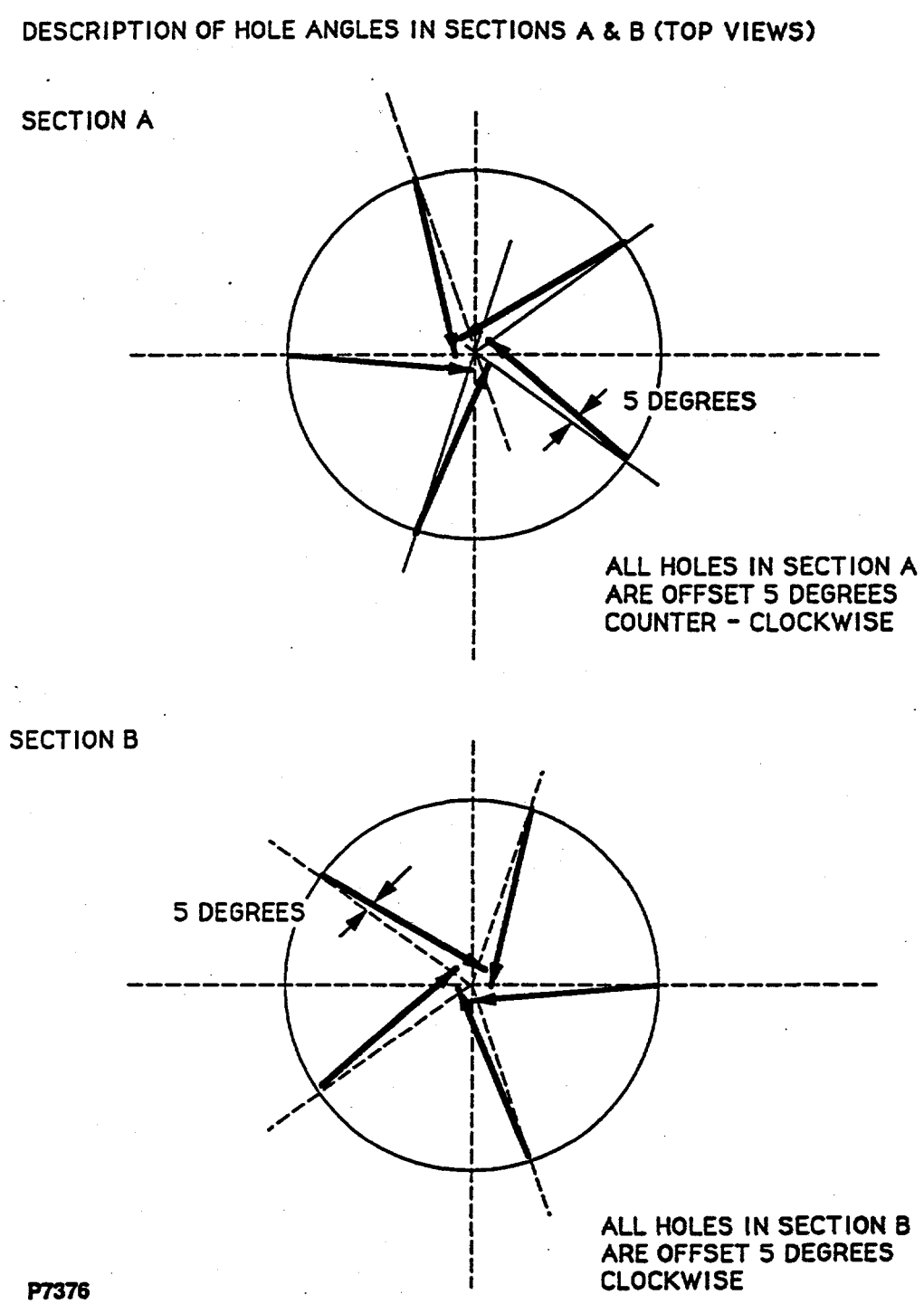

Figure 2-9. Quench Jet Configuration for 30° Silicon Nitride Mixing Sleeve.

in order to reduce flow reversal and to augment mixing.

Regarding sorbent deposition, the deposits on the silicon nitride sleeve were collected and weighed after several tests. The sorbent mass deposited on the 60^{o} silicon nitride sleeve was typically 3-5% of the sorbent injected into the system during a test. The sorbent mass deposited on the 0^{o} sleeve was nominally 18% of the sorbent injected into the system during a test.

2.3.8 MAIN DUCT

The main duct sections were fabricated from 8" pipe. Initially, the duct consisted of three 20" long modules and two 12" long spool pieces. This resulted in a total length of 84". The 20" long modules (some from the existing hot flow facility) had 1" ports for instrumentation. However, the 1" ports were too small for mounting the solid sampling probe which was 'L' shaped for isokinetic sampling. Therefore, the 12" long spool pieces were provided with 3" ports.

The insulation in the main duct consisted of high alumina liners (Zircar Products) with high temperature ceramic blanket insulation (Cotronics) wrapped on the outside. The liner/blanket assembly was placed in the 8" diameter modules. This insulation package was chosen over cast refractory because the alumina liner and blanket combination has approximately half the thermal conductivity compared to cast refractory. Therefore, lower heat losses and a more uniform axial temperature profile were expected with the liner and blanket arrangement. Another significant advantage over cast refractory was the shorter heat-up time due to the much lower specific heats of the liner and ceramic blanket.

During the middle of the experimental program the reaction time in the main duct was increased by adding two more modules (one 20" long and the other 12" long).

2.3.9 INSTRUMENTATION

All the gas flows were measured using Dwyer Instruments and Brooks flowmeters. Standard temperature and pressure corrections were made to calculate true flow rates.

Type T, R, and B thermocouples were used to measure all gas temperatures. Type T thermocouples were used to measure supply gas and gas sampling probe temperatures. Alumina sheathed type R thermocouples were used to measure the gas temperatures in the side ducts and in the main duct. Alumina sheathed and bare wire Type B thermocouples were used to measure activation flame temperatures.

Gas sampling was conducted at three locations along the main duct. Each sampling train consisted of a water cooled sampling probe followed by a Balston filter and a membrane dryer (Permapure Products). The cooling water for the probes was heated to approximately 150 F in order to avoid condensation and sulfur capture inside the probe (this was done only after it was discovered that in-probe wet scrubbing effects were significant). The gas line from the sampling probe to the dryer was also heated to approximately 150 ^{o}F to prevent condensation. The sulfur gas (SO_2, H_2S) concentration was measured using an on-line Western Research analyzer. The CO, CO_2, and O_2 concentrations were measured using Anarad and Beckman analyzers.

Solid sampling was conducted at the bottom of the main duct. The sampling train consisted of a 'L' shaped nitrogen (gas) cooled/quenched probe followed by a Balston filter/housing assembly (Type 30/25 housing, and 100-25 DH filter), flowmeter, thermocouples, and a vacuum pump. The construction of the nitrogen quenched, solids sampling probe is very similar to that used by DoE/METC in their investigation[4] of non-equilibrium sulfur capture. Conversion of calcium oxide collected on the filter into calcium hydroxide and carbonate was a concern. However, the gas temperatures at the filter were typically between 450-550 ^{o}F. At these temperatures both hydration and recarbonation reactions are slow. Typical sampling times were between 20-30 minutes.

2.3.10 DATA ACQUISITION AND CONTROL

A spreadsheet was used for recording and reducing the data. The raw data consisted of flowmeter settings, all gas temperatures and pressures, and sulfur gas concentrations before and during sorbent injection. Based on these inputs, the spreadsheet calculated the velocity and residence time in the duct, the theoretical baseline sulfur gas concentrations, and the sulfur capture.

The experiment operation and control was completely manual. In a typical run, the cooling water flow was started and the nitrogen flows were first set to the desired values. Next the propane/oxygen torches were lit and mounted in the side ducts. The sintered burner flame was then lit using a spark ignition system. The carrier gas flows (oxygen and nitrogen) were increased to the set values and propane added to the carrier gas. The carrier gas jet ignited spontaneously on coming in contact with the sintered burner gases. This completed the start-up phase of the experiment. Heat-up of the rig typically took approximately 0.75 hr to attain 700°K and 1.5 hr to attain 1400°K in the main duct.

After heat-up, baseline sulfur gas measurements were recorded from each sampling probe and compared with the expected value based on the SO_2 flowmeter setting. The next phase of the experiment (sorbent injection) was started only if greater than 90% of the expected sulfur was accounted for. Common causes for low sulfur baselines were: leaks in the moisture removing membrane dryers and sample lines, and disconnected sampling probe heating tapes. Once the baseline sulfur gas data was recorded the sorbent flow was started and the sulfur gas concentration measured from all the probes. Typically, the sulfur capture at probe #3 (lowermost) was measured first. The solid sampling was started after the gas sampling at probe #3 was completed. Sorbent injection for each test condition lasted 30 minutes, although gas phase data were acquired within 5-7 minutes. The sulfur gas concentrations were monitored as they increased to their original values after switching off the sorbent flow.

In a typical test, data at several conditions were taken. System/process parameters, such as Ca/S ratio, activation temperature, gas stoichiometry, sorbent type, and SO_2 concentration, could be changed easily during a run. Changing the duct temperature was also possible but the activation time could be varied only after shutdown as it involved a change in the number of activation duct modules (see Figure 2-2). The most commonly changed variables during a test were the Ca/S ratio, the SO_2 concentration, and the activation and sulfation temperature.

Activation burner or torch flameout was a concern in the beginning, and it did occur on a few occasions. However, a flameout was easily monitored by a decrease in the gas temperature and by looking through the viewports. On such occasions the main propane and oxygen valves were closed, and the system purged with nitrogen before relighting the flames.

Post run procedures included opening and cleaning the activation duct, collecting the deposits on the silicon nitride sleeve, cleaning all the sampling probes, and removing the wall deposits in the main duct.

3.0 FACILITY SHAKEDOWN AND MODIFICATIONS

Experimental testing, Task 2 of the two-step sulfur capture project, consisted of facility shakedown, survey experiments, and two-step process optimization studies. The work accomplished during facility shakedown and the survey experiments is reported in this section.

Facility shakedown consisted of several diverse activities ranging from component development to system tests. The specific shakedown activities were: testing of the activation burners and sorbent feed systems, shakedown of the assembled facility, measurement of activation gas and particle temperatures, comparison of the 'set' stoichiometry (based on flowmeters) and the actual stoichiometry, measurement of sorbent wall losses, and sulfur mass balance in the absence of solids and in the presence of inert solids.

Several facility improvements were made after the start of experimentation. The most important of them were improvements in the sorbent feed system, and addition of extra modules in the main duct to increase the residence time. These changes are also reported in this section.

Survey experimental results are also reported here because, in a real sense, these were very preliminary experiments. Several facility modifications were made after the survey experiments.

3.1 ACTIVATION BURNER SHAKEDOWN

3.1.1 PERFORATED COPPER DISK BURNER

The perforated copper disk premixed burner and the fluidized bed feeder system (see Figure 2-6) were tested in order to determine performance and address problems. The propane flow was set to provide a thermal input of 15,000-20,000 Btu/hr. Oxygen enriched air was used to fluidize and convey the limestone (Marblewhite 325 mesh) to the burner. Propane was added to the two-phase flow just before entry to the diffuser. The limestone flow rate was approximately 1 lb/hr.

The burner was tested with and without sorbent flow. Under both circumstances, a stable

premixed flame was established. The flame demonstrated remarkable stability to air flow variation, and plugging due to sorbent deposition. The sorbent distribution across the flame looked uniform.

However, after approximately 10 minutes of operation sorbent deposition on the back side of the perforated disk resulted in significant flame distortion. Typically, 1/3rd of the burner surface was plugged in 10 minutes. Even with one-third of the burner holes blocked, the flame did not blow off. In later tests a pneumatic vibrator was installed on the water cooled burner housing in order to shake loose the deposits. The vibrator did not improve the burner performance. In another test 0.5% by wt of Cab-O-Sil (a fluidizing agent) was added to the limestone. While fluidization improved significantly, sorbent deposition in the burner still remained a problem.

Several options were available to further improve the perforated disk burner performance, but none were pursued because the second burner, the sintered burner, performed well from the beginning.

3.1.2 SINTERED BURNER AND SCREW FEEDER SYSTEM

The sintered burner performed adequately from the beginning because plugging was never an issue. The main concerns in this design were attaining a high particle heating rate, maintaining a steady feed rate, and estimating the activation time due to the velocity difference between the sintered burner gas and the carrier jet.

The sintered burner flame stability, sorbent flow steadiness, carrier jet/flame gas mixing, and sorbent particle heat-up were assessed visually. The sintered burner flame was found to be quite stable to large changes in fuel and carrier gas flow rates. The sorbent flow appeared steady to the eye. Particle luminosity was used to evaluate carrier jet/flame gas mixing. The particle jet appeared as a cone with its tip near the burner. The jet spread to a diameter of 1.5" in a length of 8" or approximately 15-20 milliseconds. Thus, the particle/flame gas mixing time was estimated to be 15-20 ms. The particle luminosity was also observed to start 1/4-1/2" from the burner surface. This indicated that the sorbent particles were heating up rapidly. Propane addition to the carrier air in quantities sufficient for establishing a combustible mixture did not have a noticeable effect on the particle luminosity as determined by the eye. However, gas temperature

measurements discussed later showed a significant increase in temperature upon propane addition to the carrier jet.

The sorbent was fed using a K-Tron model T-20 feeder which was calibrated and mounted on an electronic scale. The loss in weight of the feeder provided a real time sorbent flow rate. The total activation flow rate was approximately 3 gm/s (thermal input 45,000 Btu/hr) with 2/3rd of the flow supplied via the carrier gas and the remaining 1/3rd through the sintered burner. Thus, the sintered burner flame was essentially a pilot flame for the combustible carrier jet. The unburnt carrier jet velocity was about 15 m/s compared to the surrounding gas velocity of 8 m/s.

3.2 SORBENT FEED UNSTEADINESS

The mounting of the feeder on an electronic scale provided accurate information of the gross particulate flow rate but the new design still suffered from sorbent flow unsteadiness on a time scale of a few seconds; an inherent characteristic of screw feeders.

The fact that the measured utilizations could be limited by fluctuations in the limestone flow due to the screw feeder was also investigated. Laser extinction signal observations of the cold sorbent jet emanating from the burner revealed cyclic fluctuations with a time period of a few 100 ms. Since the flow mixing time in the interface module is at most 50 ms, the feed unsteadiness persists in the main duct. Therefore, over part of the cycle the Ca/S ratio is greater than the average Ca/S ratio, and this decreases the maximum possible utilization. The sorbent feed fluctuation should manifest itself in the H_2S/SO_2 analyzer data. However, the sulfur gas concentrations were constant suggesting that flow mixing was occurring in the gas sampling system[2].

A laser light extinction experiment was set up to study the unsteadiness in the limestone feed. The light beam from a He-Ne laser was passed through the two-phase sorbent jet and detected by a Pin-10 Diode. A digital oscilloscope was used to analyze the voltage and frequency

[2] Cyclic fluctuations in the sulfur gas analyzer data were observed when a larger screw feeder was used at low sorbent flow rates.

data. The signal consisted of a primary cyclic component with a time period of 100-200 ms. Smaller but faster fluctuations were also present on the main signal. Analysis of the voltage data showed that at an average Ca/S=1, the actual Ca/S was varying between 1/3 and 2. The maximum possible utilization is 1, 1, and 0.5 at a Ca/S of 1/3, 1, and 2 respectively. Assuming equal weight at these three ratios results in a maximum possible utilization of 0.84. Since the best experimental utilization measured when these tests were conducted was 0.1, this suggested that the sorbent feed fluctuation was not limiting the maximum attainable sulfur capture.

3.3 ACTIVATION BURNER TEMPERATURES

The activation flame temperature is a very important variable in the two-step process. Therefore, tests were conducted to measure both the activation gas and the sorbent temperatures. Type B thermocouples and a ratio pyrometer were used. The activation flame temperature measurements were also used to determine the mass of room air entrained by the eductor (see Figure 2-5).

Figures 3-1 and 3-2 show a plot of the radiation corrected gas temperatures in the activation duct as a function of distance from the duct wall at two locations downstream of the activation burner; 10 and 30 cm. Data for three flames with adiabatic flame temperatures (AFT) in the range 2315^{o}K to 2740^{o}K are reported. There was no propane addition to the carrier jet in these flames. The shape of the temperature-distance plots in Figures 3-1 and 3-2 shows the penetration of the cold carrier jet at 10 cm, but complete mixing with the sintered burner gas by 30 cm. The gas temperatures are approximately 300^{o}C lower than the AFT's. This could be due to heat losses in the water cooled burner and in the activation duct. The particle heating rate in these flames will be low because of the absence of propane in the carrier gas. Also shown on Figure 3-1 are pyrometer measured particle temperatures. The temperatures was 1811^{o}K at an AFT of 2550^{o}K and 2311^{o}K at an AFT of 2740^{o}K. The pyrometer data represent an 'average' over the optical path length and the particle size distribution. The pyrometer reading is known to be biased towards the temperature of the fine particles (< 5 microns) which have a higher emissivity than large particles.

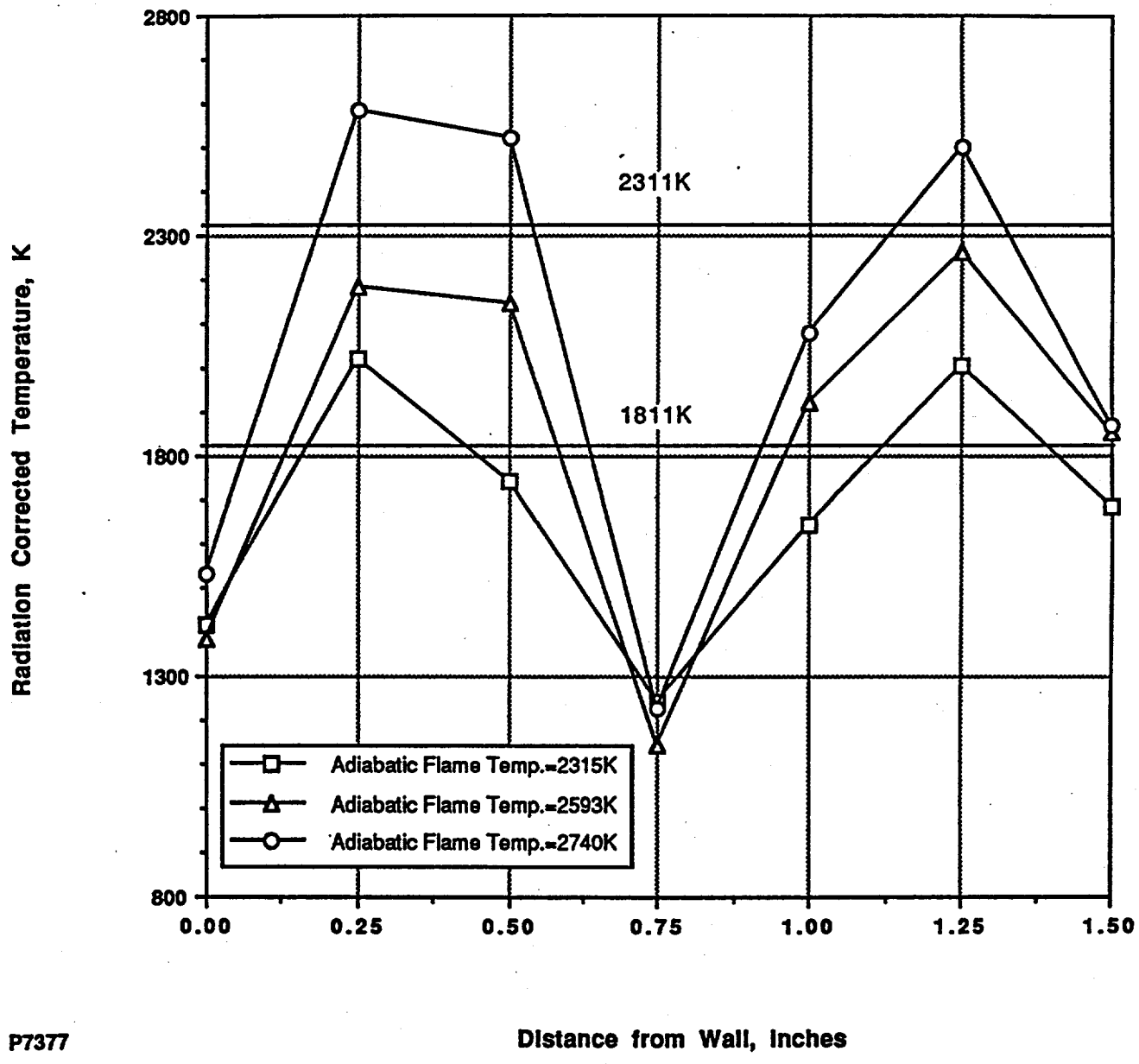

Figure 3-1. Radiation Corrected Gas Temperatures 10 cm (10 ms) from the Burner.

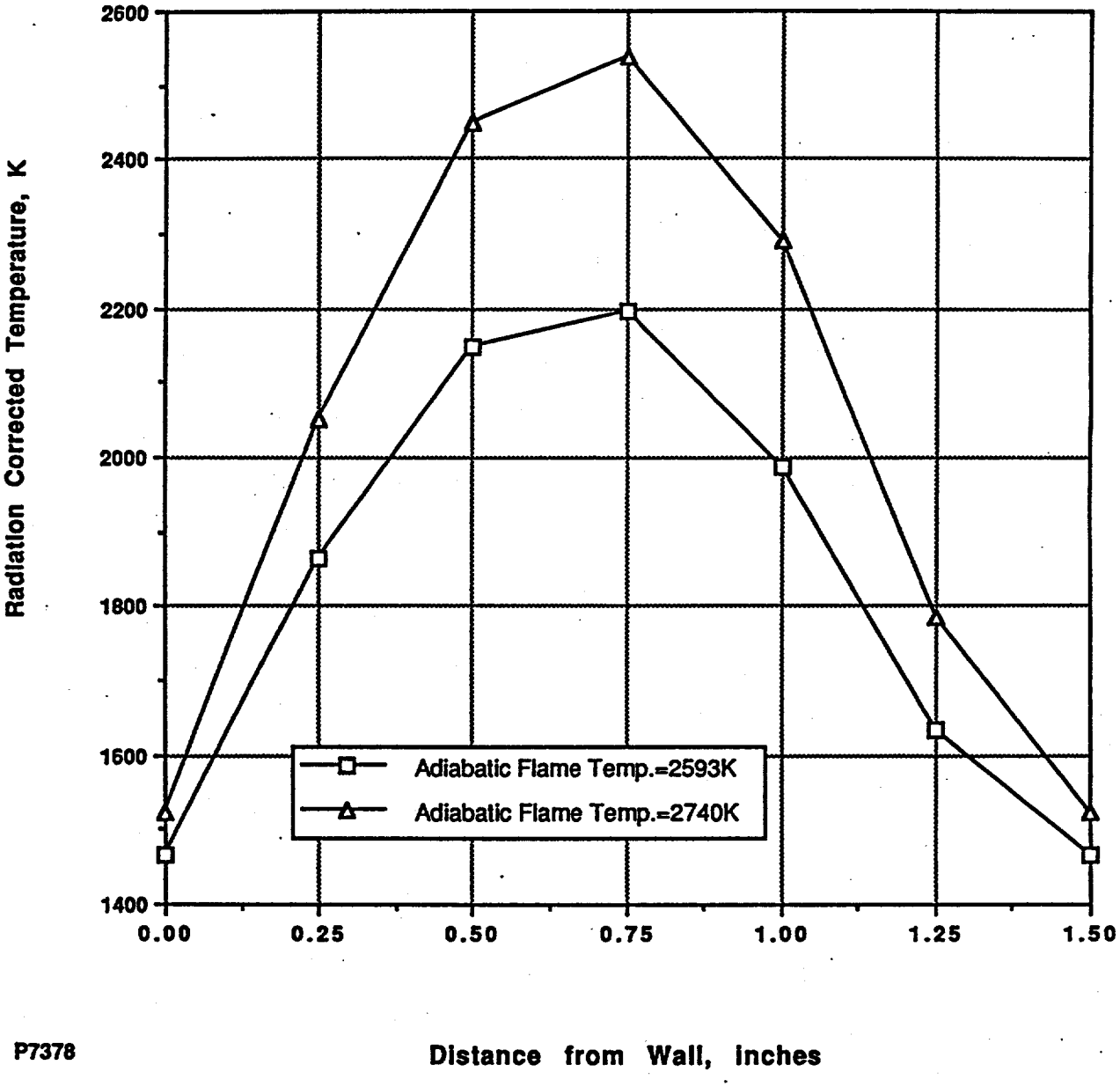

Figure 3-2. Radiation Corrected Gas Temperatures 30 cm (30 ms) from the Burner.

The effect of propane addition to the carrier jet on gas temperatures was significant. Figure 3-3 shows the activation burner centerline temperature as a function of distance from the burner. These measurements were performed by operating the burner in the open. As can be seen, with propane addition the temperature rises to its maximum value within 5 ms, in contrast to 10-30 ms in the absence of propane.

3.4 FACILITY SHAKEDOWN

A few tests were performed to shakedown the test facility. Besides fixing water and gas leaks, the most significant improvement was installation of a spark ignition system for the activation burner. Right from the first test, it proved possible to obtain the desired range of desulfurization temperature and stoichiometry in the main duct.

During experimental testing, only minor modifications such as flowmeter changes have been required. Due to the low mass and thermal conductivity of the alumina liners in the main duct, the time to heat-up to the maximum desired temperature of 1500^{o}K is only 1.5 hour. Over the test period the main burners, interface module, silicon nitride sleeve, and the main duct modules have required no repairs.

The activation duct on the other hand had to be recast on several occasions. This is hardly surprising given the high temperatures in the activation duct and the eutectic forming reaction of limestone with zirconia oxide.

3.5 SULFUR MASS CLOSURE

A sulfur mass closure check was performed during each test by comparing the baseline sulfur gas data from three locations along the main duct with the expected gas concentration based on all the gas flows. Typically, more than 90% of the input sulfur was accounted for showing that the sulfur loss in the duct and gas sampling system was minimal. Figure 3-4 shows the sulfur detected data from a number of tests. As can be noticed, there is some probe to probe variation in the baseline sulfur measured. The sulfur capture and utilization for each gas sampling probe was calculated based on the sulfur gas data without and with sorbent flow. Verification of gas

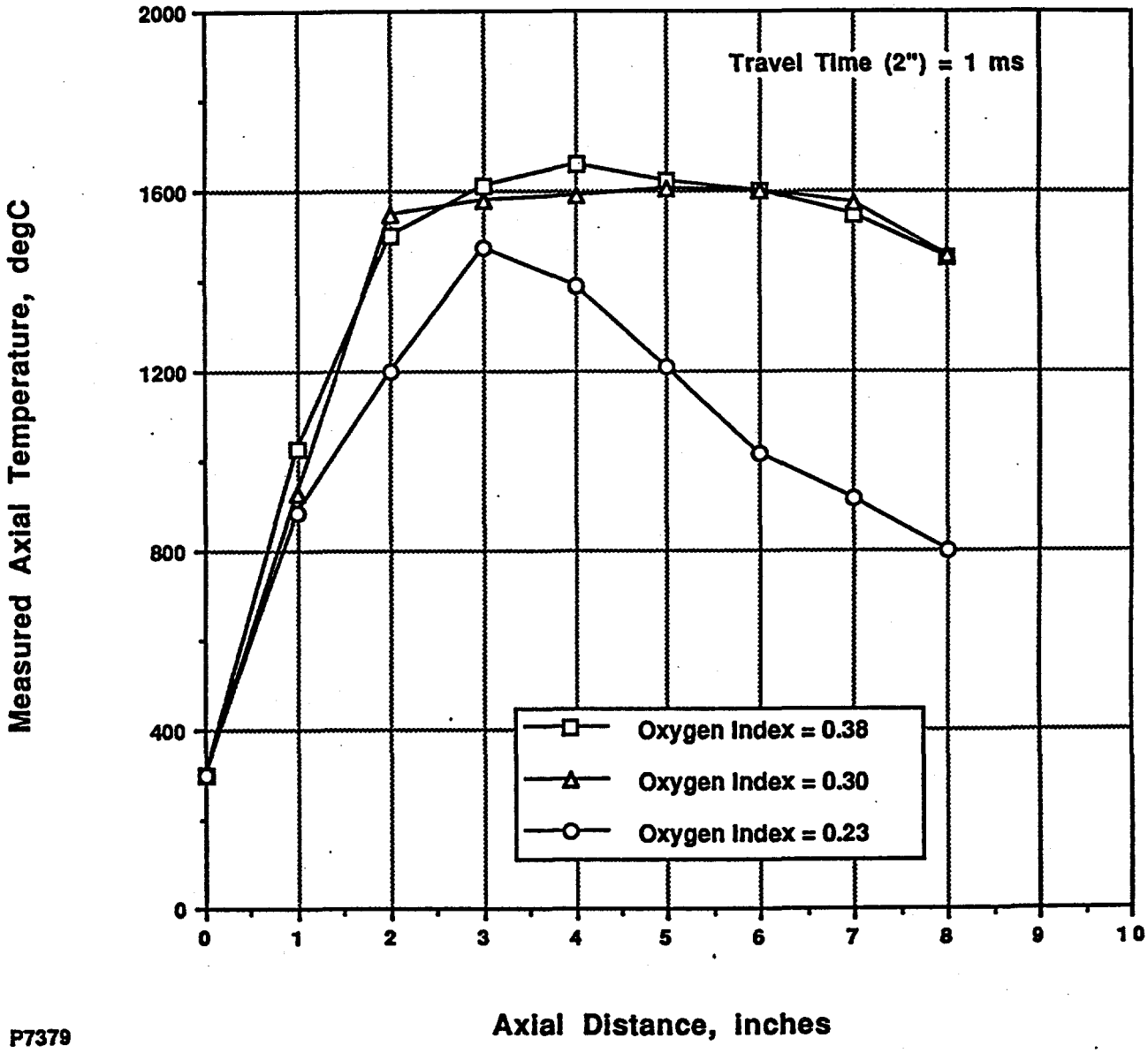

P7379

Figure 3-3. Activation Burner Axial Temperature Profile - Propane in Carrier Jet.

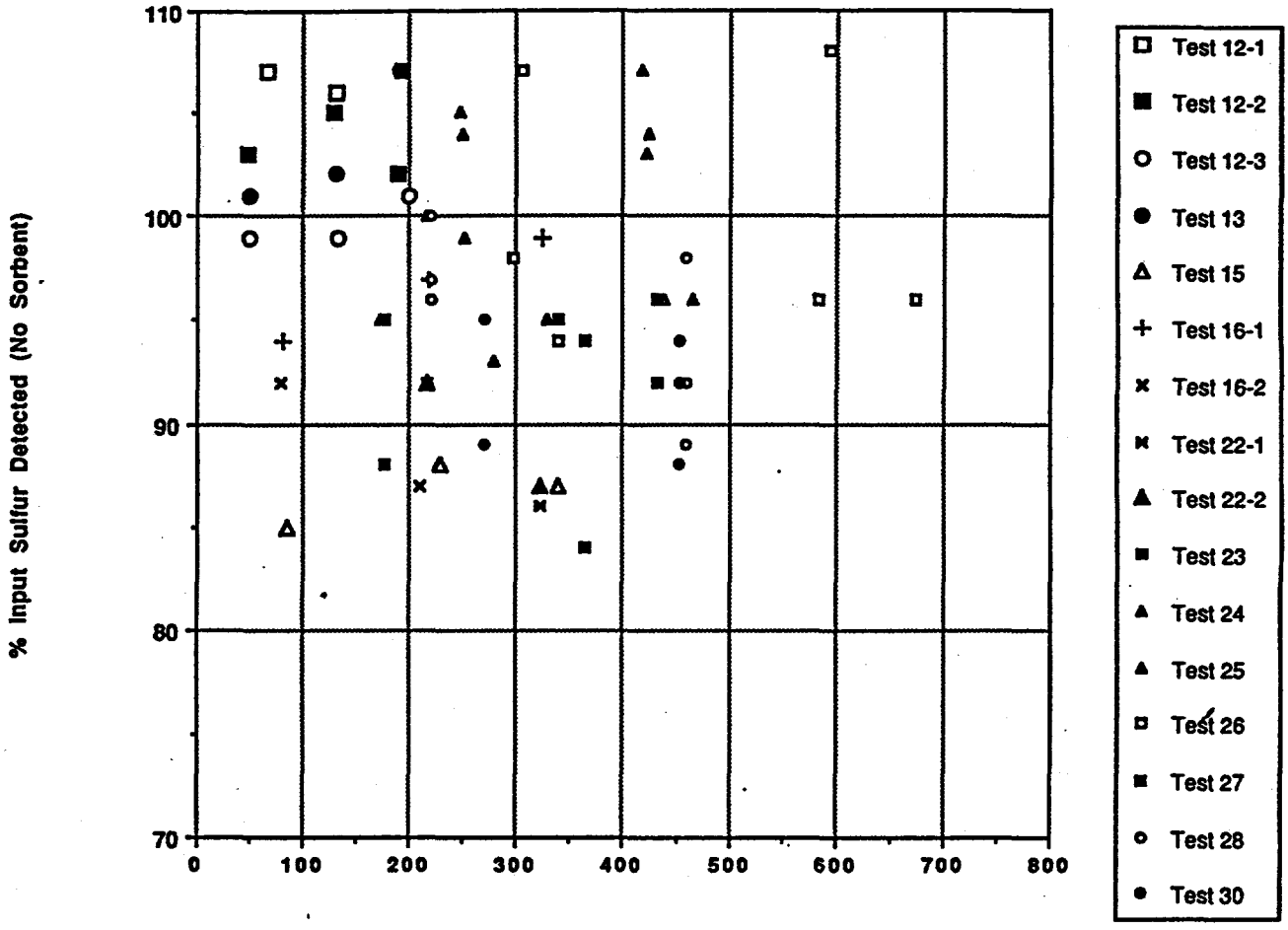

Figure 3-4. Baseline Sulfur Data from Several Tests.

phase sulfur capture was confirmed by the sulfur present in the solid samples.

Silica was injected during one test to determine the sulfur mass closure in the presence of an inert solid. There was no sulfur capture on silica injection.

3.6 AXIAL TEMPERATURE PROFILE

The gas temperatures in the main duct are reported in Figure 3-5 as a function of flow time for several temperature levels. Data for two different temperature levels, 700°K and 1400°K, are reported. A drop of 250°K was measured at the higher temperature level while a drop of only 100°K was measured at the lower temperature level over the 3 m long duct.

3.7 MAIN REACTOR STOICHIOMETRY CHECK

The true stoichiometry in the main duct was compared with the calculated stoichiometry based on all the gas flows. Gas samples extracted from the main duct were analyzed for carbon monoxide, carbon dioxide, and oxygen in order to verify the actual gas stoichiometry in the duct. The measurements were made at a duct temperature of 1000°K. The nitrogen and oxygen flows were kept constant, and the stoichiometry (calculated) was varied from 0.75 (fuel-lean) to 1.45 (fuel-rich) by varying the propane flow. A discrepancy between the measured $CO/CO_2/O_2$ concentrations and the moisture free concentrations calculated at the 'set' stoichiometry was observed. In general, the measured $CO/CO_2/O_2$ concentrations corresponded to a stoichiometry 10-15% richer than the stoichiometry based on the flowmeters. For example, a 'set' stoichiometry of 0.91 corresponds to a true stoichiometry of 1.05, and 1.25 corresponds to 1.44. The $CO/CO_2/O_2$ data were obtained for each test condition. Since most of the experiments were conducted under slightly fuel-lean conditions, the O_2 measurement was used to check the overall stoichiometry in the main duct. For most tests, the oxygen concentration was in the 2-6% range.

3.8 LIMESTONE WALL LOSS CHECK

A cold flow test was conducted to determine the limestone loss on the duct walls. Limestone was supplied at a rate of 2 lb/hr for 1 hour. Only nitrogen was supplied in the three

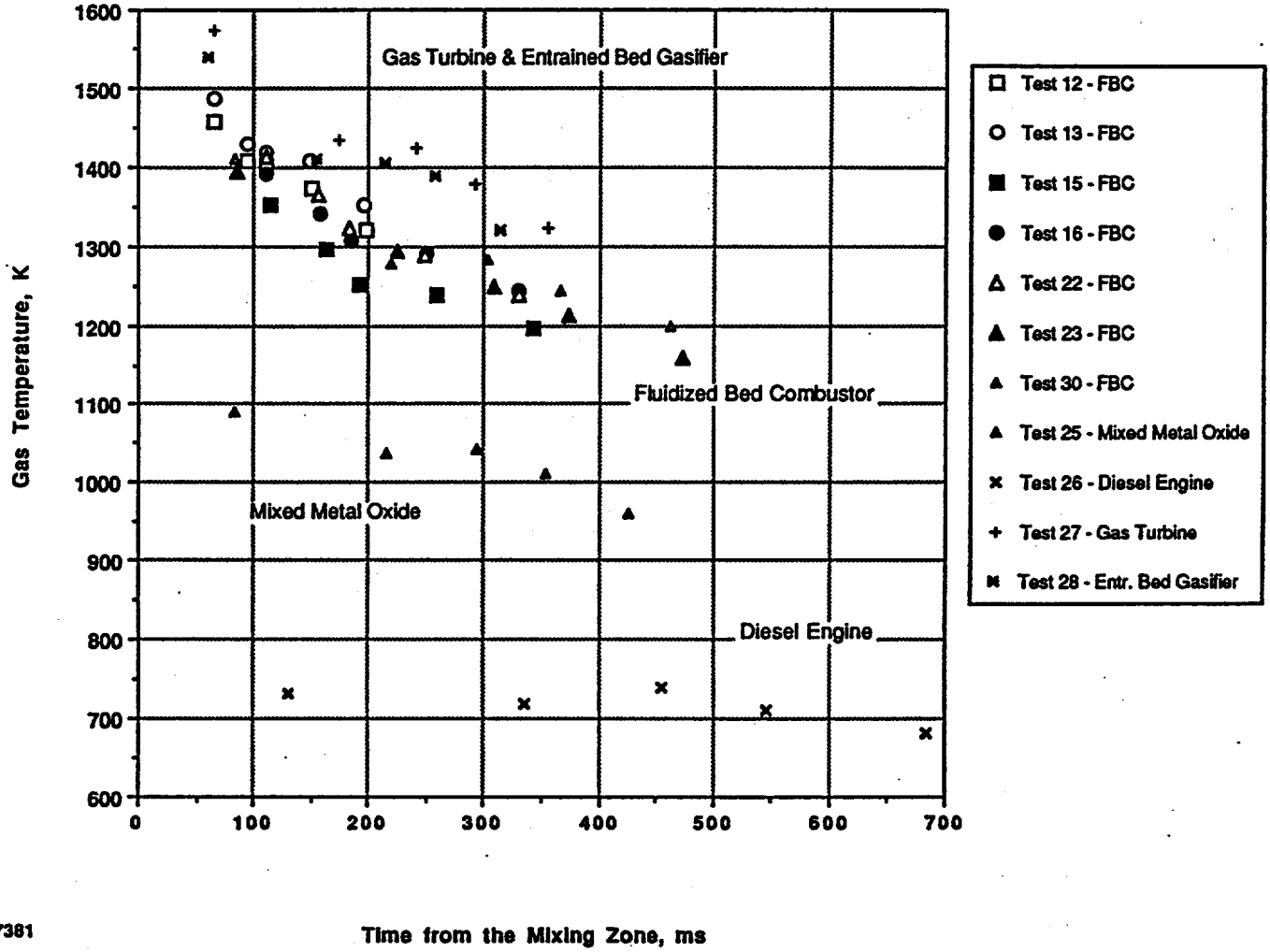

P7381

Figure 3-5. Main Duct Gas Temperatures.

burners. The duct plug flow velocity was only 2 m/s because of the room temperature flow. The limestone in the gas was scrubbed out at the bottom of the main duct by four water sprays, and the scrubbing water was decanted to determine the limestone escaping the duct. The limestone mass balance was as follows: 36 gms were deposited on the silicon nitride sleeve (60^{o} quench/mixing section), 90 gms were collected after blowing limestone off the main duct walls, and 800 gms were found in the scrubbing water. This implies that about 14% of the injected limestone is lost on the walls. However, the 14% wall loss is an upper bound because the wall deposits after a typical sulfur capture run appear to be much less. This could be either due to the higher velocities (10 m/s) and/or calcination of the limestone during a sulfur capture test. Later a few other tests were conducted. Typically 10-20% of the solids are deposited on the walls on the duct.

3.9 SURVEY EXPERIMENTS

Once the facility shakedown was completed, a few survey experiments were conducted. The principal aim of the survey experiments was: 1) to determine the actual temperature-stoichiometry-residence time envelope of the test facility and compare it with the design specifications, and 2) to perform sulfur capture tests at various temperature-stoichiometries at fixed activation conditions in order to determine the advanced coal application(s) which held the greatest potential for the two-step sulfur capture process.

In Test 2 (see Appendices A through C for a listing of conducted tests) the facility's capability to meet the temperature-stoichiometry specifications was confirmed. There were two main concerns prior to testing: 1) inability to attain high temperatures, 2) inability to meet sufficiently fuel-rich or fuel-lean conditions. It proved very easy to control the desulfurization temperature by changing the propane/oxygen torch thermal input and diluent nitrogen flow. The propane/oxygen flame also has a much wider stability range compared to a propane/air torch. Experiments in room air had showed the torch to be stable for mixtures as fuel-lean as $\phi = 0.5$. Therefore, secondary fuel or oxygen addition in the side burner ducts was not required. It was easier to establish off stoichiometry conditions at higher temperatures because any incomplete reactions at the torch tip were completed in the 30" long side burner ducts. Typically, for any experiment, the duct was first heated up at stoichiometric conditions. Then the desired

stoichiometry was set by either increasing the oxygen or propane flow.

Regarding the second goal of the survey experiments, the activation conditions were fixed at 2400°K and 20 ms, and a stoichiometry of $\phi = 1$. This choice was guided by the temperature-time conditions present in the batch reactor testing program[1]. Sulfur capture was first measured under slightly fuel-lean conditions typical of mixed metal oxide and fluidized bed combustor. The sulfur capture was found to increase as the desulfurization temperature was increased from 1000°K to 1300°K. At similar desulfurization temperatures, the captures at fuel-rich conditions ($\phi = 1.5$) were much lower than at slightly fuel-lean conditions.

These trends are in agreement with data from the previous non-equilibrium sulfur capture work at TDS and thermodynamic equilibrium sulfur capture calculations. The batch reactor experiments[1] also showed lower captures under fuel-rich conditions as compared to stoichiometric and near stoichiometric ($0.9 < \phi < 1.2$) conditions. At a fixed stoichiometry, the captures are also expected to decrease at low temperatures due to slower kinetics.

In view of these results, it was decided to optimize the two-step process for the fluidized bed combustor applications first.

4.0 PROGRAM EVOLUTION

4.1 PHILOSOPHICAL REFLECTIONS

If it is assumed that a traveler knows the conclusion of a journey in detail before hand, whether it be the final destination, the knowledge gained, or the experiences encountered, the journey would be pointless. This reasoning suggests that a journey involves encounters with the unknown and that the traveler will not know the journey's conclusion exactly.

In many cases the traveler may have prior knowledge or experience that allows reasonable prediction of a journey's conclusion. These could be called predictable journeys, which encompass most of the journeys undertaken during the span of a person's lifetime.

There are cases in complete contrast to predictable journeys. These could be called adventures. Here, by implication, the traveler is not cognizant of the extent of the unknown regions of the journey and is not very concerned with the ultimate conclusion, only the possibility that the adventure may yield new knowledge, experiences, or gratification. The traveler relies on fundamental tools, such as reason and basic knowledge, and the ability to apply these tools spontaneously and skillfully to steer the adventure in directions that suit the traveler's needs. Adventures are a very important aspect of a person's life, since they stimulate the imagination. Yet, because of their questionable utility, they are not undertaken as frequently as the more common place predictable journey.

The last cases considered span the gulf lying between the predictable journey and the adventure. These could be called expeditions and the traveler could be called an explorer. The features that make the expedition distinctly different from the predictable journey and adventure can be summarized as follows. The explorer undertakes an exploration for the purpose of acquiring new knowledge or experience in a specific area. More specifically, the explorer intends to confront the unknown with the goal of gaining an understanding of that which was previously unknown. Since the explorer has defined a goal or goals, in effect bounds have been placed on the expedition. Prior to embarking, the explorer defines a plan for the expedition. The plan may be very detailed, since the explorer anticipates encountering the unknown. The planning process usually includes refining goals, identifying unknowns which are to be probed, reflecting on the skills and knowledge that may be needed to explore the unknown, obtaining the skills and knowledge needed that are not presently held by the explorer, and, in an iterative process, the

explorer begins constructing a series of steps, a formal plan, that will efficiently guide the explorer to the chosen goal(s). Since the unknown may present the unexpected, the explorer, within the limits of knowledge held prior to embarking, usually includes strategies in the plan that provide alternate paths at critical points based on information gained up to that point. The most gratifying alternative is the one which takes the explorer beyond the goals of the original plan, beyond the explorer's expectations. The most severe being the one that involves clear indications that the original goals are not achievable and that the expedition must be halted. The explorer must be prepared for both of these alternatives, as well as the possibilities that lie between these extremes.

Although researchers would probably prefer to view themselves as adventurers, the fact that research has specific goals requiring methodical plans and that utility of results takes priority over the unpredictable returns of adventures, it is not possible to hold fast to this view. Researchers cannot view themselves as travelers on predictable journeys, and rightly so, since they pursue the unknown with skills exceeding matter of fact knowledge. Rather, researchers are explorers conducting research programs (expeditions) that have methodical plans for achieving specific goals.

This report describes a research program that was based on a plan that was carefully constructed and supported by knowledge gained during previous research programs and by that of a few very capable researchers. Inasmuch as careful planning supported by specialized knowledge is necessary for successfully achieving a research program's goals, it does not guarantee success. By its very nature, research involves probing the unknown, which can yield unexpected results. The unexpected, in return, can result in a program conclusion that is completely different from that initially anticipated or hoped for. During this research program an ancillary effect, which mimicked the anticipated behavior of the phenomena being studied, went unrecognized. Since this ancillary effect so convincingly mimicked the primary effect under study, it was very difficult to detect its presence. The researchers were fooled by this ancillary effect for an extended period. Through the perseverance of one of the researchers and his attempts to resolve an inconsistency between two measures that should yield the same result, the ancillary effect was discovered.

The impact of the ancillary effect on this program was severe. Results that were very encouraging became very unsatisfactory. Attempts were made to find regimes where the primary effect produced satisfactory results, but these attempts were unsuccessful. By the end of this program it was clear that the original Phase I goals would not be met and that the research would

not proceed into the optional phases (Phases II and III). This, in turn, warranted exercising the strategy in the original plan that defines the course of action to be taken when confronted with unexpected and unfavorable results. As a result, this research project was halted at the conclusion of the Phase I effort. This is disappointing, but the results allow no other alternative.

Much of the experimental data acquired prior to and during resolution of the catastrophic ancillary effect is invalid. Most of the data acquired after resolving this effect is valid. Since presenting invalid data would cause, without doubt, a great deal of confusion, invalid results acquired prior to and during resolution of the ancillary effect will not be presented. A great deal of experimental effort, however, was invested during that period. In order to give a complete picture of this program, one which conveys the efforts invested prior to resolution of the ancillary effect, the remainder of this section will present a program history, which follows in Section 4.2, Summaries of the tests conducted during Phase I (Base), Phase IA, and Phase IB are given in Appendices A through C, respectively. These appendices list the tests conducted plus, for each test, a synopsis giving test conditions and brief comments. Not only is a clear picture of the effort invested in this program conveyed by providing a program history at this juncture, but doing so filters out invalid results thereby allowing an unfettered presentation of valid results in Section 5.0.

4.2 PROGRAM HISTORY

Figure 4-1 presents a comparison of the actual program schedule with the original. This comparison provides a framework which gives coherence to the following discussion. The upper half of the schedule in Figure 4-1 shows the original plan. The lower half gives the schedule that reflects actual progress.

4.2.1 ORIGINAL PROGRAM

The original program was a three phase effort having an overall duration on nominally 33 months. The objectives of the overall program were to evaluate the Two-Step Rapid Sulfur Capture process over a wide range of process conditions (700-1400^{o}K for both oxidizing and reducing atmospheres); determine viable applications among advanced coal utilization systems; confirm feasibility in a proof-of-concept test facility; and determine economic feasibility by performing economic evaluations comparing this concept with existing sulfur removal

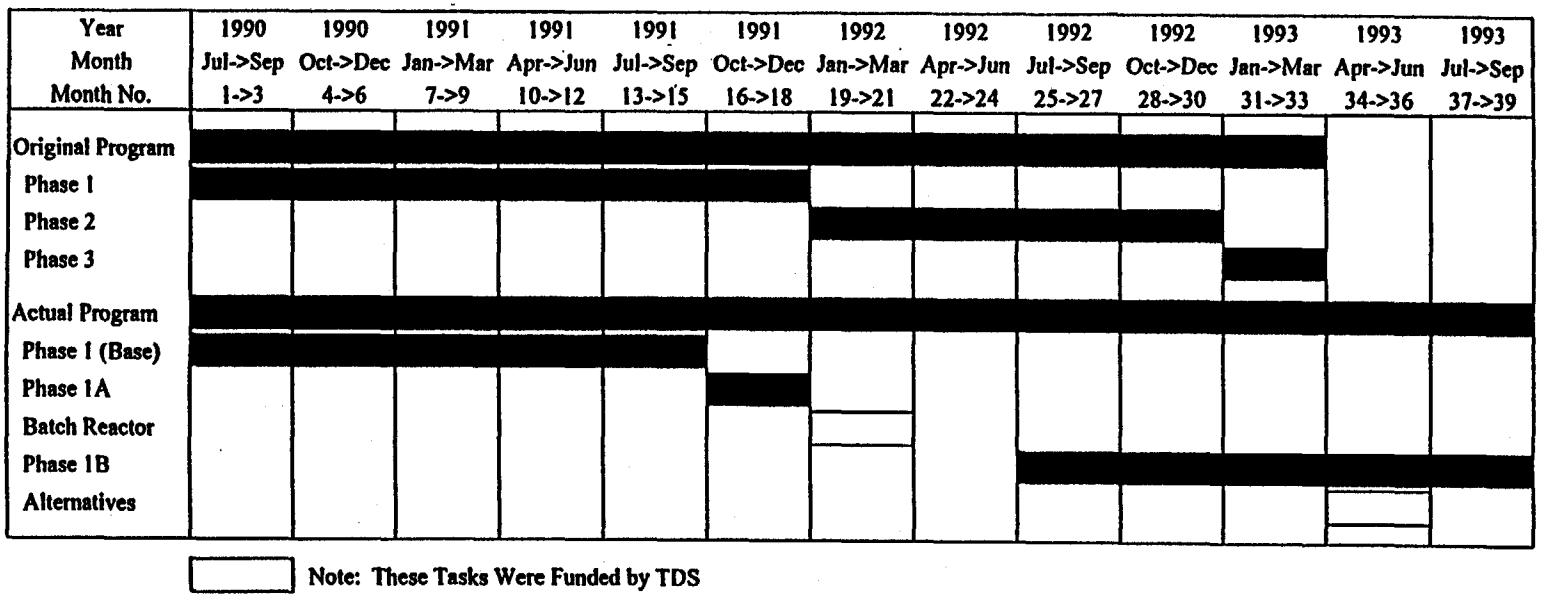

Figure 4-1. Comparison of Actual Versus Original Program Schedule.

technologies. The later phases of this program (II and III) were optional, with advancement contingent upon the success of the preceding phase. The overall goal of this program was to develop the proposed sulfur capture technology to the point where industry would support further development.

Phase I of the original program was to be an 18 month effort. In this phase a small scale flow facility was to be constructed and experiments were to be conducted over a wide range of operating conditions. The purpose was to gain a better understanding of the intricacies of limestone heat-up, calcination, and sulfur capture reactions. This information was to be used in Phase I to determine viable areas of application for the proposed sulfur capture process, e.g., coal-fueled turbines and diesels, fluid bed combustors/gasifiers, and for off-gases from mixed metal oxide sulfur removal systems. Technical and economic evaluations, comparing the proposed process with existing sulfur capture technologies, were to be conducted based on the identified viable application areas. An engineering model of the Two-Step Sulfur Capture process was to be developed during Phase I, which included limestone heat-up, calcination, and sulfur capture reactions. This model would be used as a tool for design of a Two-Step Sulfur Capture limestone injection system for testing in the advanced coal utilization proof-of-concept facility selected for Phase II. It is important to note that all of the work defined in the original Phase I plan was performed during the course of the actual Phase I effort.

Since Phases II and III of this program have not be undertaken, and will not be undertaken, no differences can be cited between the original and actual plans for these phases. Phase II of this program was to be 12 month effort. The objective of the Phase II effort was to conduct optimization testing of the Two-Step Sulfur Capture technology at an advanced coal utilization facility identified in Phase I. Based on the information gained during Phase I, a limestone injection unit would be designed, constructed, and optimized that would be capable of processing and injecting limestone into the proof-of-concept facility. The optimization tests would be conducted at TDS. After optimization, the injection unit would be installed in the proof-of concept facility identified in Phase I. Short duration testing would follow with the intent of determining optimum operating parameters and for developing a data base for economic analyses. The findings of the Phase II effort would be submitted to DoE/METC for review, followed by a decision determining whether the program would advance to Phase III.

The Phase III program was to be a three month effort. The objective of the Phase III effort was to conduct longer-term testing in the proof-of-concept facility setup during Phase II to

confirm satisfactory longer-term operation of the complete system. Sulfur capture tests in the proof-of-concept facility were to be conducted to confirm operation of the complete system with each test involving continuous operation for durations of no less than 48 hours. Calcium utilizations and the nature of the spent sorbent were to be determined. At least 200 hours of operation testing were to be logged during the Phase III effort.

4.2.2 ACTUAL PROGRAM

Since Phases II and III have not been and will not be undertaken, the following discussion pertains only to the progress made during Phase I. Referring to Figure 4-1, the actual Phase I effort is made up of five elements, namely: the base program {Phase I (Base)}; two extensions {Phases IA and IB}; and two relevant, yet not required, studies funded by TDS, i.e., additional batch reactor experiments {Batch Reactor}, and proof-of-concept experiments for two alternative sulfur capture concepts {Alternatives}. Before discussing the progress made during the actual Phase I program, the "Alternatives" testing effort will be briefly discussed and discharged, since it is not really germane to the contract work.

When it became clear that the Two-Step Sulfur Capture process would not provide calcium utilizations needed for economic feasibility, TDS conducted internally funded experimental studies ("Alternatives," Figure 4-1) in an attempt to produce an alternative sulfur capture process that would offer the government and industry a technology that may fill the void left by the dwindling prospects of the Two-Step Sulfur Capture process. This testing was conducted over a three month period. Two alternatives were tested. The first alternative was based on iron oxide as the sorbent. The second was based on a different calcium compound sorbent. The first alternative involved substituting iron oxide powder for the limestone powder in the Two-Step Sulfur Capture process. This approach was based on the significant reductions in exhaust sulfur observed near stoichiometric conditions, in the absence of sorbent injection, during coal combustion tests[2] involving the TDS 6 atm 12 MMBtu/hr Toroidal Vortex Combustor. There was some evidence that the sulfur reduction may be attributable to the iron oxide in the coal, coupled with a nearly/slightly oxidizing atmosphere. The iron oxide Two-Step Sulfur Capture tests conducted under "Alternatives" produced negligible sulfur capture. The second alternative, which used the Two-Step Sulfur Capture process, but a completely different calcium compound sorbent, produced interesting results. Albeit, the calcium utilizations were not

sufficient to warrant offering this process as a viable alternative to the process central to the Two-Step Sulfur Rapid Capture program. TDS feels the second alternative may have potential and that further study is needed to demonstrate its potential and to produce a more mature technology. No more will be said regarding approaches tested under "Alternatives," except that a suitable one was not identified.

The actual Phase I program was carried out over a 39 month period. It consisted of three program related elements, namely Phases I (Base), IA, and IB, and a TDS Internally funded, yet not required, Batch Reactor study. The rationale for the Batch Reactor study was to determine if the devastating ancillary effect discovered during Phase IB was responsible for the high utilizations measured in the TDS batch reactor facility under a previous DoE/METC program[1]. Since the results of the previous batch reactor study formed the basis of the present program, the objective of the new Batch Reactor experiments was to either substantiate or refute the results of the previous work. The findings of the new Batch Reactor study are presented later.

4.2.2.1 Phase I (Base) Study

Most of the work planned for the original Phase I effort was carried out during Phase I (Base) in the actual program. This effort was conducted over a 15 month period and involves the activities performed prior to discovering the devastating ancillary effect. Phase I (Base) contained the following technical tasks, namely:

Task 1 Test Plan and Test Facility Design and Fabrication.
Task 2 Experimental Testing.
Task 3 Two-Step Rapid Sulfur Capture Mechanism.
Task 4 Feasibility/Applicability Study.

Task 1: Test Plan and Test Facility Design and Fabrication. During this task a Test Plan was prepared and submitted to DoE/METC for review and approval. The Test Plan refined program goals, identified advanced coal utilization systems where the Two-Step Rapid Sulfur Capture process may have applicability, defined limits for each process parameter for each advanced coal utilization system, defined specifications for the test facility based on identified parameter limits, and presented a detailed test plan identifying the number of tests to be

conducted, the configuration of the test facility for each test, parameter variations to be tested during each test, and a schedule for all tests. After DoE/METC approved this plan, a detailed design for the test facility was prepared, followed by component fabrication and assembly, and facility construction. This task consumed the first five months of the program, which resulted in a well defined test plan and a facility ready for shakedown tests. The details of this task are reported in Section 2.0 Test Plan Development and Facility Design.

Task 2: Experimental Testing. This task embodied all testing conducted during Phase I (Base) and spanned the last nine months of this element of the actual program. This task contained multiple objectives, which are briefly summarized in the following. The first objective was to perform facility shakedown tests for the purpose of defining facility deficiencies and corrective modifications, and to implement the corrective modifications in order to arrive at a well behaved experimental facility. The second objective was to identify the highest potential application areas by conducting a series of survey experiments using fixed sorbent activation conditions and sulfation conditions reflecting the advanced coal utilization systems identified as potential applications for the Two-Step Rapid Sulfur Capture process. The third objective was to perform Two-Step Rapid Sulfur Capture process optimization tests for the highest potential application area. These test results were needed for Task 4 for producing an accurate evaluation, relative to existing sulfur capture technologies, of the economic feasibility of the Two-Step Rapid Sulfur Capture process. The fourth objective was to perform tests that would provide an understanding of the intricacies of the Two-Step Rapid Sulfur Capture process, namely: limestone heat-up, calcination, and sulfur capture reaction mechanisms. These test results were useful for verification of the engineering model developed in Task 3.

The four objectives just outlined were addressed during Task 2 in Phase I (Base) by conducting facility shakedown tests, sulfur capture survey experiments, and optimization tests. The shakedown tests and ensuing facility modifications will not be presented here since they are reported in Section 3.0 Facility Shakedown and Modifications. The following will focus on the survey and optimization tests, much of which will not be discussed elsewhere in this report. Since most of the results acquired during the survey and optimization tests are considered invalid, presentation of quantitative results will be held to a minimum.

Survey Experiments. Referring to Appendix A, a total of 30 tests were conducted during Phase I (Base). Since several parameter variations were examined during each test, a total of 119

cases were explored. Since refinements were made to the experimental test facility throughout the Phase I (Base) effort, a clear demarcation cannot be defined between shakedown and optimization testing. It can be said, however, that most system modifications were completed by Test 16. During Test 16 a brief survey was performed to identify the most favorable conditions (sulfation duct stoichiometry and temperature) for the Two-Step Rapid Sulfur Capture process. Sorbent activation temperature and time were fixed at 2600°K and 10 ms, respectively. These conditions were chosen based on the results of tests conducted prior to Test 16. During Test 16 the sulfation duct temperature was fixed at nominally 1350°K, where chemical equilibrium considerations indicate maximum captures can be expected. Three sulfation stoichiometries were tested, namely ϕ = 0.95, 1.04, and 1.40. As expected from results from the previous batch reactor program [1], the slightly fuel lean stoichiometry (ϕ = 0.95) gave the greatest apparent calcium utilizations. Based on this result most of the remaining experimental studies focussed on optimizing the Two-Step Rapid Sulfur Capture process for stoichiometric and slightly fuel lean applications such as fluidized bed combustors.

Later in the Phase I (Base) testing program, more detailed tests were conducted that attempted to quantify the effectiveness of the Two-Step Rapid Sulfur Capture process when applied to the applications defined earlier in Figure 2-1. Test 26 explored diesel and fixed bed gasifier effectiveness. Test 27 explored gas turbine effectiveness and Test 28 explored the effectiveness of the Two-Step Rapid Sulfur Capture process when applied under entrained bed, fluidized bed combustor, and fluidized bed gasifier conditions. These tests confirmed that the greatest apparent calcium utilizations occurred under fluidized bed combustor conditions, which substantiated devoting most optimization testing to slightly fuel lean sulfation duct stoichiometries with sulfation temperatures in the range 1100 - 1400°K.

Optimization Tests. Sulfur capture optimization tests were performed during Tests 17 through 25 and 29 through 30. These tests were conducted under slightly fuel lean sulfation conditions with sulfation gas temperatures in the range 1100 - 1400°K. These conditions reflect those of fluidized bed combustor applications. The system was operated in three different modes during this testing, namely: Two-Step Rapid Sulfur Capture (TS), Non-Equilibrium Sulfur Capture (NE), and Activation (Act.) modes. TS mode operation was achieved by injecting SO_2 into the side duct burners. The side duct burners were on, thereby producing elevated temperature, sulfur containing, simulated flue gases. The NE mode was achieved by injecting

SO_2 into the oxidizer flow of the carrier burner in the sorbent activation module. The side duct burners could be either on or off. The Act. mode was achieved by injecting no SO_2 into the system. The side burners could be either on or off.

The TS mode testing dominated the focus of the optimization testing. The influence of activation conditions and sulfation conditions were investigated to define process parameter combinations that produced optimum sulfur capture and calcium utilization. Although TS mode testing was the focus of the optimization tests, NE and Act. tests were performed also. Act. tests were performed to obtain the properties (degree of calcination, specific surface area, porosity, and pore volume) of the sorbent just after activation, yet without/before sulfation. NE tests were performed to verify if this phenomena, which was observed in the batch reactor[1], was present in the present continuous flow system.

The parameters influencing Two-Step Sulfur Capture performance are: activation temperature (T_{act}) and time (τ_{act}); activation burner stoichiometry (ϕ_{act}); interface module mixing effectiveness; sulfation duct sulfur gas concentration; sulfation duct temperature (T_s) and time (τ_s); sulfation duct stoichiometry (ϕ_s); and sulfation duct calcium to sulfur molar ratio (Ca/S). The parameters dictating mixing section effectiveness are the mass flow ratio of side duct burner flow to activation burner flow and mixing section jet injection angle (θ). Sorbent properties, such as sorbent type (limestone, hydrated lime, etc.), sorbent size, and sorbent composition, also influence performance. During Phase I (Base) the mixing section jet injection angle was fixed at 60^o. Table A-1 (Appendix A) lists most of these parameters for each test case. Table 4-1 lists the parameter ranges investigated during Phase I (Base).

A broad range of tests were conducted during the Phase I (Base) effort beyond the tests which specifically addressed process optimization via process parameter variations. These studies were done to characterize system component behavior and to develop an better understanding of calcination, mixing, and sulfation processes. With SO_2 injected through the carrier burner and without sorbent injection, radial SO_2 profiles were measured at various distances downstream of the mixing section inlet. This was done to obtain a mixing time for the 60^o mixing section. Streamwise sulfation duct temperature profiles were measured during each run to quantify the thermal history during sulfation. Calcium balances were performed after several tests to quantify

Table 4-1. Parameter Ranges for Phase I (Base) Optimization Testing.

Parameter	Range		
Activation Burner			
ϕ_{act}	0.9 - 1.2		
T_{act} (^{o}K)	1300 and 2000 - 2800		
τ_{act} (ms)	0 - 40		
Sorbent	Marblewhite Limestone	Linwood Hydrated Lime	Vicron 45-3 Limestone
Sorbent Size (mesh)	325	200	325
Sorbent Cut (full/μm)	Full & ≤ 5 15-25 25-45	Full	Full
Mixing Section			
Injection Angle (Deg.)	60		
Sulfation Duct			
ϕ_s	0.8 - 1.0		
T_s (^{o}K)	TS Mode NE Mode Act. Mode	900 - 1450 500 - 1450 450 - 1300	
Ca/S	1.0 - 3.0		
Sulfur Gas	SO_2 or H_2S (mostly SO_2)		
Sulfur Gas Concentration	1,050 - 10,680 (ppmv)		

the amount of sorbent deposited to various surfaces in the system. Mixing section deposits were of greatest interest since a fine balance exists between satisfactory quench-flow/activation-flow mixing time and sorbent segregation to mixing section walls. The ratio of quench flow rate to activation burner flow rate was varied to produce different mixing time scales in order to examine the influence of quench time on Two-Step and Non-Equilibrium Sulfur Capture performance. Stoichiometry checks were made during a major fraction of the Phase I (Base) tests by monitoring combustion product species via on-line gas analyzers. The effect of sorbent loading on carrier activation burner and ensuing sulfur capture performance was investigated. Sorbent loading is define as the ratio of the mass flow rate of sorbent to the mass flow rate of the carrier burner reactant gases. Activation burner NO_x measurements were made while varying activation burner equivalence ratio. This was important to do because the activation burners were operating in a temperature regime where thermal NO_x production could be significant. Not only were different sorbents tested, but the sulfur capture performance of different cut sizes of Marblewhite 325 limestone were investigated. Based on the range of tests conducted, a very comprehensive data base was developed characterizing parametric influences on the Two-Step Rapid Sulfur Capture process.

Task 3: Two-Step Rapid Sulfur Capture Mechanism. This task was performed in parallel with Task 1, Test Plan and Test Facility Design and Fabrication, and Task 2, Experimental Testing. The results of this effort are described in Section 6.0 of this report. The point of this task was to develop a predictive computer model describing the Two-Step Sulfur Capture process. The model includes sorbent heat-up mechanisms and calcination and sulfur capture reactions. This model was intended to be used for providing design information for development of the injection unit to be installed in the proof-of-concept facility during Phase II. This model was used, however, to design the injection system for the experimental test facility used during the Phase I effort.

Task 4: Feasibility/Applicability Study. This task was performed in the later stages of the Phase I (Base) effort. The results of this study are summarized in Section 7.0. Since the Two-Step Sulfur Capture Process was ultimately shown to yield unsatisfactory performance, thus poor economic feasibility, Section 7.0 briefly describes the less-than-satisfactory economics of this sulfur removal technology. It does not contain the details describing the methodology used to

derive the economics of this process. Rather, Appendix I gives the original feasibility analysis that was done prior to discovery of the ancillary experimental effect, which was when it looked as though this process could produce 96% sulfur capture at Ca/S = 2, or a utilization of 48%. These results have since been shown to be false.

Phase I (Base) Summary. During this phase of the overall program a detailed test plan was constructed, a reasonably well behaved experimental test facility was designed and made operational, a detailed and extensive test matrix was executed providing a comprehensive data base for the Two-Step Rapid Sulfur process, an engineering model of the process was developed, and a feasibility study was performed. Albeit, the best performance measured during the Phase I (Base) program of the Two-Step Rapid Sulfur Capture process fell short of what the Batch Reactor program[1] said should be achievable (i.e., the best calcium utilization (apparent) achieved during the Phase I (Base) program was 48%, while the Batch Reactor program[1] said 90% should be achievable). Although the Phase I (Base) results suggested the Two-Step Rapid Sulfur Capture process would be economically competitive with the Riley Stoker LIMB process, a 50% increase in utilization would be needed to be competitive with wet FGD and in-bed desulfurization technologies. If the utilization achieved in the Batch Reactor program[1] could be achieved in the Two-Step Rapid Sulfur Capture process, then this technology would have significant advantages over most desulfurization technologies. These considerations made it clear that more development work was needed.

There was an experimental artifact that further reinforced the need for further development work. This artifact would later delineate the devastating ancillary effect that changed the course of this program. Simply stated, the calcium utilizations determined by gas phase analysis (both on-line gas analyzers and gas chromatography) were three to four times greater than those based on chemical analyses applied to collected samples of spent sorbent. This discrepancy was of great concern to TDS since it was unclear which to interpret as the correct result.

The need to achieve higher utilizations and to improve gas and solids sampling techniques (to obtain agreement between utilizations derived from these techniques) formed the basis of the first extension to the Two-Step Rapid Sulfur Capture program, which is referred to in this report as Phase IA. Phase IA is described next in Section 4.2.2.2

4.2.2.2 Phase IA Study

The best apparent, yet erroneous, Two-Step Rapid Sulfur Capture performance measured during Phase I (Base) was 96% at Ca/S = 2 or, equivalently, a calcium utilization of 48%. This utilization falls short of the utilization that the Batch Reactor program[1] says should be possible by nominally a factor of two. TDS recognized that further work was required to achieve higher Two-Step Rapid Sulfur Capture performance. Since the activation process is key to achieving better sulfur capture performance, it was clear that future work should be designed to provide a better understanding of the activation process. The most sensitive tests for investigating the activation process were determined to be Non-Equilibrium Sulfur Capture and sorbent activation studies. Furthermore, the Phase I (Base) sulfur captures determined by gas phase analysis (i.e., by on-line gas analyzer) were found to be a factor of three to four greater than those determined by chemical analysis of collected spent sorbent. Based on these considerations, the main objectives of the Phase IA effort were to perform Non-Equilibrium and sorbent activation studies to obtain a better understanding of the activation process and, at the same time, to optimize the activation process and resolve the discrepancy between utilizations derived via gas phase and spent sorbent analyses.

Phase IA Testing: Referring to Figure 4-1, the Phase IA element of the actual program was a three month effort that began at the conclusion of the Phase I (Base) effort. Phase IA was strictly an experimental effort. The tests conducted during Phase IA were designed to answer many questions. For example, will Non-Equilibrium sulfur Capture be observed in the Two-Step Sulfur Capture facility? If not, why not? If Non-Equilibrium Sulfur Capture is observed, is it occurring under the temperature and time conditions observed in the Batch Reactor[1] program, and is the calcium utilization level similar to the 90% level observed in the Batch Reactor program? If the answer to the two previous questions is yes, then why aren't the Two-Step Sulfur Capture utilizations higher than 50%? The answer to this question might result in significant improvements in the Two-Step Rapid Sulfur Capture process efficiency.

Appendix B gives a summary of the tests conducted during Phase IA. This appendix lists the tests conducted plus, for each test, a synopsis giving test conditions and brief comments. A total of 20 tests were conducted. Since each test included several parameter variations, a total of

75 cases were studied during Phase IA. Table 4-2 lists the parameter ranges investigated during Phase IA.

Non-Equilibrium Sulfur Capture studies were the main focus of the tests conducted during Phase IA. During these tests the activation time was varied over the range $0 \leq \tau_{act} \leq 40$ ms and the activation temperature was varied over the range $2000 \leq T_{act} \leq 2750^{o}K$, with one point at $1100^{o}K$. The interface module mixing time scale was varied by changing the ratio of the quench flow rate to activation burner flow rate (i.e., m_q/m_a). For most of the Non-Equilibrium Sulfur Capture tests, the side duct burners were off, with only cold nitrogen supplied to the mixing section from the side duct burners. A few Non-Equilibrium Sulfur Capture tests were performed with the side duct burners on, thereby producing elevated temperature sulfation duct conditions. The effects of varying the molar ratio of calcium to sulfur (Ca/S) and SO_2 concentration were investigated also. During these tests sulfur capture was measured by monitoring the reduction in sulfation duct SO_2 concentration when sorbent was cycled on and off. During a few tests, spent sorbent was collected and analyzed for surface area, porosity, pore volume, and pore size.

Since it was important to quantify the influence of activation conditions on the morphology of the activated sorbent particles, sorbent activation tests were conducted during Phase IA also. The parameters varied during the sorbent activation tests, and the range over which these parameters were varied, were almost identical to the parameters and parameters ranges investigated during the Non-Equilibrium Sulfur Capture tests performed during Phase IA. During these tests, activated sorbent samples were collected and analyzed for specific surface area, porosity, pore volume, pore size, and degree of calcination. SEM photographs were taken of some of the activated sorbent to determine if sintering was present. These analyses and resulting sorbent properties give a clear indication if a highly active sorbent is being produced.

Later in Phase IA testing, a series of Two-Step Rapid Sulfur Capture tests were performed to correct the discrepancy between calcium utilizations determined via gas phase and spent sorbent analyses. Thinking at that time raised the possibility that the gas sampling probes, which were cooled with cold water, could be condensing the moisture in the sulfation duct gases, thereby providing conditions where in-probe wet scrubbing could occur. The presence of this sulfur capture mechanism could explain the factor of three to four difference in calcium utilizations

Table 4-2. Parameter Ranges for Phase IA Activation Optimization Testing.

Parameter	Range	
Activation Burner		
ϕ_{act}	0.9 - 1.1	
T_{act} (^{o}K)	1100 and 2000 - 2750	
τ_{act} (ms)	0 - 40	
Sorbent	Marblewhite Limestone	
Sorbent Size (mesh)	325	
Sorbent Cut (full/μm)	Full	
Mixing Section		
Injection Angle (Deg.)	60	
Sulfation Duct		
ϕ_s	TS Mode	0.96 - 0.98
	NE Mode	0.98 (Side Burners On) or n/a (Side Burners Off)
	Act. Mode	0.98 (Side Burners On) or n/a (Side Burners Off)
T_s (^{o}K)	TS Mode	1035 - 1325
	NE Mode	375 - 1080
	Act. Mode	470 - 1330
Ca/S	1.0 - 3.0	
Sulfur Gas	SO_2	
Sulfur Gas Concentration	590 - 9110 (ppmv)	

determined via gas phase analyses and spent sorbent analyses. The first test attempted to verify if in-probe wet scrubbing was taking place by using ceramic lined gas sampling probes that were cooled with 100°F water. This approach attempted to eliminate condensation in gas sampling lines until the sample gas reached a membrane dryer where the moisture could be extracted from the gas. A noticeable decrease in calcium utilization was measured when the probes were ceramic lined and cooled with 100°F water.

For the range of sulfation duct stoichiometries associated with Two-Step Sulfur Capture process ($0.8 \leq \phi_s \leq 1.0$), the dew point of the sulfation duct gases was determined to be nominally 150°F. To ensure that the gas sampling probes were maintained above the dew point, inline water heaters were installed in the water cooling lines supplying cooling water to the gas sampling probes for the next series of Two-Step Rapid Sulfur Capture tests. During these tests the activation conditions were set at T_{act} = 2600°K and τ_{act} = 10 ms, the sulfation temperature was T_s = 1375°K, and Ca/S = 2. Two-Step Rapid Sulfur Capture tests were then conducted while varying the gas sampling probe cooling water temperature over the range 70 - 150°F. The apparent sulfur capture determined by gas phase analysis (i.e., by an online SO_2 gas analyzer) decreased smoothly with increasing cooling water temperature and demonstrated an abrupt drop when the dew point was encountered. Under the Two-Step Rapid Sulfur Capture operating conditions noted above, the apparent sulfur capture dropped from 65% to 20%. These results clearly showed that very significant in-probe wet scrubbing was occurring. They also characterize the ancillary effect that changed the course of this program. From this point on in Phase IA, all gas sampling probes where cooled with nominally 150°F water to eliminate in-probe scrubbing. This practice brought gas and solids analyses based utilizations into agreement. The results of this in-probe study will be discussed further under "Phase IA Summary."

After resolving the discrepancy between gas and solids analyses based calcium utilization measurements, Phase IA was concluded by performing a limited series of optimization tests to investigate the actual performance of Two-Step Rapid Sulfur Capture and Non-Equilibrium Sulfur Capture processes, with some activation tests to characterize activated sorbent properties. As alluded to earlier, the results of these tests were not at all encouraging. The best Two-Step Sulfur Capture utilizations were no better than 12%. The best Non-Equilibrium Sulfur Capture utilizations were no better than 10%. Since elevated heating rates of limestone particles by

radiative heat fluxes emanating from activation and sulfation duct walls could result in particle sintering, thus reduced sulfur captures, some of the tests in the later part of Phase IA were devoted to investigating whether cold walls, versus hot walls, influenced Two-Step Rapid Sulfur Capture performance. Cold wall conditions were achieved by performing sulfur capture experiments immediately after lighting and adjusting system burners. Doing so did not allow time for the internal walls of the system to achieve elevated temperatures, thus significant radiative heat flux levels. Cold wall conditions did not yield utilization results that differed significantly from the hot wall results.

Phase IA Summary. The main focus of the Phase IA study was to perform a more detailed study of the sorbent activation process, with the goal of gaining a better understanding of this process and, ultimately, to determine activation conditions that would yield optimum/improved Two-Step Rapid Sulfur Capture performance. After correcting the in-probe wet scrubbing problem, the best Non-Equilibrium Sulfur Capture performance occurred at an activation temperature of 2600^{o}K, an activation time of 10 ms, and a Ca/S of nominally 1. The Non-Equilibrium Sulfur Capture calcium utilization measured under these conditions was only 9-10%. These tests indicated that activation temperature had a weak effect, while activation time had a moderate influence (utilizations decreased with increasing time, which is indicative of sintering). The best Two-Step Rapid Sulfur Capture performance occurred at an activation temperature in the range 2200 - 2600^{o}K (weak activation temperature effect), an activation time of 10 ms, and a Ca/S of nominally 2. It should be noted that varying Ca/S had a weak effect on calcium utilization. The Two-Step Sulfur Capture calcium utilization measured under these conditions was only 11-12%.

The sorbent activation studies revealed the following. SEM photographs of collected activated limestone sorbent indicated that there are more fine particles relative to raw limestone. However, size distribution measurements, by both laser diffraction sizing and mercury porosimetry, indicate that there is little change in size distribution. The difference in these two measurements can be reconciled if it is realized that the fines constitute only a small fraction of the total mass of the sorbent. For an activation temperature of 2600^{o}K and an activation time of 10 ms, the SEM photographs of activated sorbent show that the surfaces of the activated limestone particles appear more fluffy and porous than the raw material. For the same activation

temperature and an activation time of 30 ms, however, the fluffy surface characteristics have disappeared and some spherical particles are apparent, which indicates that sintering occurs at the longer activation times. Despite the appearance of a more porous surface for the 10 ms activation time sample, nitrogen multipoint surface area, adsorption isotherm, and pore distribution analyses indicate that the actual porosity of the activated sorbent is nominally 10% of that calculated from degree of calcination assuming no change in particle size. Thus, the activated limestone has relatively low porosity. Specific surface area results showed that activation at 2200 - 2600°K for 10 - 30 ms does produced a modest increase in surface area. The activated samples had surface areas as high as 14 m^2/gm, as compared with 1.7 m^2/gm for the raw limestone. This increase is due largely to an increase in internal surface area (due to increases in particle porosity) rather than an increase in external area (due to particle shattering). A simple calculation shows that even doubling the number of fine particles leads to a minor increase in surface area. Albeit, the achieved surface areas are nominally a factor 3 - 4 lower that those desirable to yield highly activated limestone sorbent.

The sorbent activation test results clearly showed that low Two-Step and Non-Equilibrium Sulfur Capture utilizations were a result of inadequate increases in activated sorbent specific surface area and porosity. The low porosities and surface areas could be due to particle sintering as a result of slow quenching in the quench/mixing section. Under high temperature activation conditions, the calcination times for limestone particles vary between a few milliseconds for fine particles to tens of milliseconds for larger ones (> 30 μm). The particle temperature may be constrained at the calcination temperature for a while, but once calcination is complete, the particle temperature rises rapidly (in a few milliseconds) to beyond the sintering temperature (> 1500°K). Very fast quenching is needed, with mixing times less than 5 - 10 ms, to prevent significant sintering (it should be noted that some sintering will always occur in a ploydispersed sorbent). As described in Section 2.0, the mixing of three gas streams (activation burner stream and two streams from the side duct burners) occurs in the silicon nitride quench/mixing section. This section was designed to achieve rapid quenching of the activated sorbent with minimal sorbent loss to walls. It is possible that the 60° mixing section was designed too conservatively regarding wall losses and that it may produce a mixing time that is too long.

SO_2 mixing studies were performed during Phase IA to check quench/mixing section time

scales. With no activation duct modules in place, which corresponds to 0 ms activation time, SO_2 was injected with the carrier burner flow and radial profiles of SO_2 concentration were measured 10 cm downstream of the inlet to the quench/mixing section. These radial profiles indicated that gas phase mixing was well underway by this station, implying a mixing time of 20 - 50 ms. The quenching of solid particles, however, should take longer due to two-phase jet penetration into the mixing zone. Solid particle quenching times are estimated to be nominally 50 ms for the 60^o mixing section. Therefore, even for the shortest activation times currently possible, which would be achieved by removing all activation duct modules, the real activation time may be as long as 50 ms.

At this point in the program, two lines of thinking dominated. First, there may be an inherent limitation of the activation process in the Two-Step Rapid Sulfur Capture scheme. If the polydispersed nature of raw limestone is considered, it is conceivable that different combinations of activation temperature and time serve only to activate a specific size cut in the size distribution of the raw limestone. Sizes above this cut are not well activated (low porosity and specific surface area due to low heating rates) and sizes below this cut become sintered because of very high heating rates. Second, if this inherent limitation does not exist, then the low utilizations, specific surface areas, and porosities are due to quench/mixing section characteristics that yield activated sorbent quenching times that are too long, which causes sintering or non-optimum activation. In an attempt to reconcile these differing lines of thinking, a Phase IB plan was developed which would investigate the influence of reduced mixing times on Two-Step Rapid Sulfur Capture performance. This plan was accepted by DoE/METC and was executed after completing a TDS funded Batch Reactor investigation (see Figure 4-1). The Batch Reactor study was performed after the conclusion of Phase IA. The details of the Batch Reactor study follow in Section 4.2.2.3 and those pertaining to the Phase IB effort are described later in Section 4.2.2.4.

Before embarking on a description of the Batch Reactor and Phase IB efforts, the following discussion presents results delineating the ancillary experimental effect (in-probe wet scrubbing phenomena) that completely changed the course of this program. During Phase I (Base) very poor agreement was being found between sulfur captures and calcium utilizations derived from gas phase sulfur species data, which was provided by an online gas analyzer, and those derived from chemical analyses applied to collected spent sorbent. During Phase I (Base) the

solids based utilizations were always a factor of three to four lower than gas phase based results.

During Phase IA it was hypothesized that the high gas phase utilization results could be due to in-probe wet scrubbing effects. This hypothesis was explored by conducting sulfur capture tests at standard conditions (i.e., an activation temperature of 2600°K, an activation time of 10 ms, the sorbent was Marblewhite 325 limestone, sulfation temperatures in the range 1350 - 1425°K, 1500 ppmv SO_2 concentration in the sulfation duct, Ca/S = 2, and a fuel lean sulfation duct stoichiometry (5% O_2) while varying the cooling water temperature of the farthest downstream gas sampling probe. The dew point for the sulfation duct gases under standard conditions is approximately 150°F. In order to avoid condensation in the gas sampling probe, the probe temperature must be maintained above 150°F before the moisture is removed in the downstream membrane dryer. In tests prior to these in-probe scrubbing tests, the gas sampling probes were running at 70 - 100°F, thus condensation could have been occurring.

Figure 4-2 presents Two-Step Sulfur Rapid Sulfur Capture results for the standard conditions noted above while the cooling water temperature to the gas sampling probe was varied between 67 and 152°F. As can be seen, the sulfur capture decreases smoothly with increasing cooling water temperature until the dew point temperature is reached. As the dew point is traversed, the sulfur capture drops suddenly with increasing temperature. This figure clearly demonstrates that in-probe wet scrubbing has been occurring in most earlier tests. These results also demonstrate that good agreement between solids and gas phase based calcium utilizations can be achieved when condensation is avoided in the gas sampling probes. The discovery of this effect, which has been referred to previously as the "ancillary experimental effect," had a very severe impact on this program. Previously, utilizations as high as 48% were being observed. After removing in-probe scrubbing effects, utilizations no greater than 11 - 12% have been obtained.

A fair question to ask is: why was this effect not discovered earlier? The reason is that in-probe scrubbing only occurs when limestone is flowing. For example, good SO_2 baseline data (no sorbent flowing) was obtained with cold probes both before injecting sorbent and after terminating sorbent flow. In fact, with the cold probes, SO_2 levels rose quickly after terminating sorbent injection. This implies that the SO_2 capture was due to formation of a water mist (two-

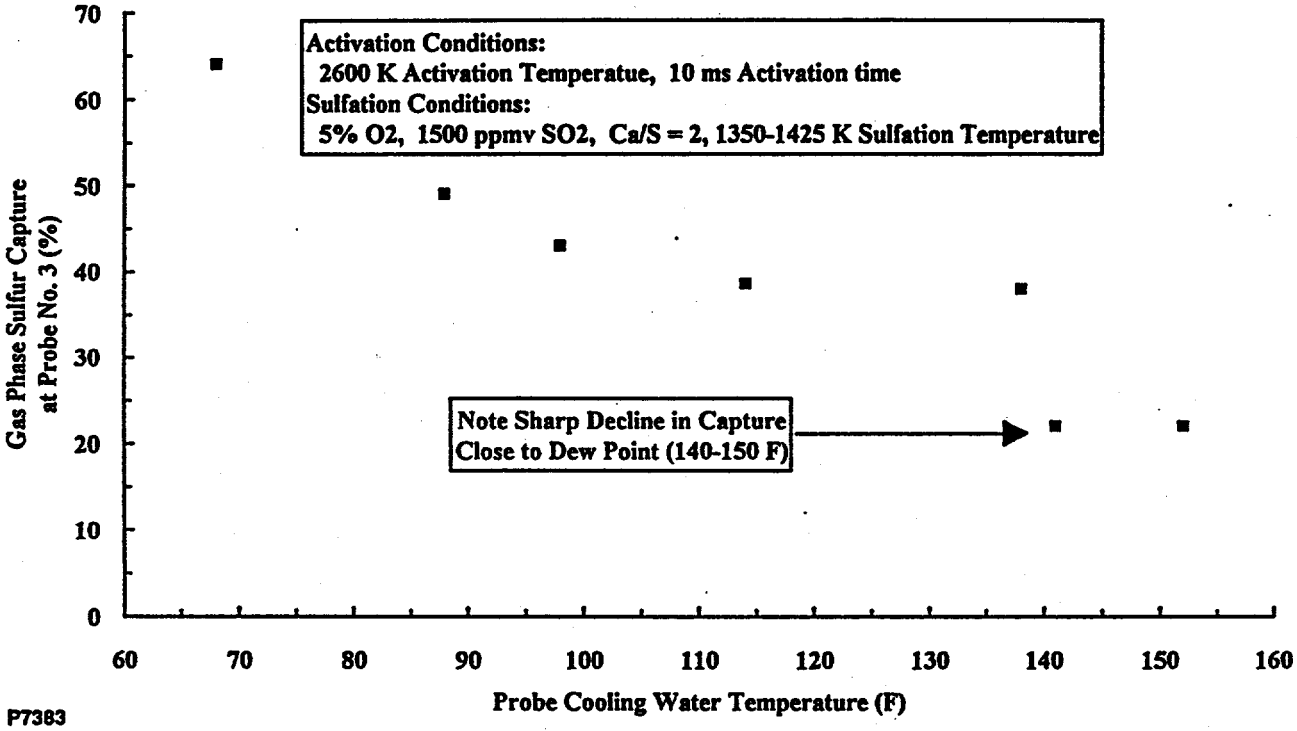

Figure 4-2. Effect of Probe Cooling Water Temperature on Apparent Sulfur Capture.

phase phenomenon) in the sample gas, rather than condensation of the internal surfaces of gas sampling probe. Until these in-probe scrubbing tests, these facts misled TDS into believing the cold probe utilization results. The low utilizations based on spent sorbent chemical analyses from earlier tests was a concern, but was not taken as the most reliable measure because of problems with the solids sampling system. Most of the solids sampling problems were corrected during Phase IA.

Since in-probe scrubbing was found to have a drastic effect on gas phase based utilizations measured during the Two-Step Rapid Sulfur Capture program, and since even higher utilizations were measured during the Batch Reactor program[1], the natural question to ask is: was in-situ wet scrubbing occurring in the batch reactor, thus leading to high utilizations? In order to verify of refute earlier batch reactor results, a brief TDS funded batch reactor study was performed. The results of this study are discussed next.

4.2.2.3 Batch Reactor Study

As noted above in Section 4.2.2.2, wet scrubbing effects in gas sampling probes masked actual Two-Step Rapid Sulfur Capture performance during a major portion of this program. It was natural to ask whether the wet scrubbing phenomena could have occurred in the cold wall vessel or gas sampling systems during the previous DoE/METC Batch Reactor program[1]. To answer this question, and to either refute or substantiate the results of the previous study, TDS conducted a brief internally funded batch reactor study following the conclusion of Phase IA. The new batch reactor study lasted three months.

Figure 4-3 presents a schematic of the batch reactor apparatus. Figure 4-4 presents a sketch of the associated gas sampling system. The batch reactor test rig was designed to be a very simple, uncomplicated apparatus. Referring to Figure 4-3, preparation and execution of a batch reactor test involved placing a known amount of limestone sorbent on the screen at the base of the test chamber, evacuating the test chamber and back-filling it to the desired pressure with oxidizer and sulfur gas constituents, then cycling the high pressure reservoir valve to admit fuel species into the chamber, allowing a reasonable amount of time for gas phase species and sorbent powder to mix, then igniting the mixture by means of a spark plug device. Issuing the fuel gases

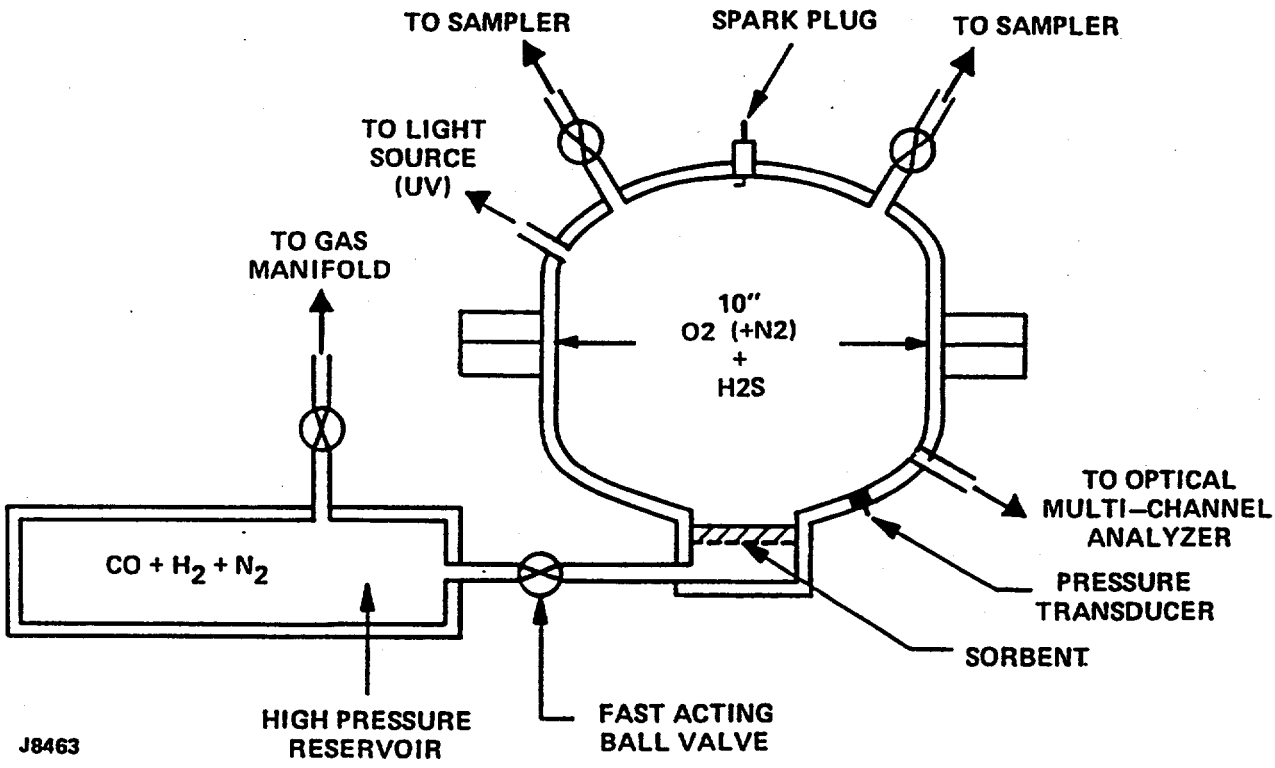

Figure 4-3. Batch Reactor Experimental Apparatus.

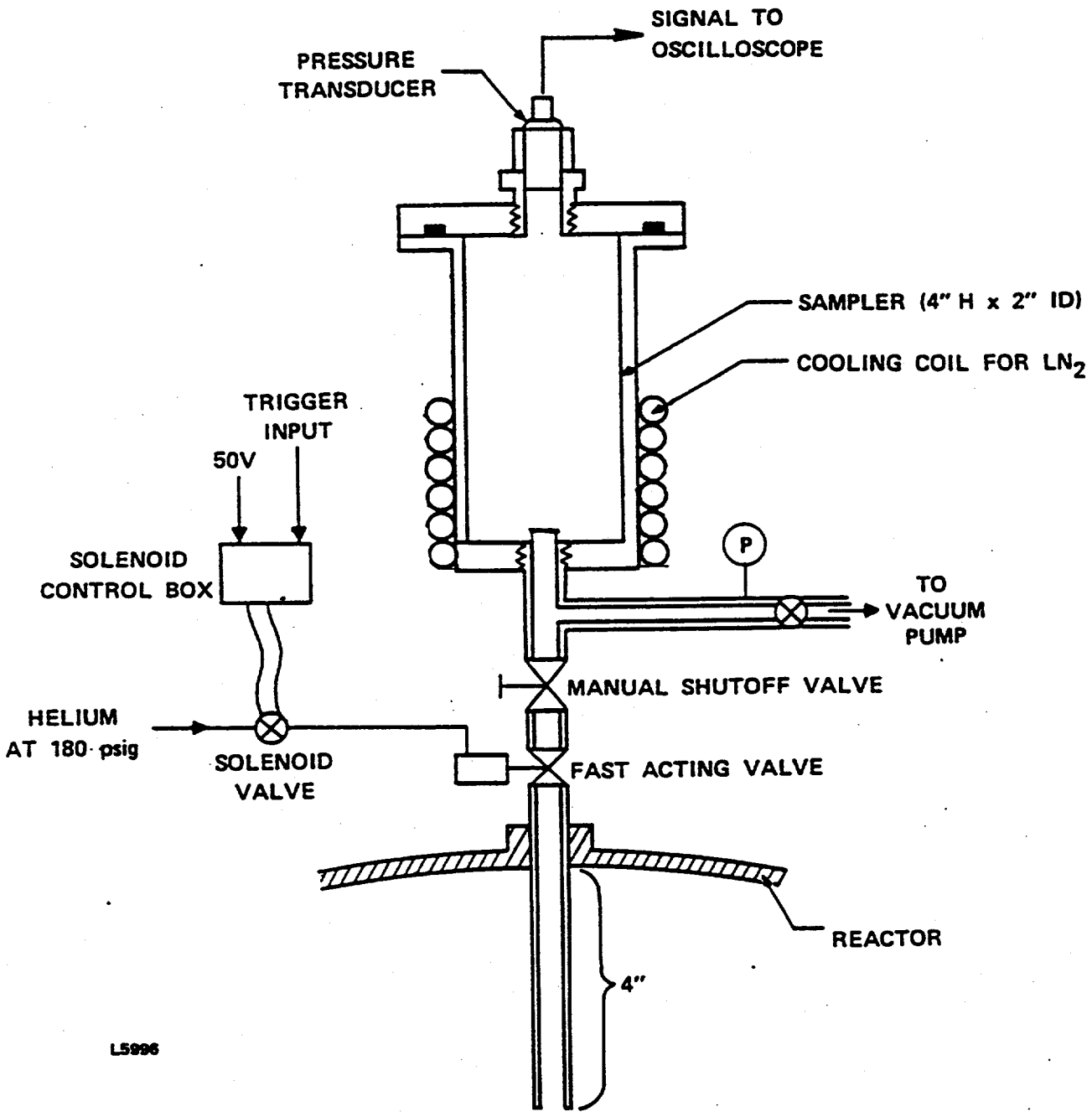

Figure 4-4. Batch Reactor Rapid Gas Sampler.

through the screen at the base of the batch reactor entrains the sorbent in the incoming flow. This process ensures that the sorbent becomes well dispersed in the batch reactor gases after a reasonable mixing time. The ensuing combustion would typically produce peak temperatures of 2600°K and pressures of 20 atm. Sulfur capture was measured as a function of time after ignition by three rapid gas samlpers. A sketch showing the features of a rapid gas sampler is given in Figure 4-4. At predefined delays after ignition, each sampler would be cycled. In this way sulfur capture could be determined as a function of time after ignition. Two different kinds of rapid samplers could be used. The small rapid sampler was used to acquire a gas sample adequate to determine sulfur gas content by gas chromatography. The volume of the small sampler was 100 cm^3 and the sampling time was nominally 4 ms. The large rapid sampler had a volume of 500 cm^3 and was used to collect solids samples. It had a sampling time of nominally 10 ms. Both samplers were cooled by liquid nitrogen in order to rapidly quench reactions that otherwise may take place after a sample has been acquired. As suggested above, gas chromatography is used to analyze acquired samples for H_2, O_2, N_2, CO, CO_2, H_2S, COS, and SO_2. Sulfur reduction is determined by using N_2 as a tracer gas. For a more detailed description of this apparatus see reference 1.

In order to achieve repeatable ignition in the batch reactor, a certain level of hydrogen must be included in the fuel gases. During the Batch Reactor program[1], the added hydrogen resulted in a combustion product moisture content of approximately 8.4%. The batch reactor tests performed after the conclusion of Phase IA were designed to minimize the moisture in the system, thereby reducing the possibility of condensation occurring at various points in the system (i.e., on the walls of the batch reactor chamber or in the gas samplers). The batch reactor tests conducted just after Phase IA used only enough hydrogen in the fuel gases to achieve repeatable ignition, which resulted in combustion product moisture levels of approximately 1.6%. Thus, the new batch reactor tests were conducted with a factor of five reduction in combustion product moisture relative to the old tests. During the new tests, all other system parameters were made identical to those used during the old tests, namely: T_{max} = 2600°K, P_{max} = 20 atm, ϕ = 1.0, Ca/S = 1.0, and Marblewhite 325 limestone was used as the sorbent. The sulfur gas was H_2S.

Figure 4-5 compares the new batch reactor data (ND - new data, LM - low moisture case) with the old data (OD - old data, HM - high moisture case). Both large (LS) and small (SS)

sampler data are presented. If attention is focused on the small sampler data (open squares (OD, HM) and open circles (ND, LM)), the sulfur capture for the new low moisture data peaks between 30 and 35 ms, whereas the old data peaks around 40 ms. The magnitude of the peak in sulfur capture for the new data seems to be approximately 60% in contrast to 90% for the old data. Reducing system moisture appears to have reduced the sulfur capture by approximately 30%. Although the large samplers provide a less reliable measure of sulfur capture due to their longer sampling time, their data also show a reduction in sulfur capture with decreasing system moisture. The results presented in Figure 4-5 imply that system moisture influences sulfur capture in batch reactor experiments.

Two explanations for the observed moisture influence can be formulated. First, and the most difficult to quantify and believe, is that sulfur/calcium reactions are occurring in the samplers. Recall that these samplers are subcooled using liquid nitrogen in order to quench reactions that would otherwise take place after a sample has been acquired. Since the sulfur capture measured by the samplers shows temporal changes, they appear to be reflecting changes in the batch reactor sulfur concentration, which qualitatively suggests that moisture influences are taking place in the batch reactor, not in the samplers. The second possibility is that condensation is forming either on the cold walls in the batch reactor or in a thin layer adjacent the cold walls. If this is occurring, the following process can be imagined. Prior to combustion initiation, a fast acting valve admits the fuel gases through a screen supporting the limestone sorbent and into the batch reactor chamber. The velocity of the incoming gases can be significant. This inflow produces a toroidal vortex in the spherical batch reactor chamber, which would tend to force the limestone particles to segregate to wall regions. Upon ignition, a combustion wave propagates, probably in a spherical manner, across the batch reactor chamber. A transient flow field is established, which generates modest velocities and significant wall currents. Condensation of the moisture in the combustion products then occurs on the cold walls of the reactor chamber and/or a mist forms in a thin layer adjacent the cold walls. Once condensation has formed, conditions are appropriate for wet scrubbing.

The wet scrubbing scenario seems like a plausible explanation for the high sulfur captures observed in the batch reactor, yet an argument must be presented that explains the transient nature of the peak in sulfur capture and the following decrease in sulfur capture. Since it takes time to

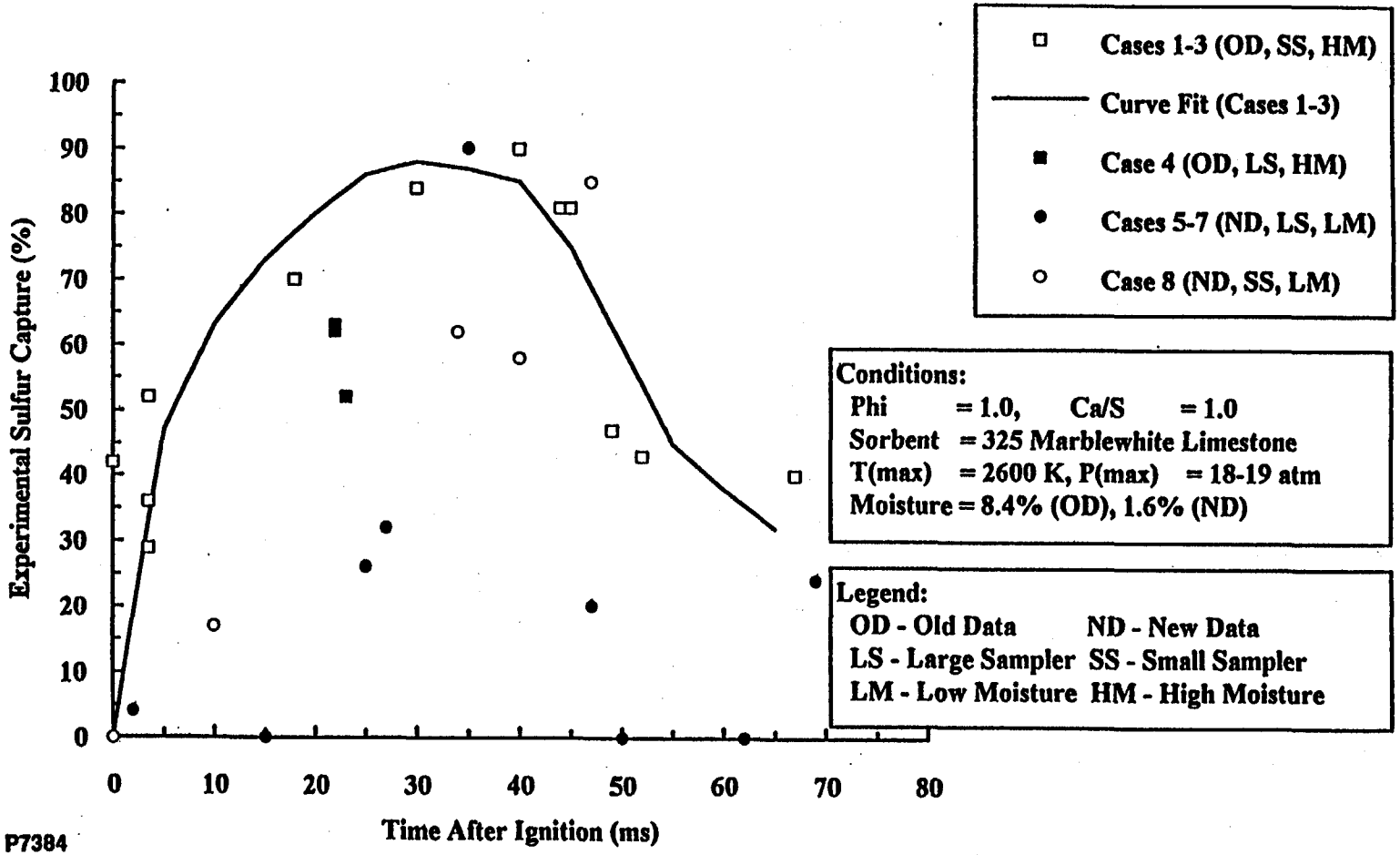

Figure 4-5. Effect of System Moisture on Batch Reactor Sulfur Capture.

establish the appropriate conditions for wet scrubbing to occur, a temporal increase in sulfur capture is expected. The fact that a maxima in sulfur capture occurs and that sulfur capture decreases following the peak implies that the conditions in the batch reactor are changing towards conditions that are no longer appropriate for wet scrubbing. There are two possible, and probably coupled, phenomena that could reduce the wet scrubbing effect. First, the wall temperature has risen to the point where condensation can no longer take place. Second, the transient flow field has decreased in strength so that the sorbent is no longer segregated in wall regions. Once these phenomena appear, any capture occurring previously is reversed due to mixing with the hot gases outside of near-wall regions.

The only phenomenon that can be partially quantified is the transient behavior of batch reactor wall temperature. The dew point for the high moisture case in Figure 4-5 is approximately 116^{o}C. The dew point for the low moisture case is 71^{o}C. If it can be shown that wall temperature increases by 50 - 100^{o}C in 35 ms (i.e., the time it takes to observe a peak in sulfur capture), then the wet scrubbing phenomena could be substantiated. To obtain an estimate of the surface temperature rise after 35 ms, the solution to the transient semi-infinite slab heat transfer problem with a convection boundary condition may be used. In order to use this solution, an estimate is needed for the hot gas side Nusselt Number. This requires computing a Reynolds number, which requires knowing a characteristic velocity. This velocity may be approximated by knowing the time it takes for the combustion wave to traverse from the ignition point to the opposite side of the chamber. Pressure trace data implies that this velocity is nominally 70 m/s. The Reynolds Number based on this velocity, the radius of the batch reactor chamber, and film properties of the combustion products is approximately 525,000. Using a flat plate or pipe Nusselt Number correlation and the estimated Reynolds Number yields a Nusselt Number of approximately 750. Using this Nusselt Number, the thermal conductivity and diffusivity of 304 stainless steel (i.e., the material of construction of the batch reactor chamber), and the transient semi-infinite slab solution, the temperature rise of the inside surface of the batch reactor chamber is estimated to be approximately 35^{o}C. Since this is of the same order as the temperature increases needed to exceed the dew points of the low and high moisture cases presented in Figure 4-5, it seems plausible that condensation effects may be occurring in the batch reactor system.

Since it will take longer to achieve inside surface wall temperatures that exceed the dew

point of the higher moisture case in Figure 4-5 (relative to the low moisture case), the peak in sulfur capture for the high moisture case should appear later than that for the low moisture case. Comparison of the open symbols in Figure 4-5 tends to support this. Since the new batch reactor data indicates that reducing combustion product moisture leads to reduced sulfur captures and reduced peak sulfur capture times, and since the estimate for wall temperature rise after 35 ms presented above implies that wet scrubbing effects should decrease at times later than 35 ms, there is some evidence suggesting that wet scrubbing effects may have interfered with true measurements of sulfur capture in the current and previous batch reactor investigations. Based on these considerations, the present and previous[1] batch reactor data should be considered questionable. Although not possible at this time, and something which was not done during the previous batch reactor studies, it would be very interesting to repeat the low moisture case with the batch reactor chamber walls heated to nominally 100°C. This would have been the definitive experiment regarding batch reactor wet scrubbing phenomena.

Since the scenario described above is somewhat speculative (i.e., wall heating results in reduced wet scrubbing capture, thus a peak in transient sulfur capture), and since the new batch reactor experiments still produced high sulfur captures, even under a factor of five reduction in system moisture, TDS defined an experimental test plan designed to explore the last avenue that could be limiting Two-Step Rapid Sulfur Capture performance. At the close of Phase IA, after eliminating gas sampling probe wet scrubbing effects, the best calcium utilizations produced by the Two-Step Rapid Sulfur Capture process were only 10 - 12%. By the conclusion of Phase IA, it was found that activation temperature had a weak effect on calcium utilization, activation time had a modest effect on calcium utilization (with indications that longer times resulted in sorbent particle sintering), and that mixing studies suggested that the quench section was producing mixing times that probably extended the activation time by as much as 50 ms. These considerations suggest that more rapid quenching of the activated limestone sorbent may lead to improved Two-Step Rapid Sulfur Capture performance, i.e., higher utilizations. The plan submitted to DoE/METC for Phase IB, the last program extension, was designed to investigate sulfur capture and calcium utilization under improved/reduced quench section mixing times. This plan was approved by Doe/METC and performed under Phase IB. The structure of Phase IB is discussed next.

4.2.2.4 Phase IB Study

Referring to Figure 4-1, the Phase IB extension commenced nominally six months after the conclusion of Phase IA and three months after the conclusion of the Batch Reactor study. The technical effort had a duration of nine months, with the balance (six months) devoted to constructing a final report that reflects the technical progress and results of the entire effort. Since a major fraction of the results obtained during Phase I (Base) and Phase IA were erroneous due to the in-probe wet scrubbing effect discovered near the end of Phase IA, the results of the Phase IB study constitute the only data, for the most part, which are presentable. This section, therefore, presents the objectives and structure of the Phase IB study, while Section 5.0 "Experiments" presents the results of the Phase IB effort. Very little from the Phase I (Base) and Phase IA studies will be presented in Section 5.0.

The overall objective of the Phase IB extension was directed towards improving activated sorbent quenching for the purpose of increasing Two-Step Rapid Sulfur Capture calcium utilization. Tests conducted during Phase IA using the two-step sulfur capture facility have produced calcium utilizations that are less than 15%. Analysis of activated limestone samples showed low porosity (< 10%) and a relatively low specific surface area (< 15 m^2/gm), while chemical analysis showed up to 90% degree of calcination. Since the theoretical porosity at 90% degree of calcination is almost 45%, it appears that calcine sintering may be responsible for the low calcium utilizations observed. Particle sintering can be avoided by affecting rapid quenching of the two-phase sorbent jet exiting the activation burner by lower temperature sulfur containing gases, thereby producing sorbent of increased surface area, thus increased activity.

As stated under "Phase IA Summary" in Section 4.2.2.2, calcination times for limestone particles vary from a few milliseconds (for fine particles) to tens of milliseconds for large particles (< 30 μm) under high temperature activation conditions. Therefore, very fast quenching is needed, with mixing times less than 5 - 10 ms, to prevent significant sintering. As described in Section 2.0, the mixing of three gas streams (activation burner stream and two streams from the side duct burners) occurs in the silicon nitride quench/mixing section. This section was designed to achieve rapid quenching of the activated sorbent with minimal sorbent loss to walls. It is possible that the 60^o mixing section was designed too conservatively regarding wall losses and

that it may be producing mixing times that are too long. Based on SO_2 mixing studies performed during Phase IA, the quenching time for the 60^o mixing section has been estimated to be 50 ms. This rather long mixing time could certainly account for the low specific surface areas and porosities observed in Phase IA.

The primary objective during Phase IB was to determine optimum quench conditions for the activation/sulfation conditions that gave the highest SO_2 captures during Phase IA. Investigating optimum quench conditions involved redesigning the silicon nitride quench/mixing section. Three new silicon nitride quench/mixing sections were designed and fabricated, which are discussed in Section 2.3.7. The number of quench jets in the quench/mixing section and their diameter, injection angle, and pattern were redefined based on a TDS computer code. The ultimate goal was to effect more rapid quenching of the two-phase sorbent jet exiting the activation burner. Mixing effectiveness, or aggressiveness, was found to be a strong function of quench jet injection angle. It was found that sorbent segregation to walls and mixing section recirculation were a function of injection angle also. The reason for fabricating three new quench/mixing sections, therefore, was to allow quench study flexibility recognizing that mixing aggressiveness and sorbent wall deposition are coupled processes.

Based on the previous results of Phase I (Base) and Phase IA, the important Two-Step and Non-Equilibrium Sulfur Capture parameters were determined to be: T_{act} - activation temperature, τ_{act} - activation time, Ca/S - calcium to sulfur molar ratio, ϕ_s - sulfation duct stoichiometry, T_s - sulfation duct temperature, and sorbent characteristics (chemical composition and size distribution). Optimum Two-Step Rapid Sulfur Capture calcium utilizations were found to occur at sulfation duct stoichiometries that were slightly fuel lean (4 - 6% O_2) and for sulfation duct temperatures in the range 1000 - 1400^oK. Based on this, the Phase IB Two-Step Rapid Sulfur Capture test matrix was limited to sulfation duct stoichiometries in the range $0.75 < \phi_s < 0.85$ and temperatures in the range $1100 < T_s < 1400$. The activation burner stoichiometry was fixed at $0.92 < \phi_{act} < 0.97$. Since varying Ca/S had a weak effect on calcium utilization, Ca/S was held near unity during the Phase IB tests. The main parameters varied during the Phase IB Two-Step Rapid Sulfur Capture tests were quench/mixing section jet injection angle ($0 < \theta < 60$), activation temperature (T_{act}) and time (τ_{act}), and sulfation duct temperature (T_s). Since the Non-Equilibrium Sulfur Capture mode gives the most sensitive indication of sorbent activation, Phase

IB included this mode of testing. Since sulfation duct stoichiometry and temperature are not germane to this mode of sulfur capture, this mode of testing was not constrained by the parameter ranges defined for the Two-Step Rapid Sulfur Capture tests. The Non-Equilibrium Sulfur Capture mode tests did conform, however, to the Two-Step Rapid Sulfur Capture mode parameter ranges defined for θ, T_{act}, τ_{act}, ϕ_{act}, and Ca/S. For the most part, Marblewhite 325 mesh limestone was used as the sorbent. Likewise, the full cut of Marblewhite 325 mesh was used. Some tests, however, were conducted using 200 mesh Linwood hydrated lime (full cut) and certain size cuts of the Marblewhite 325 mesh limestone. Table 4-3 lists the parameter ranges investigated during Phase IB.

After discovering the devastating in-probe scrubbing effect, and subsequent realization that the Two-Step Rapid Sulfur Capture process was delivering calcium utilizations that were far below those which would make the process economically viable, the remainder of this program became exploratory in nature. That is, conditions were being sought where the Two-Step Sulfur Capture process may give utilizations comparable to those suggested by previous batch reactor tests. Inasmuch as quench optimization studies were the main thrust of Phase IB, which included Two-Step Rapid Sulfur Capture and Non-Equilibrium Sulfur Capture tests, other tests were conducted to support this thrust and to find parameter conditions that produce batch-reactor like utilizations. In support of quench optimization, SO_2 mixing studies were performed during Phase IB in order to experimentally verify that the new quench/mixing sections were producing shorter mixing times. Spent sorbent deposits on the silicon nitride quench/mixing section walls were monitored to determine if severe sorbent segregation was occurring with the more aggressive quench/mixing sections.

To support exploratory efforts, cut sizes of Marblewhite 325 limestone were tested under Two-Step Sulfur Capture mode operation, as well as using 200 mesh Linwood hydrated lime as the sorbent. Sulfur capture performance using different size cuts of limestone was investigated to obtain information that might reveal inherent limitations of the Two-Step Rapid Sulfur Capture activation process. As noted earlier, the activation process may have limitations due to the polydispersed characteristics of the raw sorbent. That is, for a given set of activation conditions, it is possible that only a narrow band of sizes are being activated. Sizes below this range are probably being sintered, whereas sizes above this range are not experiencing heating rates that

Table 4-3. Parameter Ranges for Phase IB Quench Optimization Testing.

Parameter	Range	
Activation Burner		
ϕ_{act}	0.92 - 0.97	
T_{act} (^{o}K)	1300 and 2200 - 2850	
τ_{act} (ms)	0 - 30	
Sorbent	Marblewhite Limestone	Linwood Hydrated Lime
Sorbent Size (mesh)	325	200
Sorbent Cut (full/μm)	Full & ≤ 5 25-45	Full
Mixing Section		
Injection Angle (Deg.)	0, 15, 30, 60	
Sulfation Duct		
ϕ_s	TS Mode NE Mode Act. Mode	0.75 - 0.85 n/a n/a
T_s (^{o}K)	TS Mode NE Mode Act. Mode	1100 - 1420 530 - 740 520 - 660
Ca/S	0.67 - 1.97	
Sulfur Gas	SO_2	
Sulfur Gas Concentration	1170 - 2100 (ppmv)	

produce high surface area, high porosity, thus highly activated sorbent particles. Examining the sulfur capture characteristics of specific cuts of the raw sorbent provides an indication if this limitation is present. Higher activation temperatures were investigated also during Phase IB to check if higher heating rates produce higher captures. The results of these efforts as well as those addressing the main thrust of the Phase IB study are documented in Section 5.0.

4.2 FOCUS OF PRESENT REPORT

The discovery of the in-probe wet scrubbing effect during the later part of Phase IA rendered most of the results of Phase I (Base) and Phase IA worthless. Thus, very little from Phases I (Base) and Phase IA will be discussed further or presented during the remainder of this report. The main reason for providing a history of this program is to demonstrate the effort invested in uncovering the actual performance of the Two-Step Rapid Sulfur Capture process. As has been shown, a very dedicated effort was applied. Regardless, only pertinent experimental results from Phase IB will be presented in the remainder of this report, which is sufficient to illustrate the viability of the Two-Step Rapid Sulfur Capture process as a sulfur removal technology. Section 5.0 will present the experimental results obtained during Phase IB. Section 6.0, however, presents the progress made during the overall effort towards producing a computer model of calcination and sulfur capture kinetics, which has been most useful during this study as an engineering tool for generating mixing section designs. Section 7.0, which presents the economic feasibility of the Two-Step Rapid Sulfur Capture process, is a brief update of the original study performed during Phase I (Base). The original study is included in this report as Appendix I. This was done to illustrate the methodology used for deriving the economics presented in Section 7.0.

5.0 EXPERIMENTS

5.1 INTRODUCTION

This section presents the results of experimental tests performed during the last portion of this program, i.e. Phase IB (see Section 4.2.2 for the structure of the present program). Only the data from Phase IB will be presented since it was found that much of the data collected in the earlier portions of this program was invalid. The cause of the erroneous results was due to in-probe wet scrubbing effects which corrupted gas phase sulfur capture determinations.

After correcting gas sampling problems, which lead to accurate sulfur capture measurements, the best Two-Step Rapid Sulfur Capture calcium utilization measured just prior to Phase IB (i.e., at the end of Phase IA) was 11 - 12%. This result was achieved at an activation temperature of 2600 ^{o}K, an activation time of 10 ms, an activation burner stoichiometry of nominally $\phi = 0.97$ (with $\phi > 1$ being fuel rich), a Ca/S ratio of 2, a sulfation temperature of 1100 ^{o}C, a sulfation time of 250 ms, and a sulfation duct stoichiometry of nominally $\phi = 0.95$. This result fell very short of the utilizations expected based on batch reactor tests conducted under a previous DoE/METC program,[1] i.e., the batch reactor experiments produced calcium utilizations of nominally 90% under similar activation conditions. It was concluded at the close of Phase IA that the low utilizations may be due to poor quench rates in the mixing section, which may cause sintering of the activated limestone sorbent, or that the activation process, thus the Two-Step Rapid Sulfur Capture process, has inherent limitations. The main thrust of Phase IB was to explore the effect of improved sorbent quench rates. Many other aspects of the Two-Step Rapid Sulfur process were explored during Phase IB, which are reported in this section also. Regardless, the results presented in this section reveal that the Two-Step Rapid Sulfur Capture process has inherent limitations which lead to calcium utilizations that are not sufficient to make this process economically viable.

Given the relatively low calcium utilizations produced by the proposed Two-Step Rapid Sulfur Capture process, it is difficult to quantify mechanisms and associated parametric values from the results presented in this section. When enhanced quenching failed to produce a significant improvement in calcium utilizations, the Phase IB effort became more exploratory in

nature. For these reasons, the results presented in this section are grouped according to the effect a particular process parameter has and observations are given regarding the influence of each parameter. Discussions involving quantification of mechanisms are held to a minimum in order to prevent this section from becoming too speculative.

As noted above, the main thrust of Phase IB was to explore the influence of enhanced quench rates on calcium utilization. There are, however, many process parameters that also influence calcium utilization. Due to program resource limitations, it was not possible to fully explore the influence of all process parameters. Based on results obtained during the earlier portions of this program (namely Phase I (Base) and Phase IA), it was found, fortunately, to be unnecessary to explore all process parameters in order to adequately characterize the performance of the Two-Step Rapid Sulfur Capture process and to illustrate its limitations. The full matrix of process parameters includes: activation temperature (T_{act}), time (τ_{act}), and stoichiometry (ϕ_{act}); activated sorbent jet and quench jets mixing parameters, which includes quench jets injection angle (θ) and the ratio of quench jets mass flow rate to activated sorbent jet flow rate (m_q/m_a); sulfation duct temperature (T_s), time (τ_s), and stoichiometry (ϕ_s); and sorbent type and size distribution.

Based on the results of the Phase I (Base) and Phase IA portions of this program, it was found that the greatest Two-Step Rapid Sulfur Capture calcium utilizations were obtained under slightly fuel lean sulfation conditions. Thus, for the Phase IB tests, the activation burner and sulfation duct stoichiometries were fixed at nominally $\phi_{act} = 0.97$ and $\phi_s = 0.8$. For $\phi_s = 0.8$, the excess oxygen in the sulfation duct is 4% by volume. During the Phase IB tests, the actual excess oxygen levels varied between 4 and 6% by volume when the test rig was operated in the Two-Step Rapid Sulfur Capture mode. Sulfation duct stoichiometry has no meaning when the test rig is operated in the Non-Equilibrium Sulfur Capture mode, since ambient temperature nitrogen is used as the quench gas.

During Phases I (Base) and Phase IA the ratio of the mass flow rate of quench gas to the mass flow rate of the sorbent jet (m_q/m_a) was varied to alter the mixing characteristics in the silicon nitride mixing sleeve in the interface module (see Figure 2-8 for the details of the silicon nitride mixing sleeve and Figure 2-7 for details of interface module). To explore the influence of enhanced mixing during Phase IB, m_q/m_a was held constant, with a value of nominally 8, and

the quench jet injection angle (θ) was varied. The quench jet injection angle (θ) was varied by using four different mixing sleeves, which provided injection angles of θ = 0, 15, 30, and 60°. The angle θ represents the angle between a horizontal reference and the axis of each quench jet.

The Phase I (Base) and IA portions of this program also indicated that optimum calcium utilization occurred at sulfation temperatures near 1100 °C. Thus, most Two-Step Rapid Sulfur Capture tests performed during Phase IB were conducted using T_s = 1100 °C, yet a few tests were conducted with T_s = 900 °C.

Based on the preceding discussion, the following process parameters were held constant during the Phase IB experiments: ϕ_{act} = 0.97, ϕ_s = 0.8, m_q/m_a = 8, and T_s = 900 and 1100 °C. The following parameters were varied: $2200 \leq T_{act} \leq 2850$ °K, $0 \leq \tau_{act} \leq 30$ ms, $0 \leq \theta \leq 60°$, $0 \leq \tau_s \leq 400$ ms, three sorbents were tested (325 mesh Marblewhite and Vicron 45-3 limestone, and Linwood hydrated lime), and three size cuts of 325 mesh Marblewhite limestone were tested (i.e., <5 and 25 - 45 μm, and full size distribution).

The results of the Phase IB tests are presented in the remainder of this section and grouped according to the influence of a parameter or parameters on sulfur capture. The influence of sorbent quench parameters is presented in Section 5.2. The influence of sorbent activation conditions are presented in Section 5.3. The influence of the molar ratio of Ca/S is presented in Section 5.4. The influence of sulfation temperature is presented in Section 5.5. The influence of sorbent size cut is presented in Section 5.6. The influence of sorbent type is presented in Section 5.7. Sorbent properties after activation are presented in Section 5.8.

5.2 INFLUENCE OF SORBENT QUENCH PARAMETERS

The results obtained during Phases I (Base) and Phase IA implied that the activated sorbent leaving the activation module of the Two-Step Rapid Sulfur Capture test rig was not being quenched rapidly enough in the sulfur containing simulated flue gases thereby causing the sorbent particles to sinter. Sintering, in turn, leads to poor calcium utilizations. Two-Step Rapid Sulfur Capture tests were performed in Phase IB that explored the effect that more rapid quenching has on calcium utilizations. Quench rate was adjusted by varying the injection angle of the quench

jets in the mixing sleeve in the interface module. Injection angles of $\theta = 0$, 15, 30, and 60^{o} were tested. The activation time was fixed at nominally $\tau_{act} = 10$ ms, which is where optimum calcium utilizations were observed earlier in this program. The Ca/S ratio was fixed at nominally Ca/S = 1. The sulfation duct temperature was fixed at $T_s = 1100\ ^{o}C$. The sorbent used was uncut 325 Mesh Marblewhite limestone. The only other parameter that was varied during this segment of tests was the activation temperature, which was varied over the range $2200 \leq T_s \leq 2600\ ^{o}K$.

Figure 5-1 presents calcium utilization as a function of activation temperature and quench jet injection angle. The calcium utilization results presented in this figure are based on sulfur captures determined by an on-line SO_2 gas analyzer. The gas analyzer drew sample gas from a probe located near the exit of the sulfation duct. The sulfation time corresponding to this location is nominally 225 ms for the stated conditions. Neglecting the lowest and highest data points (2), we find, given the low levels of measured calcium utilizations, that calcium utilization appears to be unaffected by quench jet injection angle or by activation temperature. For 10 ms activation time, the best utilization, namely 9%, may be occurring at 2600 ^{o}K using the 15^{o} mixing sleeve.

Figure 5-2 compares the calcium utilizations just presented in Figure 5-1, which were determined using an on-line SO_2 gas analyzer, with those based on chemical analysis of collected spent sorbent. The spent sorbent was collected using an isokinetic, nitrogen quenched solids sampling probe, which is nearly identical to the design used by DoE/METC in their investigation[4] of non-equilibrium sulfur capture (see Section 2.3.9 for comments on the solids sampling system).

Figure 5-2 shows a drastic discrepancy between calcium utilizations based on gas phase and solids determinations. After pondering this discrepancy it was concluded that sulfation was occurring in the collection filter during the relatively long sampling time (typically 20 minutes) under excess oxygen conditions. It should be noted that the collection filter achieved temperatures of nominally 300 ^{o}C during solids collection, which was thought to be low enough to prevent sulfation from occurring during sampling. Regardless, a simple set of tests were conducted to resolve this discrepancy, tests that would clearly show which diagnostic was giving the correct sulfur capture level.

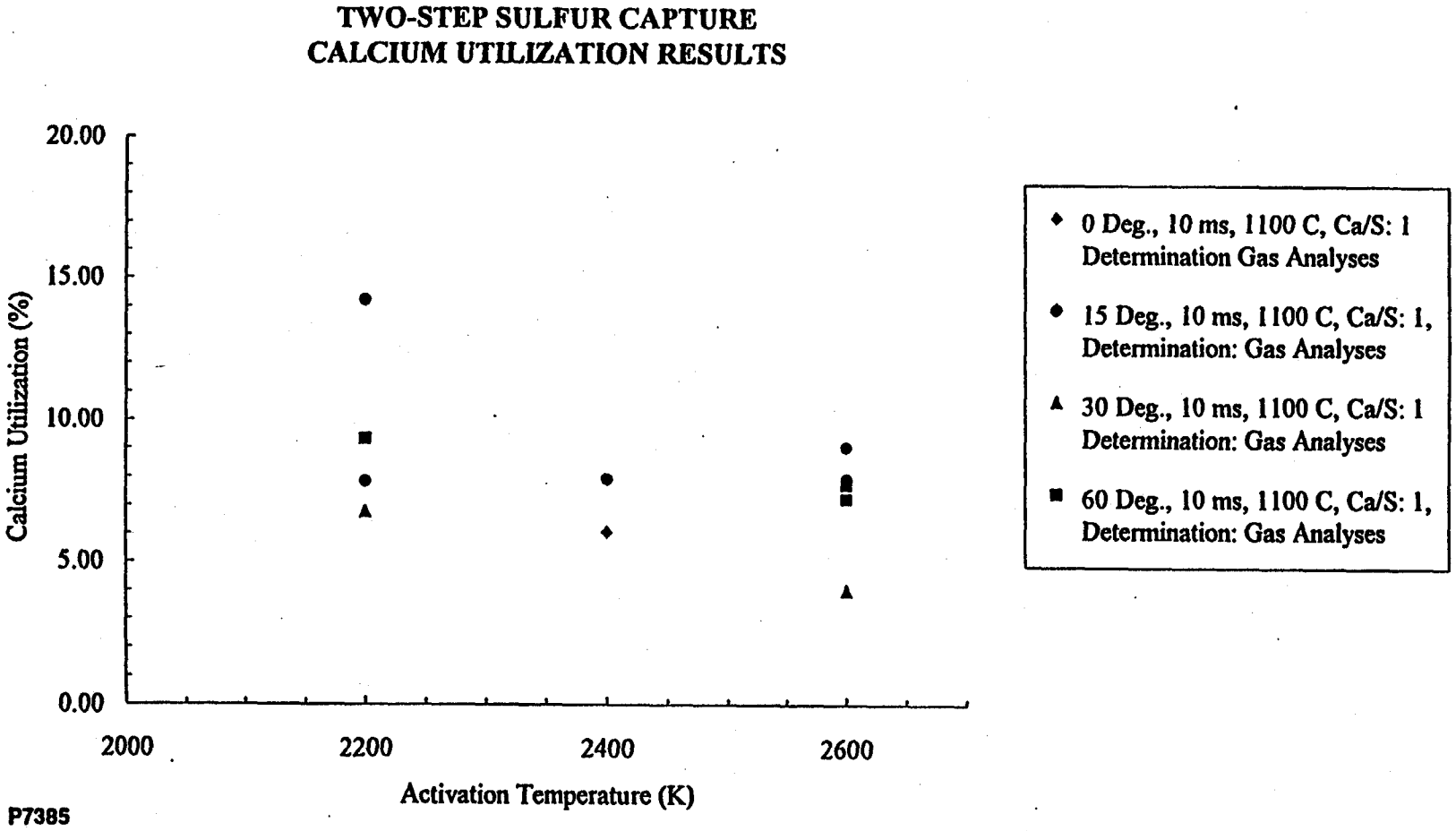

Figure 5-1. Two-Step Calcium Utilization Results.

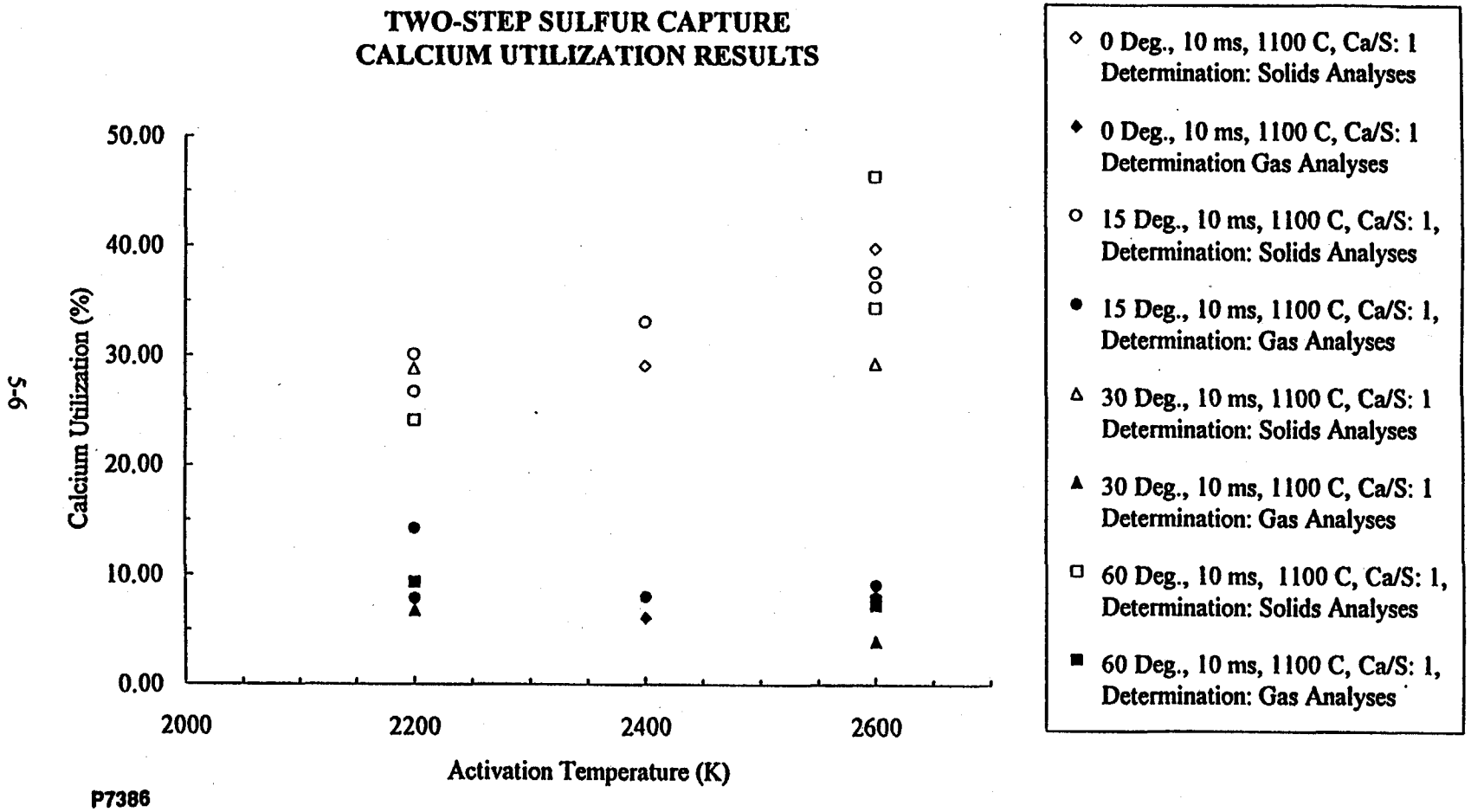

Figure 5-2. Two-Step Calcium Utilization Results.

The in-filter sulfation tests were conducted as follows. The process conditions for the in-filter sulfation check were identical to those producing the results in Figures 5-1 and 5-2 except that the were conducted at only one activation temperature, namely T_{act} = 2600 ^{o}K. Without any sulfur gas flowing through the system, and all other parameters set to simulate the Two-Step Rapid Sulfur Capture process, a solids sample was taken, which was labeled "control sample." Next, another solids sample was taken without sulfur gas flowing through the system. This sample was acquired in the same manner as the control sample, but was not removed from the collection filter. After the second sample had been acquired, the sorbent flow was terminated and the sulfur gas flow was started. The solids sampling system is allowed to draw the sulfur laden gas through the filter assembly for an amount of time typical of a solids sampling period (20 minutes). The second solids sample represents the situation where sulfation is allowed to take place only in the solids sampling filter assembly. Chemical analyses applied to the control sample produced a low calcium utilization, nominally 1%. These same analyses applied to the second sample exposed to in-filter sulfation produced relatively high calcium utilizations, nominally 40%. These tests clearly show that the elevated calcium utilizations presented in Figure 5-2 based on solids determinations, rather than gas phase determinations, are a result of in-filter sulfation. This demonstrates that the gas phase determinations are giving true sulfur capture levels, whereas the solids based results are giving erroneous results.

It should be noted, however, that the in-filter sulfation tests imply that 40% of the sulfur passing through the filter assembly is being captured (i.e., for Ca/S = 1), which is somewhat impressive given the relatively low temperatures (300 ^{o}C) present in the filter assembly. Since the solids collection process takes place over 20 minutes, this may be viewed as the long sulfation time performance of limestone activated via the Two-Step Rapid Sulfur Capture process.

In the following sections certain results are presented for tests conducted where the test rig was operated in the Non-Equilibrium Sulfur Capture mode. For this mode, ambient temperature nitrogen was injected into each side duct burner at rates producing mass flows equivalent to that which would have been provided by the side duct burners if they were lit. As a result, the oxygen levels and temperatures produced in the solids collection filter are much lower in this mode than under the Two-Step Rapid Sulfur Capture mode. Thus, in-filter sulfation effects are negligible during solids sampling when performing Non-Equilibrium Sulfur Capture tests.

Tests were performed during Phase IB that compared how rapidly the sorbent and quench jets mix in the quench section in the interface module. These tests were performed operating the test rig in the Non-Equilibrium Sulfur Capture mode. Gas phase mixing was studied by injecting SO_2 in the carrier jet of the activation burner and measuring radial profiles of SO_2 concentration in the mixing sleeve. Radial SO_2 profiles were measured at z/d = 2.5, where z is the distance downstream of the inlet of the mixing sleeve and d is the inside diameter of the mixing sleeve. These tests were conducted with the activation burners on and with and without sorbent injection.

Figure 5-3 presents radial profiles of SO_2 concentration at z/d = 2.5 without sorbent injection for two quench jet angles (θ = 15 and 60^o), two activation temperatures (T_{act} = 2400 and 2600 ^{o}K), and an activation time of 20 ms. The SO_2 concentration profiles were normalized by the centerline (r = 0) SO_2 concentration and then plotted in Figure 5-3. This figure shows that gas phase mixing is not very well completed by this axial location for the 60^o mixing sleeve. The 15^o sleeve mixing results suggest that gas phase mixing is very well completed by z/d = 2.5, but the corresponding SO_2 profiles are somewhat asymmetric. The asymmetry was found to be due to poor alignment of the sorbent carrier jet in the activation burner with the axial centerline of the mixing sleeve. The reduction in asymmetry between tests B-14 and B-15 is due to sorbent carrier jet realignment prior to test B-15. Based on the plug flow velocities of the sorbent carrier jet in the activation duct and the conditions under which the mixing tests were performed, and the fact that gas phase mixing is completed by z/d = 2.5 for the 15^o mixing sleeve, the gas phase mixing time for the 15^o sleeve is estimated to be nominally 10ms. Based on the plug flow velocity in the mixing sleeve, the gas phase mixing time for the 15^o sleeve is 50 ms. The actual mixing time for the 15^o sleeve lies somewhere between these two limits, probably midway, which is nominally 30 ms. The mixing time for the 60^o sleeve is estimated to be more like 50 ms, thus the 15^o sleeve did provide more rapid mixing. Unfortunately, the 40% decrease in mixing time provided by the 15^o sleeve was not sufficient to yield improved Two-Step Rapid Sulfur Capture calcium utilizations. Since the 0 and 30^o mixing sleeves did not produce improvements in Two-Step Rapid Sulfur Capture calcium utilizations over those achieved by the 15 and 60^o degree mixing sleeves, no mixing studies were performed using the 0 and 30^o mixing sleeves.

Figures 5-4 and 5-5 present SO_2 radial concentration profiles with and without limestone injection for activation temperatures of 2600 and 2400^o K, respectively. The test rig was operated

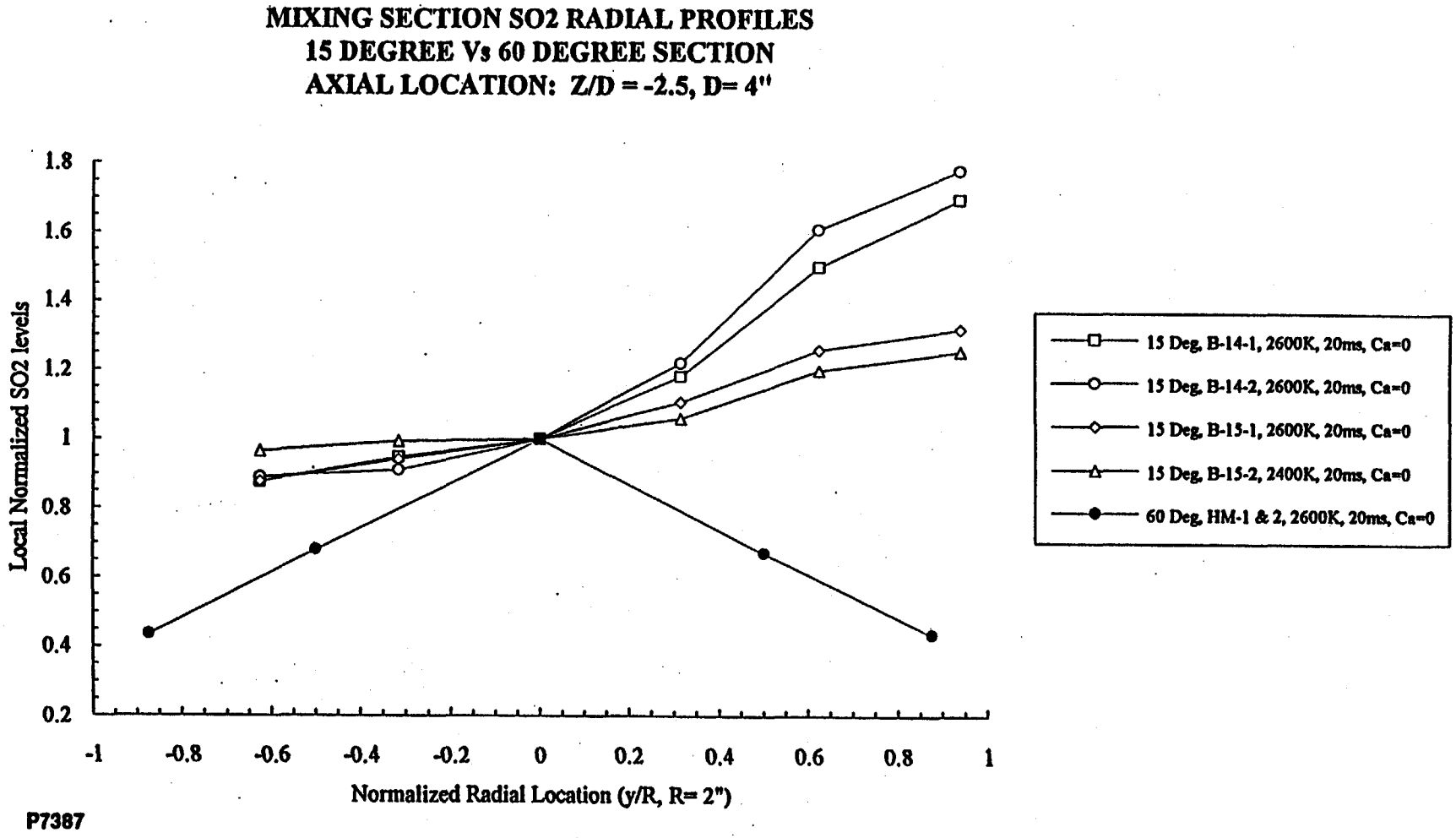

Figure 5-3. Comparison of the Performance of the 15 and 30 Degree Mixing Sections.

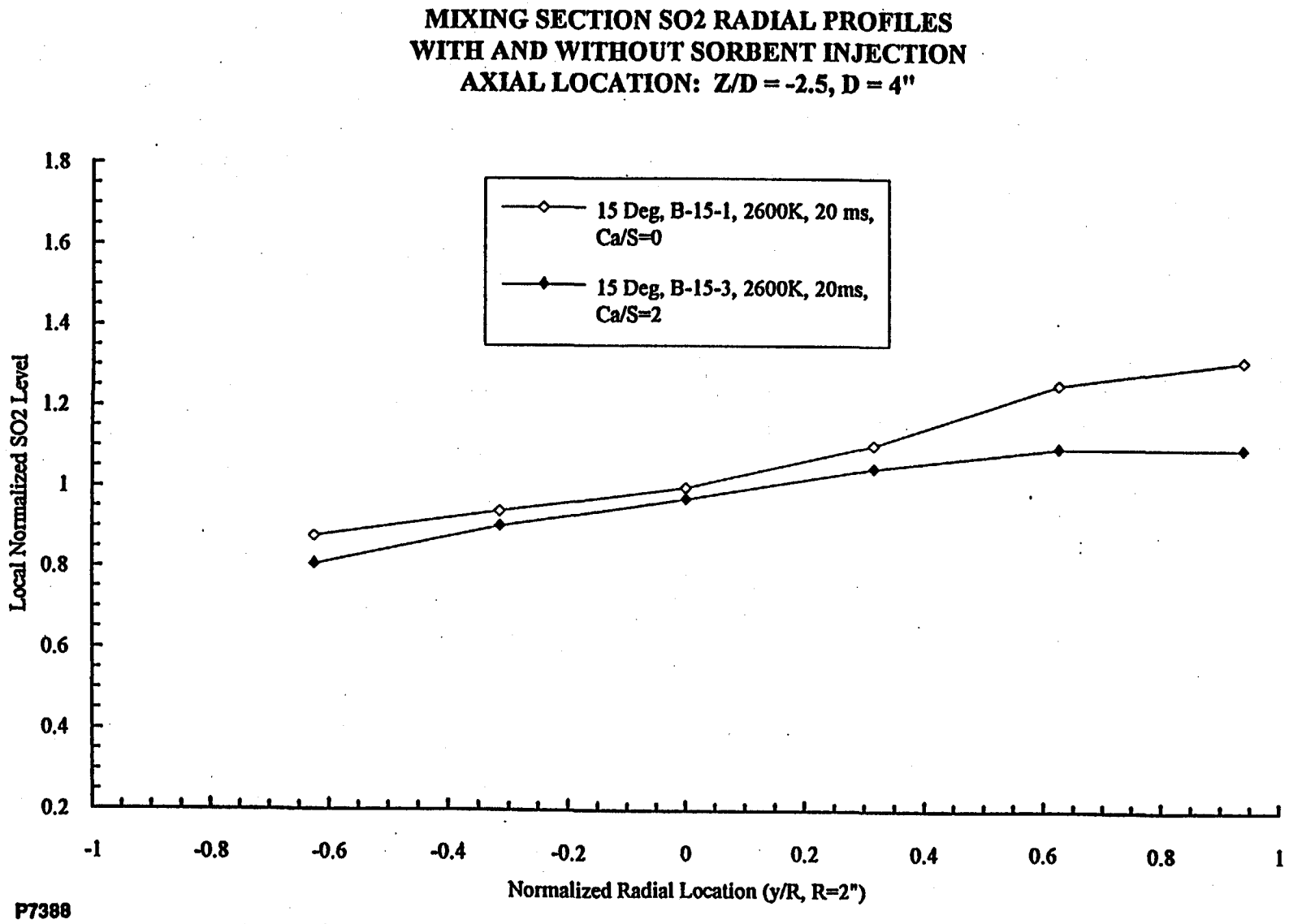

Figure 5-4. Non-Equilibrium Sulfur Capture Profiles in the 15 Degree Mixing Section for an Activation Temperature of 2600 ^{O}K.

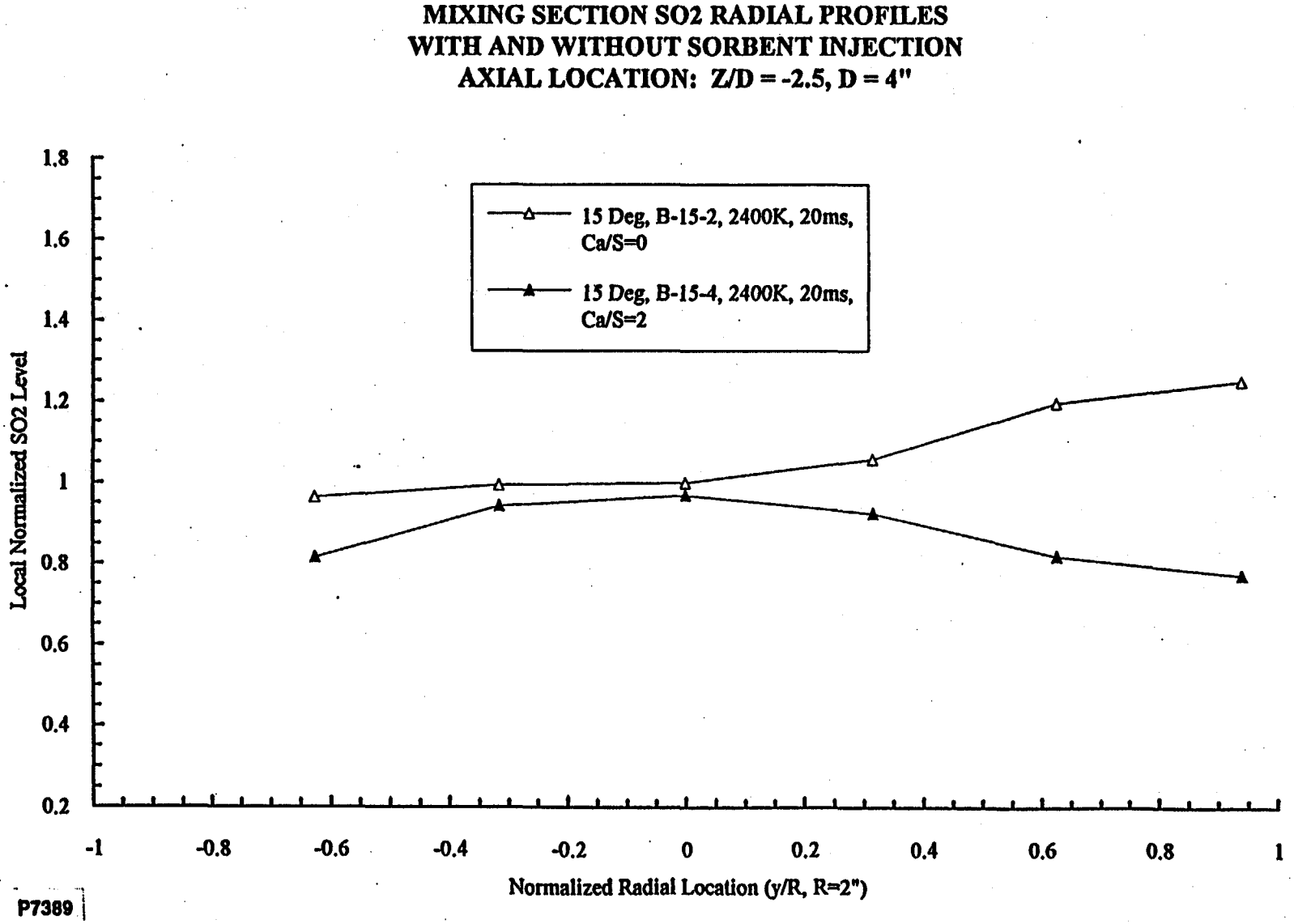

Figure 5-5. Non-Equilibrium Sulfur Capture Profiles in the 15 Degree Mixing Section for an Activation Temperature of 2400 ^{O}K.

in the Non-Equilibrium Sulfur Capture mode with Ca/S = 2 when limestone was being injected and with an activation time of 20 ms. The radial profiles of SO_2 concentration were measured at z/d = 2.5, with z/d = 0 corresponding to the inlet of the mixing sleeve. The SO_2 profiles measured during limestone injection are normalized with the centerline value measured just prior to initiating limestone injection. Several observations can be made regarding these figures. First, the sulfur capture increases as the wall is approached. This is probably due to sorbent segregation in wall regions due to the interaction of the quench jets with the sorbent jet. Second, wall region non-equilibrium sulfur capture appears to increase with decreasing activation temperature. Albeit, the overall non-equilibrium calcium utilization is still, at best, only 3 - 4% at an activation temperature of 2400°K.

The following conclusions can be drawn regarding influence of quench parameters on the Two-Step Rapid Sulfur Capture process. First, reduced mixing times were achieved by the 15° mixing sleeve relative to the 60° unit. The mixing time reduction was nominally 40%. It is expected that the 0° sleeve probably gives even smaller mixing times and that the 30° unit gives somewhat longer times. Regardless, it was found that the 0, 15, and 30° mixing sleeves did not produce significant improvements in Two-Step Rapid Sulfur Capture calcium utilizations. The best utilization measured was 9% using the 15° mixing sleeve with an activation temperature in the range 2200 - 2600°K, an activation time of 10 ms, a sulfation temperature of 1100°C, and Ca/S = 1. The reasons for poor calcium utilization will be discussed in Section 5.8 "Sorbent Properties After Activation." Regardless, it seems evident that the proposed activation process has an inherent limitation, which probably stems from the polydispersed nature of the sorbents tested, i.e., it is probably impossible to uniformly achieve highly activated calcia across the broad size distribution of the parent limestone feed.

5.3 INFLUENCE OF SORBENT ACTIVATION CONDITIONS

The process parameters that control sorbent (limestone) activation are activation temperature (T_{act}), activation time (τ_{act}), and activation burner sorbent loading. Sorbent loading, which is the ratio of the mass flow rate of sorbent to activation burner gaseous reactants mass flow rate, has little effect on sulfur capture as long as the proportions of carrier burner reactants are controlled to yield the desired flame temperature. The loading ratio was fixed in the range

6 - 8%. Limestone size distribution is also a factor, but this will be dealt with separately in Section 5.6 "Influence of Sorbent Size Cut."

Figure 5-6 illustrates the influence of T_{act} and τ_{act} on calcium utilization when the test rig is operated in the Non-Equilibrium Sulfur Capture mode. The reason for conducting sulfur capture tests in this mode was to define activation conditions that optimize calcium utilization without the ambiguities introduced by variations in the sulfation duct parameters associated with Two-Step Rapid Sulfur Capture mode. The sulfation time at which these utilizations were measured was fixed at nominally 300 ms. The sulfation temperature was low, nominally 573°K, which is a result of the mode under which these tests were performed. The calcium to sulfur ratio was fixed in the range $1 \leq Ca/S \leq 1.5$. The activation temperature was varied over the range $2200 \leq T_{act} \leq 2850^{o}K$ and the activation time was varied over the range $0 \leq \tau_{act} \leq 30$ ms. Activation time is based on the plug flow time in the activation duct and does not include the effects of finite mixing times during the quench process.

Figure 5-6 shows a considerable temperature shift between the utilizations obtained using the 15 and 60° mixing sections. We believe this shift is due to the possibility that the less aggressive mixing provided by the 60° sleeve produces a hot core flow exiting the mixing sleeve, which persists for a certain distance, thus time, into the sulfation duct. This provides temperature conditions after quenching where sulfation can occur. In essence, Two-Step Rapid Sulfur Capture is being achieved with the 60° sleeve. Since more rapid and complete quenching is being achieved with the 15° mixing sleeve, a hot core flow is not being discharged from the mixing sleeve, thus conditions are not favorable for sulfur capture reactions to proceed in the sulfation duct. It is clear in Figure 5-6 that non-equilibrium calcium utilizations increase with decreasing τ_{act} and increasing T_{act}. Albeit, the best Non-Equilibrium Sulfur Capture mode utilization was found to be 9%, which was obtained at $T_{act} = 2850^{o}K$, $\tau_{act} = 0$ ms, $\theta = 15^{o}$, and $Ca/S = 1$.

Figure 5-7 presents Two-Step Rapid Sulfur Capture calcium utilizations as a function of mixing sleeve quench jet angle (θ), activation temperature (T_{act}), and activation time (τ_{act}) for $Ca/S = 1$ and a sulfation duct temperature of 1100°C. The following points can be made regarding the data presented in this figure. Quench jet injection angle ($\theta = 0, 15, 30^{o}$) has some influence on calcium utilization, i.e., at lower activation temperatures ($T_{act} = 2200^{o}K$), calcium

NON-EQUILIBRIUM SULFUR CAPTURE COMPARISONS
ACTIVATION TEMPERATURE/TIME RESULTS

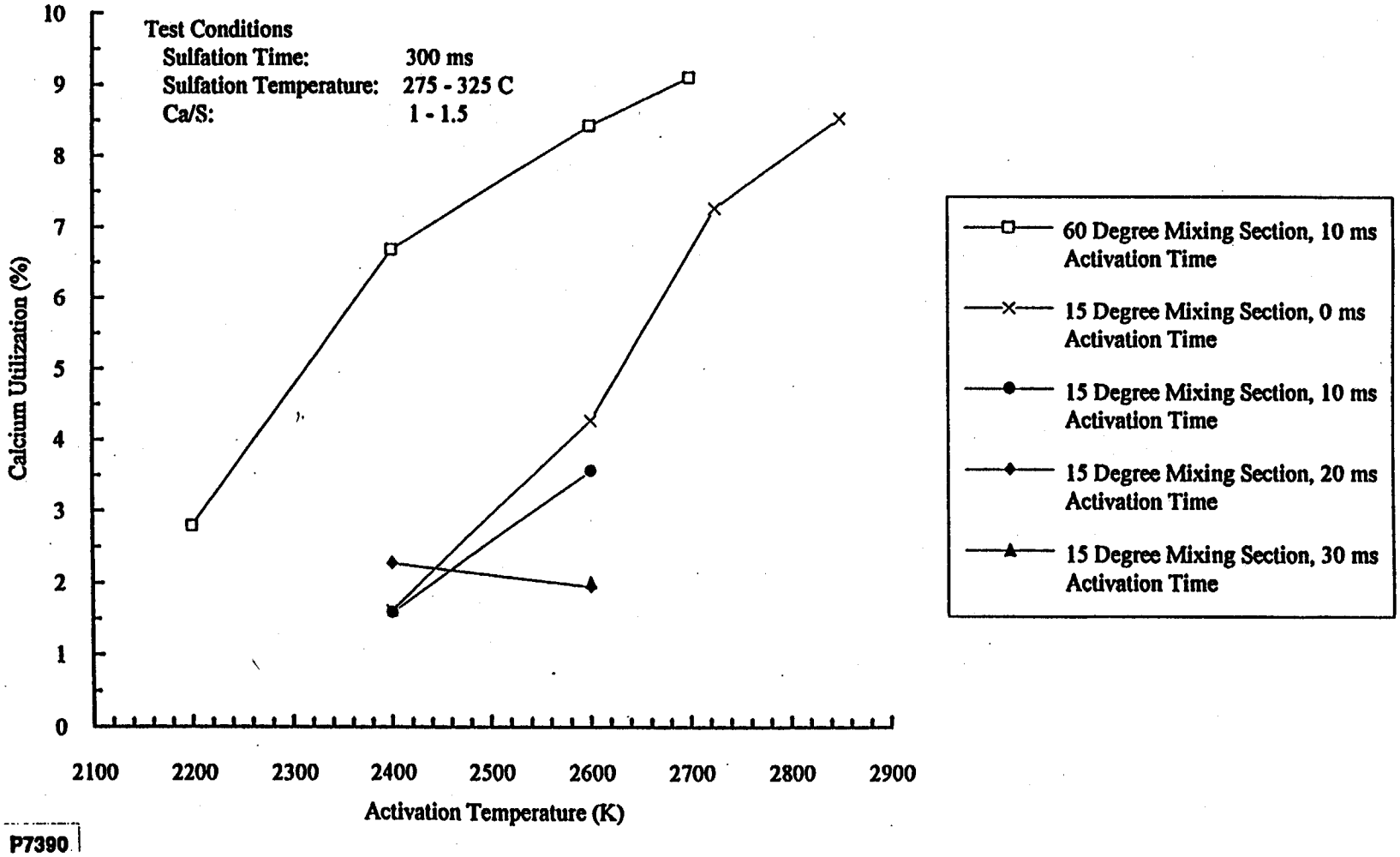

Figure 5-6. Effect of Activation Temperature and Time on Non-Equilibrium Sulfur Capture Performance.

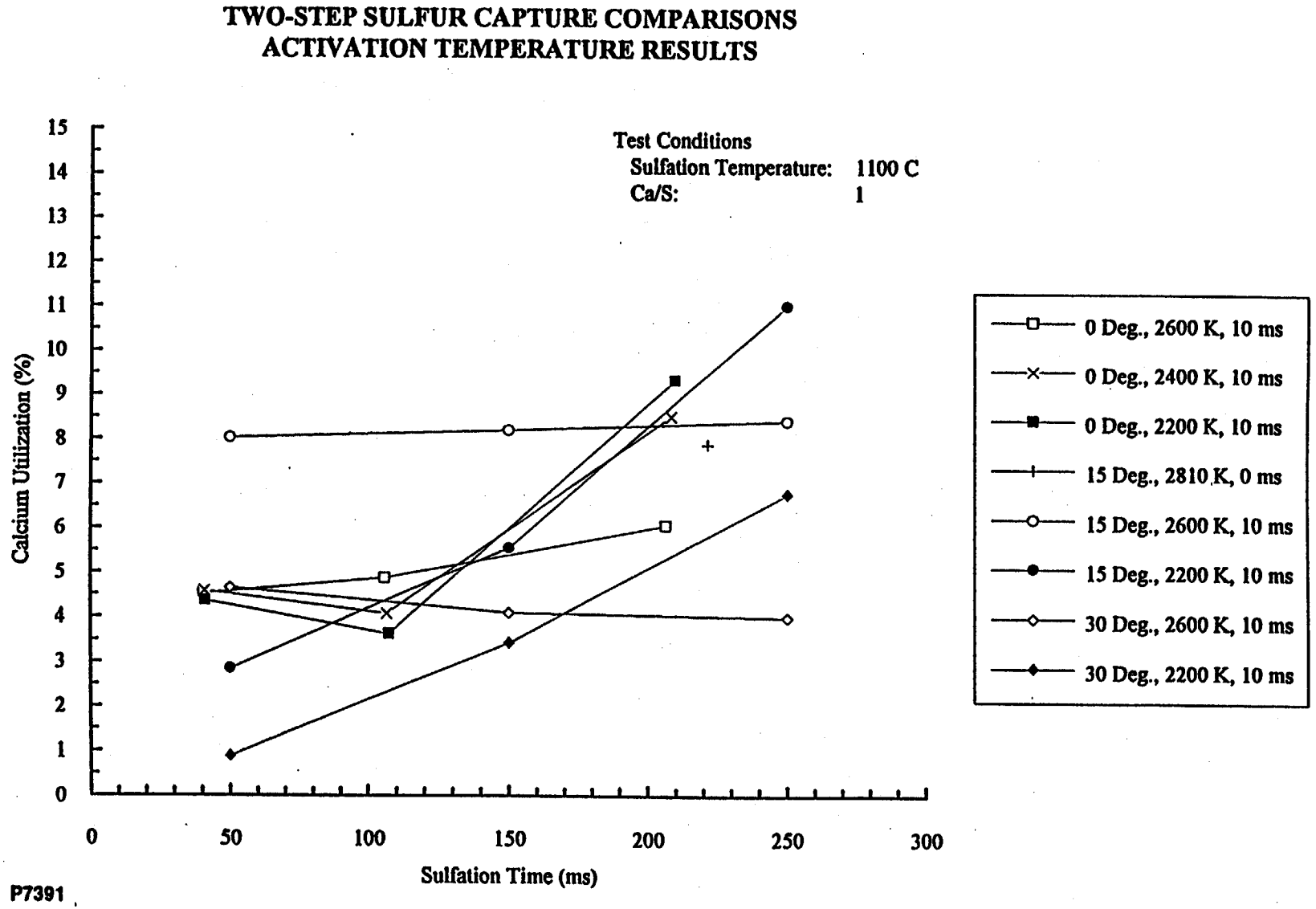

Figure 5-7. Activation Temperature Influence on Two-Step Sulfur Capture for the 15 and 30 Degree Mixing Sections.

utilizations increase with decreasing θ, whereas at the higher activation temperatures (T_{act} = 2600°K) there appears to be an optimum angle, apparently θ = 15°. The presence of an optimum angle θ implies that the quenching process impacts the activation process, either through sorbent wall segregation effects or modified activation times.

The effect of activation temperature on Two-Step Rapid Sulfur Capture calcium utilizations is rather complex. When the data in Figure 5-7 corresponding to the solid symbols is compared with the open symbols (T_{act} equal to 2200 and 2600 °K, respectively), it is found that the higher activation temperature yields calcium utilization versus sulfation time profiles that are nominally flat, whereas the lower activation temperature yields profiles that have significant slope. Also, the early sulfation time calcium utilization levels produced by the lower activation temperature are much lower that those produced by the higher activation temperature. Although the higher activation temperature yields very rapid sulfur capture, the lower activation temperature data always achieves higher calcium utilizations at the longest sulfation times. These results imply that higher activation temperatures are producing a somewhat more highly active sorbent. One with higher porosity and surface area, but lower median pore diameter. The higher porosity and surface area will yield higher initial sulfur capture rates, but these rates fall quickly due to pore blockage, which is a result of the reduced median pore diameters produced at higher activation temperatures that are quickly plugged during product layer development.

5.4 INFLUENCE OF Ca/S RATIO

The calcium to sulfur ratio (Ca/S, molar basis) is an important process parameter since, for a required sulfur reduction, it will determine the relative amount of solid waste that must be disposed of. Since regulations dictating landfill availability and use are getting more stringent, and are expected to become even more so in the near future, a viable sulfur capture process must be able to achieve high sulfur captures (~90%) at calcium to sulfur ratios near unity. It is important, therefore, to examine the influence of Ca/S on calcium utilization.

Figure 5-8 shows calcium utilization as a function of sulfation time, Ca/S, and activation temperature for fixed activation and sulfation temperatures, using the 60° mixing section. This figure indicates that calcium utilization is not very sensitive to Ca/S. There may be as much as

a 35% decrease in utilization for T_{act} = 2200°K when Ca/S is increase from Ca/S = 1 to Ca/S = 2 at sulfation times of nominally 120 ms. The decrease in calcium utilization at T_{act} = 2600°K is less, namely 25%, for the same increase in Ca/S. These results, although obtained under conditions producing very low calcium utilizations, indicate the greatest sorbent efficiencies are achieved when calcium to sulfur ratios near unity are employed.

5.5 INFLUENCE OF SULFATION TEMPERATURE

As noted in Section 1.1, and illustrated in Figure 1-1, sulfation temperature and excess oxygen both have a significant effect on sulfur capture. Equilibrium sulfur capture computations show that the maximum temperature wherein 100% sulfur capture is possible increases from 800 to 1400 °K as the equivalence ratio ϕ is decreased from unity to 0.5, which corresponds to an increase in excess oxygen from 0.1 to 10%. For the stoichiometries explored during Phase IB ($0.75 \leq \phi_s \leq 0.85$), which is a fairly narrow band, these equilibrium considerations suggest that varying sulfation temperature in the range $1100 \leq T_s \leq 1400$ °K should have a minor effect on sulfur capture. Pore diffusion rates and sulfation kinetics rates, however, are strongly dependent on sulfation temperature, so finite rate considerations suggest that sulfation temperature variations should have an effect on Two Step Rapid Sulfur Capture calcium utilization.

Figure 5-9 presents calcium utilization results as a function of sulfation duct temperature and sulfation time. Standard activation conditions were used, i.e., T_{act} = 2600 °K and 10 ms. The calcium to sulfur ratio was fixed at Ca/S = 1. The results presented in Figure 5-9 were generated using the 60° mixing section. Two sulfation temperatures were tested, i.e., 1173 and 1373 °K. Figure 5-9 shows that calcium utilization increases with increasing sulfation temperature. This trend will probably persist until nominally 1600 °K, which is the maximum stable temperature for calcium sulfate under excess oxygen conditions. These results indicate that a 24 - 37 % increase in calcium utilization occurs as the sulfation temperature is increased from 1173 to 1373 °K. The higher increase limit (37%) occurs at short sulfation times (50 ms), whereas the lower increase limit occurs at the longest sulfation time (250 ms). The fact that calcium utilization increases with increasing sulfation temperature is consistent with increasing pore diffusion and sulfation kinetics rates. The fact that the increase in calcium utilization decreases with increasing sulfation time is consistent with trends expected as a reaction approaches equilibrium.

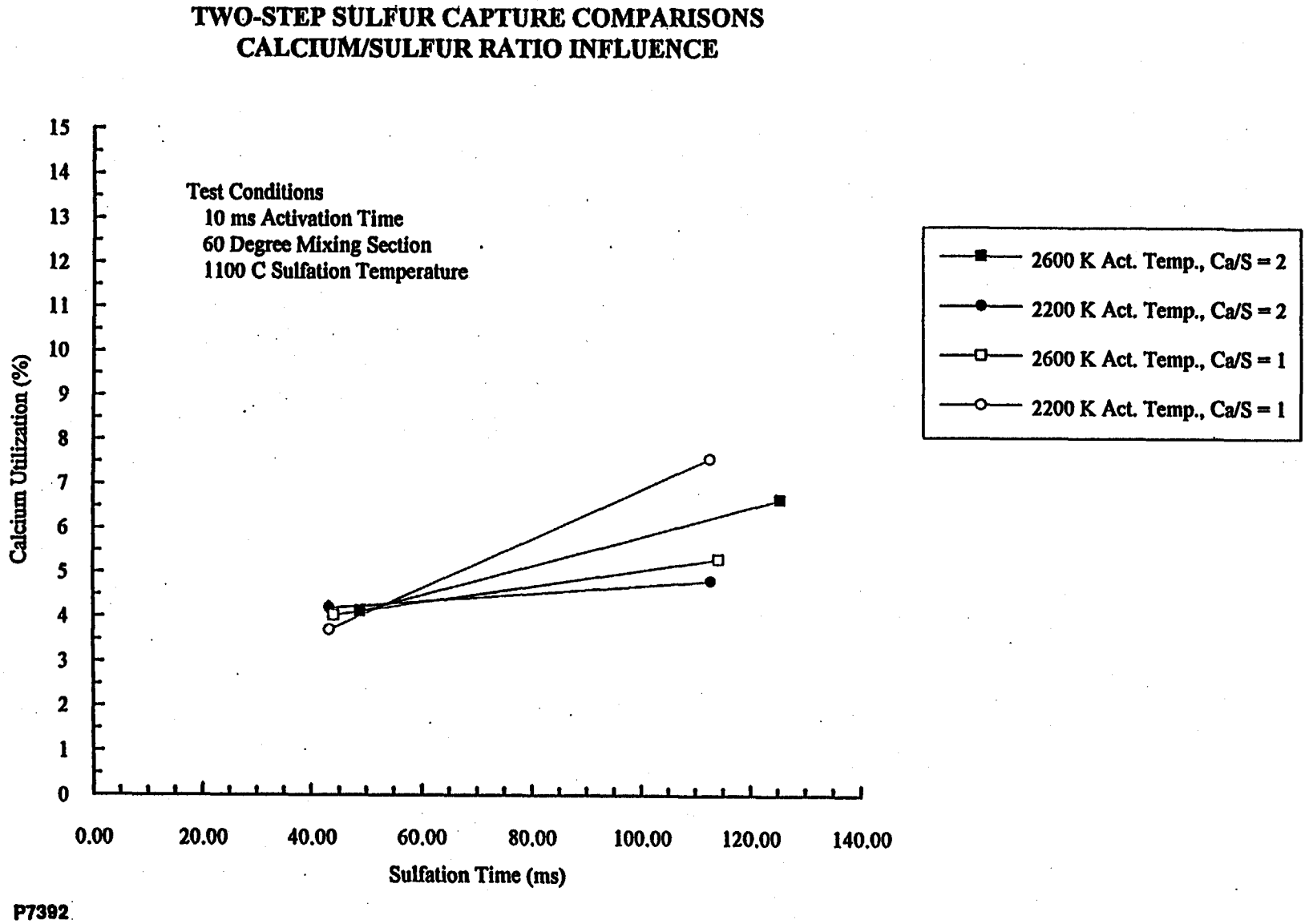

Figure 5-8. Influence of Ca/S on Two-Step Calcium Utilization.

5.6 INFLUENCE OF SORBENT SIZE CUT

It was noted earlier that the Two Step Rapid Sulfur Capture process may have inherent limitations. More specifically, it may be impossible to achieve highly activated and uniformly activated calcia across the broad size distribution of the parent limestone feed. To investigate this, different size cuts of Marblewhite limestone were tested, i.e., less than 5 μm size cut and 25 - 45 μm size cut were tested and compared to the full size distribution 325 Marblewhite limestone results. The objective was to determine if more narrow size cuts lead to increased calcium utilizations and to determine what size range gave the best results. Significant differences in calcium utilization due to variations is sorbent size distribution would support the proposed process limitation.

The sorbent size cut tests were conducted using the standard activation time (τ_{act} = 10 ms) and two activation temperatures (T_{act} = 2200 and 2600 ^{o}K). The 60^{o} degree mixing section was used during these tests. The sulfation duct temperature was held constant at T_s = 1373 ^{o}K and the calcium to sulfur ratio was held in the range $1 \leq Ca/S \leq 1.4$.

Figure 5-10 shows the results of the size cut tests. The T_{act} = 2200 ^{o}K results are given by the circular symbols, with the open symbols depicting the 0 - 5 μm size cut results and the closed symbols depicting the 25 - 45 μm results. The T_{act} = 2600 ^{o}K results are given by the square symbols, with similar meanings for the open and closed symbols. Three trends are present in the results shown in Figure 5-10. First, smaller size cuts yield higher calcium utilizations. Second, under similar conditions, the uncut Marblewhite 325 calcium utilizations (see Figure 5-1, solid square symbols) fall midway between the 0 - 5 and 25 - 45 μm results shown in Figure 5-10. Third, calcium utilizations increase with increasing activation temperature, even for the smallest size cut.

Regarding the third trend: a three-fold increase in calcium utilization for the 0 - 5 μm size cut was not expected to occur as the activation temperature increased from 2200 to 2600 ^{o}K. Sintering was expected to dominate at the higher activation temperature for this size cut, thereby

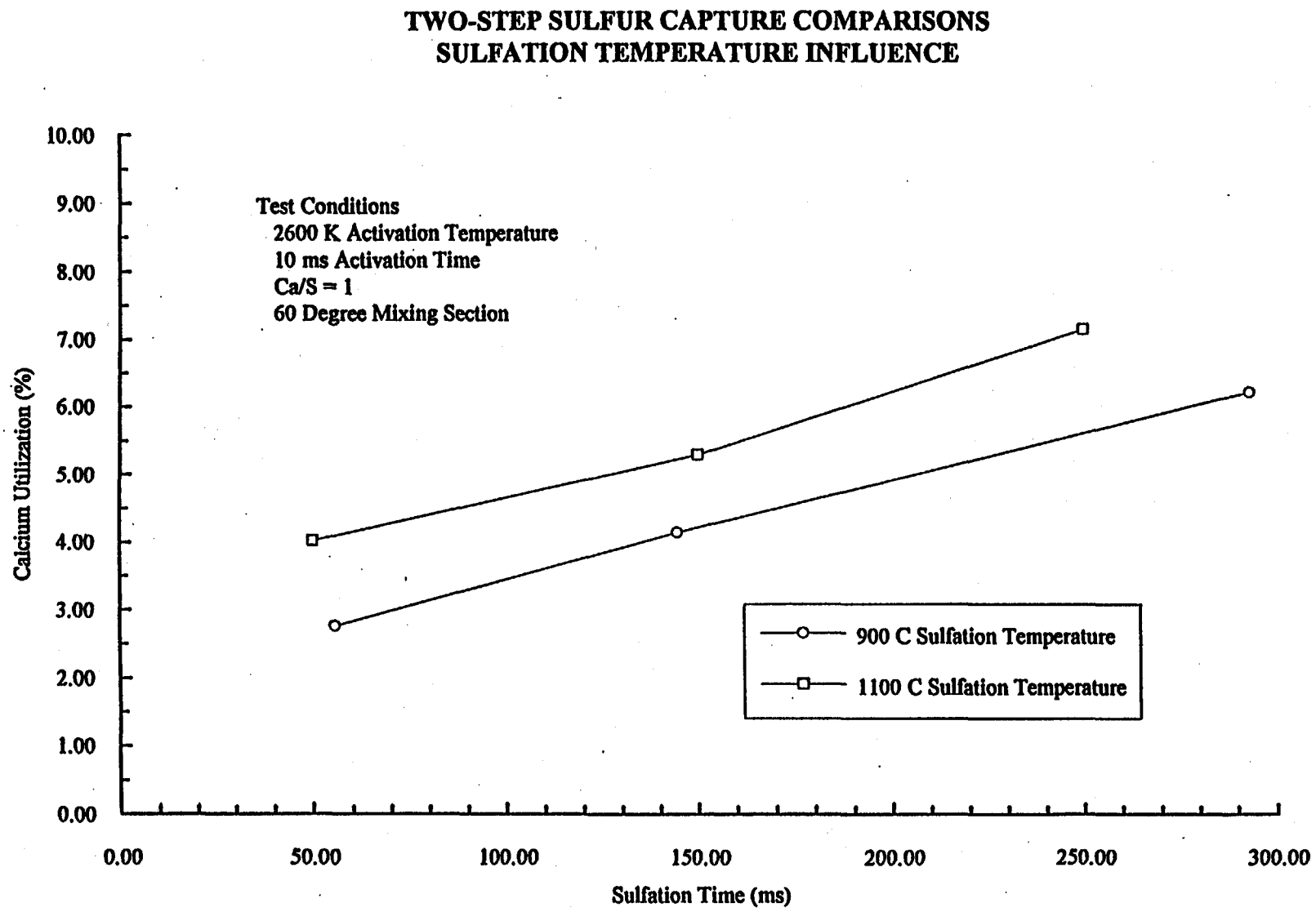

Figure 5-9. Influence of Sulfation Temperature on Two-Step Calcium Utilization.

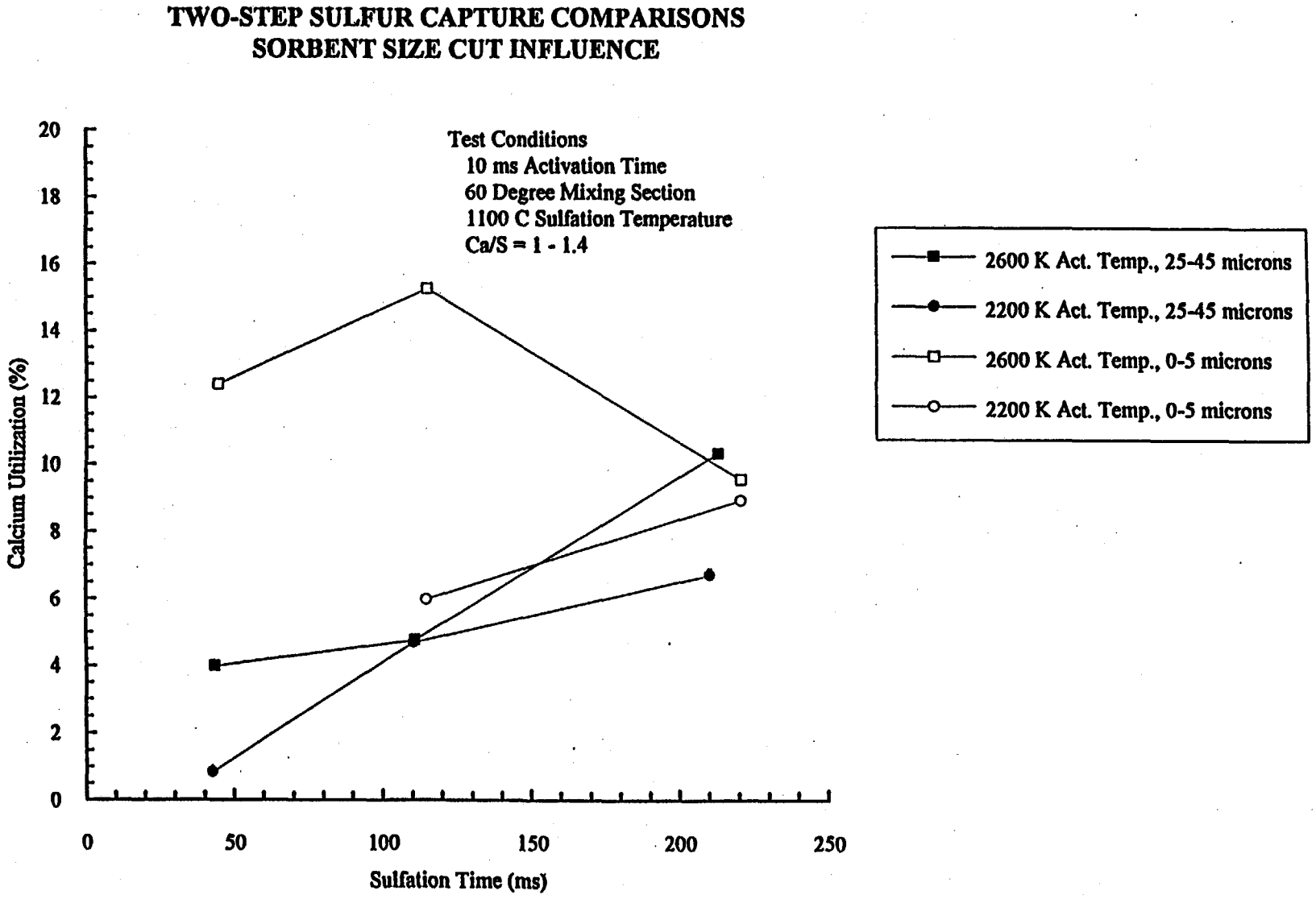

Figure 5-10. Influence of Sorbent Size Cut on Two-Step Calcium Utilization.

degrading the associated calcium utilizations significantly. In contrast, an increase in calcium utilization with increasing activation temperature was expected for the more coarse 25 - 45 μm size cut, which is what is shown in Figure 5-10.

Regarding the second and third trends noted above: based on a fixed Ca/S ratio and the difference in mass mean diameter of the two size cuts tested, the surface area of the 0 - 5 μm size cut before activation is estimated to be nominally five times greater than the uncut 325 Marblewhite limestone. The surface area of the 25 - 45 μm size cut, also before activation, is estimated to be nominally 2.5 less than the uncut 325 Marblewhite limestone. Based on the Two Step Rapid Sulfur Capture results given in Figure 5-1, the calcium utilization for uncut 325 Marblewhite limestone is nominally 7.5% for T_{act} = 2600 ^{o}K, τ_{act} = 10 ms, T_s = 1373 ^{o}K, τ_s = 250 ms, Ca/S = 1, and ϕ_s= 0.8. For these same conditions, Figure 5-10 indicates that the 0 - 5 μm size cut yields a calcium utilization of at most 15%, which is only at factor of two, not five times the uncut 325 Marblewhite limestone results. This implies that significant sintering of the 0 - 5 μm size cut is occurring. If sintering was not occurring, we would expect the 0 - 5 μm size cut to produce calcium utilizations in the 35 - 40% range. Also, Figure 5-10 indicates that the 25 - 45 μm size cut produces 10% calcium utilization at the longest sulfation time. This level is comparable to that produced by the uncut 325 Marblewhite 325 limestone, where the surface area scaling discussed above says the 25 - 45 μm size cut results should be nominally a factor of 2.5 less.

The observations just noted imply the following. First, since full activation temperature and time scans were not performed on the 0 - 5 and 25 - 45 μm size cuts of 325 Marblewhite limestone, we cannot draw any definitive conclusions regarding the limitations of the Two Step Rapid Sulfur Capture process because optimized activation conditions were not derived nor used for the tested size cuts. Second, since the 25 -45 μm size cut did not show any signs of calcium utilization level degradation (i.e., in contrast with the levels produced by the uncut 325 Marblewhite limestone), it is clear, however, that size cut does have an effect and that this tends to support the hypothesized limitation of the Two Step Rapid Sulfur Capture process, i.e., it may be impossible to achieve highly activated and uniformly calcia from a parent limestone feed that has a broad size distribution. This limitation is due to the possibility that for fixed activation time and temperature conditions only a particular size cut is being highly activated, that sizes above

the optimum range are not heated rapidly enough produce highly activated calcia, and that sizes below the optimum range are sintering because they experience very high heating rates. As suggested, heating rate is the key to producing highly activated calcia. Since the Two Step Rapid Sulfur Capture process effects particle heating via surface heat transfer mechanisms, and since the surface area to volume ratio decreases with increasing particle size, it is clear that any method which relies on surface heat transfer mechanisms will not be able to uniformly activate polydispersed sorbent feeds. A volumetric heat source would be most appropriate for sorbent activation, but we have not been able to identify such a source.

5.7 INFLUENCE OF SORBENT TYPE

Two other sorbents were tested in the Two-Step Rapid Sulfur Capture Facility during this program, namely: Linwood hydrated lime and Vicron 45-3 (a limestone). Linwood hydrated lime was tested in an attempt to obtain higher Two-Step Rapid Sulfur Capture utilizations than those produced by 325 Marblewhite limestone. Vicron 45-3 sorbent was tested because it had been tested in several single-step studies.[5,6] Since the Vicron 45-3 properties and utilization results were nearly the same as those of the 325 Marblewhite limestone, they are not reported here.

Figure 5-11 compares Two-Step Rapid Sulfur Capture calcium utilizations using Linwood hydrated lime and 325 Marblewhite limestone. The operating conditions are given in this figure, which correspond to conditions that yield nearly optimum 325 Marblewhite calcium utilizations. Strictly optimum conditions would have included an activation time of 10 ms and a mixing section quench jet angle of 15 or 30°. Since these measurements were made prior to receipt of the 0, 15, and 30° mixing sections, the 60° mixing section was used for these tests. An activation time of 0 ms was used instead of 10 ms because lime has a lower calcination temperature and because the Linwood hydrated lime had a smaller mass mean size (3 - 4 μm) relative to the 325 Marblewhite limestone (13 μm). These considerations demand use of less severe activation conditions.

Figure 5-11 shows that the hydrated lime sorbent yields calcium utilizations that are always higher than that produced by the 325 Marblewhite limestone. This figure also implies that significant sintering of the hydrated lime is occurring at the highest activation temperature

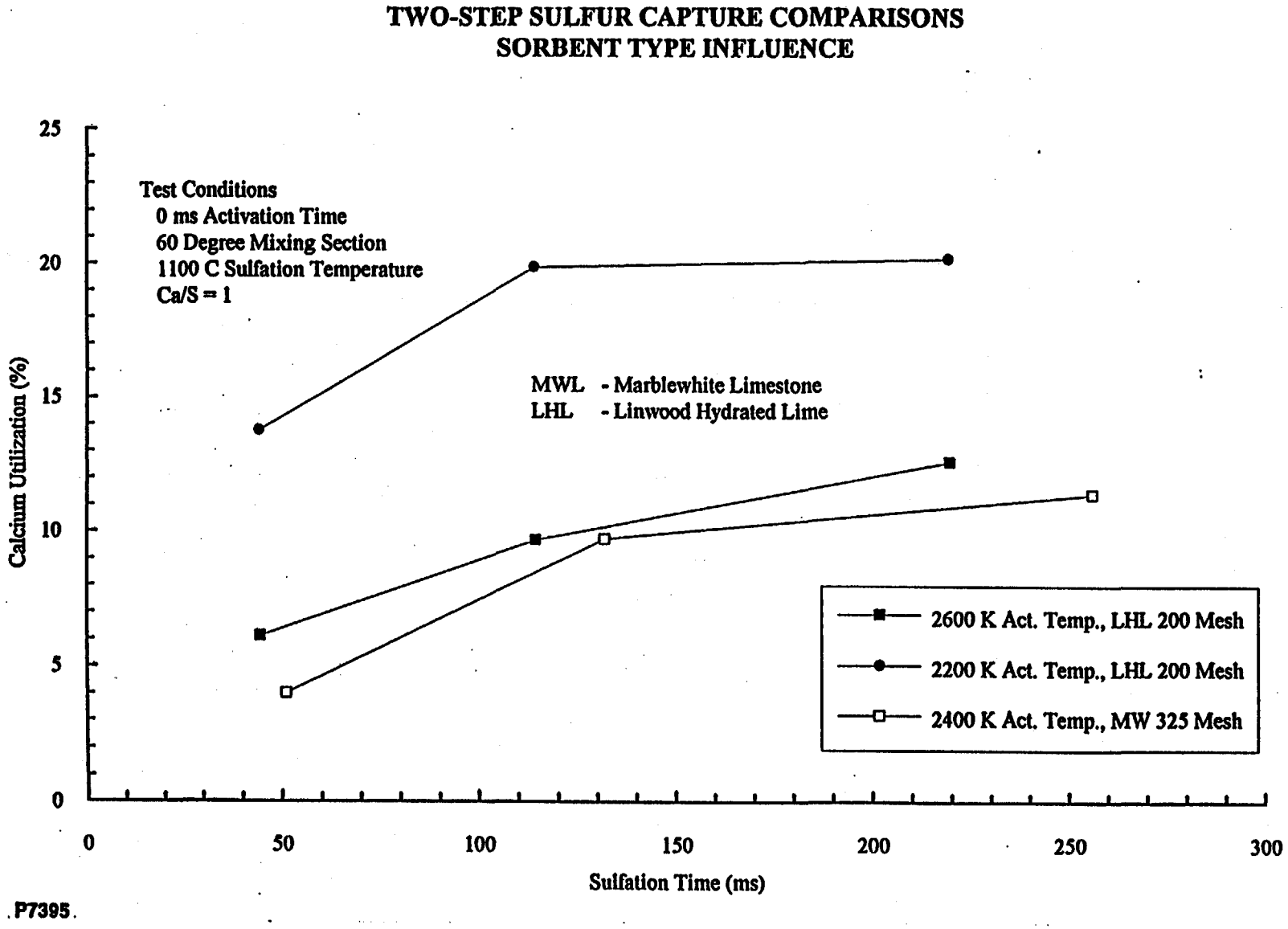

Figure 5-11. Influence of Different Sorbent Types on Two-Step Calcium Utilization.

(2600°K), and that a factor on nominally two increase in utilization is obtained as the activation temperature is decreased from 2600 to 2200°K. The maximum hydrated lime utilization measured was 20%, which occurred at an activation temperature of 2200°K, an activation time of 0 ms, a Ca/S ratio of 1, a sulfation time of 230 ms, a sulfation temperature of 1100°C, and a sulfation duct stoichiometry of ϕ_S = 0.81. Other tests were conducted at lower activation temperatures during Phase I (Base) period of this program. At an activation temperature of 1300°K a utilization of 32% was measured for the Linwood hydrated lime. This level of utilization is close to that obtained during the single-step experiments conducted by Milne and Pershing[7], which produced a calcium utilization of 30% at Ca/S = 2. Since these experiments and those performed by Milne and Pershing[7] give similar results (i.e., two-step and single-step processes give same results for hydrated lime), hydrated lime does not offer a viable option for increasing the effectiveness of the Two-Step Rapid Sulfur Capture process.

5.8 SORBENT PROPERTIES AFTER ACTIVATION

There are several processes that control sulfur capture rates during the sulfation step of the Two-Step Rapid Sulfur Capture process. The rate controlling processes are intrinsic chemical kinetics rates, mass transfer rates, pore diffusion rates, and product layer diffusion rates. Calculations performed considering 10 μm particles showed that intrinsic chemical kinetics rates are typically three orders of magnitude greater than mass transfer rates; mass transfer rates are typically three orders of magnitude greater than pore diffusion rates; and pore diffusion rates are typically three orders of magnitude greater than product layer diffusion rates. The picture of sulfur capture that emerges is that initial sulfur capture rates are limited by mass transfer effects, which, all else constant, is determined by the specific surface area of the activated sorbent particles. Once the calcia sites on the surface of a sorbent particle have reacted, sulfation rates are controlled by pore and product layer diffusion rates. Most of the sulfur capture occurs during the stage where pore and product layer diffusion rates are controlling sulfation rates.

Based on these considerations, specific surface area plays an important role in both initial mass transfer controlled sulfur capture and, in later stages, where sulfur capture rates are controlled by pore and product layer diffusion rates. In contrast, porosity and pore size play an important role in the later stages where sulfur capture rates are determined by pore and product

layer diffusion rates. Therefore, the limestone activation process must produce calcia particles that have high specific surface area, high porosity, and large pore size to achieve high calcium utilizations. It should be possible, therefore, to develop an understanding of the underlying reasons for the poor calcium utilizations produced by the Two-Step Rapid Sulfur Capture process by examining the morphological properties (specific surface area, porosity, and pore size) of limestone sorbents after the activation step of the Two-Step Rapid Sulfur Capture process. This section, therefore, explores limestone sorbent characteristics after activation.

5.8.1 ACTIVATED SORBENT SIZE DISTRIBUTIONS

Since particle shattering may occur during the activation process due to high heating rates, it is informative to examine the change in size distribution of sorbent particles before and after activation. Particle shattering leads to higher overall surface area due to generation of more particles of smaller size. To examine this phenomena, 325 Marblewhite limestone was activated for 10 ms at 2200, 2400, and 2600^{o}K during Test 11, which was conducted during the Phase I (Base) element of this program. The system was operated in the Non-Equilibrium Sulfur Capture mode, but no SO_2 was injected into the system. The activation burner stoichiometry was set to $\phi_{act} = 0.98$. Sorbent loading was 15 - 17%, which is nominally a factor of two greater than used under standard operating conditions. Solid samples were collected and sent out for mercury porosimetry analysis. A Malvern laser diffraction particle sizer was used to determine the size distribution of the 325 Marblewhite limestone before activation for comparison with the supplier's size distribution data.

Figure 5-12 presents the measured size distributions. The ordinate axis gives the weight percent below a certain particle size. This figures shows good agreement between the suppliers size distribution data (Pfizer) and the Malvern laser diffraction distribution measured by TDS. The Test 11 results were determined via mercury porosimetry. Comparison of the Test 11 results with the unactivated 325 Marblewhite distribution, which was also derived via mercury porosimetry, shows little change in particle size distribution between activated and unactivated samples. This data implies that significant particle shattering is not occurring during the activation process.

RAW & CALCINED LIMESTONE SIZE DISTRIBUTIONS USING THREE TECHNIQUES - NO SIZE CHANGES UPON ACTIVATION

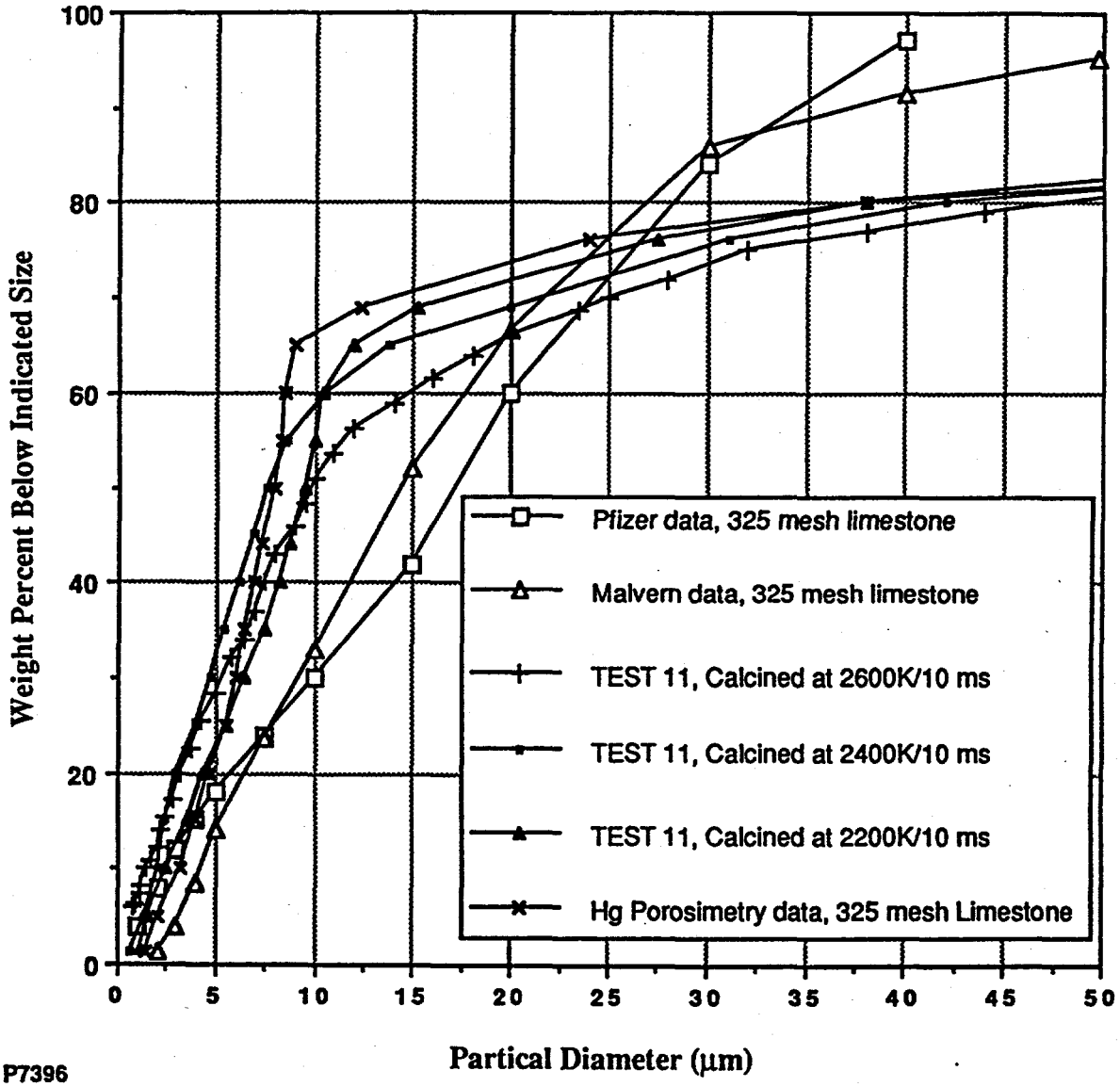

Figure 5-12. Limestone Size Distributions Before and After Activation.

5.8.2 SURFACE STRUCTURE VIA ELECTRON MICROSCOPY

Although the particle size distributions discussed in Section 5.8.1 imply that the activation process causes insignificant particle shattering, scanning electron microscopy photomicrographs were taken of several samples activated under a variety of conditions to explore this further and to obtain a visual picture of the surface structure of activated limestone particles. These photomicrographs not only make statements about shattering, but also indicate conditions under which sintering takes place.

Figures 5-13 through 5-16 show scanning electron photomicrographs of raw limestone (Marblewhite 325), limestone activated at 2200 and 2600°K for 10 ms, and limestone activated at 2600°K for 30 ms, respectively. The activated samples were collected in Tests A-5 and A-6, which were conducted during Phase IA of this program. The specific surface area and porosity corresponding to the samples in Figures 5-13 through 5-16 are summarized in Table 5-1. This table also gives corresponding particle size distribution data obtained using Malvern laser diffraction particle sizing, composition data obtained via chemical analysis, degree of calcination in percent, porosity by direct measure and based on degree of calcination, and average pore size. Multipoint nitrogen adsorption with BET analysis was used to determine specific surface area, the direct measure of porosity, and average pore size. An expression relating maximum theoretical porosity to degree of calcination was developed during this program. This expression, which is given below, is based on the assumption of constant particle size and the effect of density change as calcium carbonate ($CaCO_3$) is converted to calcium oxide (CaO) during calcination. If the densities of calcium carbonate and calcium oxide are represent by $\rho(CaCO_3)$ and $\rho(CaO)$, respectively, the molecular weights of calcium carbonate and calcium oxide represented by $M(CaCO_3)$ and M(CaO), respectively, and α and β represent the maximum theoretical porosity and degree of calcination, respectively, the expression relating α and β is:

$$\alpha = \beta \left(1 - \frac{M(CaO)}{M(CaCO_3)} \frac{\rho(CaCO_3)}{\rho(CaO)} \right) \qquad (5\text{-}1)$$

Substitution of M(CaO) = 56, $M(CaCO_3)$ = 100, ρ(CaO) = 3.32 gm/cc, and $\rho(CaCO_3)$ = 2.71 gm/cc reduces equation (5-1) to:

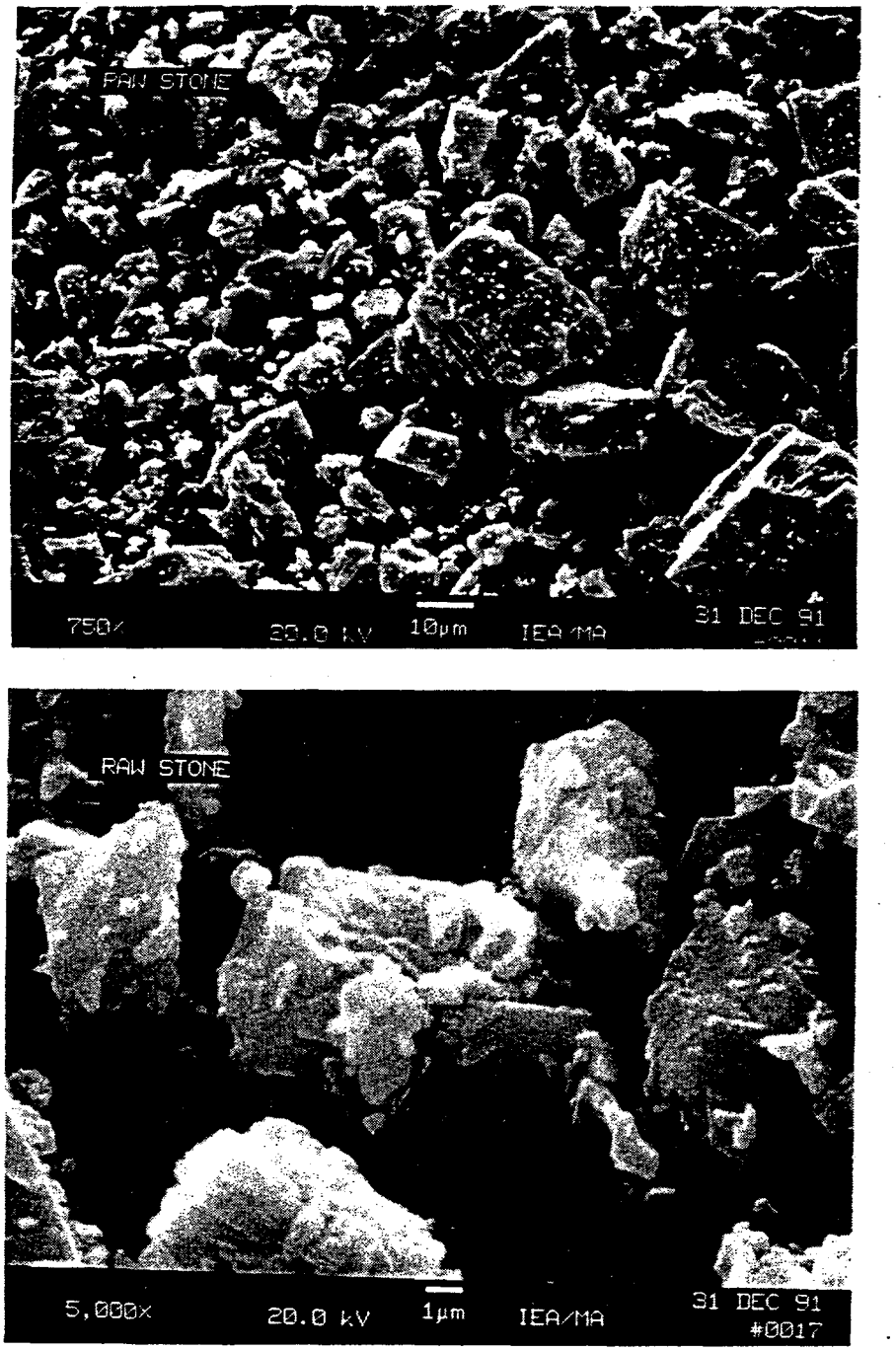

Figure 5-13. SEM Photographs of Raw Marblewhite 325 Limestone.

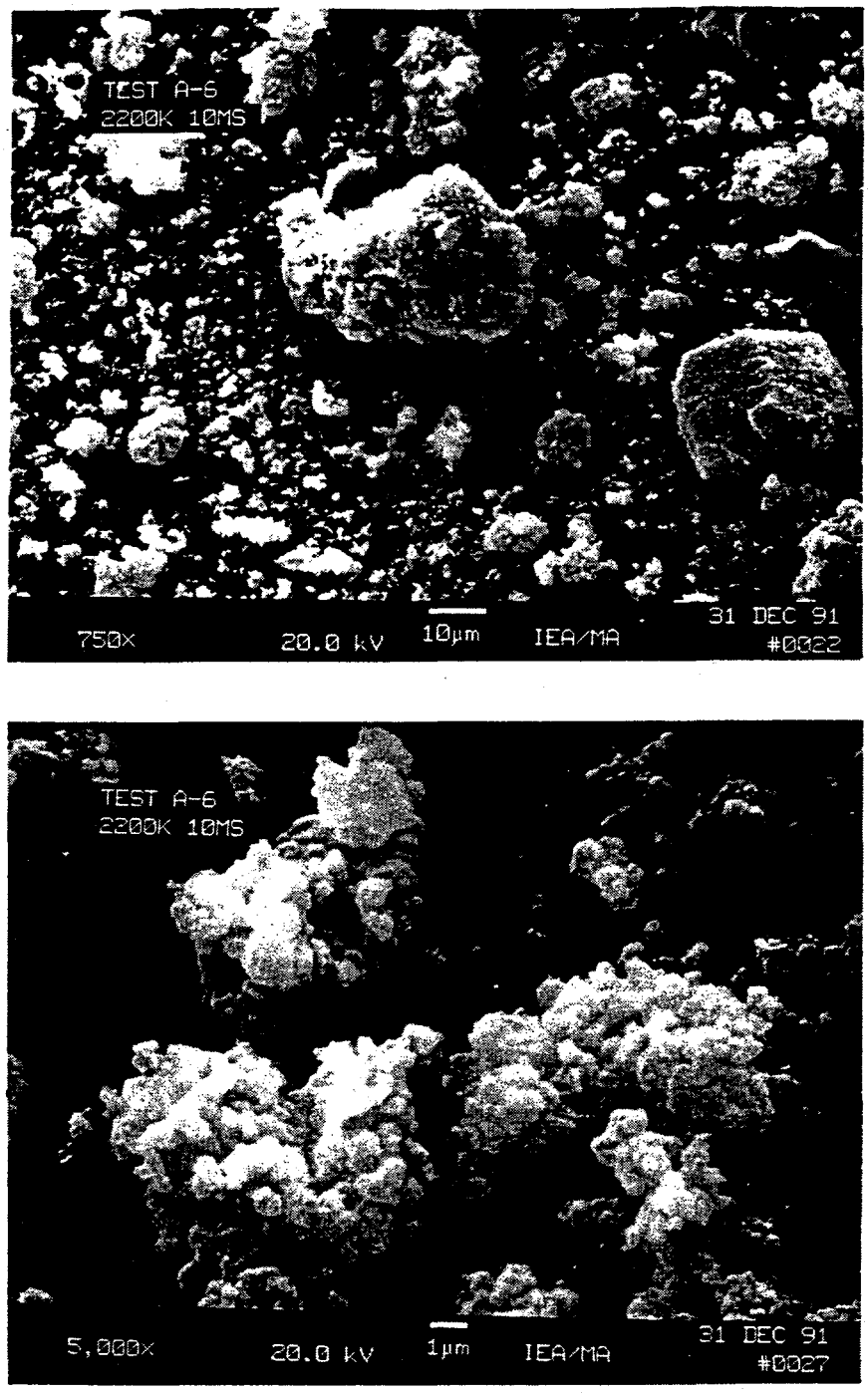

Figure 5-14. SEM Photographs of Marblewhite 325 Limestone Activated at 2200 ^{o}K and 10 ms.

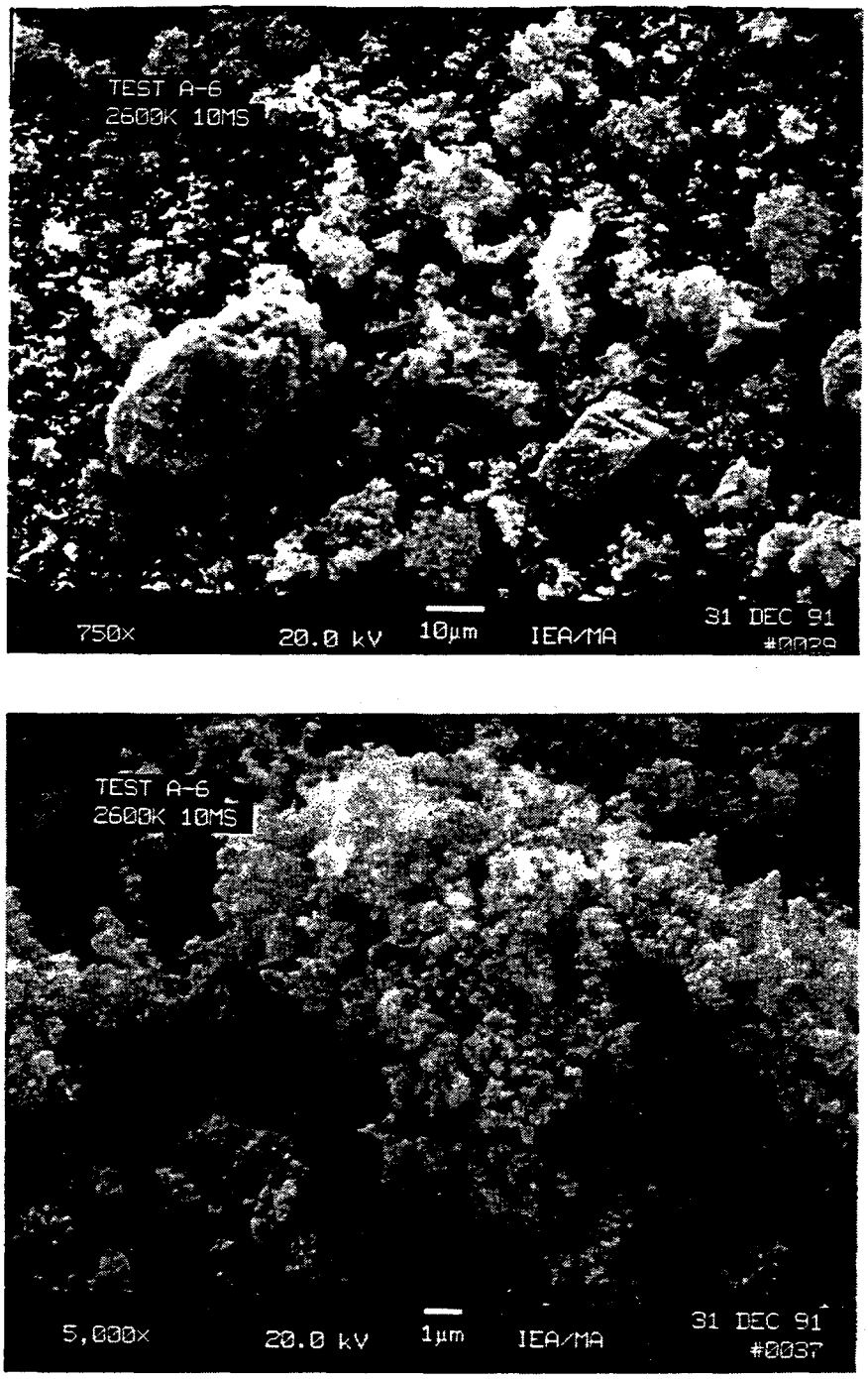

Figure 5-15. SEM Photographs of Marblewhite 325 Limestone Activated at 2600 ^{o}K and 10 ms.

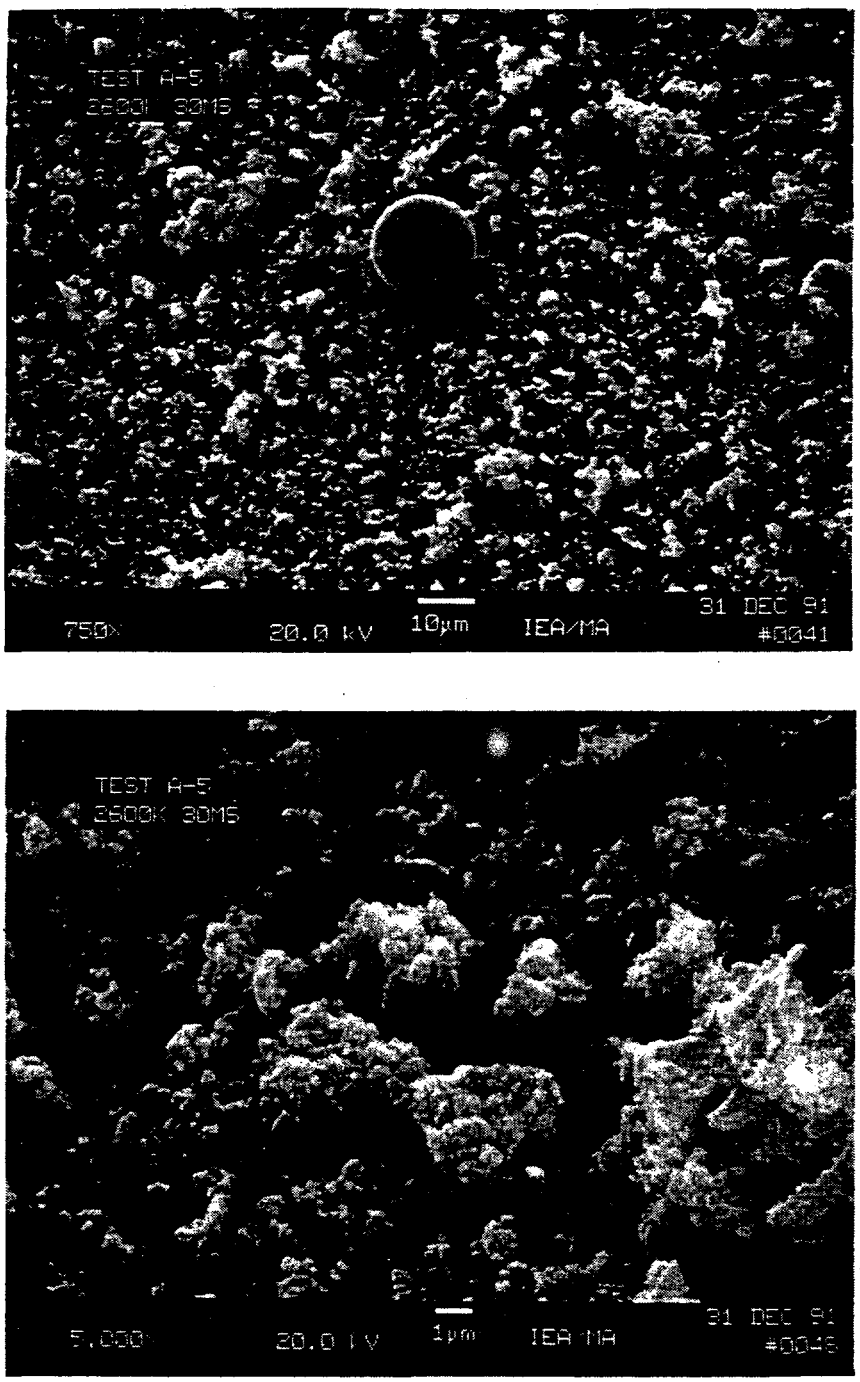

Figure 5-16. SEM Photographs of Marblewhite 325 Limestone Activated at 2600 ^{o}K and 30 ms.

Table 5-1. Physical Properties of Activated Limestone Particles.

Sorbent: 325 Mesh Marblewhite Limestone

Photomicrographs of Highlighted Samples Given in Figures 5-13 Through 5-16

Activation Time: 10 ms

Sample Conditions	$CaCO_3$	CaO	$CaSO_4$	Calcination (%)	Sp. Area (m^2/gm)	Porosity (%) Measured	Porosity (%) Calcination	Ave. Pore Size (Å)
Unactivated	**95**			**0**	**1.7**	**2.0**		**173**
2200°K	**30.8**	**52.5**	**0**	**69.2**	**7.2**	**4.1**	**37.4**	**86.2**
2400°K	19.3	68.7	0	80.7	9.7	5.0	43.6	79.5
2600°K	**18.1**	**73.5**	**0**	**81.9**	**12.2**	**5.5**	**44.2**	**70.0**

Particle Size Measurements of Activated Samples using a Laser Diffraction Particle Size Analyzer (particles dispersed in denatured alcohol):

Sample Conditions	D(10) (μm)	D(50) (μm)	D(90) (μm)
Unactivated	**3.9**	**13.0**	**29.3**
2200°K	**4.9**	**16.1**	**42.0**
2400°K	4.7	11.4	25.0
2600°K	**6.2**	**17.5**	**40.0**

Activation Time: 30 ms

Sample Conditions	$CaCO_3$	CaO	$CaSO_4$	Calcination (%)	Sp. Area (m^2/gm)	Porosity (%) Measured	Porosity (%) Calcination	Ave. Pore Size (Å)
2200°K	19.8	59.0	0	80.2	7.0	4.3	43.3	93.4
2400°K	15.2	70.2	0	84.8	7.2	4.1	45.8	87.2
2600°K	**15.4**	**64.9**	**0**	**84.6**	**13.9**	**6.8**	**45.7**	**77.1**

Particle Size Measurements of Activated Samples using a Laser Diffraction Particle Size Analyzer (particles dispersed in denatured alcohol):

Sample Conditions	D(10) (μm)	D(50) (μm)	D(90) (μm)
2200°K	3.6	11.7	25.4
2400°K	4.1	12.4	28.0
2600°K	**3.8**	**12.8**	**41.4**

$$\alpha = 0.54\ \beta \qquad (5\text{-}2)$$

Equation (5-2) indicates that the maximum theoretical porosity for a 100% calcined limestone particle (β = 100%) is α = 54%.

Figures 5-13 through 5-16 each contain two photomicrographs that were taken under magnifications of 750X and 5000X. Observations regarding the photomicrographs presented in Figures 5-13 through 5-16 and the data presented in Table 5-1 follow.

Change in Particle Size Distribution Upon Activation: A comparison of the photomicrographs in Figures 5-14 through 5-16 (activated samples) with those in Figure 5-13 (raw, unactivated limestone) shows that many more fine particles (< 5 microns) are present in the activated samples. It should noted that solids sampling was performed using an isokinetic probe, so size distribution bias should be minimal. Thus, the high heating rate activation process appears to result in more fine particles.

As noted above, Table 5-1 presents particle size distribution data for the raw and activated samples that were measured using a Malvern laser diffraction particle sizer. The particles were dispersed in denatured alcohol; water was not used in order to avoid lime hydration. The laser diffraction measurements show little change in the particle size distribution upon activation. Limestone particle size measurements performed on earlier samples using mercury porosimetry also indicated no significant change in particle size upon activation. These conflicting sets of data may be reconciled if it is observed that the fine particles constitute only a small mass fraction of the powder. This is borne out by the laser diffraction measurements which show that approximately 10% of the mass is present as fine particles. Therefore, the number density of fine particles may increase by a factor of 2-5 upon activation, but this does not change the mass size distribution significantly. Hence, it can be concluded that a small degree of particle shattering occurs during the activation process.

Change in Surface Characteristics Upon Activation: Comparison of Figures 5-14 through 5-16 with Figure 5-13 indicates that the activated samples have a fluffier and more porous

surface compared to the raw limestone particles, which have little porosity. Despite the appearance of a reasonably porous surface the actual porosity in the activated samples is small, which is demonstrated in Table 5-1. In fact the measured porosities are roughly 1/10th of the porosity calculated from the degree of calcination data (via equation (5-2)) assuming no change in particle size. The maximum porosity of fully calcined limestone is approximately 50%. Despite the low porosity, however, Figures 5-14 and 5-15 show no clear indication of particle sintering. However, Figure 5-16, which corresponds to the most extreme activation conditions, shows a reduction in fluffy appearance, with a few spherical particles present. This clearly indicates that sintering has occurred under the most extreme activation conditions (i.e., 2600°K for 30 ms). A comparison of Figures 5-14 through 5-16 shows that the most fluffy surface structure appears in Figure 5-15, which is for activation conditions of 2600°K for 10 ms. Regardless, Table 5-1 shows that the actual porosity and surface area of the three samples show in Figures 5-14 through 5-16 are low and within a factor of two.

Increase in Specific Surface Area Upon Activation: As documented in Table 5-11, Limestone activation at 2200°K to 2600°K for 10-30 ms results in a modest increase in the specific surface area of the sorbent; from 1.7 m^2/gm for the raw limestone to up to 14 m^2/gm for the activated sorbent. This increase is largely due to an increase in the internal surface area (due to an increase in the particle porosity) rather than an increase in the external area (due to particle shattering and creation of fine particles). A simple calculation shows that even a doubling of the number of fine particles (< 5 microns) causes a minor increase in the specific surface area.

Surface Structure Summary: The results presented in Table 5-2, together with the photomicrographs of raw limestone and activated limestone presented in Figures 5-13 through 5-16, show that the activation process does alter the number of fine particles and the surface texture of the particles. Albeit, the effect is not as profound as desired since porosity only increases from 2% to maybe 7% and surface area only increases from 1.7 to maybe 14 m^2/gm. It was hoped that specific surface areas near those produced the under slow calcination conditions (1100°K for several hours) explored by Stouffer and Yoon[8] (60 m^2/gm) could be achieved. This goal, as shown, was not achieved. Although Table 5-1 shows that nearly complete calcination is being achieved at activation temperatures greater than 2400°K, the low surface areas, porosities, and pore sizes (pore size actually decreases as a result of activation) suggest that sintering and non-

optimum activation is occurring over most of the size distribution of the polydispersed limestone powder. More specifically, the results presented in this subsection (Section 5.8.2) tend to support the inherent limitation proposed earlier in Section 5.0, namely: it is probably impossible to uniformly achieve highly activated calcia across the broad size distribution of the parent limestone feed. This hypothesis is drawn from the observation that particle heating by imposing a surface heat flux generated by fixed activation temperature and time conditions will result in fines being sintered, some small size band being highly activated, and top sizes being less than optimally activated due to low heating rates. This limitation is adopted as the explanation for the poor calcium utilizations produced by the Two-Step Rapid Sulfur Capture process. In light of this the remainder of Section 5.8, thus Section 5.0, will be devoted to documenting results obtained under a variety of activation conditions; results that pertain to degree of calcination, specific surface area, porosity, and pore size.

5.8.3 DEGREE OF CALCINATION TRENDS

During the first step of the Two-Step Rapid Sulfur Capture process the limestone is heated rapidly at activation temperatures in the range 2200 - 2850^{o}K for durations in the range 0 - 40 ms. During the early stages of this step, calcination takes place which tends to moderate the rate at which particle temperature increases due to the exothermic nature of this reaction. The degree of calcination, which is the fraction of calcium converted from $CaCO_3$ to CaO during the activation process, is the first major indicator of the effectiveness of the activation process. This subsection explores, therefore, calcination degree for activation temperatures in the range 2200 - 2600^{o}K, activation times in the range 0 - 30 ms, and for mixing section quench jet angles of 0, 15, 30, and 60^{o}. Both Two-Step Rapid Sulfur Capture and Non-Equilibrium Activation mode results are presented.

Figure 5-17 presents degree of calcination results versus activation temperature based on solids samples collected during several Two-Step Rapid Sulfur Capture tests. The sorbent feed was 325 Marblewhite limestone. The calcium to sulfur ratio range was in the $1 \leq Ca/S \leq 2$ and sulfation temperature was either $T_s = 900^{o}C$ or $1100^{o}C$. The activation time was either τ_{act} = 0 or 10 ms. Results for all four mixing sections are presented in this figure, which provided quench jet angles of 0, 15, 30, and 60^{o}. Using the four mixing sections provided a means for

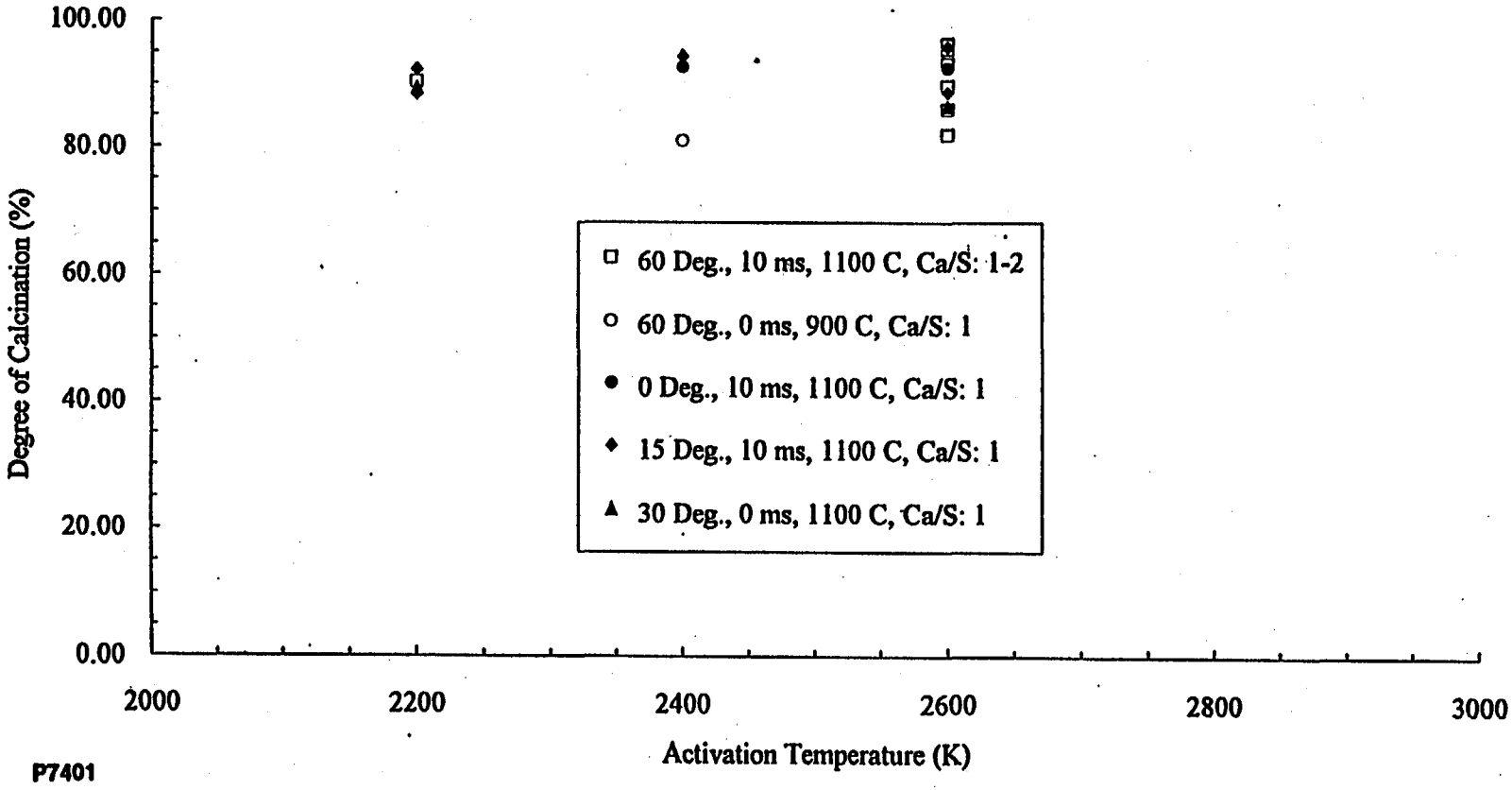

Figure 5-17. Two-Step Sulfur Capture Calcination Results.

testing the influence of quench time on degree of calcination. After close inspection of Figure 5-17, it became clear that no clear trends could be identified, i.e., any differences due to variations in activation temperature and time, mixing section quench jet angle, or sulfation temperature are not distinguishable. The only comment that can be made regarding the data in Figure 5-17 is that for activation temperatures greater than 2200°K the Two-Step process yields values for degree of calcination that are greater than 80% and perhaps as high as 95%. This result is very good, since it says that the activation process is producing very complete calcination, which is the first step towards producing a highly activated sorbent.

Figure 5-18 presents degree of calcination results versus activation temperature based on solids samples collected during several Non-Equilibrium Activation tests. For these tests the activation burner conditions were varied, but no SO_2 was injected into the system and ambient temperature nitrogen was injected as the quench gas, i.e., the side duct burners were not lit, rather only ambient temperature nitrogen gas was supplied to the side duct burners. The results presented in Figure 5-18 are based on four activation times (τ_{act} = 0, 10, 20, and 30 ms) and two mixing section injection angles (θ = 15 and 60°). The activation temperature was varied over the range $2200 \leq T_{act} \leq 2600$°K. Again, no discernable trends can be identified. If high and low data are neglected, it can be concluded that better than 80% of the calcium in the calcium carbonate is being converted to calcium oxide for activation temperatures greater than 2400°K. It may be that the degree of calcination for the 2200°K activation temperature is reduced compared to the higher activation temperatures, which is to be expected. The Non-Equilibrium Activation data seems to be somewhat lower than the Two-Step Rapid Sulfur Capture data, which could be due to the higher sulfation duct temperatures that are present during the Two-Step Rapid Sulfur Capture test. Sulfation duct temperatures were between 900 and 1100°C for the Two-Step Rapid Sulfur Capture test, whereas the Non-Equilibrium Activation tests produced sulfation duct temperatures of nominally 300°C. Thus calcination may have continued during the residence time in the sulfation duct during the Two-Step Rapid Sulfur Capture tests.

The Two-Step Rapid Sulfur Capture and Non-Equilibrium Activation results presented in Figures 5-17 and 5-18, respectively, clearly show that nearly complete calcination is taking place under the activation times and temperatures surveyed during this study. This is important since the activation process must thoroughly convert $CaCO_3$ to CaO as a first step toward producing

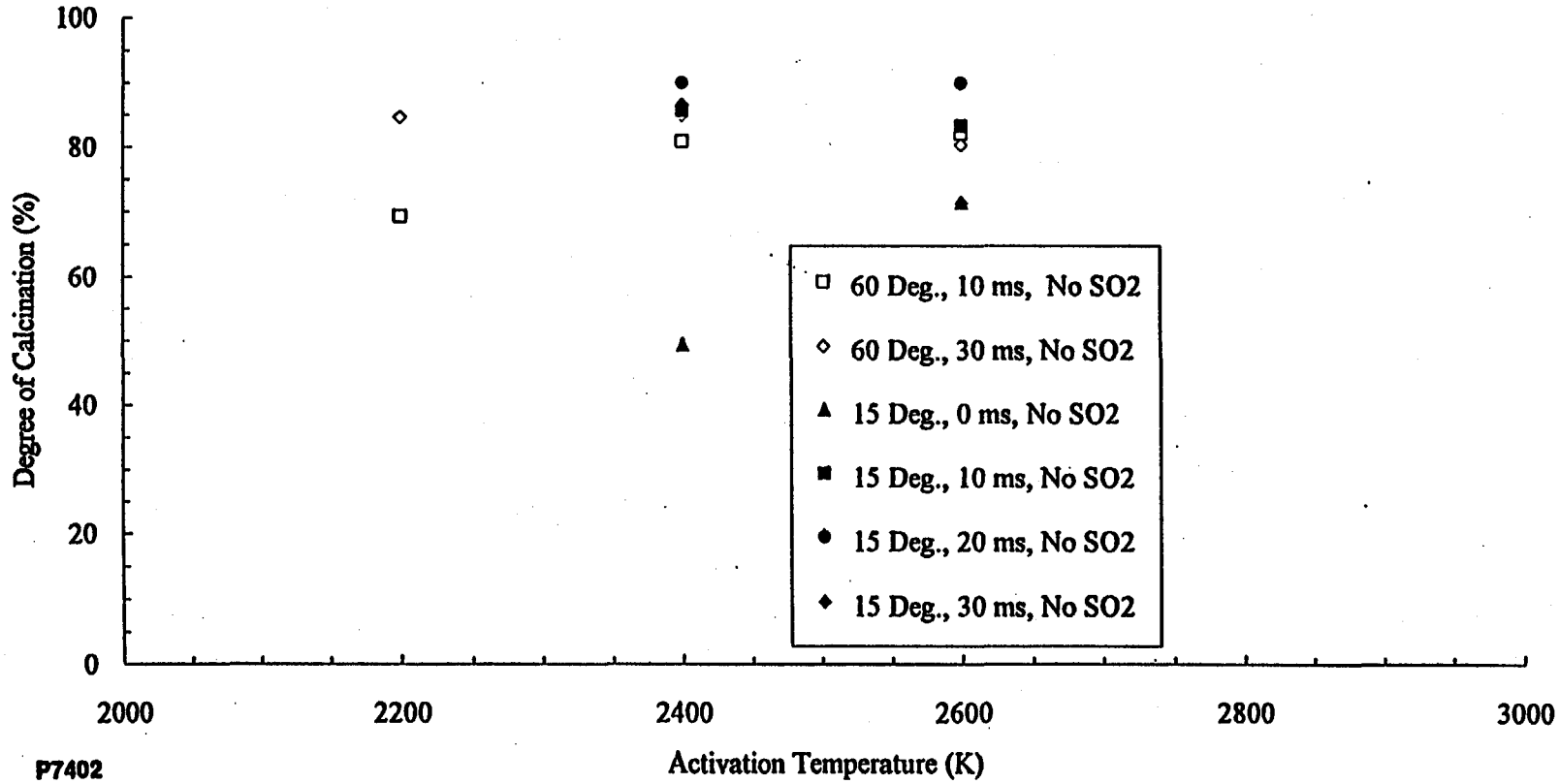

Figure 5-18. Non-Equilibrium Activation Calcination Results.

a highly activate sorbent.

5.8.4 SPECIFIC SURFACE AREA TRENDS

As noted in Section 5.8.2, the specific surface area of the activated sorbent plays an important role in all stages of the sulfur capture process. It is important, therefore, to examine the dependence of specific surface area on activation process parameters. Figure 5-19 does so by presenting specific surface area versus activation temperature for 325 Marblewhite limestone. This figure includes the influence of four activation times (τ_{act} = 0, 10, 20, and 30 ms) and two mixing section quench jet angles. The activation temperature was varied over the range $2200 \leq T_{act} \leq 2600^{o}K$. Activated sorbent surface areas were determined by applying nitrogen adsorption with BET analysis to solid samples collected while operating the test rig in the Non-Equilibrium Activation mode. If the spurious data point corresponding to 31 m^2/gm at $2600^{o}K$ is neglected, Figure 5-19 implies that specific surface area increases slightly with increasing temperature. The 15^{o} degree mixing section data at an activation temperature of $2400^{o}K$ implies an optimum activation time between 10 and 20 ms. This optimum may also apply at $2600^{o}K$, or one slightly less, but the scatter in the data prevents making definitive conclusions.

The major conclusion to be drawn from Figure 5-19 is that no real significant increase in specific surface area was achieved by varying activation temperature and time, and mixing section quench jet angle over their full or nearly full ranges. The best specific surface area was measured to be nominally 14 m^2/gm at an activation temperature of $2600^{o}K$ and an activation time of 30 ms using the 60^{o} mixing section. The data in Figure 5-6, however, suggests that this long activation time should not be optimum in terms of calcium utilization (see the 15^{o} mixing section data in Figure 5-6). Regardless, even 14 m^2/gm falls far short of the 60 m^2/gm Stouffer and Yoon[8] achieved at slow calcination rates.

5.8.5 POROSITY TRENDS

As noted in Section 5.8.2, porosity plays an important role in the later stages of the sulfur capture process where most sulfur capture occurs. High porosity and large pore size lead to pore diffusion rates that yield enhanced sulfur capture. Thus, highly activated limestone sorbents must

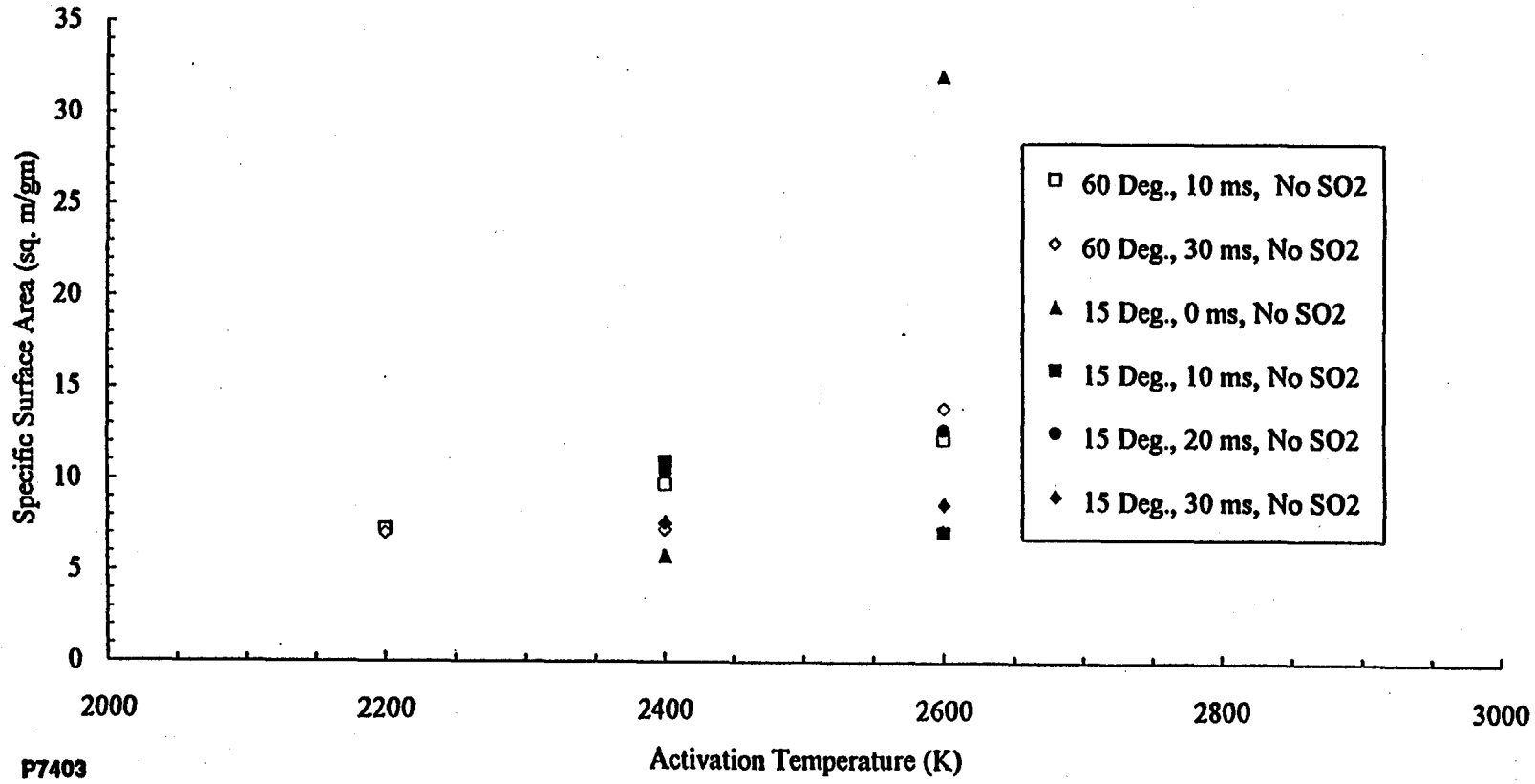

Figure 5-19. Specific Surface Area Results for Non-Equilibrium Mode Activation.

have high porosity, i.e., porosities approaching the theoretical limit (~50%). It is important, therefore, to examine the dependence of porosity on activation process parameters. Figure 5-20 does so by presenting porosity results versus activation temperature for 325 Marblewhite limestone. This figure includes the influence of four activation times (τ_{act} = 0, 10, 20, and 30 ms) and two mixing section quench jet angles. The activation temperature was varied over the range $2200 \leq T_{act} \leq 2600^{o}K$. Activated sorbent porosities were determined by applying nitrogen adsorption with BET analysis to solid samples collected while operating the test rig in the Non-Equilibrium Activation mode. As with the calcination results presented in Section 5.8.3 and the specific surface area results presented in Section 5.8.4, no discernable trends regarding the dependence of porosity on activation time or mixing section quench jet injection angle can be formulated based on the results in Figure 5-20. The only trend clearly visible is that porosity tends to increase slightly with increasing activation temperature. Albeit, the best measured porosity (~ 6 - 7%) falls far short of the maximum theoretical value (~50%). Since the porosity is low, pore diffusion rates will be significantly reduced relative to perceived optimums, which will significantly slow down the sulfur capture process.

5.8.6 PORE SIZE TRENDS

As noted in Section 5.8.2, pore size also plays an important role in the later stages of the sulfur capture process. Large pore size leads to pore diffusion rates that yield enhanced sulfur capture. Thus, highly activated limestone sorbents must have reasonably large pore sizes, i.e., optimum pore sizes should be much greater than those of the feed limestone, which, as shown in Table 5-1, is nominally 170 Å for 325 Marblewhite limestone. To explore reasons for the poor calcium utilizations produced by the Two-Step Rapid Sulfur Capture process, it is important to examine the dependence of pore size on activation process parameters. Figure 5-21 does so by presenting mean pore diameter versus activation temperature for 325 Marblewhite limestone. This figure includes the influence of four activation times (τ_{act} = 0, 10, 20, and 30 ms) and two mixing section quench jet angles. The activation temperature was varied over the range $2200 \leq T_{act} \leq 2600^{o}K$. Activated sorbent mean pore diameters were determined by applying nitrogen adsorption with BET analysis to solid samples collected while operating the test rig in the Non-Equilibrium Activation mode. As with the calcination, specific surface area, and porosity results presented in Sections 5.8.3 through 5.8.5, no discernable trends regarding the dependence of pore size on

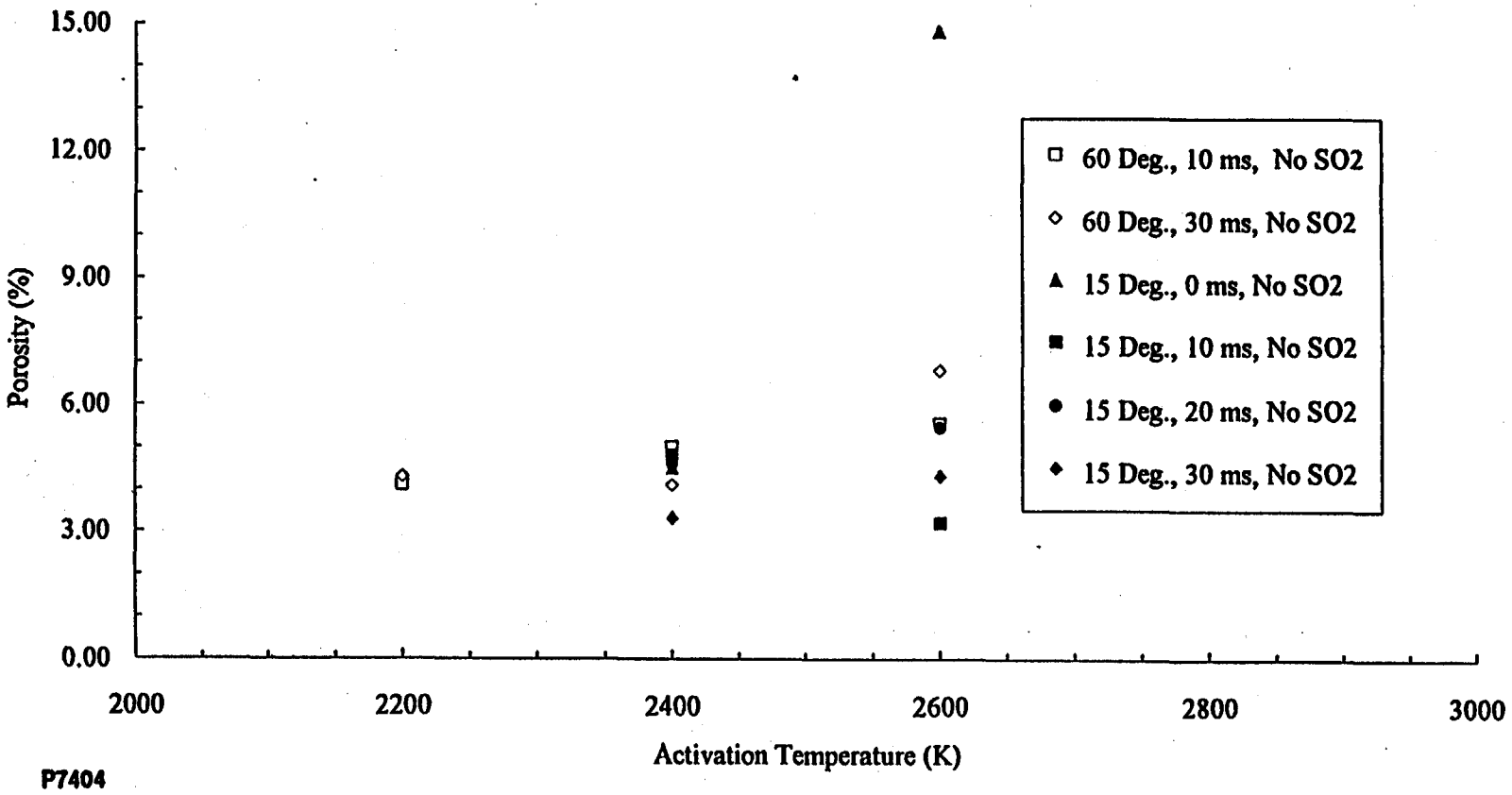

Figure 5-20. Porosity Results for Non-Equilibrium Mode Activation.

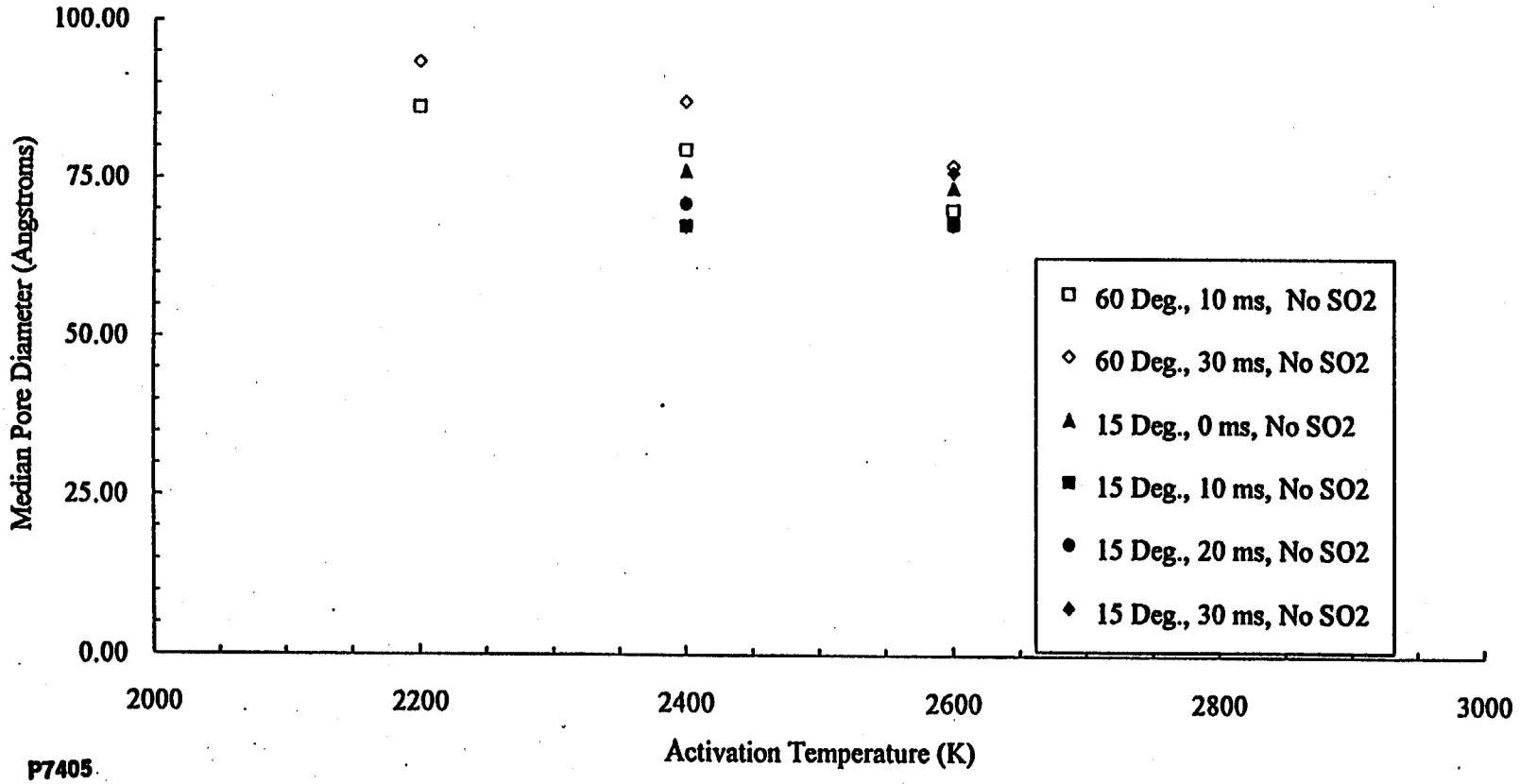

Figure 5-21. Median Pore Size Results for Non-Equilibrium Mode Activation.

activation time or mixing section quench jet injection angle can be formulated based on the results in Figure 5-21. The only trend clearly visible is that pore diameter tends to decrease with increasing activation temperature. It should also be noted that the maximum pore diameter in Figure 5-21 is nominally a factor of two less than the pore diameter of the unactivated 325 Marblewhite limestone. As noted above, it is necessary to achieve pore diameters that are at least greater than the unactivated limestone. Since the best pore diameters are significantly lower than unactivated limestone pore diameter, pore diffusion rates will be very low, which will lead to low sulfur capture rates.

5.8.7 CLOSURE TO SECTION 5.8

As noted in Section 5.2, the best Two-Step Rapid Sulfur Capture calcium utilization measured during this program was nominally 10%. This level was achieved at activation temperatures in the range 2200 - 2600^{o}K (utilization did not appear to be strongly dependent on activation temperature in this range), an activation time of 10 ms, a slightly fuel lean stoichiometry ($0.8 \leq \phi_s \leq 0.9$), a sulfation temperature of nominally 1100^{o}C, and using the 15^{o} mixing section. This level of calcium utilization makes the Two-Step Rapid Sulfur Capture process very unattractive economically, which is elaborated on in more detail in Section 7.0 and in Appendix I. This subsection (Section 5.8) has taken a close look at the morphology of limestone particles after activation under a variety of conditions. The reason for doing this was to gain some insight into what is responsible for the poor calcium utilizations. The following summarizes morphological characteristics which are hindering the Two-Step process from achieving competitive sulfur capture performance.

The specific surface area results presented in this subsection are at best a factor of four less than those achieved by Stouffer and Yoon[8] under slow calcination conditions. Thus, the Two-Step process is hindered by its inability to produce a high surface area calcia sorbent. The porosity of the activated sorbent produced by the Two-Step process is at best a factor of seven below the theoretical maximum. Thus, the Two-Step process fails to produce a highly porous calcia sorbent. Lastly, the Two-Step process produces activated limestone sorbent that has a mean pore diameter that is less than the unactivated limestone. Thus, the Two-Step process fails to produce activated calcia that has modest pore sizes. In order for a sorbent to efficiently capture

sulfur, it must have high surface area, high porosity, and large pore size. The sorbent produced by the Two-Step process falls short on all three counts. It is understandable now why the Two-Step Rapid Sulfur Capture process produces such low calcium utilizations.

Low surface area, low porosity, and small pore size all tend to support the process limitation posed early in Section 5.0, namely: it is probably impossible to uniformly achieve highly activated calcia across the broad size distribution of the parent limestone feed. This hypothesis is based on the observation that particle heating by means of a surface heat flux generated by fixed activation temperature and time conditions will result in fines being sintered, some small size band being highly activated, and top sizes being less than optimally activated due to low heating rates. This limitation is adopted, as noted earlier, as the explanation for the poor calcium utilizations produced by the Two-Step Rapid Sulfur Capture process.

6.0 TWO-STEP RAPID SULFUR CAPTURE MECHANISM MODELING

6.1 INTRODUCTION

The key objective of model development is to provide a tool suitable for effective prediction of sulfur capture processes, while minimizing the investment in code development, and retaining simple operation on conventional hardware. To achieve this, a model structure is chosen which focuses on particle centered rate controlling mechanisms, while treating the bulk fluid mechanics in a simple but adequate ad hoc manner. Available subroutines were extensively used and adapted to satisfy this specific application, minimizing the need for new code development.

The critical physical and thermal processes occurring in gas phase sulfur compound capture by pulverized calcium compounds are described by the numerical model. It serves as a tool for investigation of the relative sensitivity of the capture process to such factors as bulk flow mixing, particle size distribution, temperatures, gas concentrations, and heterogeneous kinetic rates. It is structured to run efficiently on an 80386/80387 or 486i based PC. Consequently, it allows rapid assessment of the sensitivity of sulfur capture to the above factors. This in turn permits effective use of the model as a tool for rapid interpretation of experimental results, and exploration of the sensitivity of sulfur capture to changes in sorbent properties and flow conditions.

6.2 PHYSICAL MECHANISMS AND CORRESPONDING MODELS

For this class of two phase flows, several key simplifying assumptions are made. First, to avoid complex fluid mixing modeling, it is assumed that the reacting fluid is instantaneously at uniform properties, and that mixing between fluid streams is a simple temporal process. Second, the gas phase chemical kinetic rates are assumed to be infinitely fast relative to heterogeneous rates, so that gas phase thermochemical equilibrium can be assumed. These approaches have been extensively used in modeling of pulverized coal combustion and glass batch heating, and found to be credible for preliminary analysis.[9-16] Also, it is assumed that particles are effectively spherical, and that they are internally homogeneous. As will be discussed below, these last two assumptions should be critically reviewed relative to high rate limestone sulfation.

Three classes of mechanisms are treated as having critical impact on overall particle - gas interaction. These are: bulk gas phase mixing; thermo-physical particle behavior; and heterogeneous chemistry.

The first addresses interaction between a gas stream carrying calcium based particles with a second gas stream. Their transient mixing process defines the gross time evolution of the bulk gas environment within which the particles interact. This is treated in a very simple manner, totally avoiding computational modeling of the fluid mixing process. Instead, as outlined in Figure 6.1, the primary gas stream is treated as being entrained into the carrier gas - particle stream over a defined time scale, with the mixed fluid being of uniform properties at any instant in time. Following completion of the mixing process, the homogeneous two phase system continues to evolve, as controlled by the finite rate particle physical and chemical processes. At all times, the bulk gas is assumed to be in local thermochemical equilibrium, providing definition of both temperature and gas phase species for treatment of the particle behavior.

Thermo-physical particle behavior is treated by modeling of coupled heat and mass transfer between the local gas conditions and the particle, for each of the particle size groups. This allows detailed treatment of the particle thermal history. Overall enthalpy balance is of course maintained by debiting the bulk gas enthalpy by the transfer to the particles.

Heterogeneous chemistry is treated for each size group in terms of coupled species transport and chemical kinetics. This directly impacts the particle energy balance through the chemical enthalpy effect of such processes as calcination and sulfation, and the mass transfer effect on gas - particle heat transfer. This also couples back to the gas phase through the local gas chemistry, affecting species mass transport, and gas temperature. Both gas enthalpy and species distribution are in turn impacted by particle evolution, including simple heating, drying and dehydration, calcination, sulfidation, and sulfation.

6.3 COMPUTER CODE STRUCTURE

The computer model is structured in a conventional manner to read input data files,

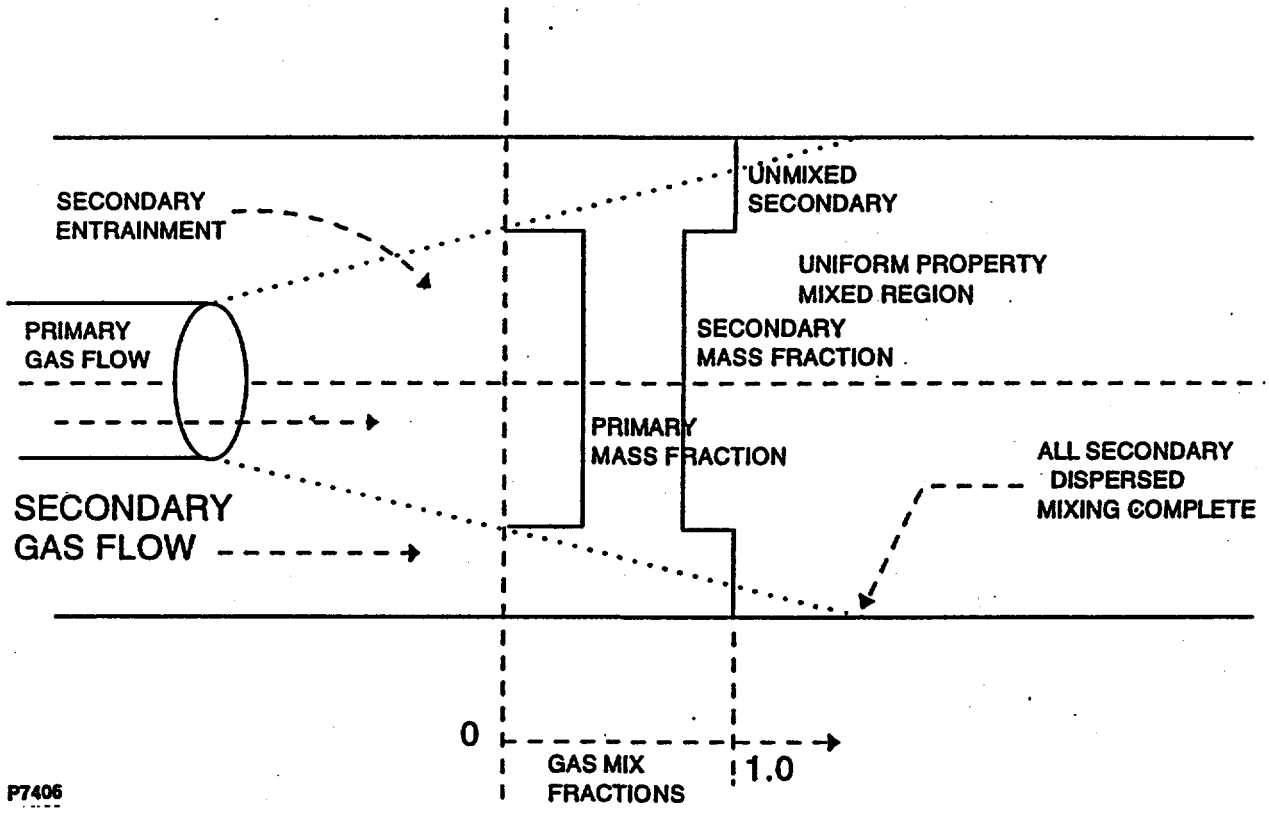

Figure 6-1. Physical Configuration of Computational Modeling.

perform a time stepped numerical integration of gas and particle properties, and generate output files showing gas and particle properties at discrete time steps. Status is shown on the computer monitor during this process. The code is written in standard Fortran 77, and is structured for compatibility with the Microsoft MS-DOS based compiler, currently version 5.1.

Input data is contained in three files. One is a standardized set of thermochemical property data. The second includes program-specific gas phase species property and kinetic data. These are used in the numerical solver to determine instantaneous gas phase chemical composition, using in fact a stiff Runge-Kutta solver for gas phase kinetics with very high rates assigned, rather than a true thermochemical solver. This is adequately fast numerically, and avoids incorporation of a thermochemical routine, while using the generalized stiff solver required for calculating the instantaneous particle properties.

The third input data file, shown in Appendix D, is specific to the modeling of the particle behavior. It specifies initial particle properties, gas properties, mixing history, numerical integration conditions, output write time interval, and completion time. Particle properties are defined in terms of the number of size groups [1 to 10]; initial diameter of each group; mass fraction in each size group; and initial particle composition, with arbitrary mass fractions of $CaCO_3$, $Ca(OH)_2$, CaO, Water, $CaSO_3$, $CaSO_4$, and CaS allowed. Particle constituent properties are also read in. Heterogeneous kinetics are set up to allow 12 different reactions, as defined in the input file. Specific reactions can be turned on or off for integration, depending on the chemical processes considered important, and to assess the relative independent effect of the various reactions. Carrier and primary gas composition, initial temperature, pressure, quantity relative to unity particle mass, and mixing behavior are also read in, followed by integration control and output requirements.

After reading these files, the code initiates cyclic updating of the mixing effect of the primary stream mass on the bulk carrier gas, while numerically integrating fully coupled particle thermal and chemical property evolution, including mass transfer blockage of heat and mass transport. Gas properties are updated for consistency with the particle energy and species balances. As noted above, a stiff Rung-Kutta routine is used, with the integration time step set in each case by the highest rate chemical or physical process, tested over all particle sizes. While

this test procedure adds a limited amount of computational overhead, it results in optimal computational accuracy and time, by continuously updating the numerical time step between prescribed bounds.

Two output files are written, with complete gas and particle property data at prescribed time steps. Also, the monitor display is updated to indicate the current output time step. One output file is a very extensive listing of all input data, intermediate computational results, and detailed calculation results. The other is a condensed tabular format, designed for import into a spreadsheet or plotting routine. A portion of each is listed for a sample case in Appendices E and F, respectively. Based on the input file CASOX.DAT specifications, the more detailed output is written at intervals of 0.5 second, and the plotting format file at intervals of 0.2 second. Data format information is incorporated throughout the detailed output material, and given as a header with the plotting file output.

6.4 SAMPLE PREDICTIONS

Two classes of calcium sorbent reaction are of direct interest for the two step sulfur capture process. These correspond to the key process steps of high temperature rapid calcination in the activation burner, and lower gas temperature non-equilibrium sulfation and thermal stabilization.

Representative input data for each of these conditions, corresponding to the working regime of the two-step experimental apparatus, is given in Appendices G and H. The inputs shown in Appendix G are set to allow description of limestone calcination in the activation burner. Appendix H describes the interaction of the calcined limestone from the activation burner as the flow mixes with the cooler simulated coal combustion products. Output files from these two cases are identical in structure to those given in Appendices E and F, and are not presented here in detail. The key results are the thermal and composition histories of the sorbent particles, and the gas phase sulfur species concentration. These are plotted in Figures 6.2 through 6.5.

Calcination behavior of pulverized limestone is shown in Figures 6.2 and 6.3. While the

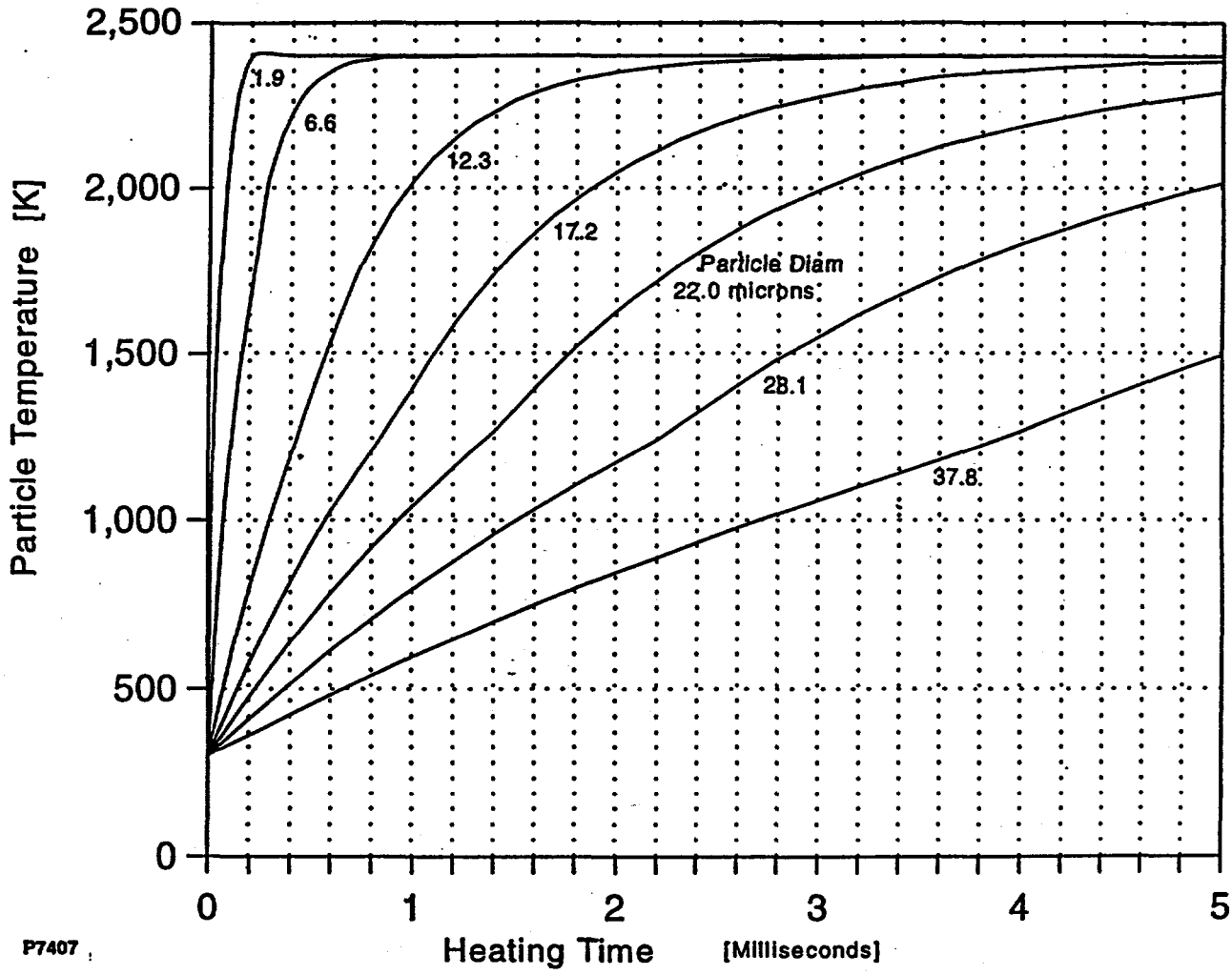

Figure 6-2. Modeled Particle Temperature History During Calcination.

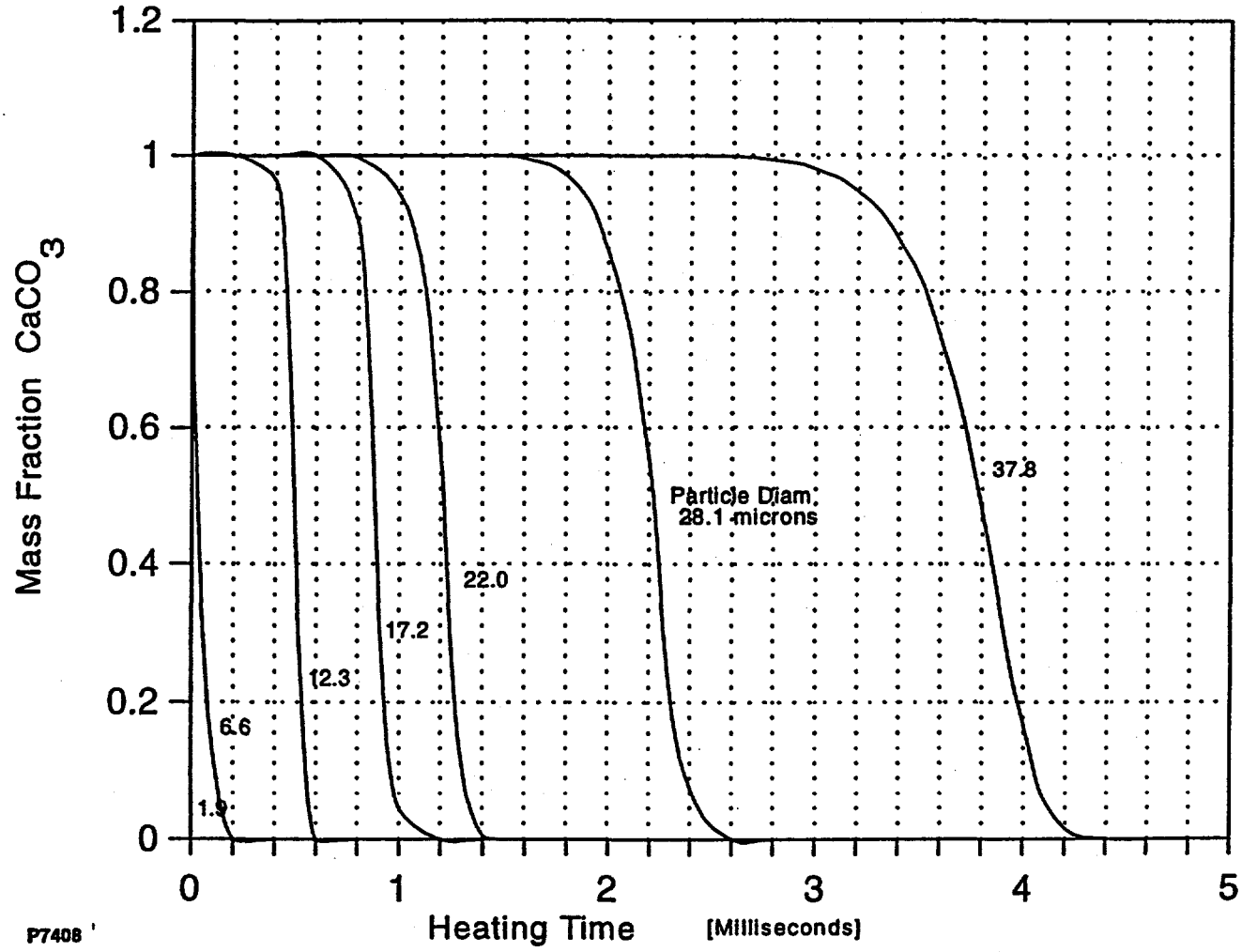

Figure 6-3. Modeled Calcium Carbonate Conversion During Calcination.

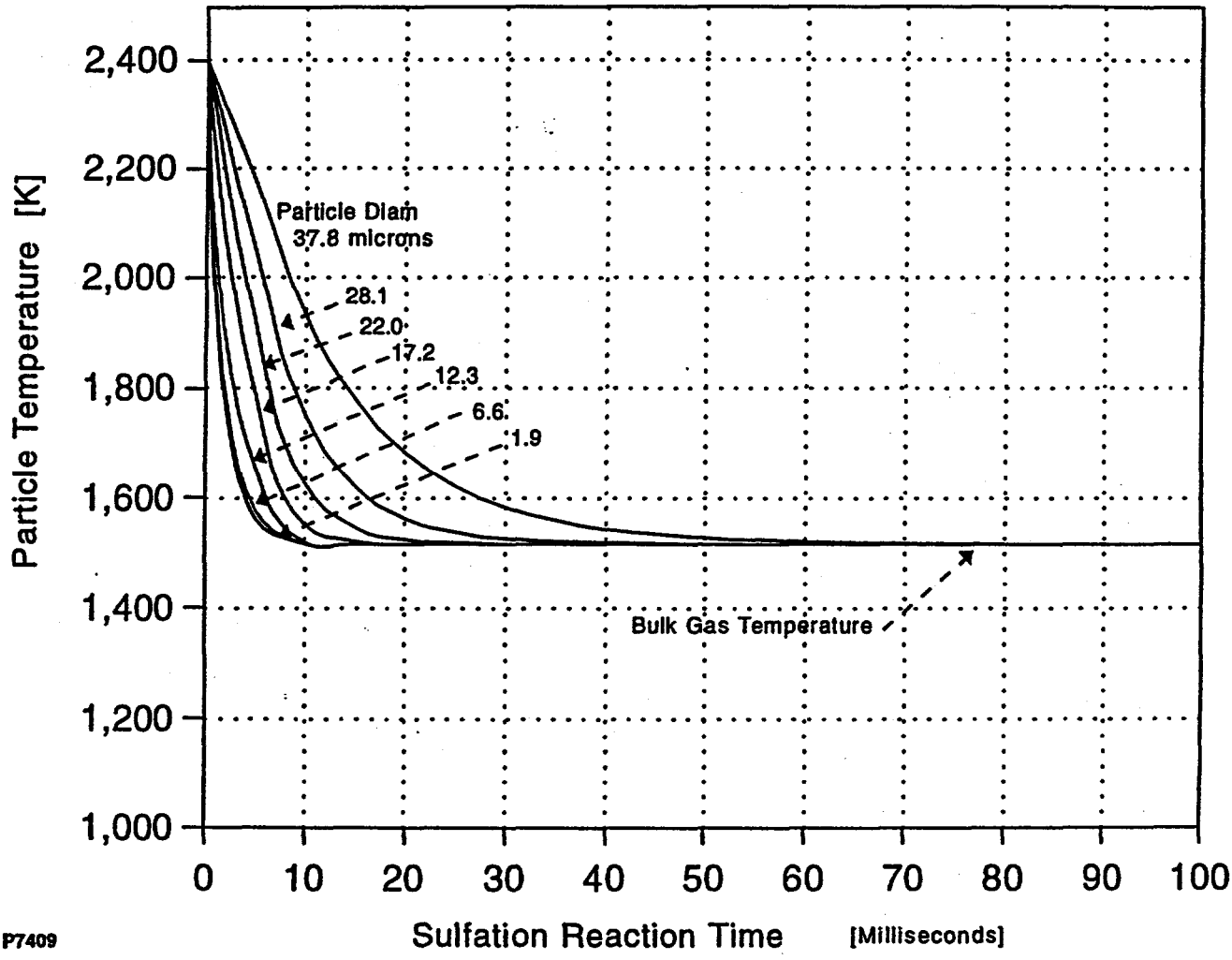

Figure 6-4. Modeled Particle Temperature During Quenching and Sulfation.

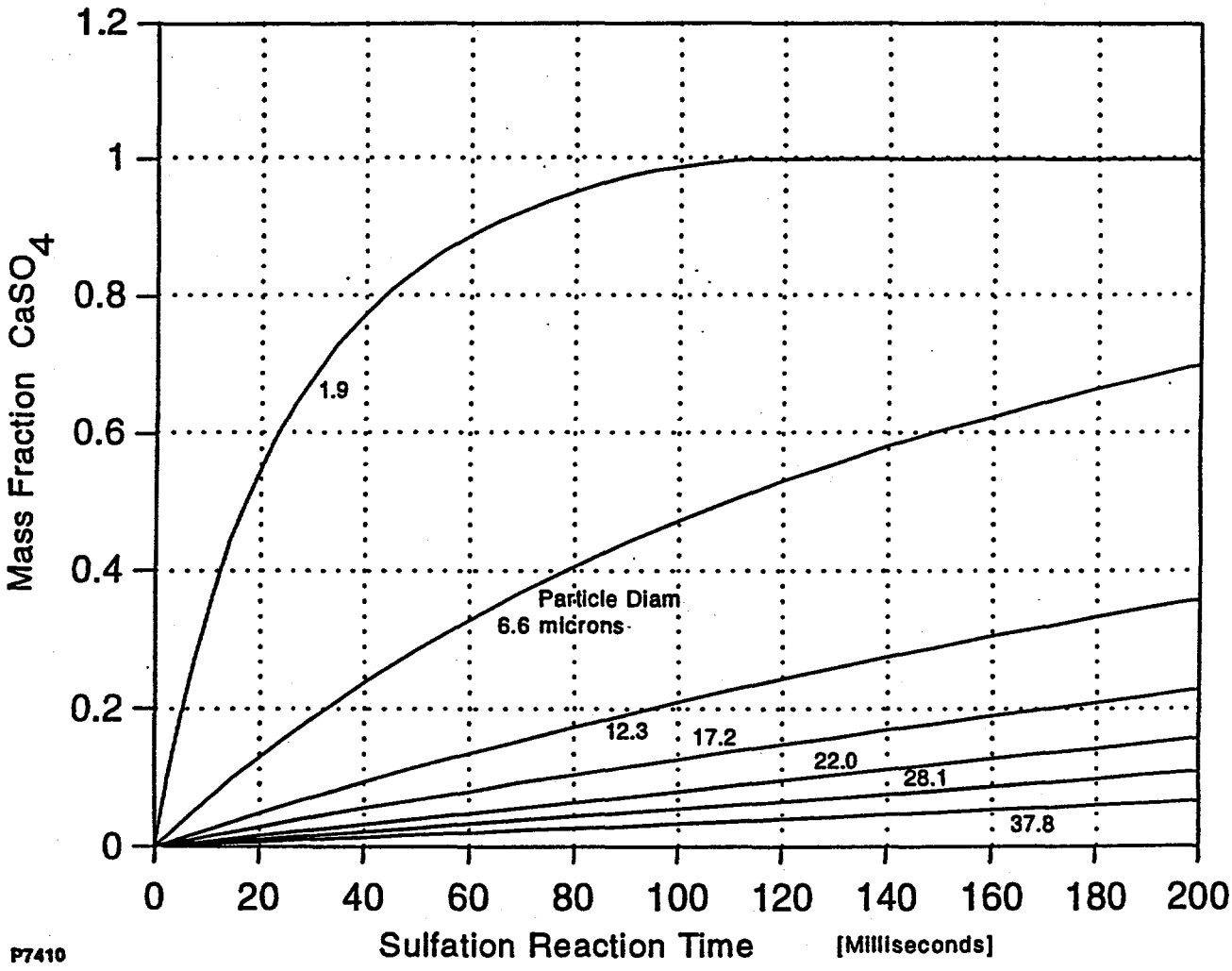

Figure 6-5. Modeled Mass Fraction of Calcium Sulfate During Sulfation.

calcination burner residence time can be up to about 70 milliseconds, the graphs terminate at 5 ms, corresponding to the completion of calcination. In this case, the limestone is initially pure $CaCO_3$ at 300 ^oK, and is exposed to combustion products at 2400 ^oK. Heat transfer from gas to particle drives particle temperature increase, with the finer particles responding fastest, as shown in Figure 6.2. As the particles increase in temperature, the finite rate endothermic calcination reaction begins, with the particle temperatures forced to flatten slightly in the 1300 ^oK range, until calcination is complete. Figure 6.3 shows the calcination behavior in terms of the variation with time of the $CaCO_3$ mass fraction of each particle size group. The solid phase product species is of course CaO. It is clear that the finer particles complete calcination rapidly, and then approach the local gas temperature, while the larger particles are calcining or heating. One obvious effect of this wide limestone particle size distribution is the potential for overheating ('Dead Burning') of the finer particles, or incomplete calcination of the larger particles.

Sulfation reaction of the hot calcined material with a cooler combustion gas containing SO_2 is shown in Figures 6.4 and 6.5. The particle temperature histories are shown in Figure 6.4, and their chemical composition evolution in Figure 6.5. The former shows the rapid thermal equilibration to the bulk gas temperature, controlled by bulk gas mixing for the finer particles, and by thermal inertia for the larger size fractions. The chemical energy term is small relative to conductive heat transfer, due to the low concentration of SO_2 in the bulk gas, and the correspondingly low effective reaction rate. Note that the time axis extends only to 100 ms., while the plot of particle sulfation covers 200 ms. The latter figure includes relative mass fractions of CaO and $CaSO_4$. Critical chemical reactions including initial sulfite formation, its oxidation to the sulfate, and reverse decomposition reactions are shown in the input file in Appendix H. While $CaSO_3$ is formed as an intermediate, the oxidation reactions forming $CaSO_4$ are rapid enough under the modeled conditions that the instantaneous $CaSO_3$ mass fraction is negligible. Under these conditions, there is very limited net sulfur dioxide capture predicted in the 200 ms residence time assumed.

6.5 MODEL SUMMARY

This model is a very effective tool for analysis of particle behavior in the research

environment. Its simple treatment of fluid dynamic processes, together with a detailed approach to particle centered energy and species variations, allows rapid and reliable numerical estimates of finite rate particle calcination and sulfation processes, with coupled heat and mass transport and heterogeneous kinetics.

It is highly effective computationally, as it is structured to focus explicitly on the controlling physical and chemical processes for calcium based sorbent reactions. Time dependent particle centered transport and chemical processes are treated in reasonable detail, with full thermal and transport coupling. Bulk gas phase mixing is simplified, to avoid unnecessary fluid dynamic computational overhead, while dealing with well defined quasi-one-dimensional flow conditions in a research environment. In that context, it is noted that this class of model, developed for pulverized coal combustion and gasification[9-15], has also been explicitly incorporated as a comprehensive particle reaction subroutine in fully three dimensional fluid dynamic combustor design calculations.[17-20] The same extension could readily be made in this case as well, if justified.

In terms of the detailed modeling of particle reactions, two areas should be refined for better representation of physical behavior. First, the particles are currently assumed to be internally homogeneous thermally and chemically. This is not correct in general, but is defensible for very fine sorbent particles, at least under moderate process conditions. However, the real issues of internal transport and temperature gradients, as well as time varying porosity, should be included to the extent that physical data allows a valid model description. In particular, it is easy to show that the relatively high heats of reaction, notably for calcination and for sulfation, coupled with their temperature dependencies and finite particle thermal and mass transport diffusivities, would be expected to create internal reaction fronts during transient processes, rather than allowing internal homogeneity during reaction.

A second area of model refinement is related to the above, but deals with gas phase transport external to the particle. The approach taken in this model is based on the traditional spherical droplet concept, in which heat and mass transfer are treated in terms of a Nusselt number correlation, with spherical symmetry assumed. That approach is quite credible for an evaporating liquid droplet, but highly questionable for a rapidly calcining solid particle. Based on observations

of rapidly devolatilizing coal particles, gas outflow as discrete jets is quite probable during rapid calcination. This can have a major impact on the overall calcination / sulfation process. It directly changes gas phase transport to the particle surface. The conventional concept of spherical 'blowing' decreases both heat and mass transfer to the particle, both limiting heat input for calcination, and preventing transport of O_2 and SO_2 to the particle during calcination. Gas jetting during sulfation would have an inverse effect on gas phase mass transport. The particle would be accelerated, enhancing simple convective transport. More significantly, the jet flow will entrain other gases, creating a substantially enhanced mass transfer rate to the particle surface. As shown in Section 6.4, the calcination process is predicted to thermostat the particle temperature in a range compatible with sulfation. Enhancing, rather than blocking transport of O_2 and SO_2 during calcination, would result in effective sulfation under non-equilibrium conditions. A modeling assessment of this, using a simple numerical description of the gas phase transport process with and without discrete gas jetting, would probably resolve some of the issues raised with non-equilibrium sulfur capture.

7.0 FEASIBILITY/ECONOMIC EVALUATION

The best Two-Step Rapid Sulfur Capture performance measured during the testing portion of this program is 10% sulfur capture at Ca/S = 1, or a calcium utilization of 10%. The sorbent used was Marblewhite 325 mesh limestone. These results were achieved using an activation temperature of 2200°K, an activation time of 10 ms, slightly fuel lean sulfation conditions, sulfation temperatures in the range 1100 - 1400°K, and the 15° mixing section. These results are certainly disappointing and show that the Two-Step Rapid Sulfur Capture process is far from being competitive with current sulfur removal technologies, which are achieving much higher sulfur captures and utilizations.

Using the same methodology applied to earlier tests results, which were more encouraging, yet in error, the cost($)/ton of SO_2 removed using coal/oxygen and natural-gas/oxygen activation burners has been calculated to be $3,614 and $4,694, respectively. Appendix I contains the original economic feasibility analysis performed early in this program when test results indicated that the Two-Step Rapid Sulfur Capture process could deliver 90% sulfur capture at a Ca/S = 2, which was shown to be in error later in this program and was due to an in-probe wet scrubbing effect that went undetected. Regardless, the original study is included in Appendix I to illustrate the approach used to derive economic feasibility. The cost/ton of SO_2 removed presented above for the Two-Step Rapid Sulfur Capture process is in no way competitive with existing sulfur removal technologies, which have a demonstrated cost($)/ton in the $300 - $700 range. The Two-Step Rapid Sulfur Capture process is even less attractive due to the greater amount of solid waste that would be produced due to its lower sulfur captures and calcium utilizations.

8.0 CONCLUSIONS

The following are the bulletized conclusions for the Phase I Rapid Sulfur Capture program. This program consisted of five elements, which are described in Section 4.2.2:

- The feasibility tests conducted during this program clearly show that the Two-Step Sulfur Capture Process is not capable of producing the calcium utilizations needed to demonstrate that the process is economically feasible. Thus, Phases II and III of the program were not undertaken and never will be.

- Since much of the data acquired during the early elements of this program were found to be invalid due to in probe wet scrubbing effects, which corrupted gas phase sulfur capture determinations, the data presented in this report is mainly that acquired during the Phase IB element of the overall program.

- The best Two-Step Rapid Sulfur Capture calcium utilization measured just prior to Phase IB (i.e., at the conclusion of Phase IA) was 11 - 12%. This result was achieved at an activation temperature of 2600^{o}K, an activation time of 10 ms, an activation burner stoichiometry of nominally $\phi = 0.97$ (with $\phi > 1$ being fuel rich), a Ca/S ratio of 2, a sulfation temperature of 1100 ^{o}C, a sulfation time of 250 ms, and a sulfation duct stoichiometry of nominally $\phi = 0.95$.

- The results of the TDS funded Batch Reactor Study showed that wet scrubbing effects may have interfered with true measurements of sulfur capture in the current and the previous batch reactor investigations; therefore all batch reactor work should be considered questionable.

- Attempts to significantly improve Two-Step Sulfur Capture utilization via experimental optimization tests involving parametric variations in activation temperature, activation time, sorbent quench parameters, and sulfation conditions were unsuccessful. However:
  - o Non-equilibrium utilization does improve somewhat with decreasing activation time and increasing activation temperature.

- Higher activation temperatures produce a somewhat more highly active sorbent; one with higher porosity and surface area, but lower median pore diameter. Higher porosity and surface area yield initially higher sulfur capture rates, but these fall quickly due to pore blockage.
- Quench jet injection angle only has a slight effect on utilization, although the best utilization (10%) was obtained with the 15^{o} mixing sleeve, an activation temperature in range 2200 - $2600^{o}K$, activation time of 10 ms, a sulfation temperature of $1373^{o}K$, and Ca/S = 1.

- Calcium utilization is not very sensitive to the Ca/S ratio; however the largest sorbent efficiencies were achieved at Ca/S ~ 1.

- Calcium utilization increases with increasing sulfation temperature up to a maximum of $1500^{o}K$, which is the maximum stable temperature for calcium sulfate under excess oxygen stoichiometries.

- Calcium utilization of limestone can be increased by taking smaller size cuts at a given activation temperature. This further implies that the Two Step process does not work well with sorbent feeds having polydispersed size distributions.

- Laser diffraction sizing and mercury porosimetry analysis applied to activated sorbent samples showed that no significant particle shattering occurs during the activation process. However, SEM photomicrographs showed that the number of very fine particles (< 5 micron) does increase during the activation process, but not enough to significantly alter the overall size distribution.

- Three morphological characteristics are hindering the Two-Step Process from achieving competitive sulfur capture performance:
  - The process is unable to produce a high surface area calcia sorbent.
  - The process fails to produce a highly porous calcia sorbent.
  - The process produces an activated sorbent with a mean pore diameter smaller than the original limestone. Basically the pore size is to small.

9.0 REFERENCES

1. Abichandani, J., Super-Equilibrium Sulfur Capture from High Temperature Gases, Final Report, DOE Contract No. DE-AC21-86MC23262, 1989.

2. "Advanced Coal-Fueled Gas Turbine Systems: Subscale Combustion Testing," Textron Defense Systems Subcontractor's Final Report for Westinghouse Electric Corporation, Power Generation Division, under DoE/METC Contract No. DE-AC21-86MC23167, 1993.

3. Gordon, S. and McBride, B. J., Computer Program for Calculation of Complex Chemical Equilibrium Compositions, Rocket Performance, Incident and Reflected Shocks, and Chapman-Jouget Detonations, NASA SP-273, 1976.

4. Richards, G.A., Lawson, W.F., Maloney, D.J., and Shaw, D.W., 1990. Rapid Sulfur Capture at High Temperatures, Technical Note, DoE/METC 91/4106.

5. Cole, J.A., Kramlich, J.C., Seeker, W.R., and Heap, M., Activation and Reactivity of Calcerous Sorbents Toward Sulfur Dioxide, Environ. Sci. Rechnol., pp. 1065, 19 (1985).

6. Newton, G.H., Chen, S.L., and Kramlich, J.C., Role of Porosity Loss Limiting SO_2 Capture by Calcium Based Sorbents, AIChE J., pp 988, Vol. 35, No. 6, 1986.

7. Milne, C.R., and Pershing, D.W, Time Resolved Sulfation Rate Measurements for Sized Sorbents, 4th Annual International Pittsburgh Coal Conference, pp. 109, 1987.

8. Stouffer, M.R., and Yoon, H., An Investigation of CaO Sulfation Mechanisms in Boiler Sorbent Injection, AIChE J., Vol. 35, No. 8, pp. 1253, 1989.

9. D.B. Stickler, R.E. Gannon, and H. Kobayashi, "Rapid Devolatilization Modeling of Coal," Eastern States Section Combustion Institute Meeting, Johns Hopkins University A.P.L., November 1974.

10. S.K. Ubhayakar, D.B. Stickler, C.W. von Rosenberg, Jr., and R.E. Gannon, "Rapid Devolatilization of Pulverized Coal in Hot Combustion Gases," Sixteenth Symposium *(International) on Combustion*, M.I.T., Cambridge, MA, August 15-21, 1976.

11. S.K. Ubhayakar, D.B. Stickler, and R.E. Gannon, "Modeling Entrained Bed Pulverized Coal Gasifiers," Fuel, Vol. 56, July 1977.

12. D.B. Stickler, F.E. Becker, and S.K. Ubhayakar, "Combustion of Pulverized Coal in High Temperature Preheated Air," 17th Aerospace Sciences Meeting, New Orleans, LA, January 15-17, 1979.

13. K. Annamalai, D.B. Stickler, R.E. Gannon, and L.A. Young, "Modeling of Pulverized Fuel Combustion Stability," Presented at the AIChE 1982 Summer National Meeting, Cleveland, Ohio, August 29 - September 1, 1982.

14. D.B. Stickler, R.E. Gannon, L.A. Young, and K. Annamalai, "An Engineering Model for Pulverized Fuel Combustion Stability," Presented at the American Flame Research Committee's Fall Symposium, Akron, Ohio, October 4-6, 1983.

15. R.E. Gannon, D.B. Stickler, W.A. Frederick, and D.R. Taschler, "Suspension Firing of Anthracite in Oxygen Enriched Air," Presented at the 1st Annual Pittsburgh Coal Technology Conference and Exhibition, Pittsburgh Hilton Hotel, September 17-24, 1984.

16. R. Tiwary, D.B. Stickler, and J. Woodroffe, "Numerical Modeling of Glass Melting in Advanced Glass Melter," Presented in the Glass Division of American Ceramic Society 90th Annual Meeting, Cincinnati, Ohio, May 1-5, 1988.

17. P.J. Loftus, A.U. Chatwani, A. Turan, and D.B. Stickler, "The Use of 3-D Numerical Modeling in the Design of a Gas Turbine Coal Combustor", ASME, Heat Transfer in Gas Turbine Engines and Three-Dimensional flows - HTD-Vol. 103, Eds., E. Elovic, J.E. O'Brien, and D.W. Pepper, 1989

18. A.U. Chatwani, A. Turan, and D.B. Stickler, "Design and Sizing of the Primary Stage of a Toroidal Vortex Gas Turbine Combustor Using a 3-D Flow Field Modeling Code," Presented at Western States Section / Combustion Institute, 1988 Spring Meeting, Univ. of Utah, March 21-22, 1988.

19. A. Turan, A.U. Chatwani, P.J. Loftus, and D.B. Stickler, "Combustor Modeling - A Maturing State of the Art", American Flame Research Foundation Conference, Pittsburgh, Pa. 1988

20. A.U. Chatwani, A. Turan, and D.B. Stickler, "Computation of 3-D Aerothermal Flow Field in a Coal Fired Combustor", Eastern States Section Meeting, Combustion Institute, Vanderbilt University, Spring 1991

21. Technical Assessment Guide, Volumes I and III, Electric Power Research Institute Report, EPRI P-4463-SR (1986).

22. Radcliffe, P., FGD Economics, pg. 33, EPRI Journal, December, 1990.

APPENDIX A

LISTING OF PHASE I (BASE) TESTS

This appendix gives a listing of the tests performed during the Phase I (Base) program (see Section 4.0 for an overview of the structure of the work performed during this project). Table A-1 lists the tests conducted, relevant process parameters for each test, and brief comments for each test. Each test may consist of one to six cases. Each case has unique process parameters. Given below are definitions or abbreviations used in Table A-1.

Mode:

TS	Two-Step Rapid Sulfur Capture mode.
NE	Non-Equilibrium Sulfur Capture mode.
Act.	Activation mode (no sulfur gas was injected into the system).

Activation Burner:

ϕ_{act}	Overall activation burner equivalence ratio.
T_{act}	Activation burner adiabatic flame temperature.
τ_{act}	Sorbent activation time based on activation duct plug flow velocity and duct length.
Sorbent	Three sorbents were tested, namely MW Marblewhite limestone, LHL Linwood hydrated lime, V45-3 Vicron 45-3 limestone.
Sorbent Size	Mesh size of sorbent.
Sorbent Cut	Indicates if the full size range of the sorbent was used (full) or the cut size range in microns (μm).
Loading	Weight percent of sorbent in activation module carrier burner.

Mixing Section:

Injection Angle	Mixing section quench gas injection angle. This is a parameter that characterizes the aggressiveness of the mixing occurring in this section. Four injection angles were studied over the entire

duration of this program, namely: 0, 15, 30, and 60 degrees. Only the 60 degree section was used during the Phase I (Base) program.

Sulfation Duct:

ϕ_s	Overall equivalence ratio in the sulfation (reactor) duct.
T_s	Average temperature in the sulfation duct.
Ca/S	Calcium to sulfur ratio in the sulfation duct.
Sulfur Gas	Identifies the sulfur gas compound injected into the system, either SO_2 or H_2S.
Concentration	Average concentration of the sulfur gas in the sulfation duct before sorbent injection.

Solids Sampling:

Type	Two types of sorbent samples were collected. Samples designated Act. (Activation) were collected when no sulfur gas was present and represent activated sorbent samples. Samples designated Capt. (Capture) were collected during sulfur gas injection and represent spent sorbent that has captured sulfur.
Chemical Anal.	Indicates whether chemical analyses were performed on the collected samples. Several samples underwent chemical analyses to determine degree of calcination, sulfur capture, and calcium utilization.
Morphology Anal.	Indicates whether surface area, porosity, or pore volume analyses were performed on a collected sample.

Table A-1. Listing of Phase I (Base) Tests.

Parameter	Test:	1			2			3
	Case:	1	2	3	1	2	3	1
Mode (TS, NE, or Act.)		n/a	n/a	n/a	n/a	n/a	n/a	n/a
Activation Burner								
Burner on or off		off	on	on	on	on	on	on
ϕ_{act}		n/a	1.00	1.00	1.00	1.00	1.00	1.00
T_{act} (^oK)		n/a	2620	2620	2620	2620	2620	2620
τ_{act} (ms)		n/a	n/a	n/a	n/a	n/a	n/a	n/a
Sorbent		none	none	none	none	none	none	none
Sorbent Size (mesh)		n/a	n/a	n/a	n/a	n/a	n/a	n/a
Sorbent Cut (full/μm)		n/a	n/a	n/a	n/a	n/a	n/a	n/a
Loading (%)		n/a	n/a	n/a	n/a	n/a	n/a	n/a
Mixing Section								
Injection Angle (Deg.)		60	60	60	60	60	60	60
Sulfation Duct								
Side Burners on or off		on	on	on	on	on	on	off
ϕ_s		1.0	1.00	1.00	0.98	1.20	0.95	n/a
T_s (^oK)		varied	800	1250	1420	1395	1010	n/a
Ca/S		n/a	n/a	n/a	n/a	n/a	n/a	n/a
Sulfur Gas (SO_2 or H_2S)		none	SO_2	SO_2	SO_2	SO_2	SO_2	none
& Concentration (ppmv)		n/a	n/a	n/a	2200	2200	1950	n/a
Solids Sampling								
Collected Sample (y/n)		no	no	no	no	no	no	no
Type (Act. or Capt.)		n/a	n/a	n/a	n/a	n/a	n/a	n/a
Chemical Anal. (y/n)		n/a	n/a	n/a	n/a	n/a	n/a	n/a
Morphology Anal. (y/n)		n/a	n/a	n/a	n/a	n/a	n/a	n/a

Comments by Test Number:

1. Shakedown of activation and side duct burners, checked thermal input and flame stability. Check on sulfation duct SO_2 baseline levels.
2. Shakedown of sulfur gas supply/sampling systems and flexibility of sulfation duct stoichiometry and temperature. Measured Sulfation duct SO_2 & H_2/S axial profiles for each condition.
3. Tested new sintered bronze activation burner. Previous stainless steel units overheated.

Table A-1. Listing of Phase I (Base) Tests, Continued.

Parameter	Test:	4		5					
	Case:	1	2	1	2	3	4	5	6
Mode (TS, NE, or Act.)		TS	n/a	n/a	n/a	TS	TS	TS	TS
Activation Burner									
Burner on or off		on	on	off	on	on	on	on	on
ϕ_{act}		0.92	0.92	n/a	1.00	1.00	1.00	1.00	1.00
T_{act} (^{o}K)		2500	2500	n/a	2620	2450	2450	2450	2620
τ_{act} (ms)		40	n/a	n/a	n/a	40	40	40	40
Sorbent		MW	none	none	none	MW	MW	MW	MW
Sorbent Size (mesh)		325	n/a	n/a	n/a	325	325	325	325
Sorbent Cut (full/μm)		full	n/a	n/a	n/a	full	full	full	full
Loading (%)		10	n/a	n/a	n/a	10	10	10	10
Mixing Section									
Injection Angle (Deg.)		60	60	60	60	60	60	60	60
Sulfation Duct									
Side Burners on or off		on	on	on	on	on	on	on	on
ϕ_s		0.92	0.92	0.95	0.95	0.91	0.92	0.95	0.91
T_s (^{o}K)		1250	1250	1320	1350	1030	1240	1300	1300
Ca/S		1.02	n/a	n/a	n/a	1.00	1.00	1.00	1.00
Sulfur Gas (SO_2 or H_2S)		SO_2	SO_2	n/a	n/a	SO_2	SO_2	SO_2	SO_2
& Concentration (ppmv)		1900	1900	n/a	n/a	2000	2000	2000	2000
Solids Sampling									
Collected Sample (y/n)		no	no	no	no	no	no	no	no
Type (Act. or Capt.)		n/a	n/a	n/a	n/a	n/a	n/a	n/a	n/a
Chemical Anal. (y/n)		n/a	n/a	n/a	n/a	n/a	n/a	n/a	n/a
Morphology Anal. (y/n)		n/a	n/a	n/a	n/a	n/a	n/a	n/a	n/a

Comments by Test Number:

4. Shakedown tests, First sulfur capture test (4-1). Measured SO_2 radial profiles at 87 cm from mixing section inlet (4-2). Determined solids deposited on walls.
5. Shakedown tests. Radial temperature profiles at 30 cm from mixing section inlet (5-1 and 2). Sulfur capture tests (5-3 through 5-6). Determined solids deposited on walls.

Table A-1. Listing of Phase I (Base) Tests, Continued.

Parameter	Test:	6						7	
	Case:	1	2	3	4	5	6	1	2
Mode (TS, NE, or Act.)		n/a	n/a	TS	n/a	TS	TS	TS	TS
Activation Burner									
Burner on or off		off	on	on	on	on	on	on	on
ϕ_{act}		n/a	1.00	1.00	1.00	1.00	1.00	1.00	1.00
T_{act} (^{o}K)		n/a	2620	2620	2450	2450	2050	2500	2400
τ_{act} (ms)		n/a	20	20	20	20	20	20	30
Sorbent		MW	MW	MW	MW	MW	MW	MW	MW
Sorbent Size (mesh)		325	325	325	325	325	325	325	325
Sorbent Cut (full/μm)		full	full	full	full	full	full	full	full
Loading (%)		10	10	10	10	10	10	10	10
Mixing Section									
Injection Angle (Deg.)		60	60	60	60	60	60	60	60
Sulfation Duct									
Side Burners on or off		off	on	on	on	on	on	on	on
ϕ_s		n/a	0.92	0.92	0.92	0.92	0.92	0.91	0.91
T_s (^{o}K)		300	1200	1200	1200	1200	1200	1100	1100
Ca/S		n/a	1.00	1.00	1.00	1.00	1.00	1.00	1.00
Sulfur Gas (SO_2 or H_2S)		none	SO_2	SO_2	SO_2	SO_2	SO_2	SO_2	SO_2
& Concentration (ppmv)		n/a	0	1800	0	1800	1800	2000	2000
Solids Sampling									
Collected Sample (y/n)		yes	yes	yes	yes	yes	yes	no	no
Type (Act. or Capt.)		n/a	Act.	Capt.	Act.	Capt.	Capt.	n/a	n/a
Chemical Anal. (y/n)		no	no	no	no	no	no	n/a	n/a
Morphology Anal. (y/n)		no	no	no	no	no	no	n/a	n/a

Comments by Test Number:

6. Sorbent supply and sampling system shakedown, and sulfur capture tests. Determined solids deposited on walls.
7. Shakedown sulfur capture tests: vary activation temperature and time, and Ca/S ratio. Determined solids deposited on walls.

Table A-1. Listing of Phase I (Base) Tests, Continued.

Parameter	Test:	7				8		
	Case:	3	4	5	6	1	2	3
Mode (TS, NE, or Act.)		TS	TS	TS	TS	NE	TS	TS
Activation Burner								
Burner on or off		on	on	on	on	on	on	on
ϕ_{act}		1.00	1.00	1.00	1.00	0.96	0.96	0.96
T_{act} (^oK)		2650	2200	2350	2350	2300	2400	2400
τ_{act} (ms)		30	30	30	30	30	30	30
Sorbent		MW	MW	MW	MW	MW	MW	MW
Sorbent Size (mesh)		325	325	325	325	325	325	325
Sorbent Cut (full/μm)		full	full	full	full	full	full	full
Loading (%)		10	30	20	20	20	20	20
Mixing Section								
Injection Angle (Deg.)		60	60	60	60	60	60	60
Sulfation Duct								
Side Burners on or off		on	on	on	on	on	on	on
ϕ_s		0.91	0.91	0.91	0.95	0.92	0.92	0.92
T_s (^oK)		1100	1150	1150	900	600	1070	1070
Ca/S		1.00	2.90	2.00	2.00	2.00	2.00	2.00
Sulfur Gas (SO_2 or H_2S)		SO_2	SO_2	SO_2	SO_2	SO_2	SO_2	SO_2
& Concentration (ppmv)		2000	2000	2000	2000	1400	1950	1950
Solids Sampling								
Collected Sample (y/n)		no	no	no	no	no	no	no
Type (Act. or Capt.)		n/a	n/a	n/a	n/a	n/a	n/a	n/a
Chemical Anal. (y/n)		n/a	n/a	n/a	n/a	n/a	n/a	n/a
Morphology Anal. (y/n)		n/a	n/a	n/a	n/a	n/a	n/a	n/a

Comments by Test Number:

7. Shakedown sulfur capture tests: vary activation temperature and time, and Ca/S ratio. Determined solids deposited on walls.
8. Shakedown tests. First non-equilibrium sulfur capture test (8-1). Two-step sulfur capture test (8-2). Radial SO_2 profile at 87 cm from mixing section inlet (8-3). Determined solids deposited on walls.

Table A-1. Listing of Phase I (Base) Tests, Continued.

Parameter	Test:	9P	9					10	
	Case:	n/a	1	2	3	4	5	1	2
Mode (TS, NE, or Act.)		n/a	TS	TS	TS	TS	TS	TS	NE
Activation Burner									
Burner on or off		on	on	on	on	on	on	on	on
ϕ_{act}		varied	0.96	0.98	0.98	0.96	0.98	0.97	0.97
T_{act} (^oK)		varied	2600	2600	2400	2600	2200	2400	2400
τ_{act} (ms)		n/a	20	20	20	20	20	30	30
Sorbent		none	MW	MW	MW	MW	MW	MW	MW
Sorbent Size (mesh)		n/a	325	325	325	325	325	325	325
Sorbent Cut (full/μm)		n/a	full	full	full	full	full	full	full
Loading (%)		n/a	15	15	15	15	15	15	15
Mixing Section									
Injection Angle (Deg.)		60	60	60	60	60	60	60	60
Sulfation Duct									
Side Burners on or off		off	on	on	on	on	on	on	on
ϕ_s		varied	0.83	0.83	0.84	0.81	0.83	0.91	0.91
T_s (^oK)		varied	1200	1200	1125	1325	1105	1375	1375
Ca/S		n/a	2.00	1.00	2.00	2.00	2.00	2.14	2.15
Sulfur Gas (SO_2 or H_2S)		none	SO_2	SO_2	SO_2	SO_2	SO_2	SO_2	SO_2
& Concentration (ppmv)		n/a	2000	2000	1900	2000	1725	2260	2250
Solids Sampling									
Collected Sample (y/n)		no	yes	yes	yes	no	no	no	no
Type (Act. or Capt.)		n/a	Capt.	Capt.	Capt.	n/a	n/a	n/a	n/a
Chemical Anal. (y/n)		n/a	yes	yes	yes	n/a	n/a	n/a	n/a
Morphology Anal. (y/n)		n/a	no	no	no	n/a	n/a	n/a	n/a

Comments by Test Number:

9P. Test 9 Preparatory shakedown tests. Installed and tested new sintered burner, which increased carrier jet diameter from 4.6 mm to 10.9 mm. Tested new sorbent feeder, mapped sorbent eductor entrained air to carrier burner, checked stoichiometries of activation and side duct burners. Side burners found to be more fuel rich than flow meters indicated - adjusted flow meter calibrations, activation burner more fuel lean due to higher levels of eductor entrained air than expected.

9. Beginning sulfur capture testing, shakedown complete. Sulfur captures varying T_{act} and T_s. Radial temperature profile at 10 cm from activation burner.

10. Partial repeat of 9 with increased activation time (10-1). Also includes a non-equilibrium capture case (10-2). Determined sorbent deposited to walls.

Table A-1. Listing of Phase I (Base) Tests, Continued.

Parameter	Test: 11 Case: 1	2	3	4	5	6	7
Mode (TS, NE, or Act.)	TS	TS	TS	NE	Act.	Act.	Act.
Activation Burner							
Burner on or off	on	on	on	on	on	on	on
ϕ_{act}	0.98	0.89	0.98	0.97	0.98	0.98	0.98
T_{act} (^oK)	2600	2600	2600	2600	2600	2400	2200
τ_{act} (ms)	10	10	10	10	10	10	10
Sorbent	MW	MW	MW	MW	MW	MW	MW
Sorbent Size (mesh)	325	325	325	325	325	325	325
Sorbent Cut (full/μm)	full	full	full	full	full	full	full
Loading (%)	8	8	15	15	15	15	17
Mixing Section							
Injection Angle (Deg.)	60	60	60	60	60	60	60
Sulfation Duct							
Side Burners on or off	on	on	on	off	off	off	off
ϕ_s	0.89	0.73	0.89	n/a	n/a	n/a	n/a
T_s (^oK)	1450	1380	1400	515	475	450	450
Ca/S	1.04	1.04	2.04	1.52	n/a	n/a	n/a
Sulfur Gas (SO_2 or H_2S)	SO_2	SO_2	SO_2	SO_2	none	none	none
& Concentration (ppmv)	2350	1875	2215	1435	n/a	n/a	n/a
Solids Sampling							
Collected Sample (y/n)	no	no	no	no	yes	yes	yes
Type (Act. or Capt.)	n/a	n/a	n/a	n/a	Act.	Act.	Act.
Chemical Anal. (y/n)	n/a	n/a	n/a	n/a	yes	yes	yes
Morphology Anal. (y/n)	n/a	n/a	n/a	n/a	yes	yes	yes

Comments by Test Number:

11. Two-Step Rapid Sulfur Capture tests varying Ca/S and sulfation oxygen levels (11-1 to 11-3). Rapidly quenched non-equilibrium test (11-4). Sorbent activation tests (11-5 to 11-7).

Table A-1. Listing of Phase I (Base) Tests, Continued.

Parameter	Test:	12			13			14	
	Case:	1	2	3	1	2	3	1	2
Mode (TS, NE, or Act.)		TS	TS	TS	NE	TS	TS	TS	NE
Activation Burner									
Burner on or off		on	on	on	on	on	on	on	on
ϕ_{act}		0.95	0.95	0.96	0.93	0.94	0.97	0.98	0.98
T_{act} (^oK)		2600	2600	2400	2600	2600	2800	2600	2400
τ_{act} (ms)		10	10	10	10	10	10	10	10
Sorbent		MW	MW	MW	MW	MW	MW	MW	MW
Sorbent Size (mesh)		325	325	325	325	325	325	325	325
Sorbent Cut (full/μm)		full	full	full	full	full	full	full	full
Loading (%)		8	16	16	15	15	15	4	8
Mixing Section									
Injection Angle (Deg.)		60	60	60	60	60	60	60	60
Sulfation Duct									
Side Burners on or off		on	on	on	on	on	on	on	on
ϕ_s		0.85	0.84	0.89	1.03	1.03	1.03	0.88	0.88
T_s (^oK)		1390	1415	1370	1450	1420	1440	1235	1255
Ca/S		1.04	2.04	1.98	1.88	2.04	2.04	1.10	2.18
Sulfur Gas (SO_2 or H_2S)		SO_2	SO_2	SO_2	H_2S	SO_2	SO_2	SO_2	SO_2
& Concentration (ppmv)		2050	1950	1990	2150	2000	2125	1080	1280
Solids Sampling									
Collected Sample (y/n)		no	no	no	no	no	no	yes	yes
Type (Act. or Capt.)		n/a	n/a	n/a	n/a	n/a	n/a	Capt.	Capt.
Chemical Anal. (y/n)		n/a	n/a	n/a	n/a	n/a	n/a	yes	yes
Morphology Anal. (y/n)		n/a	n/a	n/a	n/a	n/a	n/a	no	no

Comments by Test Number:

12. Two-Step Rapid Sulfur Capture tests varying Ca/S using higher sulfation oxygen levels.
13. Non-equilibrium sulfur capture using H_2S and Two-Step Sulfur Capture using SO_2 at higher activation temperatures.
14. Shakedown of new sorbent feeder. Sorbent flow oscillations observed. Will correct in near future. Problems plagued test yielding poor SO_2 baseline levels. Attempted Two-Step Sulfur Capture measurements, yet test results should be discarded due to problems encountered.

Table A-1. Listing of Phase I (Base) Tests, Continued.

Parameter	Test:	15			16			17	
	Case:	1	2	3	1	2	3	1	2
Mode (TS, NE, or Act.)		TS	TS	NE	TS	TS	TS	Act.	TS
Activation Burner									
Burner on or off		on	on	on	on	on	on	off	off
ϕ_{act}		0.96	0.96	0.98	0.98	1.00	1.01	n/a	n/a
T_{act} (^oK)		2600	2600	2600	2725	2725	2200	n/a	n/a
τ_{act} (ms)		10	10	10	10	10	10	n/a	n/a
Sorbent		MW	MW	MW	MW	MW	MW	MW	MW
Sorbent Size (mesh)		325	325	325	325	325	325	325	325
Sorbent Cut (full/μm)		full	full	full	full	full	full	full	full
Loading (%)		4	8	4	8	8	30	34	34
Mixing Section									
Injection Angle (Deg.)		60	60	60	60	60	60	60	60
Sulfation Duct									
Side Burners on or off		on	on	on	on	on	on	on	on
ϕ_s		0.93	0.95	0.96	0.95	1.40	0.98	0.90	0.90
T_s (^oK)		1250	1270	1305	1315	1350	1365	1300	1310
Ca/S		1.03	2.09	1.02	1.80	1.91	1.04	n/a	1.07
Sulfur Gas (SO_2 or H_2S)		SO_2	SO_2	SO_2	SO_2	SO_2	SO_2	none	SO_2
& Concentration (ppmv)		1300	1270	1340	1650	1600	10680	n/a	10000
Solids Sampling									
Collected Sample (y/n)		yes	yes	no	yes	no	yes	yes	yes
Type (Act. or Capt.)		Capt.	Capt.	n/a	Capt.	n/a	Capt.	Act.	Capt.
Chemical Anal. (y/n)		yes	yes	n/a	yes	n/a	yes	yes	yes
Morphology Anal. (y/n)		no	no	n/a	no	n/a	no	no	no

Comments by Test Number:

15. Two-Step Sulfur Capture tests varying Ca/S, but at lower carrier burner loadings (15-1 and 15-2). Non-equilibrium test at lower carrier burner loadings (15-3).
16. Two-Step Sulfur Capture under fuel lean and fuel rich conditions and at higher activation temperatures (16-1 and 16-2). High SO_2 concentration sulfur capture (16-3).
17. Sorbent activation (17-1) and sulfur capture (17-2 and 3) tests with activation burners off. Sulfur capture tests simulate single step injection processes.

Table A-1. Listing of Phase I (Base) Tests, Continued.

Parameter	Test:	17	18				19		
	Case:	3	1	2	3	4	1	2	3
Mode (TS, NE, or Act.)		TS	Act.	Act.	Act.	Act.	TS	TS	TS
Activation Burner									
Burner on or off		off	on	on	on	on	on	on	on
ϕ_{act}		n/a	0.99	0.98	0.98	1.00	0.99	0.99	0.99
T_{act} (^oK)		n/a	2700	2600	2400	2200	2600	2600	2400
τ_{act} (ms)		n/a	10	10	10	10	5	5	5
Sorbent		MW	MW	MW	MW	MW	MW	MW	MW
Sorbent Size (mesh)		325	325	325	325	325	325	325	325
Sorbent Cut (full/μm)		full	full	full	full	full	full	full	full
Loading (%)		11	8	15	16	29	6	10	10
Mixing Section									
Injection Angle (Deg.)		60	60	60	60	60	60	60	60
Sulfation Duct									
Side Burners on or off		on	off	off	off	off	on	on	on
ϕ_s		0.87	n/a	n/a	n/a	n/a	0.95	0.95	0.94
T_s (^oK)		1305	540	540	510	585	1260	1300	1255
Ca/S		2.01	n/a	n/a	n/a	n/a	1.15	2.01	2.01
Sulfur Gas (SO_2 or H_2S)		SO_2	none	none	none	none	SO_2	SO_2	SO_2
& Concentration (ppmv)		1650	n/a	n/a	n/a	n/a	1760	1700	1705
Solids Sampling									
Collected Sample (y/n)		no	yes	yes	yes	yes	yes	yes	yes
Type (Act. or Capt.)		n/a	Act.	Act.	Act.	Act.	Capt.	Capt.	Capt.
Chemical Anal. (y/n)		n/a	yes	yes	yes	yes	no	no	no
Morphology Anal. (y/n)		n/a	yes	yes	yes	yes	no	no	no

Comments by Test Number:

17. Sorbent activation (17-1) and sulfur capture (17-2 and 3) tests with activation burners off. Sulfur capture tests simulate single step injection processes.
18. Sorbent activation tests varying Ca/S with rapid quench to determine degree of calcination, specific surface area, and porosity.
19. Two-Step Sulfur Capture Tests at shorter activation time. Varied Ca/S ratio.

Table A-1. Listing of Phase I (Base) Tests, Continued.

Parameter	Test:	19		20				
	Case:	4	5	1	2	3	4	5
Mode (TS, NE, or Act.)		Act.	Act.	TS	TS	TS	TS	TS
Activation Burner								
Burner on or off		on	on	on	on	on	on	off
ϕ_{act}		0.99	0.99	0.99	1.02	0.97	0.99	n/a
T_{act} (^oK)		2400	2600	2600	2600	2400	2400	n/a
τ_{act} (ms)		5	5	10	10	10	10	n/a
Sorbent		MW	MW	LHL	LHL	LHL	LHL	LHL
Sorbent Size (mesh)		325	325	200	200	200	200	200
Sorbent Cut (full/μm)		full	full	full	full	full	full	full
Loading (%)		10	10	4	8	4	8	8
Mixing Section								
Injection Angle (Deg.)		60	60	60	60	60	60	60
Sulfation Duct								
Side Burners on or off		off	off	on	on	on	on	on
ϕ_s		n/a	n/a	0.98	0.96	0.97	0.96	0.96
T_s (^oK)		450	690	1315	1330	1280	1310	1215
Ca/S		n/a	n/a	1.00	2.09	1.00	2.07	2.08
Sulfur Gas (SO_2 or H_2S)		none	none	SO_2	SO_2	SO_2	SO_2	SO_2
& Concentration (ppmv)		n/a	n/a	1670	1750	1560	1625	1390
Solids Sampling								
Collected Sample (y/n)		yes	yes	no	yes	no	no	no
Type (Act. or Capt.)		Act.	Act.	n/a	Capt.	n/a	n/a	n/a
Chemical Anal. (y/n)		no	no	n/a	no	n/a	no	n/a
Morphology Anal. (y/n)		no	no	n/a	no	n/a	no	n/a

Comments by Test Number:

19. Two-Step Sulfur Capture Tests at shorter activation time. Varied Ca/S ratio.
20. Two-Step Sulfur Capture tests using Linwood Hydrated Lime as the sorbent. Varied activation temperature and Ca/S.

Table A-1. Listing of Phase I (Base) Tests, Continued.

Parameter	Test:	21				22		
	Case:	1	2	3	4	1	2	3
Mode (TS, NE, or Act.)		TS	TS	n/a	TS	TS	TS	TS
Activation Burner								
Burner on or off		on	on	off	on	on	on	on
ϕ_{act}		1.00	0.99	n/a	0.99	0.99	0.99	1.00
T_{act} (^oK)		2400	2400	n/a	1300	2600	2400	1300
τ_{act} (ms)		10	10	n/a	10	10	10	10
Sorbent		LHL	LHL	LHL	LHL	MW	MW	MW
Sorbent Size (mesh)		200	200	200	200	325	325	325
Sorbent Cut (full/μm)		full	full	full	full	full	full	full
Loading (%)		8	29	8	9	8	13	14
Mixing Section								
Injection Angle (Deg.)		60	60	60	60	60	60	60
Sulfation Duct								
Side Burners on or off		on	on	on	on	on	on	on
ϕ_s		0.97	0.97	0.98	0.88	0.94	0.94	0.89
T_s (^oK)		1305	1300	1215	1240	1325	1245	1115
Ca/S		2.08	1.06	2.08	2.09	2.04	2.41	2.40
Sulfur Gas (SO_2 or H_2S)		SO_2	SO_2	SO_2	SO_2	SO_2	SO_2	SO_2
& Concentration (ppmv)		1575	10863	1385	1505	1360	1875	1760
Solids Sampling								
Collected Sample (y/n)		yes	yes	yes	yes	no	no	no
Type (Act. or Capt.)		Capt.	Capt.	Capt.	Capt.	n/a	n/a	n/a
Chemical Anal. (y/n)		no	no	no	no	n/a	no	n/a
Morphology Anal. (y/n)		no	no	no	no	n/a	no	n/a

Comments by Test Number:

21. Additional Two-Step Sulfur Capture tests using Linwood Hydrated Lime as the sorbent. Varied activation temperature and sulfation duct SO_2 concentration. This concludes the hydrated lime tests.

22. This test was intended to resolve solid sampling problems, i.e., prior tests revealed poor collection efficiencies. However, the solids sampling system suction pump failed and these tests could not be conducted. Instead, repeats were done of previous conditions using Marblewhite limestone, but adding a lower activation temperature case, i.e., no propane supplied in the carrier burner, which drops the activation temperature to 1200-1400 ^oK.

Table A-1. Listing of Phase I (Base) Tests, Continued.

Parameter	Test:	23						24	
	Case:	1	2	3	4	5	6	1	2
Mode (TS, NE, or Act.)		TS	TS	TS	TS	TS	TS	TS	TS
Activation Burner									
Burner on or off		on	on	on	on	on	on	on	on
ϕ_{act}		0.99	1.00	0.99	0.98	0.98	0.99	1.00	1.00
T_{act} (^oK)		2600	2600	2600	2400	2400	2600	2600	2600
τ_{act} (ms)		10	10	10	10	10	10	10	10
Sorbent		MW	MW	MW	MW	MW	MW	MW	MW
Sorbent Size (mesh)		325	325	325	325	325	325	325	325
Sorbent Cut (full/μm)		full	full	full	full	full	full	full	full
Loading (%)		7	8	4	9	8	8	8	8
Mixing Section									
Injection Angle (Deg.)		60	60	60	60	60	60	60	60
Sulfation Duct									
Side Burners on or off		on	on	on	on	on	on	on	on
ϕ_s		0.94	0.95	0.95	0.95	0.95	0.94	0.96	0.95
T_s (^oK)		1260	1280	1260	1260	1260	1130	1290	1300
Ca/S		2.04	1.53	0.97	1.59	2.02	1.53	2.04	1.53
Sulfur Gas (SO_2 or H_2S)		SO_2	SO_2	SO_2	SO_2	SO_2	SO_2	SO_2	SO_2
& Concentration (ppmv)		1470	1900	1430	1870	1495	1400	1500	1995
Solids Sampling									
Collected Sample (y/n)		yes	no	yes	yes	no	no	no	no
Type (Act. or Capt.)		Capt.	n/a	Capt.	Capt.	n/a	n/a	n/a	n/a
Chemical Anal. (y/n)		yes	n/a	yes	yes	n/a	no	n/a	n/a
Morphology Anal. (y/n)		no	n/a	no	no	n/a	no	n/a	n/a

Comments by Test Number:

23. Two-Step Rapid Sulfur Capture tests at longer sulfation times.
24. Two-Step Rapid Sulfur Capture tests using varying size cuts of Marblewhite limestone. Made NO_x measurements to assess emissions of activation burner. Data imply that activation burner NO_x is nominally 1900 ppmv.

Table A-1. Listing of Phase I (Base) Tests, Continued.

Parameter	Test:	24				25			
	Case:	3	4	5	6	1	2	3	4
Mode (TS, NE, or Act.)		TS	TS	TS	TS	n/a	TS	TS	TS
Activation Burner									
Burner on or off		on	on	on	on	on	on	on	on
ϕ_{act}		1.00	1.00	1.00	1.00	varied	1.00	1.00	1.22
T_{act} (^{o}K)		2600	2600	2600	2600	2600	2600	2600	2600
τ_{act} (ms)		10	10	10	10	n/a	10	10	10
Sorbent		MW	MW	MW	MW	none	MW	MW	MW
Sorbent Size (mesh)		325	325	325	325	n/a	325	325	325
Sorbent Cut (full/μm)		5-15	<5	15-25	25-45	n/a	full	full	full
Loading (%)		8	8	8	8	n/a	8	8	8
Mixing Section									
Injection Angle (Deg.)		60	60	60	60	60	60	60	60
Sulfation Duct									
Side Burners on or off		on	on	on	on	off	on	on	on
ϕ_s		0.95	0.95	0.95	0.95	n/a	0.86	0.86	0.92
T_s (^{o}K)		1305	1315	1330	1325	613	1030	1060	1230
Ca/S		1.53	1.53	1.53	1.53	n/a	1.91	1.53	1.53
Sulfur Gas (SO_2 or H_2S)		SO_2	SO_2	SO_2	SO_2	none	SO_2	SO_2	SO_2
& Concentration (ppmv)		2025	2075	2100	2060	n/a	1090	1544	1310
Solids Sampling									
Collected Sample (y/n)		no	no	no	no	no	yes	no	no
Type (Act. or Capt.)		n/a	n/a	n/a	n/a	n/a	Capt.	n/a	n/a
Chemical Anal. (y/n)		n/a	n/a	n/a	n/a	n/a	no	n/a	n/a
Morphology Anal. (y/n)		n/a	n/a	n/a	n/a	n/a	no	n/a	n/a

Comments by Test Number:

24. Two-Step Rapid Sulfur Capture tests using varying size cuts of Marblewhite limestone. Made NO_x measurements to assess emissions of activation burner.

25. Measured activation NO_x emissions (25-1). For ϕ_{act} = 1.0, 1.2, 1.3, NO_x levels in activation burner were measured to be 956, 197, and 109 ppmv, respectively. Studied Two-Step Rapid Sulfur Capture under mixed metal oxide sulfur removal system conditions (25-2 through 25-4). To reduce activation burner NO_x, operated activation burner at ϕ_{act} = 1.22 during case 25-4.

Table A-1. Listing of Phase I (Base) Tests, Continued.

Parameter	Test:	26				27		28	
	Case:	1	2	3	4	1	2	1	2
Mode (TS, NE, or Act.)		TS	TS	TS	TS	TS	TS	TS	TS
Activation Burner									
Burner on or off		on	on	on	on	on	on	on	on
ϕ_{act}		1.00	1.00	1.00	1.00	1.00	1.00	1.02	1.02
T_{act} (^{o}K)		2600	2600	2600	2600	2600	2600	2600	2600
τ_{act} (ms)		10	10	10	10	10	10	10	10
Sorbent		MW	MW	MW	MW	MW	MW	MW	MW
Sorbent Size (mesh)		325	325	325	325	325	325	325	325
Sorbent Cut (full/μm)		full	full	full	full	full	full	full	full
Loading (%)		8	8	8	8	8	8	8	8
Mixing Section									
Injection Angle (Deg.)		60	60	60	60	60	60	60	60
Sulfation Duct									
Side Burners on or off		off	off	on	on	on	on	on	on
ϕ_s		n/a	n/a	1.70	1.70	0.50	0.50	1.80	1.80
T_s (^{o}K)		700	675	650	650	1425	1430	1410	1415
Ca/S		2.04	1.46	2.04	1.53	2.04	1.53	2.04	1.53
Sulfur Gas (SO_2 or H_2S)		SO_2	SO_2	SO_2	SO_2	SO_2	SO_2	SO_2	SO_2
& Concentration (ppmv)		1115	1390	1110	1750	1290	1560	1050	1400
Solids Sampling									
Collected Sample (y/n)		no	no	no	no	no	no	no	no
Type (Act. or Capt.)		n/a	n/a	n/a	n/a	n/a	n/a	n/a	n/a
Chemical Anal. (y/n)		n/a	n/a	n/a	n/a	n/a	n/a	n/a	n/a
Morphology Anal. (y/n)		n/a	n/a	n/a	n/a	n/a	n/a	n/a	n/a

Comments by Test Number:

26. Two-Step Rapid Sulfur Capture tests targeting diesel (26-1 through 26-2) and fixed bed gasifier (26-3 through 26-4) applications. Side duct burners not fired for diesel simulation, yet excess oxygen (9.5% O_2) added via quench flow. Side duct burners fired fuel rich to achieve gasifier conditions.
27. Two-Step Rapid Sulfur Capture tests targeting gas turbine applications.
28. Two-Step Rapid Sulfur Capture tests targeting entrained bed gasifier (28-1 through 28-2), fluidized bed combustor (28-3), and fluidized (28-4) bed gasifier applications.

Table A-1. Listing of Phase I (Base) Tests, Continued.

Parameter	Test:	28		29				
	Case:	3	4	1	2	3	4	5
Mode (TS, NE, or Act.)		TS	TS	TS	TS	TS	TS	TS
Activation Burner								
Burner on or off		on	on	on	on	on	on	on
ϕ_{act}		1.00	1.00	1.00	1.00	1.00	0.99	0.99
T_{act} (^oK)		2600	2600	2600	2600	2600	2400	2400
τ_{act} (ms)		10	10	10	10	10	10	10
Sorbent		MW	MW	V45-3	V45-3	V45-3	V45-3	V45-3
Sorbent Size (mesh)		325	325	325	325	325	325	325
Sorbent Cut (full/μm)		full	full	full	full	full	full	full
Loading (%)		8	8	8	8	8	8	8
Mixing Section								
Injection Angle (Deg.)		60	60	60	60	60	60	60
Sulfation Duct								
Side Burners on or off		on	on	on	on	on	on	on
ϕ_s		0.89	1.8	0.95	0.95	0.95	0.95	0.95
T_s (^oK)		1450	1270	1290	1285	1300	1250	1255
Ca/S		2.04	2.04	2.04	1.53	1.53	1.53	2.04
Sulfur Gas (SO_2 or H_2S)		SO_2	SO_2	SO_2	SO_2	SO_2	SO_2	SO_2
& Concentration (ppmv)		1240	1020	1315	1930	1950	1360	1905
Solids Sampling								
Collected Sample (y/n)		no	no	no	no	no	no	no
Type (Act. or Capt.)		n/a	n/a	n/a	n/a	n/a	n/a	n/a
Chemical Anal. (y/n)		n/a	n/a	n/a	n/a	n/a	n/a	n/a
Morphology Anal. (y/n)		n/a	n/a	n/a	n/a	n/a	n/a	n/a

Comments by Test Number:

28. Two-Step Rapid Sulfur Capture tests targeting entrained bed gasifier (28-1 through 28-2), fluidized bed combustor (28-3), and fluidized (28-4) bed gasifier applications.
29. Two-Step Sulfur Capture tests using Vicron 45-3 limestone as the sorbent. This test used activation and sulfation conditions optimum for Marblewhite 325 limestone. Varied activation temperature and Ca/S.

Table A-1. Listing of Phase I (Base) Tests, Continued.

Parameter	Test:	30				
	Case:	1	2	3	4	5
Mode (TS, NE, or Act.)		TS	TS	TS	TS	TS
Activation Burner						
Burner on or off		on	on	on	on	on
ϕ_{act}		0.99	0.99	0.99	0.99	0.99
T_{act} (^oK)		2600	2600	2600	2600	2600
τ_{act} (ms)		10	10	10	10	10
Sorbent		MW	MW	MW	MW	MW
Sorbent Size (mesh)		325	325	325	325	325
Sorbent Cut (full/μm)		full	full	full	full	full
Loading (%)		8	8	8	8	8
Mixing Section						
Injection Angle (Deg.)		60	60	60	60	60
Sulfation Duct						
Side Burners on or off		on	on	on	on	on
ϕ_s		0.95	0.96	0.96	0.96	0.96
T_s (^oK)		1280	1280	1285	1305	1290
Ca/S		2.04	2.04	2.18	2.20	1.91
Sulfur Gas (SO_2 or H_2S)		SO_2	SO_2	SO_2	SO_2	SO_2
& Concentration (ppmv)		1395	1360	1350	1220	1305
Solids Sampling						
Collected Sample (y/n)		no	yes	yes	yes	yes
Type (Act. or Capt.)		n/a	Capt.	Capt.	Capt.	Capt.
Chemical Anal. (y/n)		n/a	no	no	no	no
Morphology Anal. (y/n)		n/a	no	no	no	no

Comments by Test Number:

30. Two-Step Rapid Sulfur Capture repeat tests under optimized activation and sulfation conditions.

APPENDIX B

LISTING OF PHASE IA TESTS

This appendix gives a listing of the tests performed during the Phase IA program (see Section 4.0 for an overview of the structure of the work performed during this project). Table B-1 lists the tests conducted, relevant process parameters for each test, and brief comments for each test. Each test may consist of one to six cases. Each case has unique process parameters. Given below are definitions or abbreviations used in Table B-1.

Mode:

TS	Two-Step Rapid Sulfur Capture mode.
NE	Non-Equilibrium Sulfur Capture mode.
Act.	Activation mode (no sulfur gas was injected into the system).

Activation Burner:

ϕ_{act}	Overall activation burner equivalence ratio.
T_{act}	Activation burner adiabatic flame temperature.
τ_{act}	Sorbent activation time based on activation duct plug flow velocity and duct length.
Sorbent	Three sorbents were tested, namely MW Marblewhite limestone, LHL Linwood hydrated lime, V45-3 Vicron 45-3 limestone.
Sorbent Size	Mesh size of sorbent.
Sorbent Cut	Indicates if the full size range of the sorbent was used (full) or the cut size range in microns (μm).
Loading	Weight percent of sorbent in activation module carrier burner.

Mixing Section:

Injection Angle	Mixing section quench gas injection angle. This is a parameter that characterizes the aggressiveness of the mixing occurring in this section. Four injection angles were studied over the entire

duration of this program, namely: 0, 15, 30, and 60 degrees. Only the 60 degree section was used during the Phase I (Base) program.

Sulfation Duct:

ϕ_s	Overall equivalence ratio in the sulfation (reactor) duct.
T_s	Average temperature in the sulfation duct.
Ca/S	Calcium to sulfur ratio in the sulfation duct.
Sulfur Gas	Identifies the sulfur gas compound injected into the system, either SO_2 or H_2S.
Concentration	Average concentration of the sulfur gas in the sulfation duct before sorbent injection.

Solids Sampling:

Type	Two types of sorbent samples were collected. Samples designated Act. (Activation) were collected when no sulfur gas was present and represent activated sorbent samples. Samples designated Capt. (Capture) were collected during sulfur gas injection and represent spent sorbent that has captured sulfur.
Chemical Anal.	Indicates whether chemical analyses were performed on the collected samples. Several samples underwent chemical analyses to determine degree of calcination, sulfur capture, and calcium utilization.
Morphology Anal.	Indicates whether surface area, porosity, or pore volume analyses were performed on a collected sample.

Table B-1. Listing of Phase IA Tests.

Parameter	Test:	A1				A2		
	Case:	1	2	3	4	1	2	3
Mode (TS, NE, or Act.)		n/a	n/a	n/a	n/a	n/a	NE	NE
Activation Burner								
Burner on or off		off	off	on	on	on	on	on
ϕ_{act}		n/a	n/a	1.00	1.00	1.00	0.99	1.00
T_{act} (^oK)		300	300	2600	2600	2600	2600	2400
τ_{act} (ms)		n/a	n/a	n/a	n/a	n/a	20	20
Sorbent		none	none	none	none	none	MW	MW
Sorbent Size (mesh)		n/a	n/a	n/a	n/a	n/a	325	325
Sorbent Cut (full/μm)		n/a	n/a	n/a	n/a	n/a	full	full
Loading (%)		n/a	n/a	n/a	n/a	n/a	7	8
Mixing Section								
Injection Angle (Deg.)		60	60	60	60	60	60	60
Sulfation Duct								
Side Burners on or off		off	off	off	off	off	off	off
ϕ_s		n/a	n/a	n/a	n/a	n/a	n/a	n/a
T_s (^oK)		300	300	510	510	480	505	500
Ca/S		n/a	n/a	n/a	n/a	n/a	0.94	0.69
Sulfur Gas (SO_2 or H_2S)		SO_2	SO_2	SO_2	SO_2	SO_2	SO_2	SO_2
& Concentration (ppmv)		1500	1500	1500	1500	1500	1380	1325
Solids Sampling								
Collected Sample (y/n)		no	no	no	no	no	no	no
Type (Act. or Capt.)		n/a	n/a	n/a	n/a	n/a	n/a	n/a
Chemical Anal. (y/n)		n/a	n/a	n/a	n/a	n/a	n/a	n/a
Morphology Anal. (y/n)		n/a	n/a	n/a	n/a	n/a	n/a	n/a

Comments by Test Number:

A1. Cold and hot flow interface module mixing tests. Cold flow tests were done in A1-1 through A1-2, whereas hot flow tests were done in A1-3 through A1-4. For all cases only ambient temperature N_2 was supplied to the side duct burners and SO_2 was supplied to the carrier burner as the tracer species for mixing measurements. In A1-1 and A1-2 no propane was supplied to the activation burners, only O_2 and N_2, which were supplied at nominal flow rates. In A1-3 and A1-4 propane was supplied to the activation burners. Radial measurements of SO_2 concentration were made at 25 cm below the inlet of the mixing section. These tests were performed with only one 20 cm module installed in the mixing duct.

A2. Comments on next page.

Table B-1. Listing of Phase IA Tests, Continued.

Parameter	Test:	A2	A3			A4			
	Case:	4	1	2	3	1	2	3	4
Mode (TS, NE, or Act.)		NE	NE	NE	NE	NE	NE	NE	NE
Activation Burner									
Burner on or off		on	on	on	on	on	on	on	on
ϕ_{act}		1.00	1.00	n/a	1.00	1.00	0.92	1.00	1.00
T_{act} (^{o}K)		2400	2600	2600	2600	2400	2400	2400	2400
τ_{act} (ms)		20	40	30	30	30	30	30	30
Sorbent		MW	MW	MW	MW	MW	MW	MW	MW
Sorbent Size (mesh)		325	325	325	325	325	325	325	325
Sorbent Cut (full/μm)		full	full	full	full	full	full	full	full
Loading (%)		8	8	8	6	8	8	8	8
Mixing Section									
Injection Angle (Deg.)		60	60	60	60	60	60	60	60
Sulfation Duct									
Side Burners on or off		off	off	off	off	off	off	off	off
ϕ_s		n/a	n/a	n/a	n/a	n/a	n/a	n/a	n/a
T_s (^{o}K)		505	430	500	425	420	420	420	420
Ca/S		1.79	0.91	1.01	0.83	0.97	0.97	2.60	2.60
Sulfur Gas (SO_2 or H_2S)		SO_2	SO_2	SO_2	SO_2	SO_2	SO_2	SO_2	SO_2
& Concentration (ppmv)		1325	1300	1300	1300	1720	1810	700	660
Solids Sampling									
Collected Sample (y/n)		no	no	no	no	yes	no	no	no
Type (Act. or Capt.)		n/a	n/a	n/a	n/a	Capt.	n/a	n/a	n/a
Chemical Anal. (y/n)		n/a	n/a	n/a	n/a	yes	n/a	n/a	n/a
Morphology Anal. (y/n)		n/a	n/a	n/a	n/a	n/a	n/a	n/a	n/a

Comments by Test Number:

A2. Hot flow mixing study, A2-1, same as in A1-3 and A1-4 except radial profiles measured at 43 cm from inlet of mixing section and installed two modules in activation duct making this duct 40 cm long. Cases A2-2 through A2-4 explored non-equilibrium sulfur capture varying activation temperature and Ca/S for fixed activation time (20 ms).

A3. Non-equilibrium and mixing tests. These tests explored mixing with three activation modules (61 cm length) at 13 cm from inlet of mixing section during non-equilibrium sulfur capture. Reduced activation burner flows were explored in A3-1 to generate a longer activation time (40 ms). A3-2 used standard activation conditions. A3-3 used higher side duct N_2 flows to achieve a more rapid quench.

A4. Non-equilibrium tests. See next page for comments.

Table B-1. Listing of Phase IA Tests, Continued.

Parameter	Test:	A4	A5					
	Case:	5	1	2	3	4	5	6
Mode (TS, NE, or Act.)		NE	NE	NE	NE	Act.	Act.	Act.
Activation Burner								
Burner on or off		on	on	on	on	on	on	on
ϕ_{act}		1.00	0.97	0.97	0.96	0.97	0.97	0.97
T_{act} (^oK)		2600	2300	2100	1200	2200	2400	2600
τ_{act} (ms)		30	30	30	30	30	30	30
Sorbent		MW	MW	MW	MW	MW	MW	MW
Sorbent Size (mesh)		325	325	325	325	325	325	325
Sorbent Cut (full/μm)		full	full	full	full	full	full	full
Loading (%)		8	7	10	10	8	8	8
Mixing Section								
Injection Angle (Deg.)		60	60	60	60	60	60	60
Sulfation Duct								
Side Burners on or off		off	off	off	off	off	off	off
ϕ_s		n/a	n/a	n/a	n/a	n/a	n/a	n/a
T_s (^oK)		460	430	430	375	430	440	460
Ca/S		2.60	2.04	3.07	3.07	n/a	n/a	n/a
Sulfur Gas (SO_2 or H_2S)		SO_2	SO_2	SO_2	SO_2	none	none	none
& Concentration (ppmv)		680	640	620	590	n/a	n/a	n/a
Solids Sampling								
Collected Sample (y/n)		yes	no	no	no	yes	yes	yes
Type (Act. or Capt.)		Capt.	n/a	n/a	n/a	Act.	Act.	Act.
Chemical Anal. (y/n)		yes	n/a	n/a	n/a	yes	yes	yes
Morphology Anal. (y/n)		yes	n/a	n/a	n/a	yes	yes	yes

Comments by Test Number:

A4. Non-equilibrium tests varying activation temperature, Ca/S, oxygen in quench, and flow rate ratio of quench flow to activation burner flow. Gas sampling probe 5 cm below inlet to mixing section.

A5. Non-equilibrium tests at longer activation times varying activation temperatures (A5-1 through A5-3). Sorbent activation tests (A5-4 through A5-6) varying activation temperature.

Table B-1. Listing of Phase IA Tests, Continued.

Parameter	Test: Case:	A6 1	2	3	4	5	6	7	8
Mode (TS, NE, or Act.)		NE	NE	NE	NE	NE	Act.	Act.	Act.
Activation Burner									
Burner on or off		on	on	on	on	on	on	on	on
ϕ_{act}		0.97	0.98	0.99	1.00	0.97	0.96	0.96	0.96
T_{act} (^oK)		2600	2600	2750	2400	2200	2200	2400	2600
τ_{act} (ms)		10	10	10	10	10	10	10	10
Sorbent		MW	MW	MW	MW	MW	MW	MW	MW
Sorbent Size (mesh)		325	325	325	325	325	325	325	325
Sorbent Cut (full/μm)		full	full	full	full	full	full	full	full
Loading (%)		7	8	8	8	9	8	8	8
Mixing Section									
Injection Angle (Deg.)		60	60	60	60	60	60	60	60
Sulfation Duct									
Side Burners on or off		off	off	off	off	off	off	off	off
ϕ_s		n/a	n/a	n/a	n/a	n/a	n/a	n/a	n/a
T_s (^oK)		530	530	580	550	510	510	560	560
Ca/S		2.29	1.06	1.06	1.08	1.08	n/a	n/a	n/a
Sulfur Gas (SO_2 or H_2S)		SO_2	SO_2	SO_2	SO_2	SO_2	none	none	none
& Concentration (ppmv)		700	1950	1960	1965	2000	n/a	n/a	n/a
Solids Sampling									
Collected Sample (y/n)		no	no	no	no	no	yes	yes	yes
Type (Act. or Capt.)		n/a	n/a	n/a	n/a	n/a	Act.	Act.	Act.
Chemical Anal. (y/n)		n/a	n/a	n/a	n/a	n/a	yes	yes	yes
Morphology Anal. (y/n)		n/a	n/a	n/a	n/a	n/a	yes	yes	yes

Comments by Test Number:

A6. Non-equilibrium sulfur capture tests varying Ca/S and activation temperature for fixed and lower activation time (10 ms). Activated sorbent samples taken varying activation temperature to explore calcination degree, surface area, porosity, and pore size.

Table B-1. Listing of Phase IA Tests, Continued.

Parameter	Test:	A7				A8			
	Case:	1	2	3	4	1	2	3	4
Mode (TS, NE, or Act.)		NE	NE	NE	NE	NE	NE	NE	NE
Activation Burner									
Burner on or off		on	on	on	on	on	on	on	on
ϕ_{act}		0.99	0.99	0.99	0.99	0.94	0.96	0.99	0.99
T_{act} (^oK)		2650	2575	2700	2575	2650	2350	2550	2575
τ_{act} (ms)		10	10	10	10	10	10	10	30
Sorbent		MW	MW	MW	MW	MW	MW	MW	MW
Sorbent Size (mesh)		325	325	325	325	325	325	325	325
Sorbent Cut (full/μm)		full	full	full	full	full	full	full	full
Loading (%)		7	8	4	4	3	4	4	8
Mixing Section									
Injection Angle (Deg.)		60	60	60	60	60	60	60	60
Sulfation Duct									
Side Burners on or off		off	off	off	off	off	off	off	off
ϕ_s		n/a	n/a	n/a	n/a	n/a	n/a	n/a	n/a
T_s (^oK)		605	825	932	1040	1020	1000	1035	1080
Ca/S		1.32	2.70	2.53	2.48	2.09	2.42	0.96	1.05
Sulfur Gas (SO_2 or H_2S)		SO_2	SO_2	SO_2	SO_2	SO_2	SO_2	SO_2	SO_2
& Concentration (ppmv)		1815	1680	1480	1970	1620	1595	4980	9110
Solids Sampling									
Collected Sample (y/n)		no	no	no	yes	no	no	no	no
Type (Act. or Capt.)		n/a	n/a	n/a	Capt.	n/a	n/a	n/a	n/a
Chemical Anal. (y/n)		n/a	n/a	n/a	yes	n/a	n/a	n/a	n/a
Morphology Anal. (y/n)		n/a	n/a	n/a	yes	n/a	n/a	n/a	n/a

Comments by Test Number:

A7. Non-equilibrium sulfur capture tests varying Ca/S and ratio of quench flow to activation burner flow (i.e., m_q/m_a). For A7-1 through A7-4, m_q/m_a = 4, 2, 1, 0.5, respectively.

A8. Non-equilibrium sulfur capture tests varying Ca/S, Activation temperature, and ratio of quench flow to activation burner flow (i.e., m_q/m_a). For A8-1 through A8-5, m_q/m_a = 0.5, 0.5, 0.5, 0.5, 0.7, respectively.

Table B-1. Listing of Phase IA Tests, Continued.

Parameter	Test:	A8	A9			A10	A11		
	Case:	5	1	2	3	1	1	2	3
Mode (TS, NE, or Act.)		NE	NE	NE	NE	Act.	Act.	Act.	Act.
Activation Burner									
Burner on or off		on	on	on	on	on	on	on	on
ϕ_{act}		0.98	1.00	1.00	1.00	0.98	0.98	0.98	0.98
T_{act} (^{o}K)		2575	2650	2600	2650	2550	2550	2425	2425
τ_{act} (ms)		10	10	10	10	10	10	10	10
Sorbent		MW	MW	MW	MW	MW	MW	MW	MW
Sorbent Size (mesh)		325	325	325	325	325	325	325	325
Sorbent Cut (full/μm)		full	full	full	full	full	full	full	full
Loading (%)		8	7	8	7	12	15	15	13
Mixing Section									
Injection Angle (Deg.)		60	60	60	60	60	60	60	60
Sulfation Duct									
Side Burners on or off		off	off	off	off	off	off	off	0ff
ϕ_s		n/a	n/a	n/a	n/a	n/a	n/a	n/a	n/a
T_s (^{o}K)		1080	545	545	485	470	480	500	505
Ca/S		1.15	0.91	1.04	0.88	n/a	n/a	n/a	n/a
Sulfur Gas (SO_2 or H_2S)		SO_2	SO_2	SO_2	SO_2	none	none	none	none
& Concentration (ppmv)		7200	1795	1890	1080	n/a	n/a	n/a	n/a
Solids Sampling									
Collected Sample (y/n)		yes	no	no	no	yes	yes	yes	no
Type (Act. or Capt.)		Capt.	n/a	n/a	n/a	Act.	Act.	Act.	n/a
Chemical Anal. (y/n)		yes	n/a	n/a	n/a	no	no	no	n/a
Morphology Anal. (y/n)		yes	n/a	n/a	n/a	yes	yes	yes	n/a

Comments by Test Number:

A8. Non-equilibrium sulfur capture tests varying Ca/S, Activation temperature, and ratio of quench flow to activation burner flow (i.e., m_q/m_a). For A8-1 through A8-5, m_q/m_a = 0.5, 0.5, 0.5, 0.5, 0.7, respectively.

A9. Non-equilibrium sulfur capture tests varying ratio of quench flow to activation burner flow (i.e., m_q/m_a). For A9-1 through A9-3, m_q/m_a = 6.5, 6.5, 11.6, respectively. Quench flow rates for test A9 are much higher than test A8.

A10. Sorbent activation test at higher carrier burner loadings.

A11. Sorbent Activation tests at higher carrier burner loadings varying activation temperature.

Table B-1. Listing of Phase IA Tests, Continued.

Parameter	Test:	A12				A13	A14	A15	
	Case:	1	2	3	4	1	1	1	2
Mode (TS, NE, or Act.)		NE	Act.	Act.	Act.	TS	TS	TS	TS
Activation Burner									
Burner on or off		on	on	on	on	on	on	on	on
ϕ_{act}		0.98	0.96	0.96	0.94	0.94	0.98	0.95	0.95
T_{act} (^{o}K)		2550	2550	2650	2375	2625	2650	2200	2400
τ_{act} (ms)		10	10	10	10	10	10	10	10
Sorbent		MW	MW	MW	MW	MW	MW	MW	MW
Sorbent Size (mesh)		325	325	325	325	325	325	325	325
Sorbent Cut (full/μm)		full	full	full	full	full	full	full	full
Loading (%)		8	8	8	8	8	7	8	8
Mixing Section									
Injection Angle (Deg.)		60	60	60	60	60	60	60	60
Sulfation Duct									
Side Burners on or off		off	off	off	off	on	on	on	on
ϕ_s		n/a	n/a	n/a	n/a	0.96	0.95	0.96	0.96
T_s (^{o}K)		560	575	590	550	1300	1315	1290	1310
Ca/S		1.12	n/a	n/a	n/a	1.98	1.81	1.98	2.17
Sulfur Gas (SO_2 or H_2S)		SO_2	none	none	none	SO_2	SO_2	SO_2	SO_2
& Concentration (ppmv)		1790	n/a	n/a	n/a	1500	1640	1570	1550
Solids Sampling									
Collected Sample (y/n)		no	yes	yes	yes	yes	no	no	no
Type (Act. or Capt.)		n/a	Act.	Act.	Act.	Capt.	n/a	n/a	n/a
Chemical Anal. (y/n)		n/a	no	no	no	yes	n/a	n/a	n/a
Morphology Anal. (y/n)		n/a	no	no	no	n/a	n/a	n/a	n/a

Comments by Test Number:

A12. Non-equilibrium and solids collection system tests. Non-equilibrium case A12-1 used a ceramic lined gas sampling probe to avoid condensation, thus wet scrubbing, when sampling. Cases A12-2 through A12-4 were to achieve improved solids sampling collection efficiencies.

A13. Two-Step Rapid Sulfur Capture using heated gas sampling probes (100 F) with ceramic inserts. Performed a detailed mass balance of calcium injected into the system. Performed chemical analyses on solids collected in system.

A14. Identical repeat of test A13. Improved solids collection efficiency.

A15. See next page.

Table B-1. Listing of Phase IA Tests, Continued.

Parameter	Test:	A15		A16				A17	
	Case:	3	4	1	2	3	4	1	2
Mode (TS, NE, or Act.)		TS	TS	TS	TS	TS	TS	NE	NE
Activation Burner									
Burner on or off		on	on	on	on	on	on	on	on
ϕ_{act}		0.98	1.07	0.98	0.98	0.98	0.96	0.95	0.94
T_{act} (^oK)		2600	2600	2600	2600	2600	2200	2600	2400
τ_{act} (ms)		10	10	10	10	10	10	10	10
Sorbent		MW	MW	MW	MW	MW	MW	MW	MW
Sorbent Size (mesh)		325	325	325	325	325	325	325	325
Sorbent Cut (full/μm)		full	full	full	full	full	full	full	full
Loading (%)		8	7	7	7	8	8	7	8
Mixing Section									
Injection Angle (Deg.)		60	60	60	60	60	60	60	60
Sulfation Duct									
Side Burners on or off		on	on	on	on	on	on	off	off
ϕ_s		0.95	0.95	0.95	0.95	0.95	0.97	n/a	n/a
T_s (^oK)		1360	1375	1295	1300	1300	1285	575	550
Ca/S		2.13	2.01	1.96	2.03	2.10	2.02	0.95	1.01
Sulfur Gas (SO_2 or H_2S)		SO_2	SO_2	SO_2	SO_2	SO_2	SO_2	SO_2	SO_2
& Concentration (ppmv)		1635	1680	1650	1700	1670	1645	1850	1850
Solids Sampling									
Collected Sample (y/n)		no	yes	no	no	no	no	no	no
Type (Act. or Capt.)		n/a	Capt.	n/a	n/a	n/a	n/a	n/a	n/a
Chemical Anal. (y/n)		n/a	no	n/a	n/a	n/a	n/a	n/a	n/a
Morphology Anal. (y/n)		n/a	no	n/a	n/a	n/a	n/a	n/a	n/a

Comments by Test Number:

A15. Two-Step Rapid Sulfur Capture tests (A15-1 through A15-3) using heated gas sampling probes (>150 F) and varying activation temperature. Fuel rich activation burner tested in test A15-4. Checking to see if condensation induced probe scrubbing is occurring.

A16. Two-Step Rapid Sulfur Capture tests exploring the effect of gas sampling probe temperature on observed sulfur captures. Did very activation temperature. Results clearly demonstrated that significant gas sampling probe scrubbing was occurring.

A17. Non-equilibrium Sulfur Capture tests with heated gas sampling probes (>150 F) varying activation temperature. Results showed minimal sulfur capture (2%).

Table B-1. Listing of Phase IA Tests, Continued.

Parameter	Test:	A17	A18				A19		
	Case:	3	1	2	3	4	1	2	3
Mode (TS, NE, or Act.)		NE	TS	TS	TS	Act.	TS	NE	TS
Activation Burner									
Burner on or off		on	on	on	on	on	on	on	on
ϕ_{act}		0.95	0.99	0.99	1.00	0.95	0.96	0.96	0.95
T_{act} (^oK)		2200	2600	2600	1100	2400	2200	2200	2400
τ_{act} (ms)		10	10	10	10	10	0	0	0
Sorbent		MW	MW	MW	MW	MW	MW	MW	MW
Sorbent Size (mesh)		325	325	325	325	325	325	325	325
Sorbent Cut (full/μm)		full	full	full	full	full	full	full	full
Loading (%)		8	7	8	10	7	8	9	8
Mixing Section									
Injection Angle (Deg.)		60	60	60	60	60	60	60	60
Sulfation Duct									
Side Burners on or off		off	on	on	on	on	on	on	on
ϕ_s		n/a	0.98	0.98	0.98	0.98	0.98	0.98	0.98
T_s (^oK)		510	1095	1295	1320	1330	1250	1250	1275
Ca/S		0.97	1.72	2.16	2.28	1.93	1.98	2.15	2.06
Sulfur Gas (SO_2 or H_2S)		SO_2	SO_2	SO_2	SO_2	SO_2	SO_2	SO_2	SO_2
& Concentration (ppmv)		1430	1550	1640	1600	1540	1640	1600	1680
Solids Sampling									
Collected Sample (y/n)		no	no	yes	yes	no	no	no	no
Type (Act. or Capt.)		n/a	n/a	Capt.	Capt.	n/a	n/a	n/a	n/a
Chemical Anal. (y/n)		n/a	n/a	no	no	n/a	n/a	n/a	n/a
Morphology Anal. (y/n)		n/a	n/a	no	no	n/a	n/a	n/a	n/a

Comments by Test Number:

A17. See previous page.

A18. Two-Step Rapid Sulfur Capture tests using heated gas sampling probes (150 F) studying cold reactor wall effects (lower radiative flux), lower sulfation temperature, and unactivated sorbent influences.

A19. Two-Step Rapid Sulfur Capture tests a shortest activation time using heated gas sampling probes (150 F). Activation temperature was varied and a non-equilibrium test was performed at an activation temperature of 2200 ^oK to compare with earlier results at longer activation times.

Table B-1. Listing of Phase IA Tests, Continued.

Parameter	Test:	A19	A20			
	Case:	4	1	2	3	4
Mode (TS, NE, or Act.)		TS	TS	TS	TS	TS
Activation Burner						
Burner on or off		on	on	on	on	on
ϕ_{act}		1.00	0.95	0.95	0.95	0.95
T_{act} (^{o}K)		1100	2250	2400	2400	2400
τ_{act} (ms)		0	0	0	0	0
Sorbent		MW	MW	MW	MW	MW
Sorbent Size (mesh)		325	325	325	325	325
Sorbent Cut (full/μm)		full	full	full	full	full
Loading (%)		8	8	7	7	7
Mixing Section						
Injection Angle (Deg.)		60	60	60	60	60
Sulfation Duct						
Side Burners on or off		on	on	on	on	on
ϕ_s		0.98	0.98	0.98	0.98	0.98
T_s (^{o}K)		1210	1090	1330	1085	1300
Ca/S		1.87	1.16	1.16	0.73	1.01
Sulfur Gas (SO_2 or H_2S)		SO_2	SO_2	SO_2	SO_2	SO_2
& Concentration (ppmv)		1560	1760	1750	1590	1700
Solids Sampling						
Collected Sample (y/n)		no	no	no	no	yes
Type (Act. or Capt.)		n/a	n/a	n/a	n/a	Capt.
Chemical Anal. (y/n)		n/a	n/a	n/a	n/a	yes
Morphology Anal. (y/n)		n/a	n/a	n/a	n/a	no

Comments by Test Number:

19. See previous page.
20. Two-Step Sulfur Capture tests using heated gas sampling probes (150 F). Studying shortest activation time sulfur captures varying quench rates and activation temperature.

APPENDIX C
LISTING OF PHASE IB TESTS

This appendix gives a listing of the tests performed during the Phase IB program (see Section 4.0 for an overview of the structure of the work performed during this project). Table C-1 lists the tests conducted, relevant process parameters for each test, and brief comments for each test. Each test may consist of one to six cases. Each case has unique process parameters. Given below are definitions or abbreviations used in Table C-1.

Mode:

TS	Two-Step Rapid Sulfur Capture mode.
NE	Non-Equilibrium Sulfur Capture mode.
Act.	Activation mode (no sulfur gas was injected into the system).

Activation Burner:

ϕ_{act}	Overall activation burner equivalence ratio.
T_{act}	Activation burner adiabatic flame temperature.
τ_{act}	Sorbent activation time based on activation duct plug flow velocity and duct length.
Sorbent	Three sorbents were tested, namely MW Marblewhite limestone, LHL Linwood hydrated lime, V45-3 Vicron 45-3 limestone.
Sorbent Size	Mesh size of sorbent.
Sorbent Cut	Indicates if the full size range of the sorbent was used (full) or the cut size range in microns (μm).
Loading	Weight percent of sorbent in activation module carrier burner.

Mixing Section:

Injection Angle	Mixing section quench gas injection angle. This is a parameter that characterizes the aggressiveness of the mixing occurring in this section. Four injection angles were studied over the entire

duration of this program, namely: 0, 15, 30, and 60 degrees. Only the 60 degree section was used during the Phase I (Base) program.

Sulfation Duct:

ϕ_S	Overall equivalence ratio in the sulfation (reactor) duct.
T_S	Average temperature in the sulfation duct.
Ca/S	Calcium to sulfur ratio in the sulfation duct.
Sulfur Gas	Identifies the sulfur gas compound injected into the system, either SO_2 or H_2S.
Concentration	Average concentration of the sulfur gas in the sulfation duct before sorbent injection.

Solids Sampling:

Type	Two types of sorbent samples were collected. Samples designated Act. (Activation) were collected when no sulfur gas was present and represent activated sorbent samples. Samples designated Capt. (Capture) were collected during sulfur gas injection and represent spent sorbent that has captured sulfur.
Chemical Anal.	Indicates whether chemical analyses were performed on the collected samples. Several samples underwent chemical analyses to determine degree of calcination, sulfur capture, and calcium utilization.
Morphology Anal.	Indicates whether surface area, porosity, or pore volume analyses were performed on a collected sample.

Table C-1. Listing of Phase IB Tests.

Parameter	Test:	B1		B2					
	Case:	1	2	1	2	3	4	5	6
Mode (TS, NE, or Act.)		n/a	n/a	TS	TS	TS	TS	TS	TS
Activation Burner									
Burner on or off		on	on	on	on	on	on	on	on
ϕ_{act}		0.96	0.95	0.96	0.96	0.96	0.96	0.96	0.96
T_{act} (^oK)		2600	2600	2600	2600	2600	2600	2200	2200
τ_{act} (ms)		10	10	10	10	10	10	10	10
Sorbent		MW	MW	MW	MW	MW	MW	MW	MW
Sorbent Size (mesh)		325	325	325	325	325	325	325	325
Sorbent Cut (full/μm)		full	full	full	full	full	full	full	full
Loading (%)		8	8	8	8	7	7	9	9
Mixing Section									
Injection Angle (Deg.)		60	60	60	60	60	60	60	60
Sulfation Duct									
Side Burners on or off		off	off	on	on	on	on	on	on
ϕ_s		n/a	n/a	0.82	0.82	0.83	0.80	0.75	0.75
T_s (^oK)		615	605	1405	1400	1385	1345	1335	1335
Ca/S		n/a	n/a	1.07	1.91	0.84	0.83	1.00	1.97
Sulfur Gas (SO_2 or H_2S)		none	none	SO_2	SO_2	SO_2	SO_2	SO_2	SO_2
& Concentration (ppmv)		n/a	n/a	2095	1170	1860	1640	1730	875
Solids Sampling									
Collected Sample (y/n)		yes	yes	no	no	no	no	no	no
Type (Act. or Capt.)		n/a	n/a	n/a	n/a	n/a	n/a	n/a	n/a
Chemical Anal. (y/n)		no	no	n/a	n/a	n/a	n/a	n/a	n/a
Morphology Anal. (y/n)		no	no	n/a	n/a	n/a	n/a	n/a	n/a

Comments by Test Number:

B1. Attempts to measure radial lime concentration profiles at r = -1, 0, +1 in. at exit of mixing section and at exit of activation duct. Sintered burner failed and experienced difficulties in obtaining the correct behavior of this burner. Problem was eventually solved, but did not get desired data.

B2. Two-Step Rapid Sulfur Capture with heated gas sampling probes (140-150 F) varying activation temperature and Ca/S.

Table C-1. Listing of Phase IB Tests, Continued.

Parameter	Test:	B3		B4		B5		B6	
	Case:	1	2	1	2	1	2	1	2
Mode (TS, NE, or Act.)		TS	TS	TS	TS	TS	TS	TS	TS
Activation Burner									
Burner on or off		on	on	on	on	on	on	on	on
ϕ_{act}		0.96	0.95	0.96	0.96	0.96	0.96	0.96	0.96
T_{act} (^oK)		2600	2600	2600	2200	2200	2200	2600	2200
τ_{act} (ms)		10	10	10	10	20	20	10	10
Sorbent		MW	MW	MW	MW	MW	MW	MW	MW
Sorbent Size (mesh)		325	325	325	325	325	325	325	325
Sorbent Cut (full/μm)		full	full	<5	<5	full	full	25-45	25-45
Loading (%)		8	8	5	7	10	10	9	11
Mixing Section									
Injection Angle (Deg.)		60	60	60	60	60	60	60	60
Sulfation Duct									
Side Burners on or off		on	on	on	on	on	on	on	on
ϕ_s		0.84	0.80	0.84	0.85	0.76	0.82	0.84	0.83
T_s (^oK)		1325	1160	1345	1350	1320	1110	1345	1340
Ca/S		1.00	1.09	0.67	1.03	1.02	1.13	1.15	1.14
Sulfur Gas (SO_2 or H_2S)		SO_2	SO_2	SO_2	SO_2	SO_2	SO_2	SO_2	SO_2
& Concentration (ppmv)		1895	1760	1890	1715	1810	1930	1840	1920
Solids Sampling									
Collected Sample (y/n)		yes	yes	no	yes	yes	yes	yes	yes
Type (Act. or Capt.)		Capt.	Capt.	n/a	Capt.	Capt.	Capt.	Capt.	Capt.
Chemical Anal. (y/n)		yes	no	n/a	yes	yes	no	no	no
Morphology Anal. (y/n)		no	no	n/a	no	no	no	no	no

Comments by Test Number:

B3. Two-Step Rapid Sulfur Capture tests using heated gas sampling probes. Varied sulfation temperature.

B4. Two-Step Rapid Sulfur Capture tests using fine sorbent cut size (<5μm) and heated gas sampling probes. Varied activation temperature.

B5. Two-Step Rapid Sulfur Capture tests using at lower activation temperature using heated gas sampling probes. Varied sulfation temperature.

B6. Two-Step Rapid Sulfur Capture tests using coarse sorbent cut (25-45μm) and heated gas sampling probes. Varied activation temperature and sulfation temperature.

Table C-1. Listing of Phase IB Tests, Continued.

Parameter	Test:	B6			B7			B8	
	Case:	3	4	5	1	2	3	1	2
Mode (TS, NE, or Act.)		TS	TS	TS	TS	TS	TS	TS	TS
Activation Burner									
Burner on or off		on	on	on	on	on	on	on	on
ϕ_{act}		0.96	0.95	0.95	0.96	0.96	0.96	0.96	0.95
T_{act} (^oK)		2600	1300	1300	2600	2600	2200	2600	2600
τ_{act} (ms)		10	10	10	10	10	10	0	0
Sorbent		MW	MW	MW	MW	MW	MW	LHL	LHL
Sorbent Size (mesh)		325	325	325	325	325	325	200	200
Sorbent Cut (full/μm)		25-45	25-45	25-45	<5	<5	<5	full	full
Loading (%)		10	11	11	9	5	5	8	6
Mixing Section									
Injection Angle (Deg.)		60	60	60	60	60	60	60	60
Sulfation Duct									
Side Burners on or off		on	on	on	on	on	on	on	on
ϕ_s		0.78	0.71	0.71	0.80	0.80	0.78	0.81	0.81
T_s (^oK)		1170	1190	1315	1325	1355	1305	1300	1330
Ca/S		1.38	1.35	1.39	1.46	0.79	0.70	1.30	0.97
Sulfur Gas (SO_2 or H_2S)		SO_2	SO_2	SO_2	SO_2	SO_2	SO_2	SO_2	SO_2
& Concentration (ppmv)		1820	1660	1580	1700	1660	1570	1620	1565
Solids Sampling									
Collected Sample (y/n)		yes	yes	yes	yes	yes	no	yes	yes
Type (Act. or Capt.)		Capt.	Capt.	Capt.	Capt.	Capt.	n/a	Capt.	Capt.
Chemical Anal. (y/n)		no	yes	no	no	no	n/a	yes	no
Morphology Anal. (y/n)		no	no	no	no	no	n/a	no	no

Comments by Test Number:

B6. Two-Step Rapid Sulfur Capture tests using coarse sorbent cut (25-45μm) and heated gas sampling probes. Varied activation temperature and sulfation temperature.

B7. Two-Step Rapid Sulfur Capture tests using fine sorbent cut (<5μm) and heated gas sampling probes. Varied activation temperature and Ca/S.

B8. Two-Step Rapid Sulfur Capture tests using Linwood Hydrated Lime. Varied activation temperature and Ca/S.

Table C-1. Listing of Phase IB Tests, Continued.

Parameter	Test:	B8	B9			B10		B11	
	Case:	3	1	2	3	1	2	1	2
Mode (TS, NE, or Act.)		TS	TS	TS	TS	TS	TS	TS	TS
Activation Burner									
Burner on or off		on	on	on	on	on	on	on	on
ϕ_{act}		0.96	0.96	0.96	0.97	0.94	0.95	0.95	0.96
T_{act} (^oK)		2200	2600	2200	2600	2600	2200	2600	2400
τ_{act} (ms)		0	10	10	10	10	10	10	10
Sorbent		LHL	MW	MW	MW	MW	MW	MW	MW
Sorbent Size (mesh)		200	325	325	325	325	325	325	325
Sorbent Cut (full/μm)		full	full	full	full	full	full	full	full
Loading (%)		7	9	9	8	7	8	8	8
Mixing Section									
Injection Angle (Deg.)		60	60	60	60	15	15	15	15
Sulfation Duct									
Side Burners on or off		on	on	on	on	on	on	on	on
ϕ_s		0.81	0.80	0.81	0.79	0.81	0.81	0.80	0.82
T_s (^oK)		1310	1325	1320	1175	1320	1340	1300	1340
Ca/S		0.98	1.14	0.93	1.00	0.96	0.97	1.17	1.15
Sulfur Gas (SO_2 or H_2S)		SO_2	SO_2	SO_2	SO_2	SO_2	SO_2	SO_2	SO_2
& Concentration (ppmv)		1520	1850	1820	1930	1695	1605	1645	1520
Solids Sampling									
Collected Sample (y/n)		no	yes	yes	yes	yes	yes	yes	yes
Type (Act. or Capt.)		n/a	Capt.	Capt.	Capt.	Capt.	Capt.	Capt.	Capt.
Chemical Anal. (y/n)		n/a	yes	yes	yes	yes	yes	yes	yes
Morphology Anal. (y/n)		n/a	no	no	no	no	no	no	no

Comments by Test Number:

B8. Two-Step Rapid Sulfur Capture tests using Linwood Hydrated Lime. Varied activation temperature and Ca/S. Used heated gas sampling probes.

B9. Two-Step Rapid Sulfur Capture tests using standard Marblewhite 325 limestone. Varied activation and sulfation temperatures. Used heated gas sampling probes.

B10. Repeat of Two-Step Sulfur Capture B9 tests using new 15^o mixing section. Used heated gas sampling probes.

B11. Two Step Sulfur capture tests with new 15^o mixing section. Fixed sulfation temperature and varied activation temperature. Used heated gas sampling probes.

Table C-1. Listing of Phase IB Tests, Continued.

Parameter	Test:	B11	B12				B13		
	Case:	3	1	2	3	4	1	2	3
Mode (TS, NE, or Act.)		TS	Act.	NE	Act.	NE	Act.	NE	NE
Activation Burner									
Burner on or off		on	on	on	on	on	on	on	on
ϕ_{act}		0.96	0.96	0.97	0.96	0.96	0.97	0.96	0.97
T_{act} (^oK)		2200	2600	2600	2400	2400	2600	2600	2400
τ_{act} (ms)		10	10	10	10	10	20	20	20
Sorbent		MW	MW	MW	MW	MW	MW	MW	MW
Sorbent Size (mesh)		325	325	325	325	325	325	325	325
Sorbent Cut (full/μm)		full	full	full	full	full	full	full	full
Loading (%)		9	9	9	8	8	7	8	8
Mixing Section									
Injection Angle (Deg.)		15	15	15	15	15	15	15	15
Sulfation Duct									
Side Burners on or off		on	off	off	off	off	off	off	off
ϕ_s		0.81	n/a	n/a	n/a	n/a	n/a	n/a	n/a
T_s (^oK)		1330	580	580	565	565	530	535	530
Ca/S		1.15	n/a	1.18	n/a	0.92	n/a	1.54	1.49
Sulfur Gas (SO_2 or H_2S)		SO_2	none	SO_2	none	SO_2	none	SO_2	SO_2
& Concentration (ppmv)		1545	n/a	1890	n/a	2060	n/a	1200	1230
Solids Sampling									
Collected Sample (y/n)		yes	yes	yes	yes	yes	yes	yes	yes
Type (Act. or Capt.)		Capt.	Act.	Capt.	Act.	Capt.	Act.	Capt.	Capt.
Chemical Anal. (y/n)		yes	yes	yes	yes	yes	yes	yes	yes
Morphology Anal. (y/n)		no	yes	no	yes	no	yes	no	no

Comments by Test Number:

B11. See previous page.

B12. Non-equilibrium Sulfur Capture and sorbent activation tests varying activation temperature. Attempting to find optimum non-equilibrium sulfur capture conditions, which will be used in subsequent Two-Step Rapid Sulfur Capture testing.

B13. Same as test B12, except increased activation time to 20 ms.

Table C-1. Listing of Phase IB Tests, Continued.

Parameter	Test:	B13	B14			B15			
	Case:	4	1	2	3	1	2	3	4
Mode (TS, NE, or Act.)		Act.	n/a	n/a	NE	n/a	n/a	NE	NE
Activation Burner									
Burner on or off		on	on	on	on	on	on	on	on
ϕ_{act}		0.96	0.96	0.96	0.96	0.97	0.97	0.96	0.96
T_{act} (^oK)		2400	2600	2600	2600	2600	2400	2600	2400
τ_{act} (ms)		20	20	20	20	20	20	20	20
Sorbent		MW	none	none	MW	none	none	MW	MW
Sorbent Size (mesh)		325	n/a	n/a	325	n/a	n/a	325	325
Sorbent Cut (full/μm)		full	n/a	n/a	full	n/a	n/a	full	full
Loading (%)		7	n/a	n/a	7	n/a	n/a	8	8
Mixing Section									
Injection Angle (Deg.)		15	15	15	15	15	15	15	15
Sulfation Duct									
Side Burners on or off		off	off	off	off	off	off	off	off
ϕ_s		n/a	n/a	n/a	n/a	n/a	n/a	n/a	n/a
T_s (^oK)		520	595	605	600	625	605	670	640
Ca/S		n/a	n/a	n/a	1.52	n/a	n/a	1.70	1.53
Sulfur Gas (SO_2 or H_2S)		none	SO_2	SO_2	SO_2	SO_2	SO_2	SO_2	SO_2
& Concentration (ppmv)		n/a	1260	1245	1275	1250	1160	1185	1220
Solids Sampling									
Collected Sample (y/n)		yes	no	no	no	no	no	no	no
Type (Act. or Capt.)		Act.	n/a	n/a	n/a	n/a	n/a	n/a	n/a
Chemical Anal. (y/n)		yes	n/a	n/a	n/a	n/a	n/a	n/a	n/a
Morphology Anal. (y/n)		yes	n/a	n/a	n/a	n/a	n/a	n/a	n/a

Comments by Test Number:

B13. Same as test B12, except increased activation time to 20 ms.

B14. Mixing studies at 10 in. below inlet of mixing section. Radial SO_2 profiles measured at r = -1.25, -0.63, 0.0, 0.63, 1.25 in. No sorbent injected during tests B14-1 and B14-2. Sorbent injected during test B14-3. Checking for flow asymmetries and degree of mixing.

B15. Repeat of B14. Adjusted alignment of activation burner/duct with mixing section to reduce asymmetries. Tests B15-1 and B15-2 were mixing studies without sorbent injection, whereas sorbent was injected during tests B15-3 and B15-4.

Table C-1. Listing of Phase IB Tests, Continued.

Parameter	Test:	B16			B17			
	Case:	1	2	3	1	2	3	4
Mode (TS, NE, or Act.)		Act.	NE	Act.	Act.	Act.	NE	NE
Activation Burner								
Burner on or off		on	on	on	on	on	on	on
ϕ_{act}		0.96	0.97	0.95	0.96	0.97	0.96	0.97
T_{act} (^oK)		2600	2600	2400	2600	2400	2600	2400
τ_{act} (ms)		30	30	30	0	0	0	0
Sorbent		MW	MW	MW	MW	MW	MW	MW
Sorbent Size (mesh)		325	325	325	325	325	325	325
Sorbent Cut (full/μm)		full	full	full	full	full	full	full
Loading (%)		10	8	8	9	8	8	8
Mixing Section								
Injection Angle (Deg.)		15	15	15	15	15	15	15
Sulfation Duct								
Side Burners on or off		off	off	off	off	off	off	off
ϕ_s		n/a	n/a	n/a	n/a	n/a	n/a	n/a
T_s (^oK)		540	575	570	655	655	660	655
Ca/S		n/a	1.59	n/a	n/a	n/a	1.46	1.39
Sulfur Gas (SO_2 or H_2S)		none	SO_2	none	none	none	SO_2	SO_2
& Concentration (ppmv)		n/a	1475	n/a	n/a	n/a	1585	1575
Solids Sampling								
Collected Sample (y/n)		yes	yes	yes	yes	yes	yes	yes
Type (Act. or Capt.)		Act.	Capt.	Act.	Act.	Act.	Capt.	Capt.
Chemical Anal. (y/n)		yes	yes	yes	yes	yes	yes	yes
Morphology Anal. (y/n)		yes	no	yes	yes	yes	no	no

Comments by Test Number:

B16. Non-equilibrium sulfur capture and activation tests. Varied activation temperature at longest activation time.

B17. Non-equilibrium sulfur capture and activation tests. Varied activation temperature at shortest activation time.

Table C-1. Listing of Phase IB Tests, Continued.

Parameter	Test:	B18		B19		B20		
	Case:	1	2	1	2	1	2	3
Mode (TS, NE, or Act.)		TS	TS	n/a	n/a	n/a	n/a	TS
Activation Burner								
Burner on or off		on	on	on	on	on	on	on
ϕ_{act}		0.97	0.97	0.96	0.96	0.97	0.96	0.96
T_{act} (°K)		2600	2200	2600	2600	2600	2600	2600
τ_{act} (ms)		10	10	10	10	10	10	10
Sorbent		MW	MW	MW	MW	MW	MW	MW
Sorbent Size (mesh)		325	325	325	325	325	325	325
Sorbent Cut (full/μm)		full	full	full	full	full	full	full
Loading (%)		9	8	7	7	7	7	6
Mixing Section								
Injection Angle (Deg.)		30	30	0	0	0	0	0
Sulfation Duct								
Side Burners on or off		on	on	on	on	on	on	on
ϕ_s		0.81	0.82	0.82	0.82	0.82	0.83	0.83
T_s (°K)		1350	1360	1300	1360	1330	1410	1420
Ca/S		1.16	1.14	n/a	1.58	n/a	0.98	0.87
Sulfur Gas (SO_2 or H_2S)		SO_2	SO_2	none	SO_2	none	SO_2	SO_2
& Concentration (ppmv)		1660	1530	n/a	1080	n/a	1660	1540
Solids Sampling								
Collected Sample (y/n)		yes	yes	yes	yes	yes	yes	no
Type (Act. or Capt.)		Capt.	Capt.	Act.	Both	Act.	Both	n/a
Chemical Anal. (y/n)		yes	yes	yes	yes	yes	yes	n/a
Morphology Anal. (y/n)		no	no	no	no	no	no	n/a

Comments by Test Number:

B18. Two-Step Rapid Sulfur Capture tests using new 30° mixing section. Standard condition used, varied activation temperature.

B19. In-filter sulfation check using new 0° mixing section . This is to verify if sulfation is occurring in solids sample collection filter during collection. Test B19-1 is a control sample, collected solids without SO_2 injection. In test B19-2 a solids sample was collected without SO_2 injection, then sorbent flow was terminated and SO_2 was injected into the system during a second sample collection period. SO_2 analyzer problems occurred impairing results.

B20. Same as B19, plus a Two-Step Rapid Sulfur Capture test with new 0° mixing section. In-filter sulfation tests verified that significant sulfation occurs in the filter housing.

Table C-1. Listing of Phase IB Tests, Continued.

Parameter	Test:	B21		B22			B23	
	Case:	1	2	1	2	3	1	2
Mode (TS, NE, or Act.)		TS	TS	TS	TS	TS	NE	NE
Activation Burner								
Burner on or off		on	on	on	on	on	on	on
ϕ_{act}		0.97	0.97	0.96	0.97	0.95	0.95	0.92
T_{act} (^oK)		2600	2400	2600	2400	2200	2600	2400
τ_{act} (ms)		10	10	10	10	10	0	0
Sorbent		MW	MW	MW	MW	MW	MW	MW
Sorbent Size (mesh)		325	325	325	325	325	325	325
Sorbent Cut (full/μm)		full	full	full	full	full	full	full
Loading (%)		7	7	7	5	4	6	4
Mixing Section								
Injection Angle (Deg.)		0	0	0	0	0	0	0
Sulfation Duct								
Side Burners on or off		on	on	on	on	on	off	off
ϕ_s		0.82	0.81	0.81	0.80	0.80	n/a	n/a
T_s (^oK)		1390	1390	1380	1390	1375	660	750
Ca/S		1.03	0.97	0.92	0.73	0.50	1.19	0.80
Sulfur Gas (SO_2 or H_2S)		SO_2	SO_2	SO_2	SO_2	SO_2	SO_2	SO_2
& Concentration (ppmv)		1480	1540	1600	1640	1610	1390	1515
Solids Sampling								
Collected Sample (y/n)		yes	yes	yes	yes	yes	yes	yes
Type (Act. or Capt.)		Capt.	Capt.	Capt.	Capt.	Capt.	Capt.	Capt.
Chemical Anal. (y/n)		yes	yes	no	no	no	no	no
Morphology Anal. (y/n)		no	no	no	no	no	no	no

Comments by Test Number:

B21. Two-Step Rapid Sulfur Capture tests using new 0^o mixing section. Standard conditions, varied activation temperature. Used heated gas sampling probes.

B22. Repeat and extension of test B21.

B23. Non-equilibrium Sulfur Capture tests using 0^o mixing section and shortest activation time. Varied activation temperature.

Table C-1. Listing of Phase IB Tests, Continued.

Parameter	Test:	B24			B25
	Case:	1	2	3	1
Mode (TS, NE, or Act.)		NE	NE	NE	TS
Activation Burner					
Burner on or off		on	on	on	on
ϕ_{act}		0.98	0.96	0.96	0.93
T_{act} (^{o}K)		2600	2725	2850	2810
τ_{act} (ms)		0	0	0	0
Sorbent		MW	MW	MW	MW
Sorbent Size (mesh)		325	325	325	325
Sorbent Cut (full/μm)		full	full	full	full
Loading (%)		8	6	7	8
Mixing Section					
Injection Angle (Deg.)		0	0	0	0
Sulfation Duct					
Side Burners on or off		off	off	off	on
ϕ_s		n/a	n/a	n/a	0.83
T_s (^{o}K)		715	740	760	1320
Ca/S		1.34	1.12	1.32	1.08
Sulfur Gas (SO_2 or H_2S)		SO_2	SO_2	SO_2	SO_2
& Concentration (ppmv)		1610	1600	1465	1720
Solids Sampling					
Collected Sample (y/n)		no	no	no	no
Type (Act. or Capt.)		n/a	n/a	n/a	n/a
Chemical Anal. (y/n)		n/a	n/a	n/a	n/a
Morphology Anal. (y/n)		n/a	n/a	n/a	n/a

Comments by Test Number:

B24. Non-equilibrium Sulfur Capture test at shortest activation time and higher activation temperatures.

B25. Two-Step Sulfur Capture test at shortest activation time and highest activation temperature.

APPENDIX D

COMPUTER CODE INPUT FILE: CASOX.DAT

Representative Case

```
CA - SOX  REACTION CODE INPUTS

Case Number (Int XXX)
101
Process:  0 = Const Pressure, 1 = Const Volume
0
Particle Properties
Number of particle size groups  [ 1 to 10 ]
7
Particle Shattering:  1 = Shatter, 0 = No Breakage
0 0 0 0 0 0 0
Particle Shattering Diameter Ratio
1. 1. 1. 1. 1. 1. 1.
Initial Particle Diameters  [ cm ]
8e-4  12e-4  16e-4  24e-4  32e-4  48e-4  64e-4
Mass Fraction of each particle size group
0.08   0.12   0.18   0.24   0.20  0.12   0.06
Particle Composition [Weight Fraction] by Species
CaCO3  Ca(OH)2   CaO      Water   CaSO3    CaSO4     CaS
0.50   0.40      0.00     0.10    0.00     0.0       0.0
Particle Constituent Specific Heat          [cal/gm K]
CaCO3  Ca(OH)2   CaO      Water   CaSO3    CaSO4     CaS
0.214  0.288     0.197    1.000   0.1      0.265     0.1
Particle Constituent Heat of Formation      [Kcal/gm]
CaCO3   Ca(OH)2  CaO      Water   CaSO3    CaSO4     CaS
-2.877  -3.186   -2.705   -3.21   -1.0     -2.466    -1.573
Particle Constituent Densities              [gm/cm^3]
CaCO3  Ca(OH)2   CaO      Water   CaSO3    CaSO4     CaS
2.22   2.343     3.346    1.0     2.0      2.45      2.18
Particle Initial Temperature  [K]
300
Calculate Particle Properties:  1 = Y, 0 = N
1
Sorbent Particle Kinetics Constants
```

Reaction	Usage Y/1 N/0	Ht. of React [Kcal/mole]	A [1/sec]	E [Kcal/M]
CaCO3 -> CaO + CO2	1	-42.17	.414e13	54.82
Ca(OH)2 -> CaO + H2O	1	-26.60	.146e14	58.01
CaO + SO2 -> CaSO3	1	47.52	.864e12	31.2
CaSO3 + 0.5O2 -> CaSO4	0	65.53	.411e14	28.32
CaSO3 + H2O -> CaSO4 + H2	1	7.74	.543e14	32.1
CaSO3 + CO2 -> CaSO4 + CO	0	-2.10	.918e14	38.93
CaSO4 -> CaO + SO2 + 0.5O2	0	-113.05	.323e13	68.33
CaSO4 + CO -> CaSO3 + CO2	0	2.10	.246e10	69.07
CaSO4 + H2 -> CaSO3 + H2O				

```
                                  0          -7.74       .463e10      64.31
CaSO3 -> CaO + SO2
                                  0         -47.52       .112e10      57.23
CaO + H2S -> CaS + H2O
                                  0          14.77       .511e13      32.12
CaS + H2O -> CaO + H2S
                                  0          -14.77      .213e14      54.79
Carrier Gas Inputs:
Carrier / Particulates  [Mass]
1.20
Species Composition  [Mass Basis; 16 required]
CH4,C6H6,C6H12,H2,O2, N2,CO,CO2,H2O,H2S, SO2,COS,H,N,O, OH
0 0 0 0 0  1.0 0 0 0 0 0  0 0 0 0 0 0  0
Carrier Gas Static Pressure     [Std. Atm.]
1.0
Carrier Gas Static Temperature  [K]
300
Carrier Gas Velocity  [cm/sec]
1.0e4
Calc Carrier Gas Heat Loss :  1 = Y; 0 = N
0
Primary Gas Inputs:
Primary / Particulates  [Mass]
80.0
Species Composition  [Mass Basis; 16 required]
CH4,C6H6,C6H12,H2,O2,  N2,CO,CO2,H2O,H2S,  SO2,COS,H,N,O,  OH
0 0 0 0 0.05   0.85 0 0 0 0.05   0.05 0 0 0 0   0
Primary Gas Static Pressure     [Std. Atm.]
1.0
Primary Gas Static Temperature  [K]
2300
Primary Gas Velocity  [cm/sec]
1.0e3
Primary Gas Physical Parameters
Calculate primary gas properties:  1 = Y, 0 = N
1
Total Flow Mixing Time  [sec]
4.0e-3
Rate Control: Turbulent = 1, Laminar = 0
1
Wall Temp [K];  Thermal Equil Time [sec]
1800.0  .20
Sutherland constant for viscosity  [gm/cm sec]
1.708e-4
Diffusivity of oxygen in air   [cm2/s]
5e-2
Solution Control Inputs
Internal Debug Control: 1 = On, 0 = Off
0
Initial Time Step  [sec]
1.0e-5
Minimum and Maximum Time Steps   [sec]
5.0e-5 2.0e-3
End of Solution Time   [sec]
6.0e-3
Time Interval for Data Plot Filing   [sec]
2.0e-4
Time Interval for Data List Output   [sec]
5.0e-4
```

APPENDIX E

COMPUTER CODE OUTPUT FILE: CASOX.OUT

Representative Case - Portion Only

```
******* OUTPUT * FROM * CALCULATIONS ********

Carrier and primary air rates
        69.41              12.05
Carrier gas properties
Time (msec.);  Carrier Temperature (K)
       3.01             2246.52
Carrier gas density, pressure, Cp
         .000159     1.000000      .309559
Fractions on Mass , Volume , Dry basis
 CH4         .1000E-09  .1822E-09  .1828E-09
 C6H6        .1000E-09  .3742E-10  .3755E-10
 C6H12       .1000E-09  .3473E-10  .3485E-10
 H2          .8725E-06  .1265E-04  .1270E-04
 O2          .4895E-01  .4472E-01  .4487E-01
 N2          .8495E+00  .8864E+00  .8895E+00
 CO          .1181E-05  .1232E-05  .1236E-05
 CO2         .1714E-02  .1138E-02  .1142E-02
 H2O         .2160E-02  .3504E-02  .3516E-02
 H2S         .4895E-01  .4199E-01  .4213E-01
 SO2         .4874E-01  .2224E-01  .2232E-01
 COS         .1000E-09  .4866E-10  .4883E-10
 H           .1000E-09  .2900E-08  .2910E-08
 N           .1000E-09  .2087E-09  .2094E-09
 O           .1000E-09  .1827E-09  .1833E-09
 OH          .1000E-09  .1719E-09  .1725E-09
Primary Gas Properties
Time =    3.01  Primary Temp =  2292.53  Density =  .1557E-03
Pressure =  .1013E+07  Cp =  .1291E+08
Primary Composition is
CH4    .0000;      C6H6    .0000;      C6H12   .0000;      H2      .0000
O2     .0500;      N2      .8500;      CO      .0000;      CO2     .0000
H2O    .0000;      H2S     .0500;      SO2     .0500;      COS     .0000
H      .0000;      N       .0000;      O       .0000;      OH      .0000
Particle Properties are
I Temp   Diam  Mass/        Mass  Fractions ...
   [K]   [um]  Initial  Water CaCO3 Ca(OH)2  CaO  CaSO3 CaSO4  CaS
1 2244.5 6.73  .764      .000   .000   .000 .576   .367  .057 .000
2 2161.6 9.17  .652      .000   .000   .000 .814   .172  .014 .000
3 2023.3 11.75 .614      .000   .000   .000 .922   .075  .003 .000
4 1367.9 19.08 .690      .000   .246   .189 .563   .002  .000 .000
5  887.8 29.69 .900      .000   .556   .444 .000   .000  .000 .000
6  381.5 44.57 .901      .001   .556   .444 .000   .000  .000 .000
7  334.1 61.29 .940      .044   .556   .444 .000   .000  .000 .000
```

APPENDIX F

COMPUTER CODE OUTPUT FILE: CASOX.PLT

Representative Case - Portion Only

File Header Information

```
PLOTTING  OUTPUTS

The Date is  04/28/1993
The Time is  17:49:32

The Computation Time is  00:00:23

Number of Plot Steps =  31
Number of Particle Sizes =  7

Listing Format:

Time [ms]; Primary gas temp  [K]; Mix Status; Carrier gas temp [K];
Carrier gas comp (16); CH4, C6H6, C6H12, H2, O2, N2
                       CO, CO2, H2O, H2S, SO2, COS
                       H, N, O, OH
Unreacted Sorbent    ; Reacted Sorbent  (Totals) ; Int. Steps
Particle:Diam[um]; Temp[K]; Density[gm/cm^3]; Sulf Frac; Rmech(Nrange)
Diam [um]; Mass Frac: Water  CaCO3  Ca(OH)2  CaO  CaSO3  CaSO4  CaS
```

Specific Time Step Outputs

Next Time Step:

```
3.01    2292.5     *ON*          2246.5
 .0000   .0000   .0000   .0000   .0490   .8495
 .0000   .0017   .0022   .0490   .0487   .0000
 .0000   .0000   .0000   .0000
 .9348   .0652                           193
    6.73      2244.5     2.6394     .3241      HETERO
    9.17      2161.6     2.9855     .1211      HETERO
   11.75      2023.3     3.1823     .0479      HETERO
   19.08      1367.9     2.7716     .0012      HETERO
   29.69       887.8     2.2730     .0000      HETERO
   44.57       381.5     2.2730     .0000        EVAP
   61.29       334.1     2.2730     .0000        EVAP
    6.73   .0000   .0000   .0000   .5759   .3666   .0575   .0000
    9.17   .0000   .0000   .0000   .8143   .1719   .0138   .0000
   11.75   .0000   .0000   .0000   .9220   .0745   .0034   .0000
   19.08   .0000   .2461   .1894   .5628   .0017   .0000   .0000
   29.69   .0000   .5555   .4444   .0000   .0000   .0000   .0000
   44.57   .0012   .5556   .4444   .0000   .0000   .0000   .0000
   61.29   .0441   .5556   .4444   .0000   .0000   .0000   .0000
```

Next Time Step:

```
3.21    2292.0     *ON*          2248.4
 .0000   .0000   .0000   .0000   .0490   .8492
 .0000   .0018   .0021   .0490   .0488   .0000
 .0000   .0000   .0000   .0000
 .9247   .0753                           210
```

```
     6.81       2246.9     2.6011       .3543       HETERO
     9.24       2171.0     2.9515       .1358       HETERO
    11.81       2055.8     3.1565       .0563       HETERO
    17.08       1457.6     3.2974       .0029       HETERO
    29.69        950.1     2.2731       .0000       HETERO
    44.55        419.4     2.2730       .0000         EVAP
    61.06        336.0     2.2730       .0000         EVAP
     6.81     .0000     .0000     .0000     .5461     .3918     .0620     .0000
     9.24     .0000     .0000     .0000     .7943     .1902     .0155     .0000
    11.81     .0000     .0000     .0000     .9089     .0869     .0042     .0000
    17.08     .0000     .0158     .0081     .9712     .0048     .0001     .0000
    29.69     .0000     .5555     .4444     .0001     .0000     .0000     .0000
    44.55     .0006     .5555     .4444     .0000     .0000     .0000     .0000
    61.06     .0386     .5555     .4444     .0000     .0000     .0000     .0000

Next Time Step:

3.41    2291.5     *ON*           2249.9
 .0000    .0000    .0000    .0000    .0490    .8493
 .0000    .0018    .0021    .0490    .0488    .0000
 .0000    .0000    .0000    .0000
 .9165    .0835                              58
     6.88       2248.8     2.5659       .3841       HETERO
     9.31       2177.8     2.9191       .1504       HETERO
    11.87       2083.0     3.1315       .0648       HETERO
    16.99       1542.7     3.3263       .0052       HETERO
    29.68       1009.3     2.2733       .0000       HETERO
    44.53        456.8     2.2730       .0000         EVAP
    60.83        338.3     2.2730       .0000         EVAP
     6.88     .0000     .0000     .0000     .5179     .4156     .0665     .0000
     9.31     .0000     .0000     .0000     .7748     .2079     .0173     .0000
    11.87     .0000     .0000     .0000     .8960     .0991     .0049     .0000
    16.99     .0000     .0000     .0000     .9911     .0087     .0002     .0000
    29.68     .0000     .5553     .4443     .0004     .0000     .0000     .0000
    44.53     .0001     .5555     .4444     .0001     .0000     .0000     .0000
    60.83     .0331     .5555     .4444     .0001     .0000     .0000     .0000

Next Time Step:

3.61    2291.1     *ON*           2250.8
 .0000    .0000    .0000    .0000    .0491    .8493
 .0000    .0017    .0020    .0491    .0488    .0000
 .0000    .0000    .0000    .0000
 .9083    .0917                              35
     6.96       2250.1     2.5335       .4135       HETERO
     9.38       2182.9     2.8882       .1650       HETERO
    11.93       2104.6     3.1072       .0732       HETERO
    17.02       1616.0     3.3158       .0080       HETERO
    29.67       1065.2     2.2744       .0000       HETERO
    44.53        495.0     2.2731       .0000       HETERO
    60.60        340.9     2.2730       .0000         EVAP
     6.96     .0000     .0000     .0000     .4911     .4380     .0709     .0000
     9.38     .0000     .0000     .0000     .7558     .2251     .0191     .0000
    11.93     .0000     .0000     .0000     .8832     .1111     .0057     .0000
    17.02     .0000     .0000     .0000     .9863     .0134     .0003     .0000
    29.67     .0000     .5543     .4438     .0018     .0000     .0000     .0000
    44.53     .0000     .5555     .4444     .0001     .0000     .0000     .0000
    60.60     .0278     .5555     .4444     .0001     .0000     .0000     .0000
```

APPENDIX G

COMPUTER CODE INPUT FILE: CALCINATION CASE

```
CA - SOX  REACTION CODE INPUTS

Case Number (Int XXX)
111
Process:  0 = Const Pressure, 1 = Const Volume
0
Particle Properties
Number of particle size groups  [ 1 to 10 ]
7
Particle Shattering:  1 = Shatter, 0 = No Breakage
0 0 0 0 0 0 0
Particle Shattering Diameter Ratio
1. 1. 1. 1. 1. 1. 1.
Initial Particle Diameters  [ cm ]
1.88e-4  6.58e-4  12.32e-4  17.23e-4  21.98e-4  28.13e-4  37.75e-4
Mass Fraction of each particle size group
14.29  14.28  14.29  14.28  14.29  14.28  14.29
Particle Composition [Weight Fraction] by Species
CaCO3  Ca(OH)2   CaO      Water   CaSO3    CaSO4     CaS
1.00   0.00      0.00     0.00    0.00     0.0       0.0
Particle Constituent Specific Heat          [cal/gm K]
CaCO3  Ca(OH)2   CaO      Water   CaSO3    CaSO4     CaS
0.214  0.288     0.197    1.000   0.1      0.265     0.1
Particle Constituent Heat of Formation      [Kcal/gm]
CaCO3   Ca(OH)2  CaO      Water   CaSO3    CaSO4     CaS
-2.877  -3.186   -2.705   -3.21   -1.0     -2.466    -1.573
Particle Constituent Densities              [gm/cm^3]
CaCO3  Ca(OH)2   CaO      Water   CaSO3    CaSO4     CaS
2.77   2.343     3.346    1.0     2.0      2.45      2.18
Particle Initial Temperature  [K]
300
Calculate Particle Properties:  1 = Y, 0 = N
1
Sorbent Particle Kinetics Constants
```

Reaction	Usage Y/1 N/0	Ht. of React [Kcal/mole]	A [1/sec]	E [Kcal/M]
CaCO3 -> CaO + CO2	1	-42.17	.23e13	49.00
Ca(OH)2 -> CaO + H2O	0	-26.60	.146e14	58.01
CaO + SO2 -> CaSO3	0	47.52	.864e12	31.2
CaSO3 + 0.5O2 -> CaSO4	0	65.53	.411e14	28.32
CaSO3 + H2O -> CaSO4 + H2	0	7.74	.543e14	32.1
CaSO3 + CO2 -> CaSO4 + CO	0	-2.10	.918e14	38.93
CaSO4 -> CaO + SO2 + 0.5O2	0	-113.05	.323e13	68.33
CaSO4 + CO -> CaSO3 + CO2	0	2.10	.246e10	69.07
CaSO4 + H2 -> CaSO3 + H2O	0	-7.74	.463e10	64.31
CaSO3 -> CaO + SO2	0	-47.52	.112e10	57.23
CaO + H2S -> CaS + H2O				

```
                                0          14.77       .511e13      32.12
CaS + H2O -> CaO + H2S
                                0         -14.77       .213e14      54.79
Carrier Gas Inputs:
Carrier / Particulates  [Mass]
12.3
Species Composition  [Mass Basis; 16 required]
CH4,C6H6,C6H12,H2,O2, N2,CO,CO2,H2O,H2S, SO2,COS,H,N,O, OH
0 0 0 0 0.014  0.626 0 0.234 0.126 0  0 0 0 0 0  0
Carrier Gas Static Pressure     [Std. Atm.]
1.0
Carrier Gas Static Temperature  [K]
2400
Carrier Gas Velocity  [cm/sec]
1357.6
Calc Carrier Gas Heat Loss :  1 = Y; 0 = N
0
Primary Gas Inputs:
Primary / Particulates  [Mass]
1000.0
Species Composition  [Mass Basis; 16 required]
CH4,C6H6,C6H12,H2,O2,  N2,CO,CO2,H2O,H2S,  SO2,COS,H,N,O,  OH
0 0 0 0 0.01   0.67 0 0.207 0.113 0   0 0 0 0 0   0
Primary Gas Static Pressure     [Std. Atm.]
1.0
Primary Gas Static Temperature  [K]
2400
Primary Gas Velocity  [cm/sec]
853.5
Primary Gas Physical Parameters
Calculate primary gas properties:  1 = Y, 0 = N
1
Total Flow Mixing Time  [sec]
1.0e-3
Rate Control: Turbulent = 1, Laminar = 0
1
Wall Temp [K];  Thermal Equil Time [sec]
2200.0  .20
Sutherland constant for viscosity  [gm/cm sec]
1.708e-4
Diffusivity of oxygen in air   [cm2/s]
5e-2
Solution Control Inputs
Internal Debug Control: 1 = On, 0 = Off
0
Initial Time Step  [sec]
1.0e-6
Minimum and Maximum Time Steps   [sec]
2.0e-6 2.0e-3
End of Solution Time   [sec]
10.0e-3
Time Interval for Data Plot Filing   [sec]
2.0e-4
Time Interval for Data List Output   [sec]
1.0e-3
```

APPENDIX H

COMPUTER CODE INPUT FILE: SULFATION CASE

```
CA - SOX  REACTION CODE INPUTS

Case Number (Int XXX)
121
Process:  0 = Const Pressure, 1 = Const Volume
0
Particle Properties
Number of particle size groups  [ 1 to 10 ]
7
Particle Shattering:  1 = Shatter, 0 = No Breakage
0 0 0 0 0 0 0
Particle Shattering Diameter Ratio
1. 1. 1. 1. 1. 1. 1.
Initial Particle Diameters  [ cm ]
1.88e-4  6.58e-4  12.32e-4  17.23e-4  21.98e-4  28.13e-4  37.75e-4
Mass Fraction of each particle size group
14.29  14.28  14.29  14.28  14.29  14.28  14.29
Particle Composition [Weight Fraction] by Species
CaCO3  Ca(OH)2   CaO      Water   CaSO3    CaSO4     CaS
0.00   0.00      1.00     0.00    0.00     0.0       0.0
Particle Constituent Specific Heat          [cal/gm K]
CaCO3  Ca(OH)2   CaO      Water   CaSO3    CaSO4     CaS
0.214  0.288     0.197    1.000   0.1      0.265     0.1
Particle Constituent Heat of Formation      [Kcal/gm]
CaCO3   Ca(OH)2  CaO      Water   CaSO3    CaSO4     CaS
-2.877  -3.186   -2.705   -3.21   -1.0     -2.466    -1.573
Particle Constituent Densities              [gm/cm^3]
CaCO3  Ca(OH)2   CaO      Water   CaSO3    CaSO4     CaS
2.77   2.343     3.346    1.0     2.0      2.45      2.18
Particle Initial Temperature  [K]
2400
Calculate Particle Properties:  1 = Y, 0 = N
1
Sorbent Particle Kinetics Constants
```

Reaction	Usage Y/1 N/0	Ht. of React [Kcal/mole]	A [1/sec]	E [Kcal/M]
CaCO3 -> CaO + CO2	0	-42.17	.23e13	49.00
Ca(OH)2 -> CaO + H2O	0	-26.60	.146e14	58.01
CaO + SO2 -> CaSO3	1	47.52	.864e12	31.2
CaSO3 + 0.5O2 -> CaSO4	1	65.53	.411e14	28.32
CaSO3 + H2O -> CaSO4 + H2	1	7.74	.543e14	32.1
CaSO3 + CO2 -> CaSO4 + CO	1	-2.10	.918e14	38.93
CaSO4 -> CaO + SO2 + 0.5O2	0	-113.05	.323e13	68.33
CaSO4 + CO -> CaSO3 + CO2	0	2.10	.246e10	69.07
CaSO4 + H2 -> CaSO3 + H2O	0	-7.74	.463e10	64.31
CaSO3 -> CaO + SO2	0	-47.52	.112e10	57.23
CaO + H2S -> CaS + H2O				

```
                                0          14.77       .511e13      32.12
CaS + H2O -> CaO + H2S
                                0         -14.77       .213e14      54.79
Carrier Gas Inputs:
Carrier / Particulates  [Mass]
37.5
Species Composition  [Mass Basis; 16 required]
CH4,C6H6,C6H12,H2,O2, N2,CO,CO2,H2O,H2S, SO2,COS,H,N,O, OH
0 0 0 0 0.012  0.630 0 0.239 0.119 0  0 0 0 0 0 0
Carrier Gas Static Pressure     [Std. Atm.]
1.0
Carrier Gas Static Temperature  [K]
2400
Carrier Gas Velocity  [cm/sec]
1926.0
Calc Carrier Gas Heat Loss :  1 = Y; 0 = N
0
Primary Gas Inputs:
Primary / Particulates  [Mass]
285.2
Species Composition  [Mass Basis; 16 required]
CH4,C6H6,C6H12,H2,O2,  N2,CO,CO2,H2O,H2S,  SO2,COS,H,N,O,  OH
0 0 0 0 0.022   0.714 0 0.168 0.092 0   0.004 0 0 0 0   0
Primary Gas Static Pressure     [Std. Atm.]
1.0
Primary Gas Static Temperature  [K]
1373
Primary Gas Velocity  [cm/sec]
1127
Primary Gas Physical Parameters
Calculate primary gas properties:  1 = Y, 0 = N
1
Total Flow Mixing Time  [sec]
8.0e-3
Rate Control: Turbulent = 1, Laminar = 0
1
Wall Temp [K];  Thermal Equil Time [sec]
2200.0  .20
Sutherland constant for viscosity  [gm/cm sec]
1.708e-4
Diffusivity of oxygen in air   [cm2/s]
5e-2
Solution Control Inputs
Internal Debug Control: 1 = On, 0 = Off
0
Initial Time Step  [sec]
1.0e-6
Minimum and Maximum Time Steps   [sec]
2.0e-6 2.0e-3
End of Solution Time   [sec]
200.0e-3
Time Interval for Data Plot Filing   [sec]
2.5e-3
Time Interval for Data List Output   [sec]
10.0e-3
```

APPENDIX I

INITIAL FEASIBILITY/ECONOMIC EVALUATION

I.1 INTRODUCTION

It should be noted that this initial Feasibility/Economic Evaluation was prepared during Phase I (Base) and is based on early experimental results which were found later in this program to be erroneous. The actual best performance of the Two-Step Sulfur Capture process was found to be 10% calcium utilization at Ca/S = 1. This section is included here for the sole purpose of presenting the methodology used for deriving the economic feasibility results presented in Section 7.0.

I.2 TWO-STEP SULFUR CAPTURE

The Two-Step Rapid Sulfur Capture performance used in the following analysis is 97% at a Ca/S=2. Early results in this program indicated that this could be achieved using limestone activation conditions of 2600^{o}K and 10 ms, sulfation of 1250-1450^{o}K and slightly fuel-lean, and with Marblewhite 325, a pulverized limestone with a mass median diameter of 14 microns, as the sorbent. As cautioned above, these results were found to be in error later in this program. Nevertheless, they are used in this section for determining economic feasibility results..

I.3 APPLICATIONS FOR THE TWO-STEP PROCESS

Based on the sulfation conditions under which the performance stated under I.2 was thought to be achievable, the ideal applications for the Two-Step Rapid Sulfur Capture Process were determined to be in furnace injection and fluidized bed combustion.

I.4 ACTIVATION BURNER DESIGN

NOx formation was a concern at the high temperatures required for limestone activation. Therefore, a fuel/oxygen burner design was preferred to a fuel/enriched air burner design. The fuel-oxygen burner is also more compact than a fuel-air burner because much greater limestone

loadings are possible at the required flame temperature of 2600°K. Thermodynamic equilibrium calculations of fuel-oxygen systems showed that a limestone loading of 50% was possible in a natural gas/oxygen flame and a loading of 46% was possible in a coal/oxygen flame. As discussed later, the coal/oxygen burner is more economical than the natural gas-oxygen burner.

I.5 ADVANCED COAL COMBUSTION SYSTEMS CONSIDERED

Sulfur dioxide removal costs for two possible applications of the Two-Step Rapid Sulfur Capture process have been calculated, namely: a pulverized coal fired boiler and an atmospheric fluidized bed combustor.

I.6 ECONOMIC ANALYSIS METHOD

The levelized revenue requirement method outlined in EPRI's Technical Assessment Guide[21] was adopted for estimating the two-step process costs. Table I-1 shows the parameters which go into the levelized revenue requirement calculation. These factors are capital cost, levelized carrying charge, consumable cost, and levelization factor for consumables. The costs can also be calculated in constant dollars or current dollars. A brief description of the differences between these analysis is shown in Table I-2. Table I-3 describes the reference advanced coal utilization systems for which the two-step process costs were calculated. Two reference systems were provided by Riley Research at Worcester (MA), with the first one being an EPRI standard that was used to evaluate FGD processes in a recently published study[22]. The EPRI analysis is in constant dollars. Table I-4 shows the EPRI and Riley system flows in detail. The SO_2 flows are approximately the same. Therefore, the activation burner size and gas/solid flows are approximately the same.

I.7 RILEY STOKER'S RETROFIT LIMB REFERENCE SYSTEM

Table I-5 shows a breakdown of the levelized capital recovery and consumable costs in mills/kWh for Riley's retrofit LIMB reference system. Also shown is the cost in $/ton of SO_2 removed. The costs for three two-step cases are compared with LIMB which is assumed to capture 50% sulfur at a Ca/S=2. Two levels of utilization were assumed for the two-step process when

this study was prepared early in this program: 96% capture at Ca/S=2 and 90% capture at Ca/S=1.2. Moreover, costs of two activation burner designs, coal/oxygen and natural-gas/oxygen were calculated. Several observations can be made from the data in Table I-5. The two-step process is approximately 23% more economical than LIMB at 48% calcium utilization and 42% more economical at 75% calcium utilization. The gas/oxygen burner is more expensive than the coal/oxygen activation burner. A point to note in this figure is that the LIMB case has lower mills/kWh but a higher \$/ton SO_2 removed cost because LIMB captures only 50% of the SO_2 in contrast to 90-96% capture levels assumed for the two-step cases.

Based on results obtained earlier in this program, the two-step process would have been two to three times more efficient in sorbent utilization and, therefore, the limestone and waste cost per ton SO_2 removed would have been less than for LIMB. The major cost in the two-step process is the coal and oxygen costs. Most of the coal cost would have been recovered because only a fraction of the activation burner energy is used to calcine the limestone. This energy recovery is represented by the 'coal credit' term in the analysis. In fact, at higher than 30% utilization the overall sulfation process is exothermic and therefore, the coal credit term is greater than the coal cost. The methodology adopted in arriving at the coal credit term is explained in Tables I-6 and I-7.

The consumable cost levelization factors, consumable costs, and capital costs used in the above analysis are shown in Tables I-8 through I-10. In Table I-8 real escalation refers to the annual rate of increase of an expenditure that is due to factors such as depletion, increased demand, and improvements in design (negative escalation). Inflation refers to the rise in price levels caused by an increase in available currency and credit without a proportional increase in available goods and services of equal quality.

An issue looming on the horizon is the regulation regarding coal waste disposal. The new acid rain legislation is going to result in a doubling of the scrubber waste. So far coal power plant wastes have been considered non-hazardous by the EPA but disposal (landfilling) requirements are expected to become more stringent because of tighter state and local laws. Therefore, sulfur removal technologies which produce less waste have an edge. A waste disposal cost of 16 \$/ton was used in the analysis. According to Dean Golden (EPRI) the coal waste disposal costs range

from $12-20 per ton at present. However, some utilities (especially in the East) are paying more for waste disposal even now. For example, Atlantic Electric based in New Jersey is currently paying $25 per ton and expects to pay on average $40 per ton over the life of their plant. There is considerable uncertainty regarding future waste disposal costs because of the uncertain regulatory environment. An upper bound might be the cost to dispose municipal incinerator waste. At present it costs $100 per ton to dispose of incinerator waste. Table I-11 shows the effect on $/ton SO2 removed if the waste disposal costs undergo a real escalation of 5% per year.

The size of the activation burner compared to the main coal burning plant is of obvious importance. The activation burner represents only 5% and 8% of the total system flow at 90% removal (Ca/S=1.2) and 96% removal (Ca/S=2) respectively.

The injection of limestone into the furnace increases the amount of solids which have to be removed downstream in a ESP or baghouse. It should be pointed out that a baghouse improves the utilization because of longer gas/solid contact. Table I-12 shows the increase in the solids loading upon limestone injection and the effect this has on the waste properties. The presence of lime in the waste results in steam generation and handling problems. The two-step process would have been better than LIMB in this respect because of the lower percentage of unreacted lime in the solid waste.

I.8 EPRI'S REFERENCE SYSTEM

Table I-13 summarizes the wet FGD and the two-step process costs. The wet FGD cost data were obtained from the study published in the EPRI Journal. The two-step costs were calculated using the same financial data and consumable costs as used in the EPRI study. The consumable costs were the same as shown in Table I-9. The financial data in this study were different than before because the costs were calculated in constant dollars (see Table I-14). As pointed in the EPRI study, the dry sorbent injection technologies have lower capital costs but higher operating costs due to low sorbent utilization. Wet FGD systems have a sorbent utilization approaching 90%. Therefore, >90% sulfur removal is achieved at Ca/S=1.1 typically.

The data in Table I-13 show the two-step process is competitive with wet FGD at 48%

utilization and more economical at 75% utilization. The two-step process at 75% utilization is more economical than wet FGD (which has a utilization of 90%) probably because the two-step levelized operating costs at 75% utilization become less than the FGD levelized capital costs.

I.9 RILEY STOKER'S AFBC SYSTEM

A comparison of the two-step costs with the in-bed desulfurization costs is shown in Table I-16. This analysis was done in current dollars levelized over 30 years. Therefore, the levelization factors shown in Table I-9 for the 30 year column were used. As can be seen the two-step process is competitive with in-bed desulfurization at 75% utilization. Also shown is the impact of escalating waste disposal costs.

TABLE I-1

METHOD OF ECONOMIC ANALYSIS - LEVELIZED REVENUE REQUIREMENTS

Levelized Revenue Requirement (or Cost)	= Initial Capital Cost * Levelized Ann. Carrying Charges + Initial Estimate of Operating Expenses * Levelization Factor
Carrying Charges	= Return on Equity + Return on Debt + Book Depreciation + Insurance + Property Taxes + Income Tax on Minimum Acceptable Return
Minimum Acceptable Return	= Return on Equity + Return on Debt
Operating Expenses	= Consumable Costs + O & M Costs

TABLE I-2

CONSTANT VERSUS CURRENT DOLLAR ANALYSIS

Current Dollars:

- Includes the Effect of Inflation
- Analysis more closely resembles Future Cash Flows
- Method is used by Utilities in Evaluating their Business Investments
- Tends to make Options Appear More Costly - Typically Twice as much as the Constant Dollar Analysis

Constant Dollars:

- Does Not Include the Effect of Inflation
- Cost Trends Due to Real Price Escalation are Clearly Visible
- Constant Dollar Analysis is usually used for Long Term Studies
- Method Preferred by Economic Analysts
- Used in the EPRI Study for Evaluating FGD Technologies

TABLE I-3

REFERENCE COAL COMBUSTION SYSTEMS

1. EPRI STANDARD FOR FGD ECONOMIC ANALYSIS

   Retrofit Plant, 300 MW, 2.6% Sulfur Coal -- 30 Year Levelized Constant Dollars

2. Riley's Retrofit LIMB

   200 MW, 3.4% Sulfur Coal -- 15 Year Levelized Current Dollars

3. Riley's AFBC Plant

   110,000 lb/hr Steam (80 MM Btu/hr Thermal), 3.3% Sulfur Coal -- 30 Year Levelized Current Dollars

TABLE I-4

REFERENCE SYSTEM FLOW RATES

	EPRI's System	Riley's LIMB Retrofit
Thermal input, MMBtu/hr	2000	1200
Coal heating value, btu/lb	13,100	10,650
Coal flow, lb/hr	151,832	113,301
Coal sulfur content, % wt	2.6	3.4
So2 flow, lb/hr	7895	7704

Limestone flow is set by the sulfur removal process Ca/S ratio. The total activation burner flow is set by the limestone flow and the maximum limestone loading to achieve 2600k in the burner.

TABLE I-5

RETROFIT SORBENT INJECTION - 15 YEAR LEVELIZED BUSBAR COSTS

	LIMB 50% Capt. Ca/S=2	TWO-STEP 96% Capt. Ca/S=2 Coal/O_2	TWO-STEP 96% Capt. Ca/S=2 Gas/O_2	TWO-STEP 90% Capture Ca/S=1.2 Coal/O_2
Activation Burner Design:				
Capital Recovery	4.44	4.62	4.62	3.71
Fixed O & M	1.03	1.03	1.03	1.03
Variable O & M	0.55	0.55	0.55	0.55
Consumables:				
Limestone	2.33	2.33	2.33	1.40
Waste Disposal	2.18	2.52	2.52	1.75
Oxygen	0	5.72	5.72	3.45
Coal or Natural Gas	0	3.08	6.44	1.85
Coal Charge	0.80	0	0	0
Coal Credit	-0.86	-4.10	-4.26	-2.83
Water	0.64	0.64	0.64	0.64
TOTAL (mills/kWh)	11.11	16.4	19.6	11.6
$/Ton-$SO_2$	682	525	626	394

TABLE I-6

FUEL CREDIT CALCULATION PROCEDURE

- Net Energy of the Calcination/Sulfation Reaction is Converted into a Coal Equivalent
- Net Energy Required (in AFBC and LIMB) =
  - + Sensible Energy to Heat CaCO3 to 1400^{o}K
  - + Calcination Energy (Assuming 100% Calcination)
  - - Heat Release Due to Sulfation
  - - Sensible Heat in Solid and Gas Products

Overall Calcination-Sulfation Reaction is slightly exothermic at AFBC & LIMB Utilizations

- In the Two-Step Process, the Heat Recovered Consists of Four Terms

+ Enthalpy Recovered in Cooling Activation Burner Gas From 2600^{o}K to 1400^{o}K (It is assumed that sulfation starts at 1400^{o}K)

+ Enthalpy Recovered from CO_2 and H_2O (formed from Coal or Gas in the Activation Burner) as the Flue Gas Cools Down from 1400^{o}K to 400^{o}K (It is assumed that the heat below 400^{o}K cannot be recovered)

+ Sulfation Energy

+ Recoverable Sensible Heat (1400^{o}K to 400^{o}K) in Solids (CaO, $CaSO_4$) and CO_2 formed due to Calcination

Note: In the two-step process the energy needed to heat the limestone up to 1400^{o}K and calcine it is implicitly accounted for in the thermodynamic equilibrium calculation.

TABLE I-7

HEAT BALANCES DURING SULFATION

LIMB & AFBC

- Heat Required To Calcine Limestone, Btu/lb

  1096

- Heat Release Due to Sulfation + Sensible Energy in Solids & CO2, Btu/lb

  432+2957X

  Where X is the Utilization

- Net Heat Input, Btu/lb

  664-2957X

Therefore, Overall Reaction is Thermoneutral at a Utilization of 22%

TWO-STEP

- Heat Content in Activation Burner Gas (2600°K to 1400°K) Btu/lb of Activation Burner Flow

  Coal/Oxygen 1177

  Gas/Oxygen 1397

- Sensible Energy in CO2 and H2O formed from Fuel Btu/lb of fuel (1400°K to 400°K)

  For Gas (2.75*0.56 + 2.25*1.1)*1000

  For Coal (3.03*0.56 + 0.50*1.1)*1000

- Heat Release in Sulfation + Sensible Heat in Solids, Btu/lb of Limestone

  432+2957X

TABLE I-8

CONSUMABLE COST LEVELIZATION FACTORS BASED ON EPRI'S TECHNICAL ASSESSMENT GUIDE - CURRENT DOLLAR ANALYSIS

Consumable	% Inflation	% Real Escalation	Levelization Factor 15 yr	30 yr
Coal	6	1	1.556	1.961
Limestone	6	0	1.452	1.748
Oxygen	6.3	0.3	1.481	1.800
Natural Gas	6	2	1.670	2.213
Waste:				
Baseline Case	6	0	1.452	1.748
Stringent Case	6	5	2.078	2.864
Annual Capital Recovery			18.6%	17.3%

TABLE I-9

CONSUMABLE COSTS

Consumable	1991 Price	Source
Coal ($/Ton)	50	TAG*
Oxygen ($/Ton)	45	Vendor Quote
Natural Gas ($/1000 SCF)	3 (Range 2-4)	Natural Gas Annual
Limestone ($/Ton)	15	TAG
Waste Disposal ($/Ton)	16 (Range 12-20)	EPRI
Water ($/1000 Gallon)	0.85	TAG

* EPRI's Technical Assessment Guide, 1986

TABLE I-10

RETROFIT SORBENT INJECTION TECHNOLOGY CAPITAL COSTS

Retrofit LIMB	24,720,000*
Two-Step Alternatives	
96% Capture at Ca/S=2	25,708,800
90% Capture at Ca/S=1.2	20,682,000

* Based on 1985 Estimates Provided by Riley Research, Worcester, MA
Cost Escalation: 1991 Costs = 1.20 * 1985 Costs
Capital Costs are assumed to be proportional to the limestone and waste flow raised to the 1/2 power

TABLE I-11

EFFECT OF ESCALATING WASTE DISPOSAL COSTS ON THE ECONOMICS

RILEY'S RETROFIT LIMB CASE

PROCESS	LEVELIZED DISPOSAL COST, $/TON	
	33.2	23
Two-Step: 96% Capture at Ca/S=2	559	525
LIMB: 50% Capture at Ca/S=2	740	682
Two-Step: 90% Capture at Ca/S=1.2	419	394

TABLE I-12

CHANGES IN WASTE CHARACTERISTICS DUE TO SORBENT INJECTION

PROCESS	TOTAL WASTE/FLYASH
No Injection	1.0
(10% Ash, 3.4% Sulfur Coal)	
LIMB	3.0
Two-Step (96% at Ca/S=2)	3.3
Two-Step (90% at Ca/S=1.2)	2.6

- Boilers can typically handle a 2-4 fold increase in solid loading
- Downstream particulate collection equipment has to be upgraded
- The unreacted lime forms a low grade cement with fly ash resulting in a low permeability waste
- Lime/Fly ash mix presents handling problems due to steam generation

TABLE I-13

WET FGD AND DRY INJECTION TECHNOLOGY COSTS

SOURCE: EPRI Journal, December, 1990.

MODEL: 300 MW Unit, 2.6% Sulfur Coal, Moderately Difficult Retrofit, 30 Year Levelized Costs in Constant Dollars.

Control Technology	Capital Requirements ($/kW)	$/Ton SO_2 Removed
Wet FGD	150 - 280	350 - 600
Dry Sorbent Injection	70 - 120	420 - 750

SOURCE: TDS Economic Feasibility Study. Same Assumptions as EPRI Study.

MODEL: Same as EPRI Model Above.

Control Technology	$/Ton SO_2 Removed
Two-Step Process (96% Capture @ Ca/S = 2)	415
Two-Step Process (90% Capture @ Ca/S = 1)	326
Riley Stoker LIMB (50% Capture @ Ca/S = 2)	540

TWO-STEP PROCESS IS ECONOMICALLY COMPETITIVE WITH FGD AT 75% UTILIZATION

TABLE I-14

WET FGD AND SORBENT INJECTION TECHNOLOGY COSTS

- Source: EPRI Journal, December, 1990
- Reference System: 300 MW, 2.6% Sulfur Coal, Moderately Difficult Retrofit, 30 Year Levelized Costs in Constant 1990 Dollars

Control Technology	Capital Cost, $/kW	$/Ton SO2
Wet FGD	150-280	350-600
Sorbent Injection	70-120	420-750

- Energy Technology Office Study Conducted under the same assumptions as the EPRI study

Two-Step (96% at Ca/S=2)	415
Two-Step (90% at Ca/S=1.2)	326
LIMB (50% at Ca/S=2)	540

The Two-Step process becomes economically competitive with wet FGD at 75% Utilization

TABLE I-15

CONSUMABLE COST LEVELIZATION FACTORS BASED ON EPRI'S TECHNICAL ASSESSMENT GUIDE - CONSTANT DOLLAR ANALYSIS

Consumable	% Inflation	% Real Escalation	Levelization Factors 15 Yr	30 Yr
Coal	6	1	1.072	1.122
Limestone	6	0	1.0	1.0
Oxygen	6.3	0.3	1.018	1.03
Natural Gas	6	2	1.151	1.267
Waste:				
Baseline Case	6	0	1.0	1.0
Stringent Case	6	5	1.33	1.882
Capital Recovery			11.7%	10.3%

TABLE I-16

AFBC COST SUMMARY - 30 YEAR LEVELIZED COSTS IN CURRENT DOLLARS

Cost Element	In-Bed 90% at Ca/S=3	Coal/Oxygen 96% at Ca/S=2	Coal/Oxygen 90% at Ca/S=1.2
Capital Recovery	0	48.4	41.3
Oxygen	0	223.2	142.9
Coal	47.9	124.2	79.5
Coal Credit	-57.6	-140.8	-104
Limestone	143.8	89.8	57.5
Waste	138.7	96.9	71.7
Water	17.5	17.5	17.5
$/Ton SO2	**290**	**459**	**306**

- If Waste Costs Escalate to 45.8 instead of 28 $/Ton

$/Ton SO2	**379**	**521**	**352**

Two-Step Process is Competitive with in-bed desulfurization at 75% Utilization